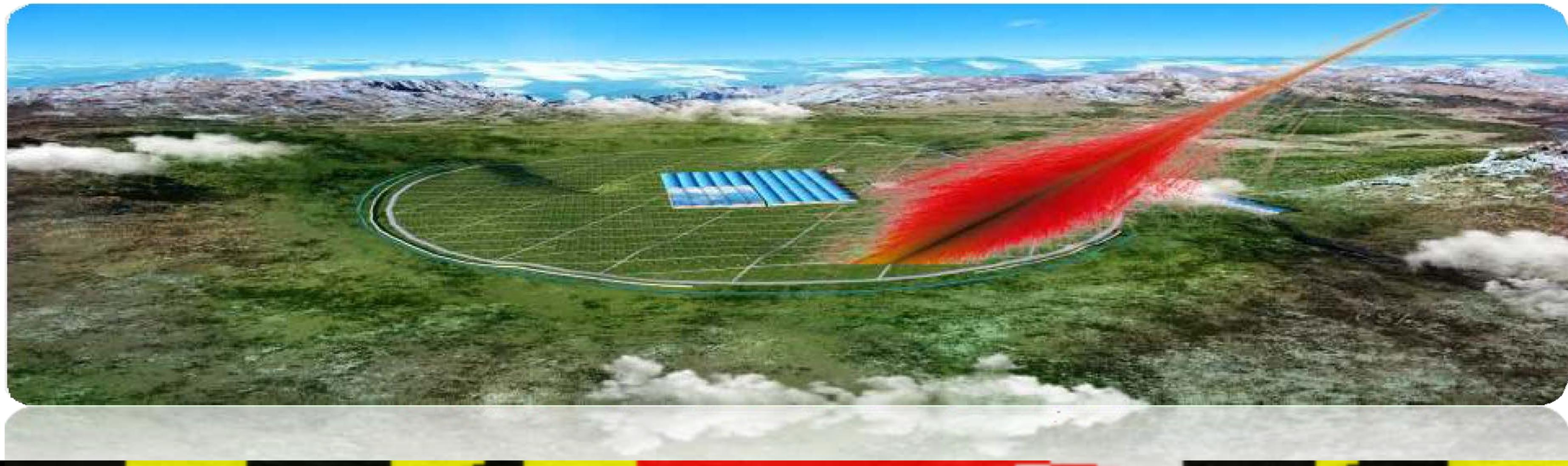
An aerial photograph of the Large High Altitude Air Shower Observatory (LHAASO) in Tibet. The site is located in a high-altitude, arid landscape with a grid-like pattern of detector modules. A large white rectangular building, likely the control center, is situated in the middle of the array. In the foreground, there are several small blue-roofed buildings and two large, circular artificial reservoirs filled with water. The background shows distant mountain ranges under a cloudy sky.

Recent Results from The Large High Altitude Air Shower Observatory (LHAASO)

Jordan Goodman
Erice Summer 2022

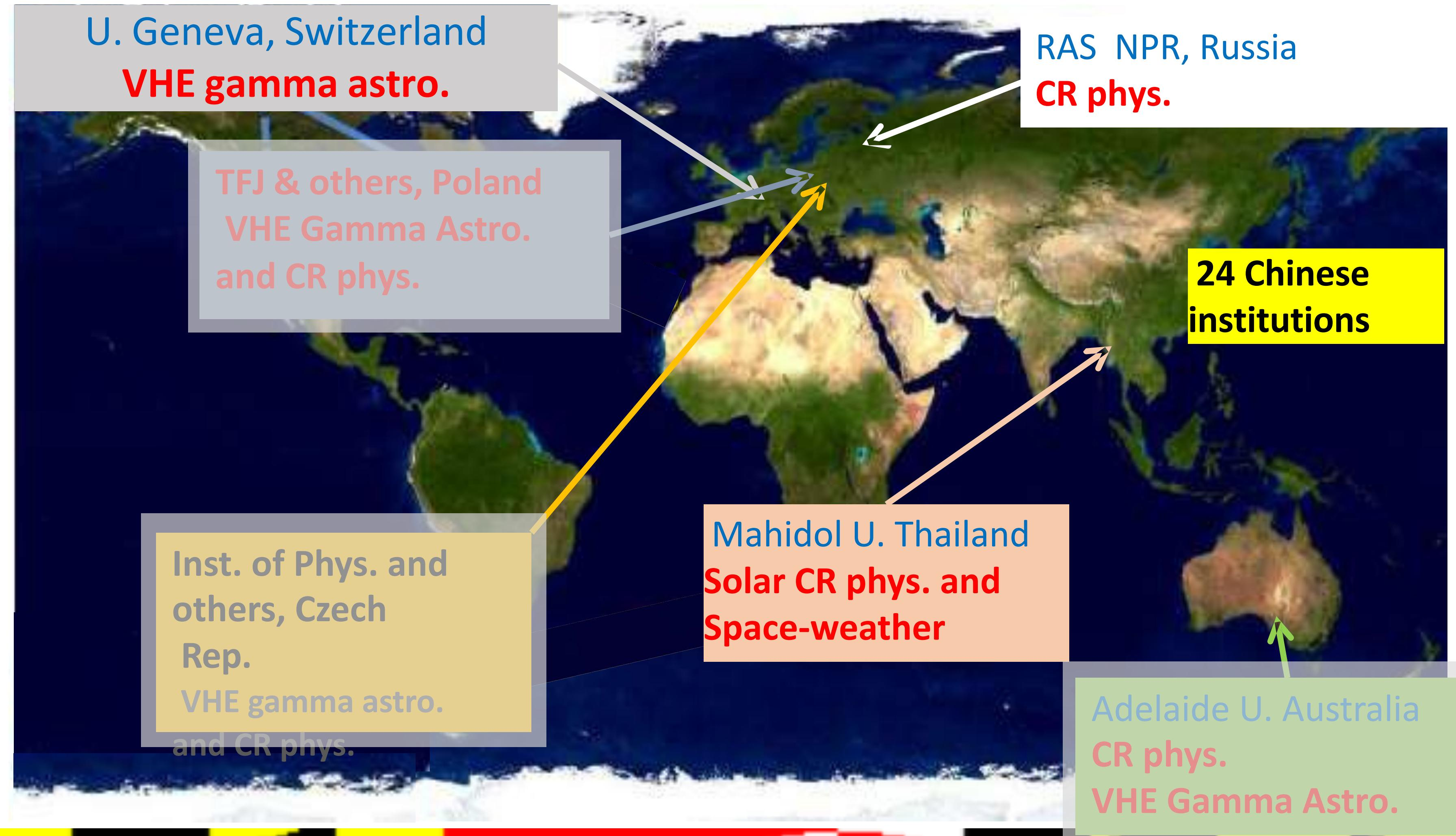
Talk Overview

- Large High Altitude Air Shower Observatory (LHAASO)
 - Disclaimer - I am not a LHAASO collaborator. (More of an envious admirer)!
 - All the material in this talk was taken from public sources or given to me by Zhen Cao
- There are many similarities between HAWC and LHAASO
 - Cost is not one of them!



LHAASO Collaboration (by country)

Yi Zhang

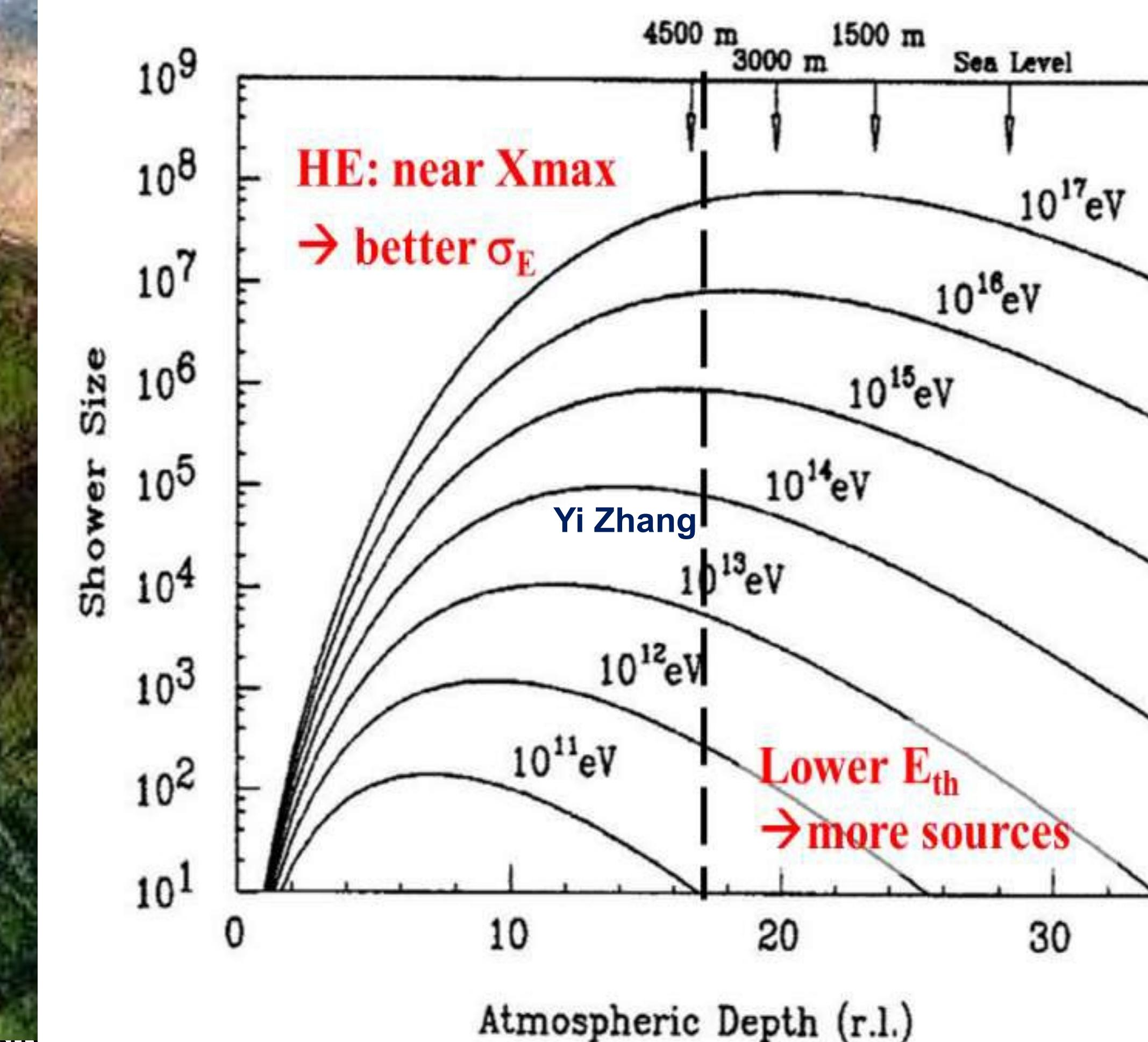




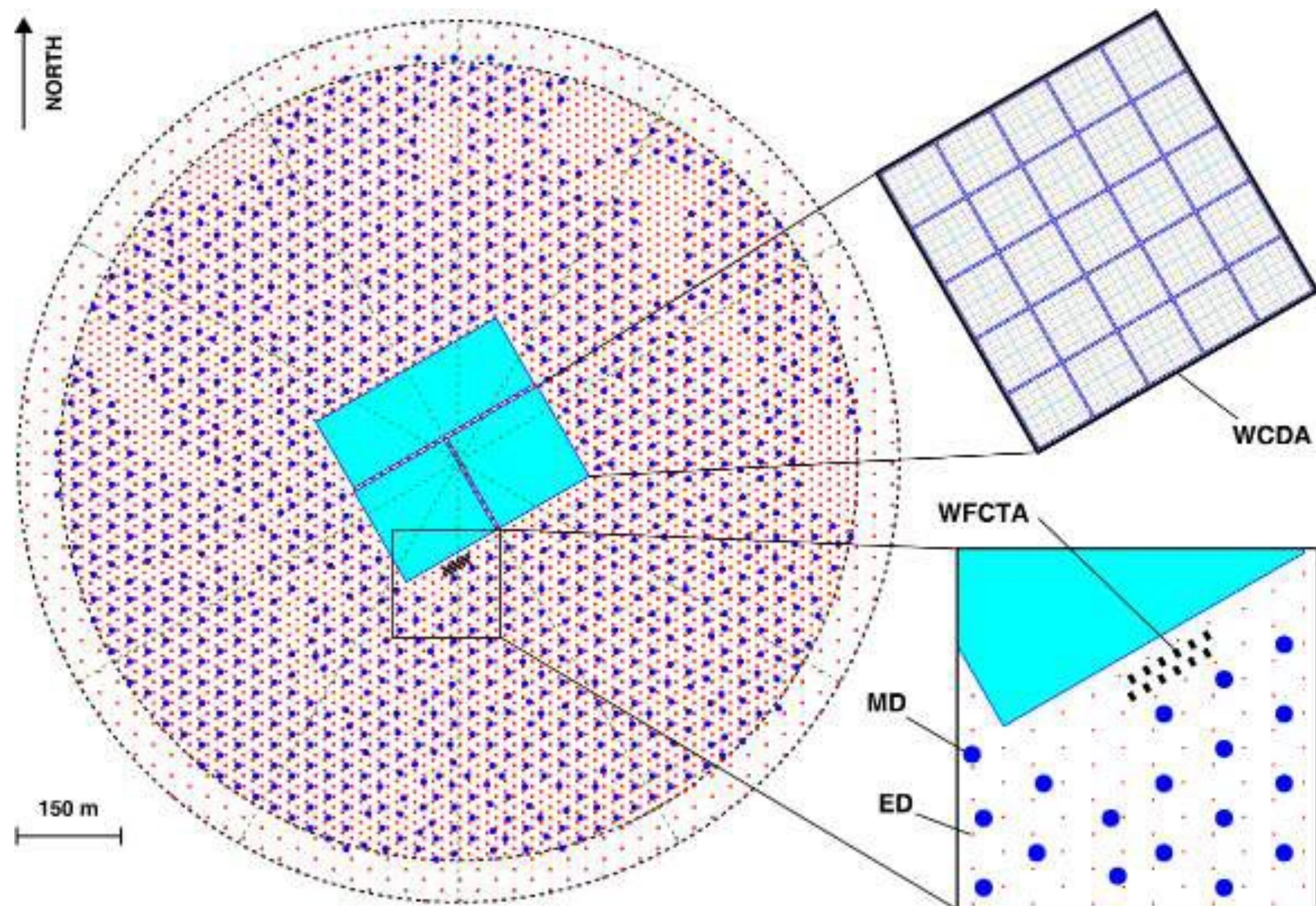
Where is LHAASO

Yi Zhang

Mt. Haizi (4410 m a.s.l., 29°21' 27.6" N, 100°08'19.6" E),
Sichuan, China



A Large area EAS array covering 1.3 km²



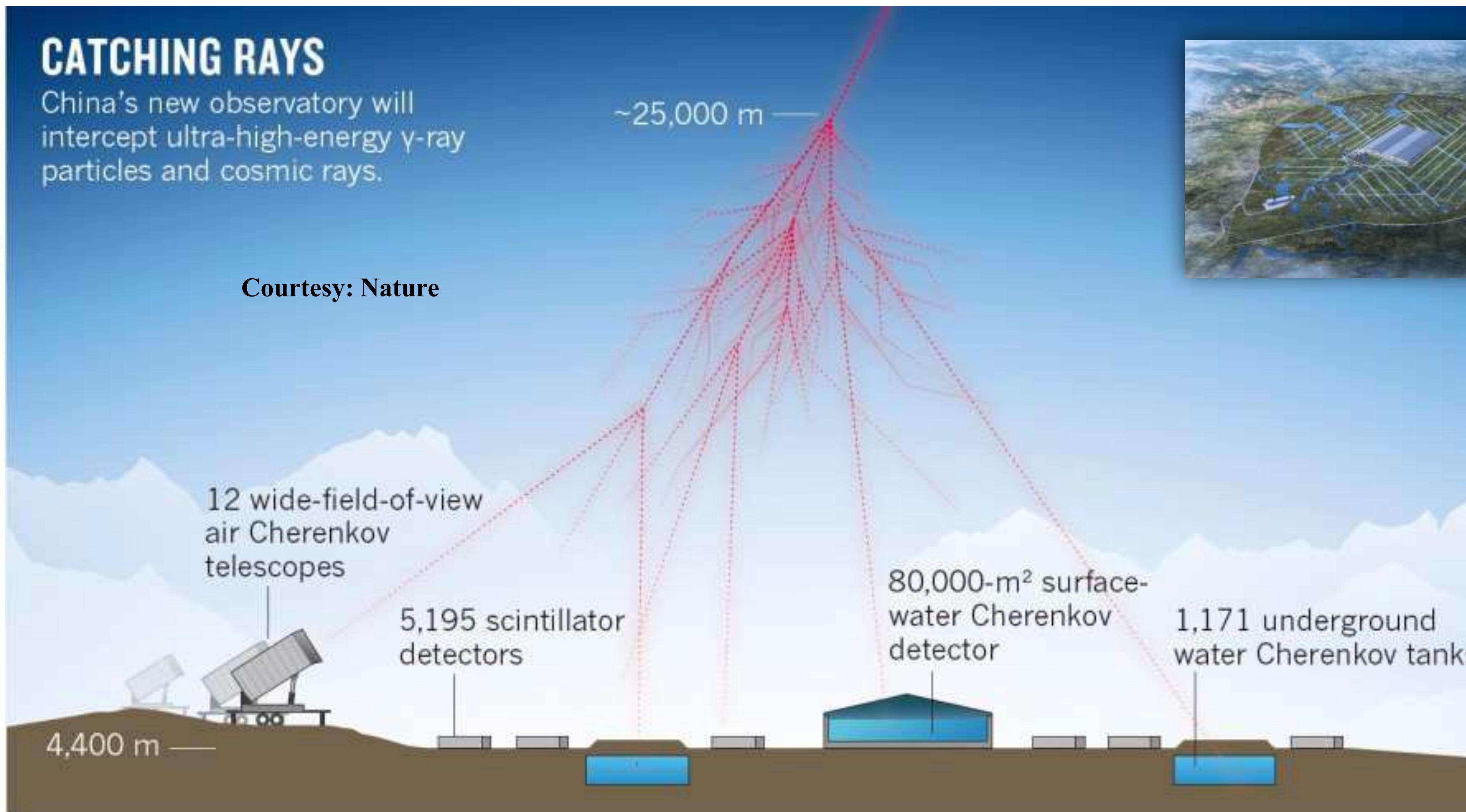
- 5242 Electron Detectors (ED)s
 - 1 m² each
 - 15 m spacing
- 1188 Muon Detectors (MD)s
 - 36 m² each
 - 30 m spacing
- 3120 Water Cherenkov Det. WCDs
 - 25 m² each
- 18 Wide Field Cherenkov Telescopes WFCTs

Main goals of LHAASO

- TeV gamma-ray survey → WCDA (100 GeV-30 TeV)
 - AGN, GRB, survey new source, ...
- >20 TeV gamma-ray survey → KM2A (10TeV-1PeV)
 - SNR, PWN, Superbubble, diffuse around 100TeV, ...
- Individual nuclei spectra → WFCTA (10TeV to EeV)
 - Different configures
 - Combined with WCDA, WCDA++, KM2A
- Benefit regions:
 - Anisotropy, Solar physics, dark matter, EBL, IGMF, Lorentz invariance, hadronic interaction, ...



Hybrid Detection of EASs by LHAASO





LHAASO birds-eye View from a drone — May. 2021



Living Space

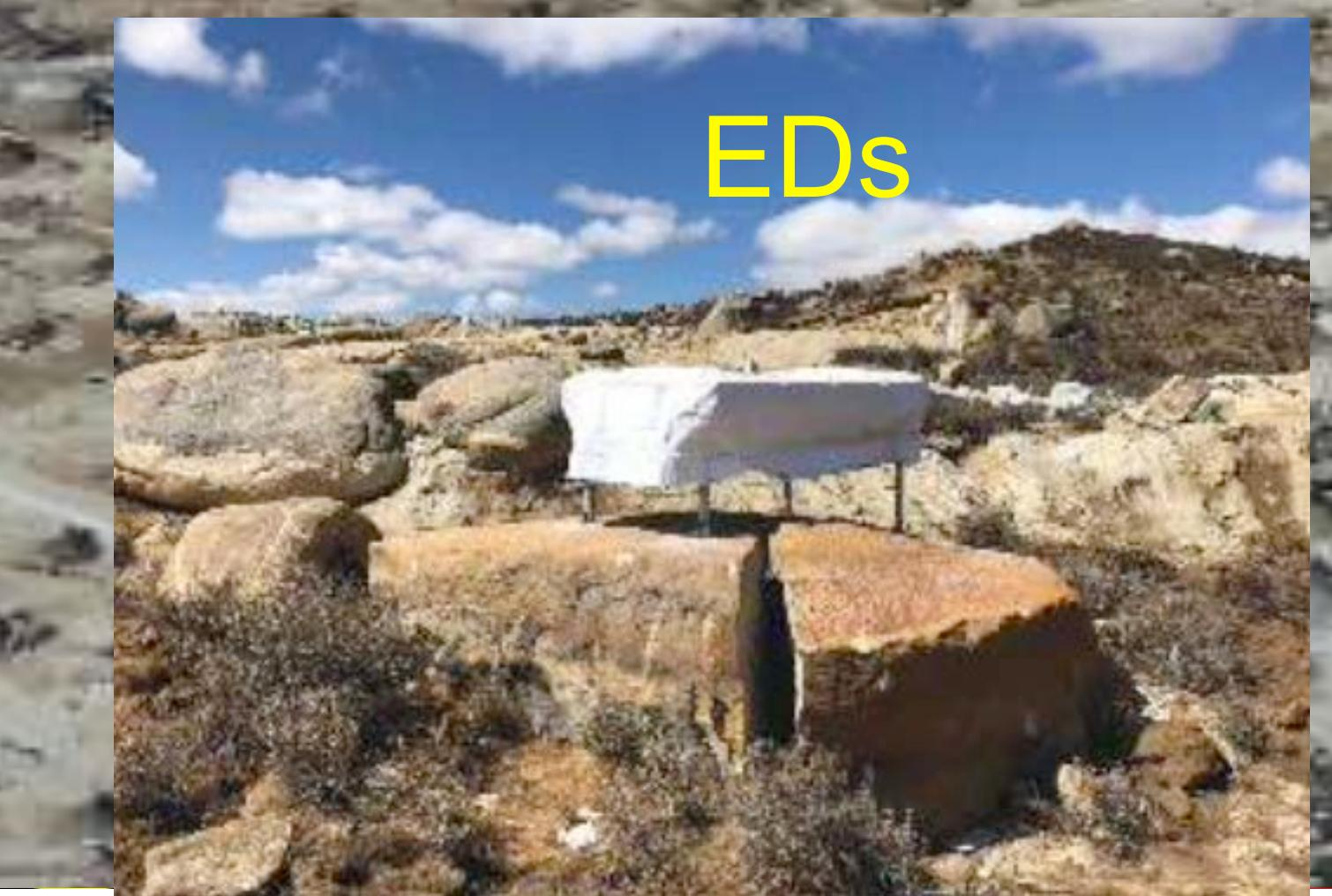


Building the Experiment

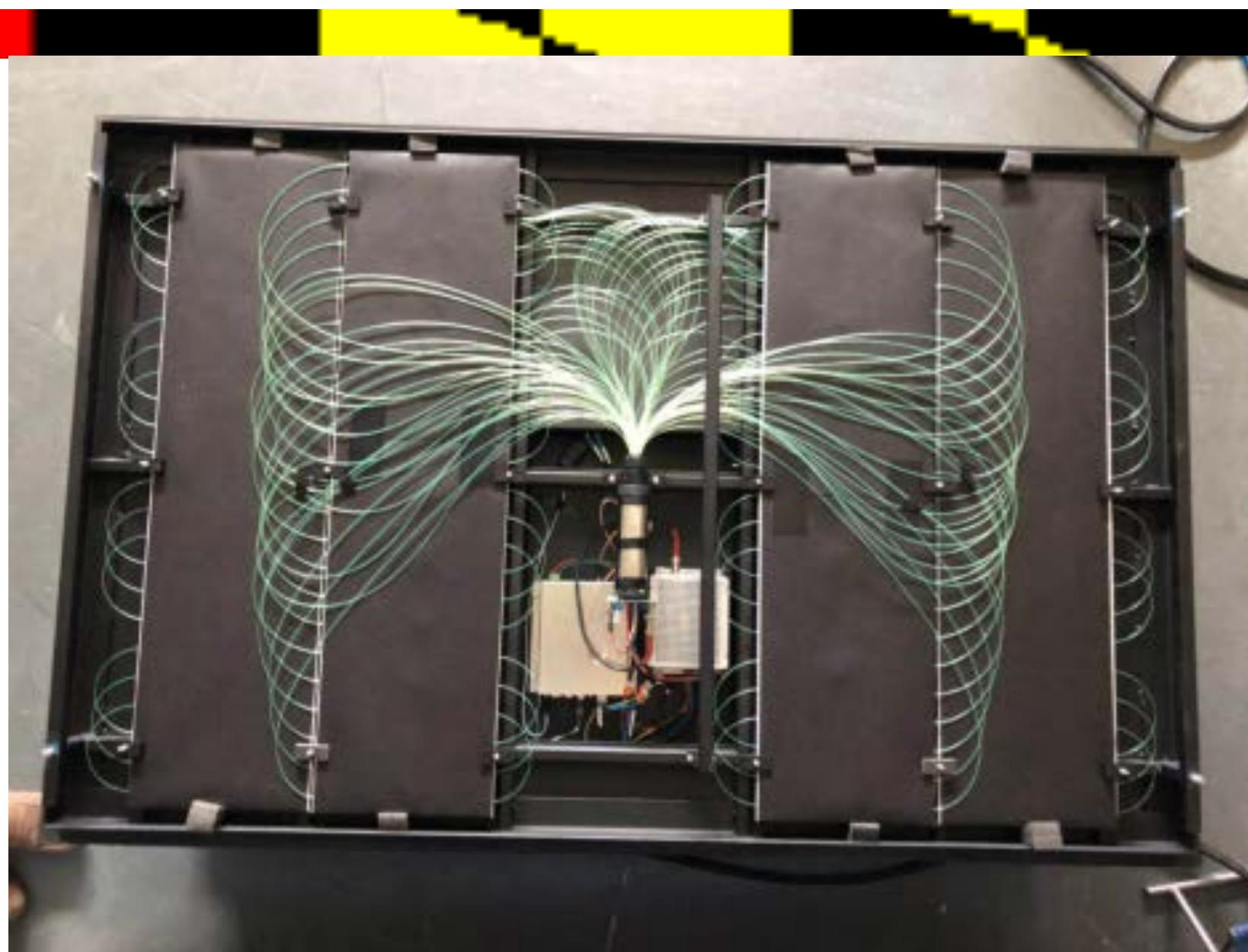
Three Gorges Dam - \$22B



LHAASO birds-eye View from a drone



KM2A Electromagnetic particle Detectors



Scintillator Detector Unit

1/2 ED array, 2365 EDs started 2019-12

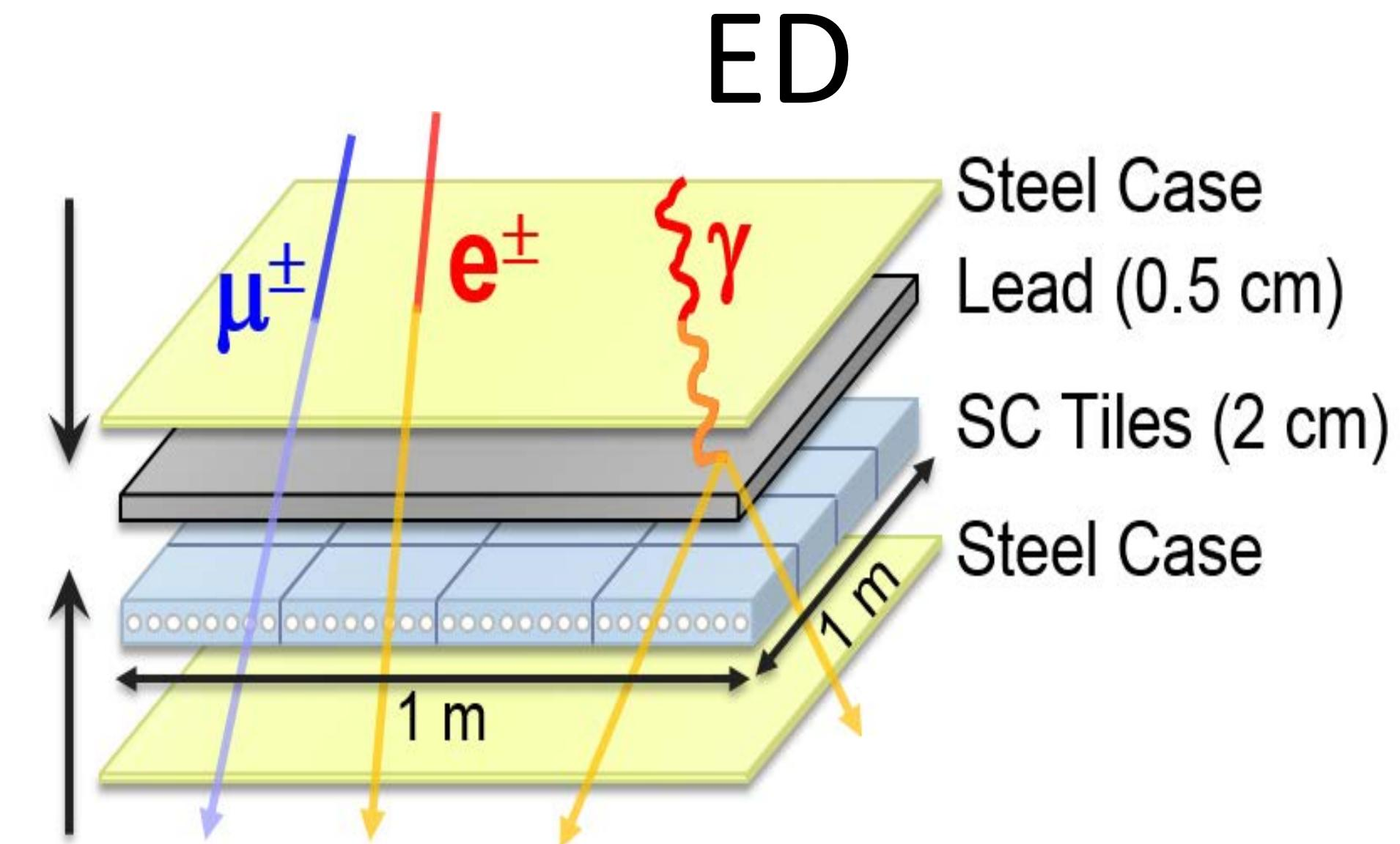
**3/4 ED array, 3978 EDs (total 5242),
started operation 6/12/2020**

Trigger rate ~ 1900Hz,

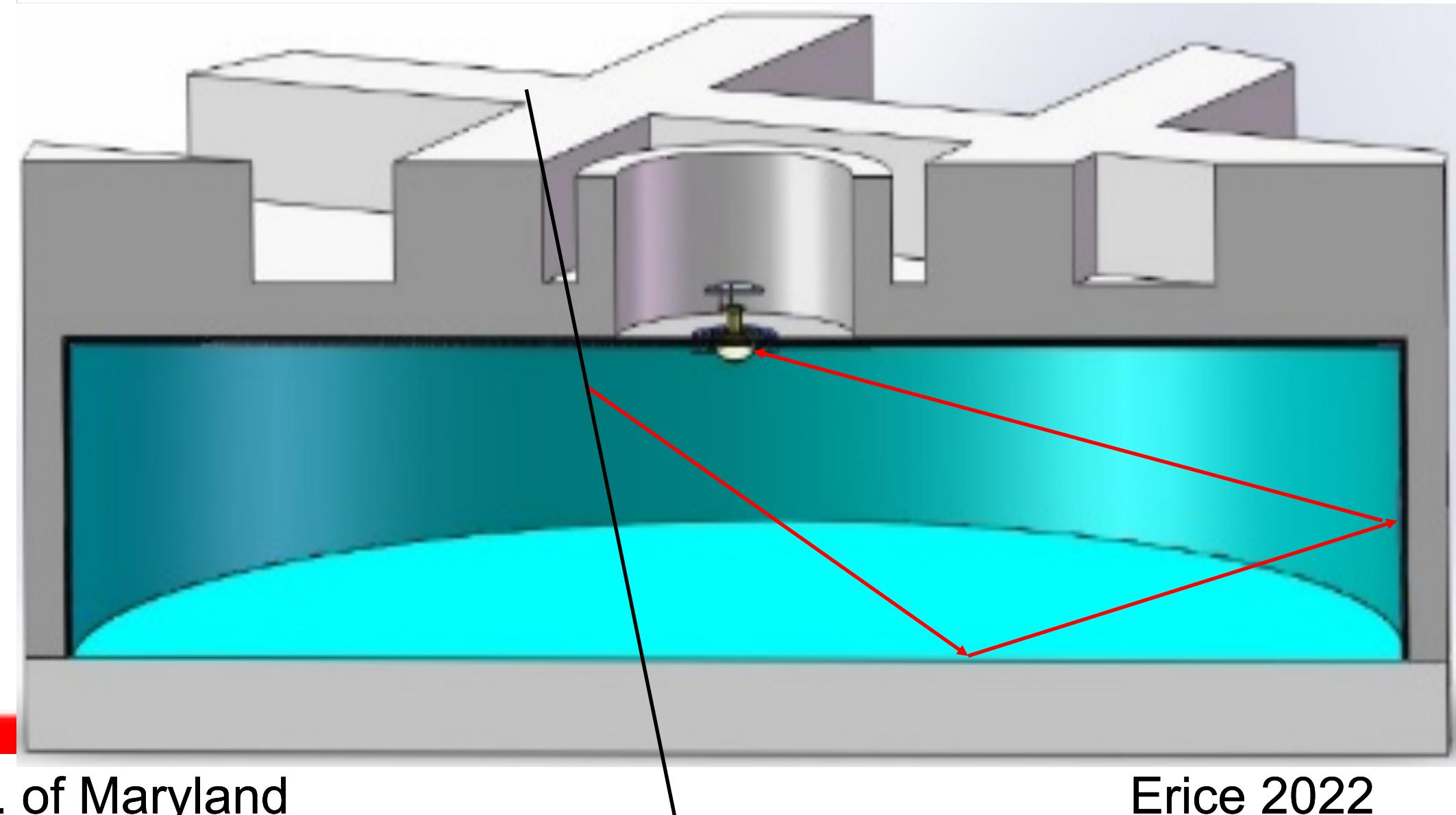
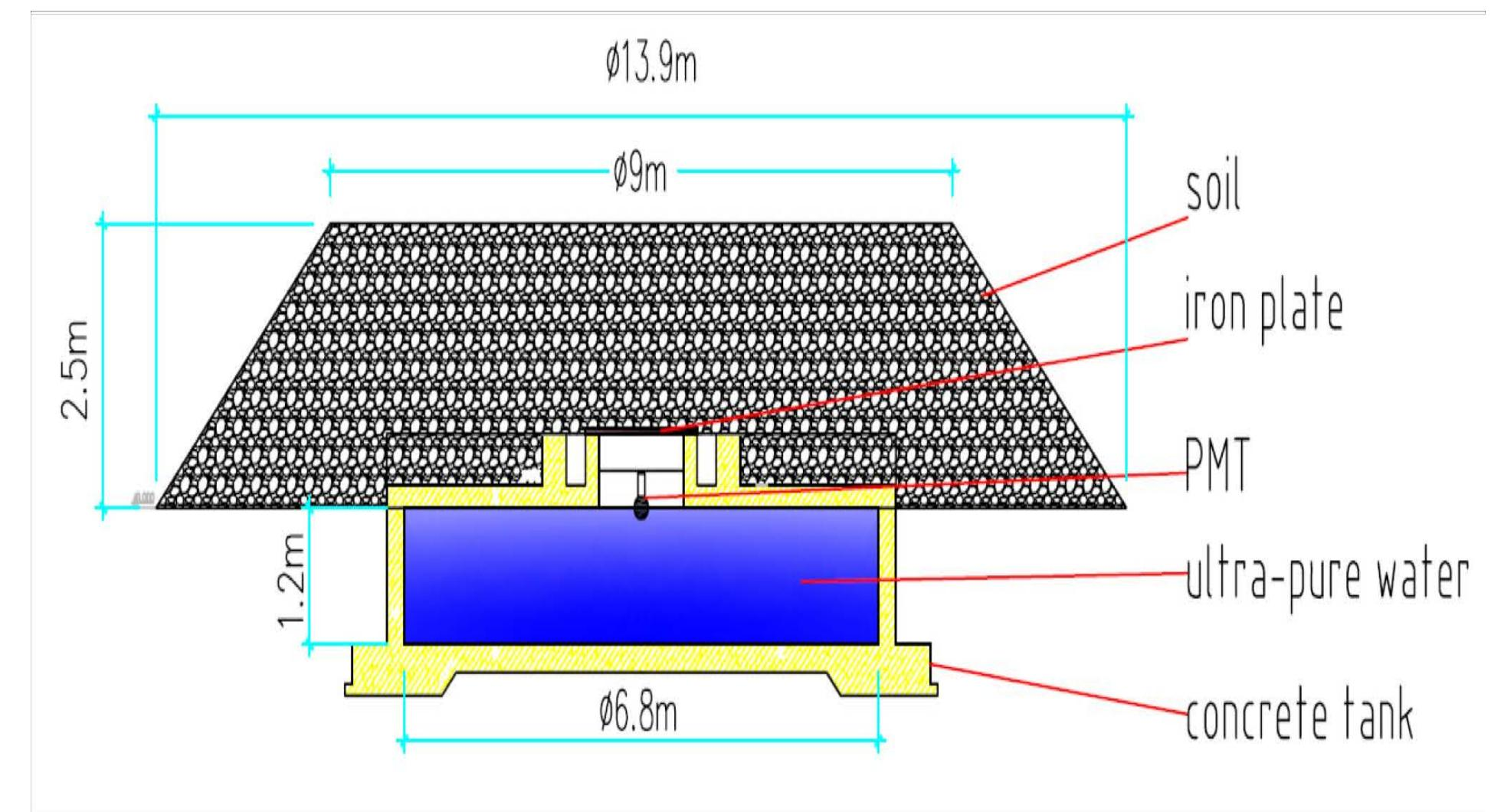
1.45TB one day

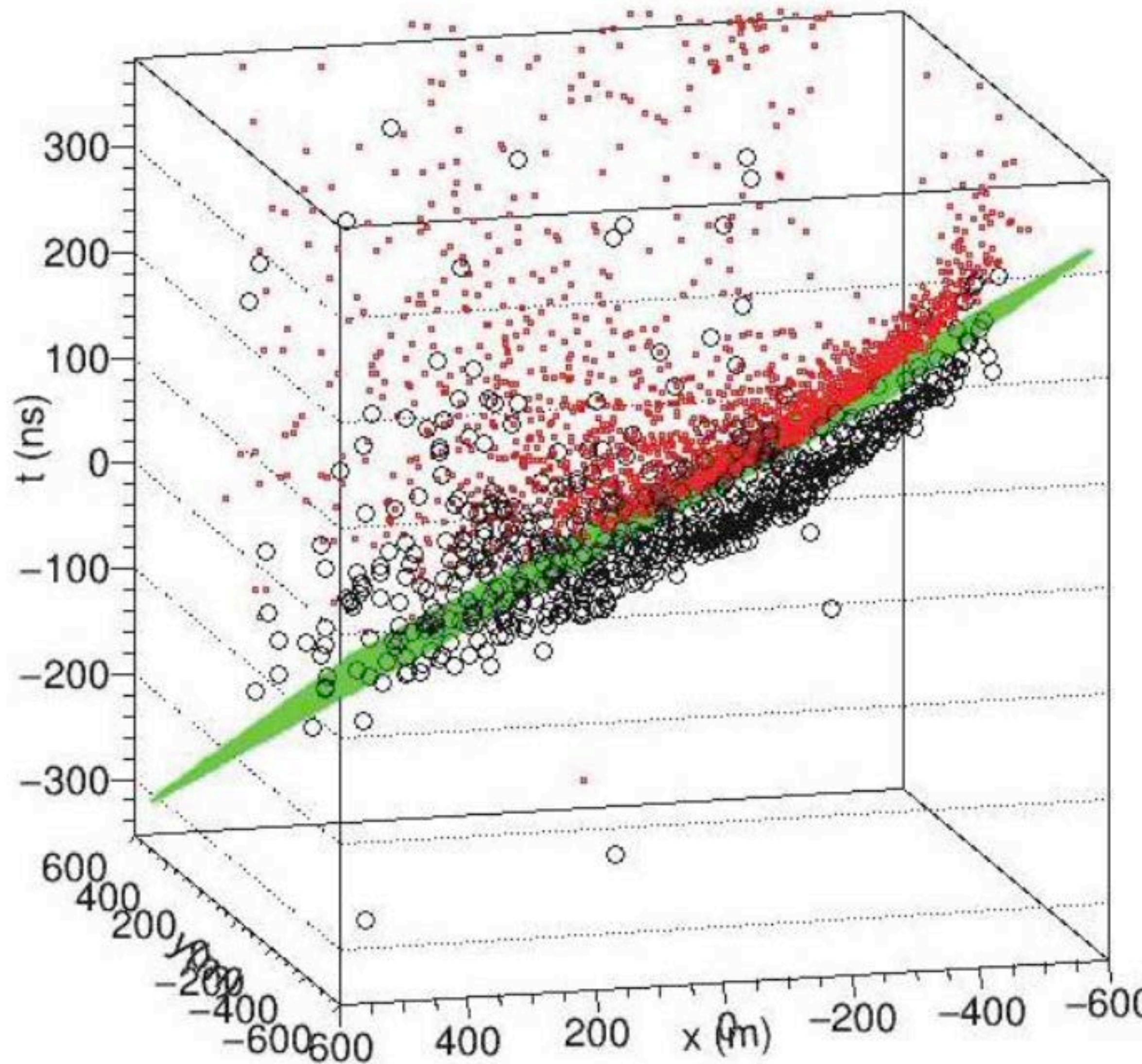
ED Specifications

Detection area	1m × 1m; 5mm Lead covered
Detection efficiency	> 95%
Time resolution	< 2ns
Dynamic range	1~10000 particles/m²; 25%@1 particle, 5%@10000 particles
single channel rate	<2kHz@working Gain
Stable operation	> 20yrs (4410m, 0.6atm., ±25°C)



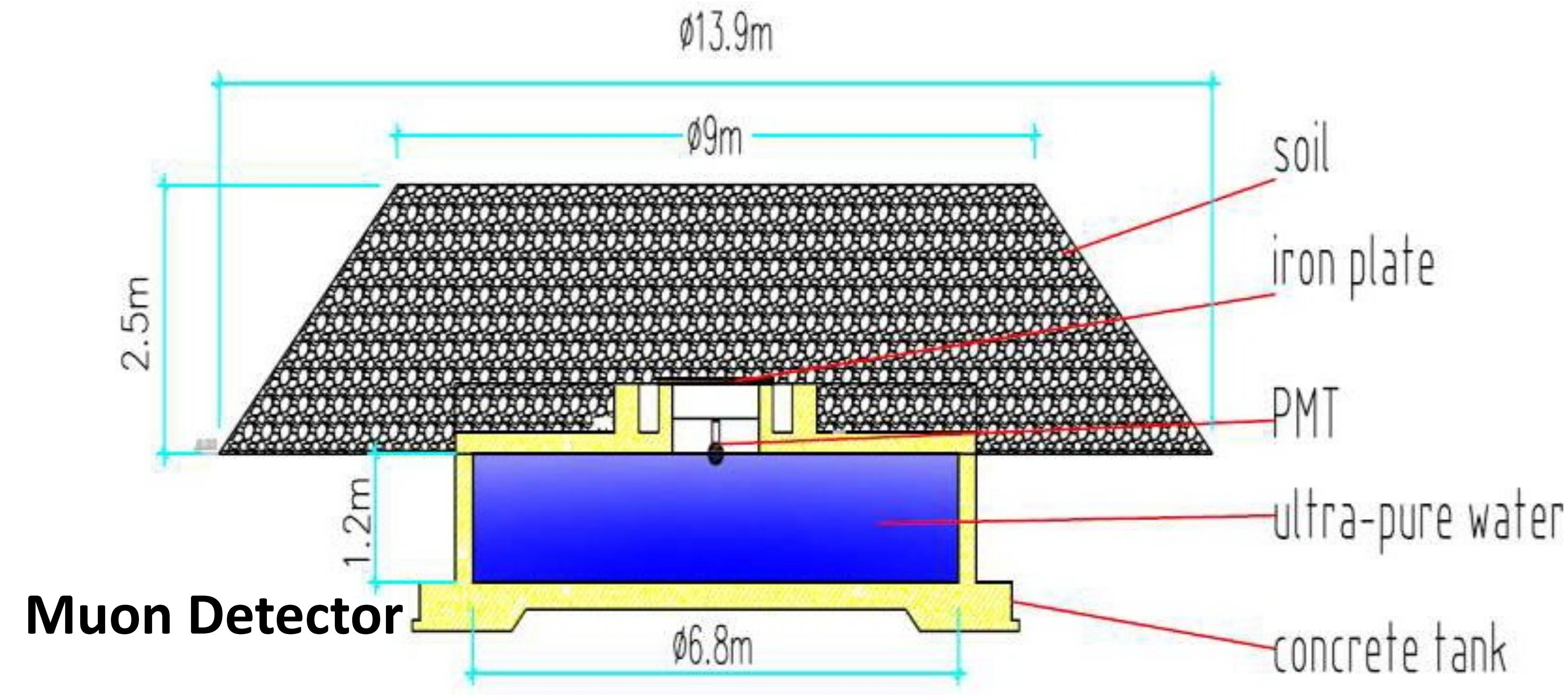
MD





Secondary particles of an EAS detected by the ED array. The green plane is EAS front plane. The red squares are the fired ED. The black circles are the fired MD. The second front is caused by MD's dead time.

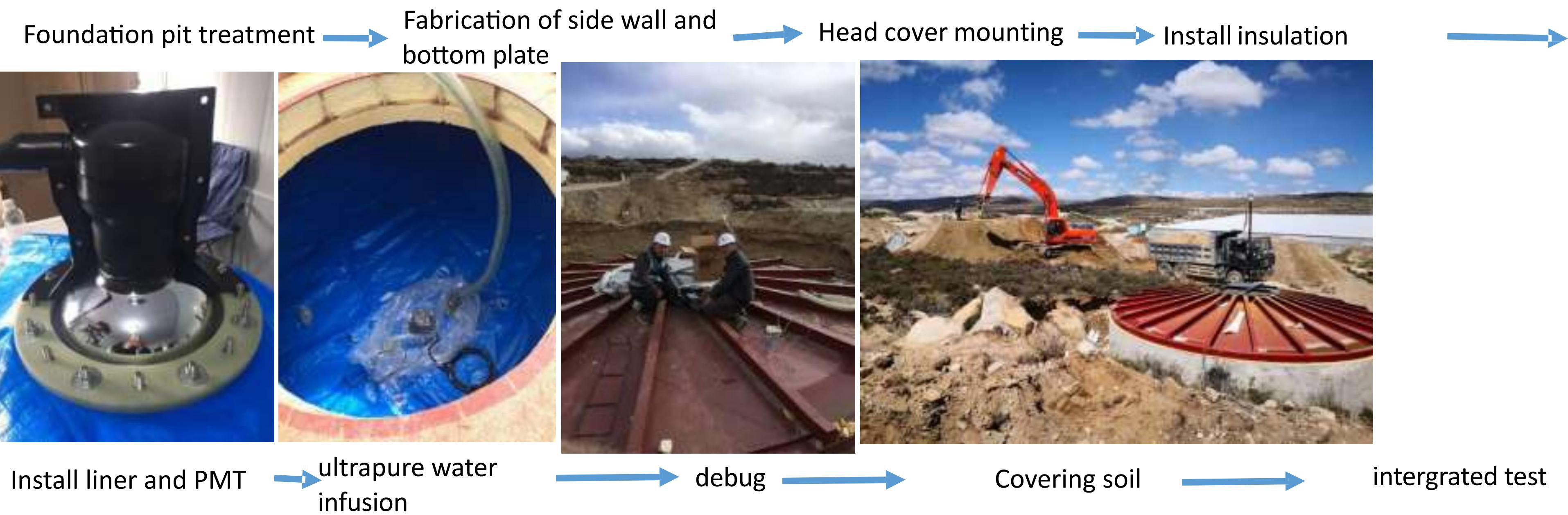
KM2A Muon Detector array



1/2 MD array, 592 MDs (total 1188) started operation from 12/2019

3/4 MD array, 914 MDs (total 1188) started operation from 12/2020

Installation of a Muon Detector

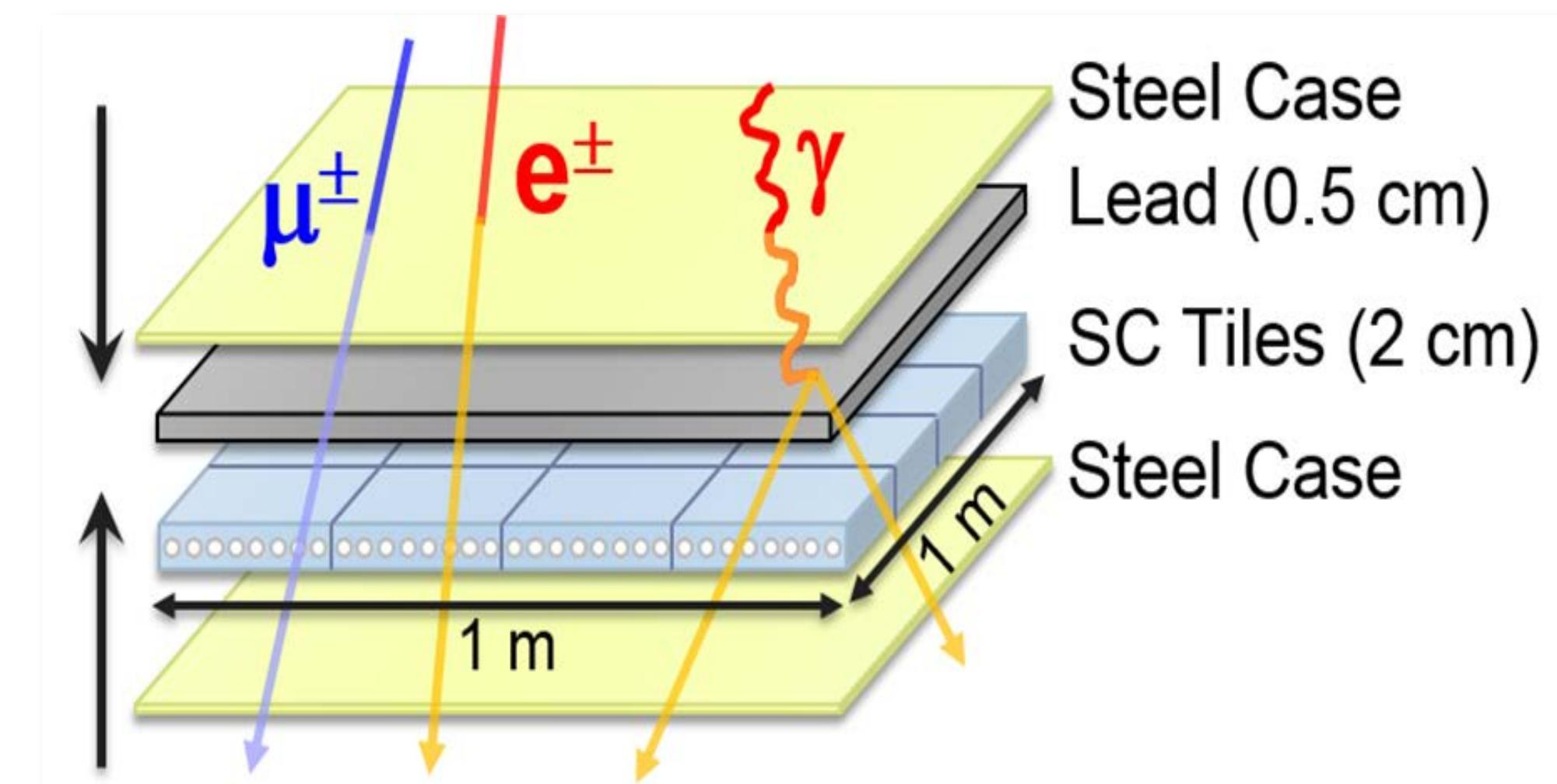


KM2A: 1.36 (km)^2

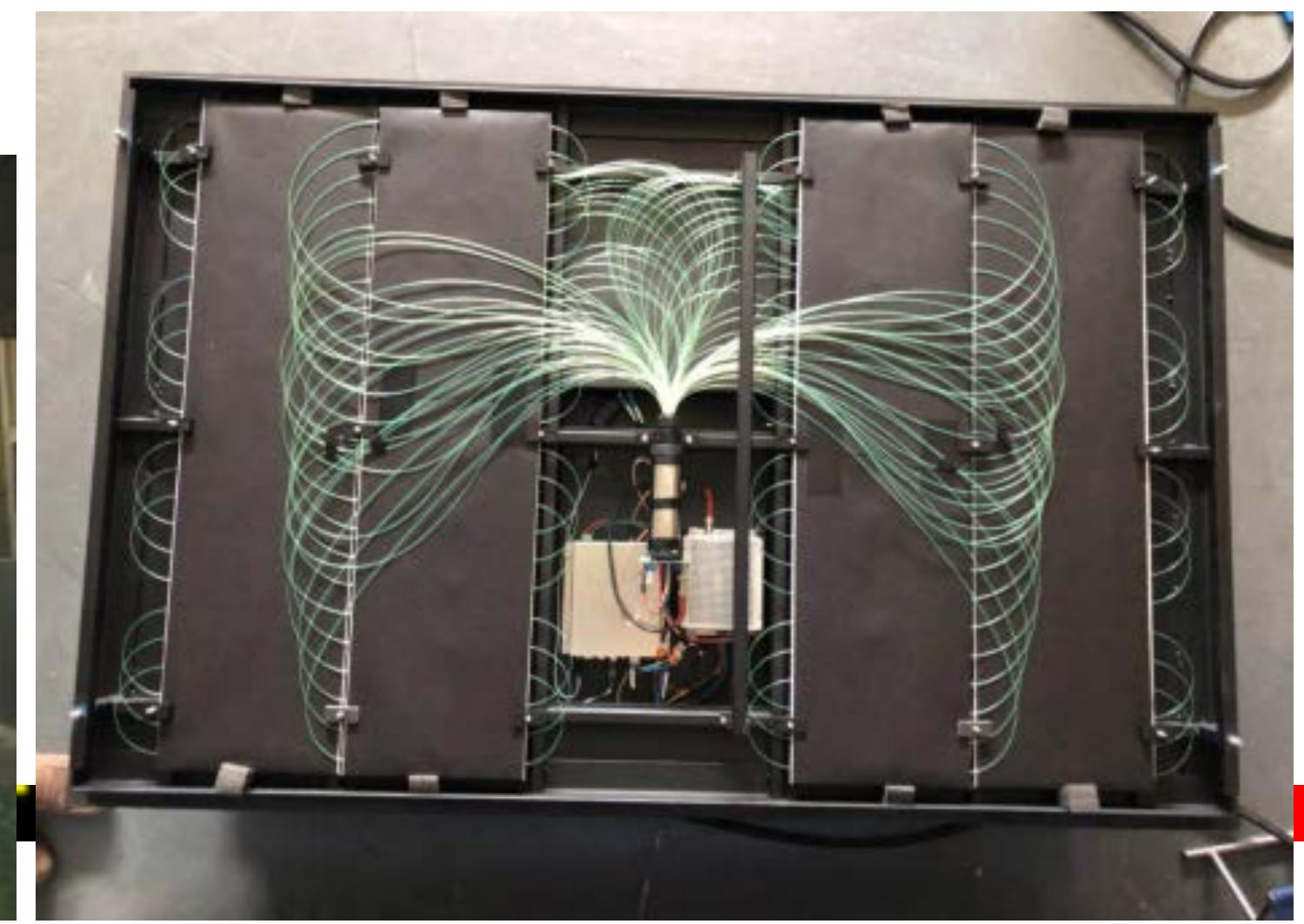
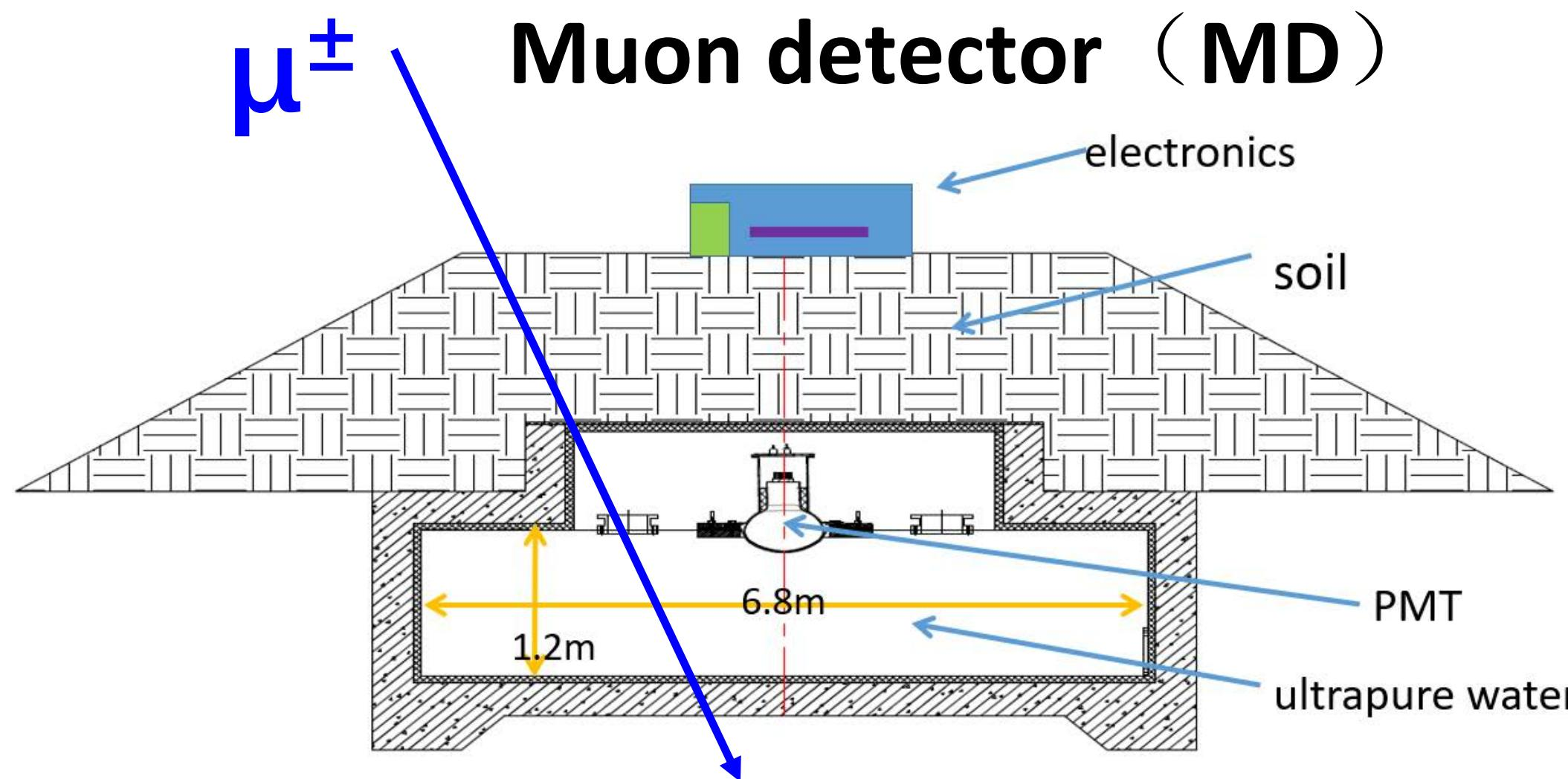


- > 5195 EDs
 - 1 m^2 each
 - 15 m spacing
- > 1188 MDs
 - 36 m^2 each
 - 30 m spacing

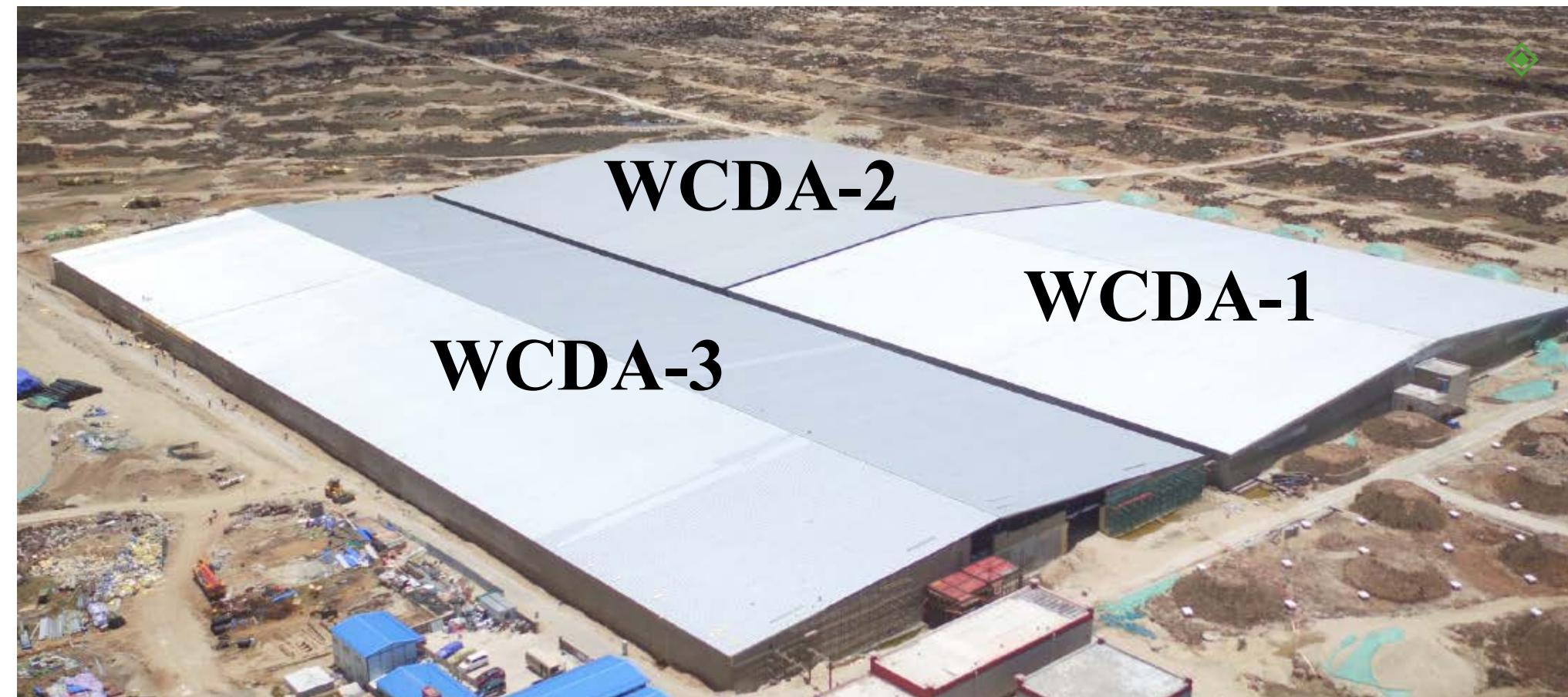
Scintillator Detectors (ED)



Inner View of one ED



Water Cherenkov Detector Array (WCDA)



Energy range

WCDA-1

- 300 GeV – 10 PeV
- WCDA-2 and WCDA-3
- 100 GeV - 10 TeV

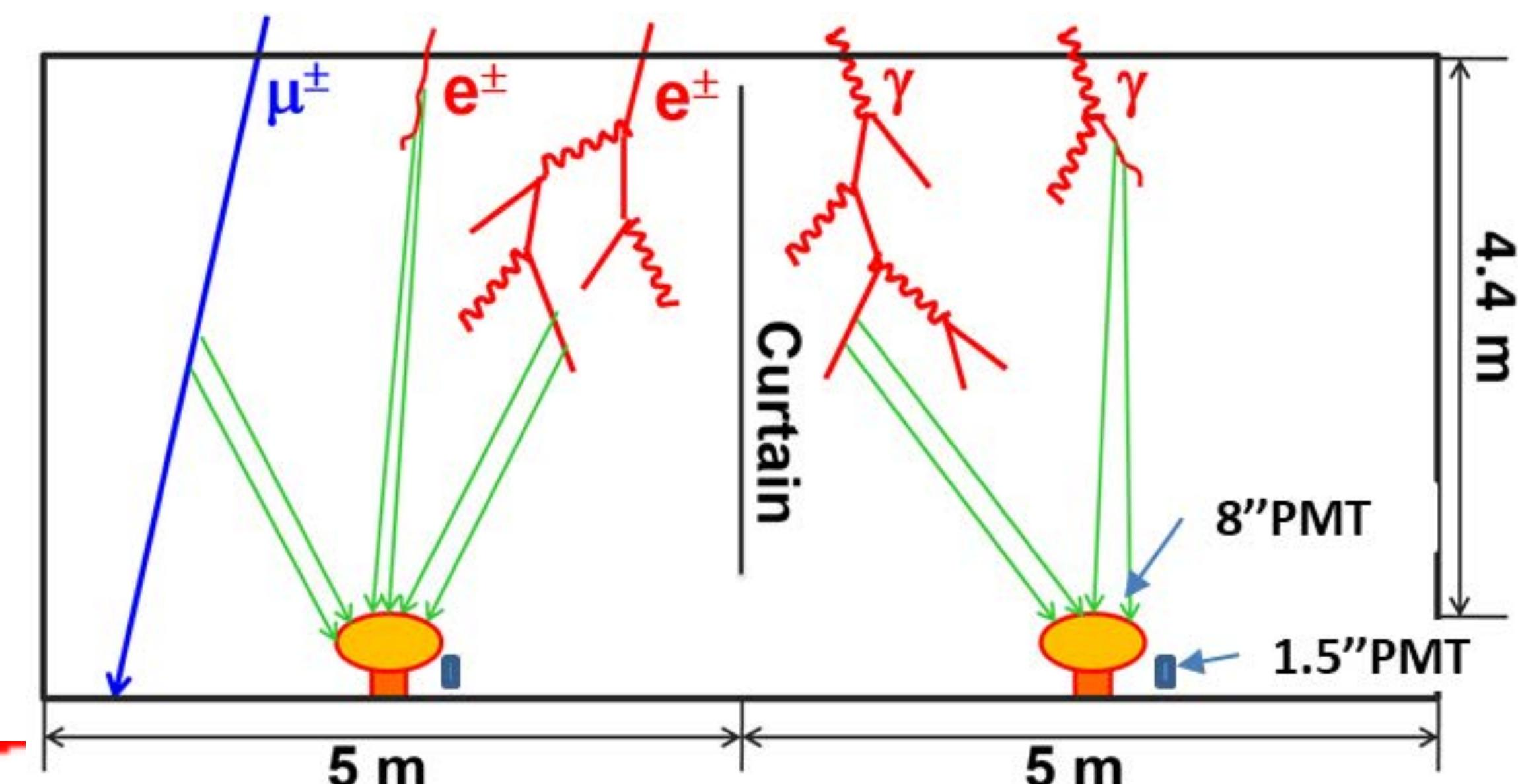
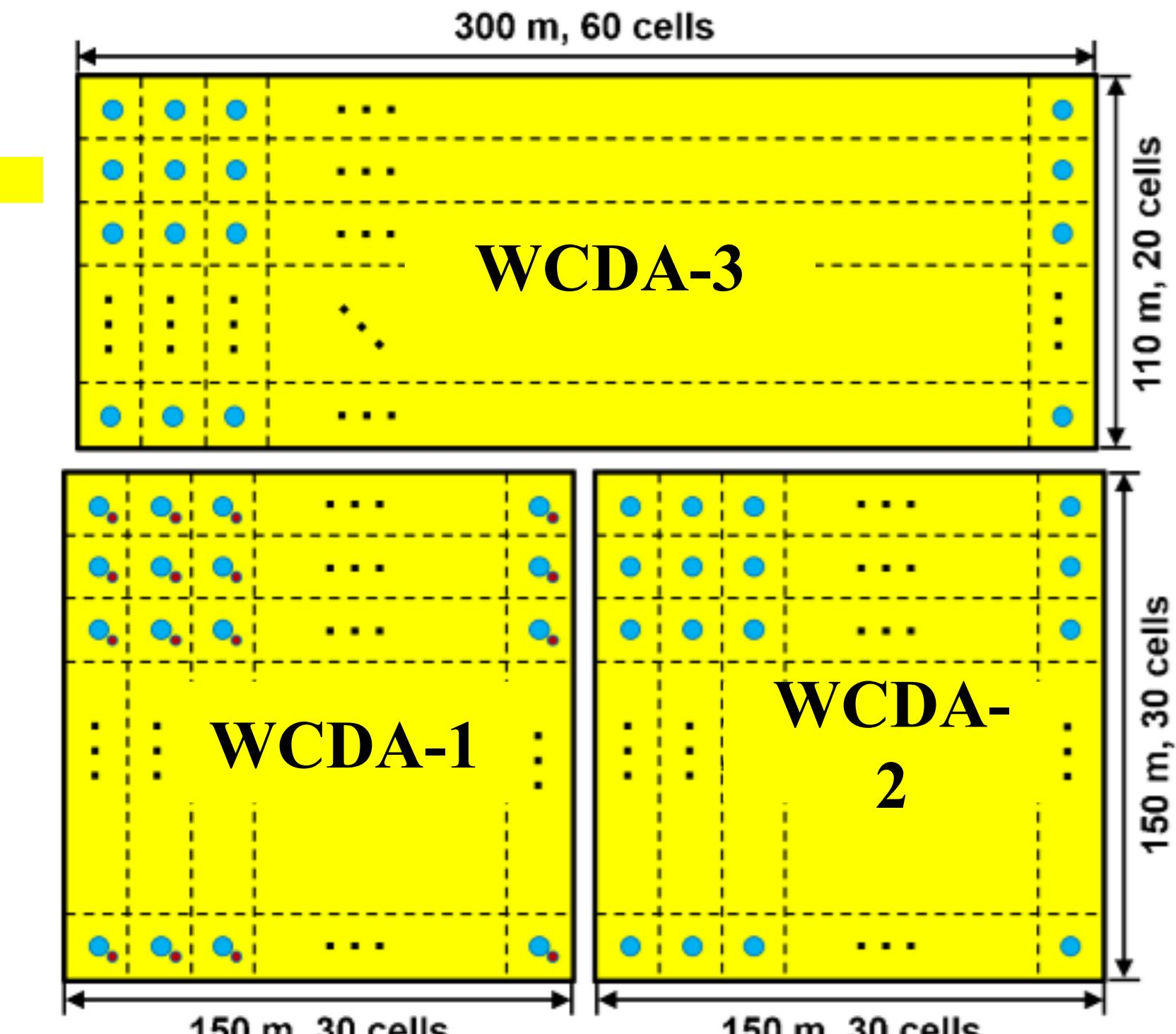
➤ Total area: $78,000\text{m}^2$ (HAWC $22,000\text{m}^2$)

➤ Total units: 3,120

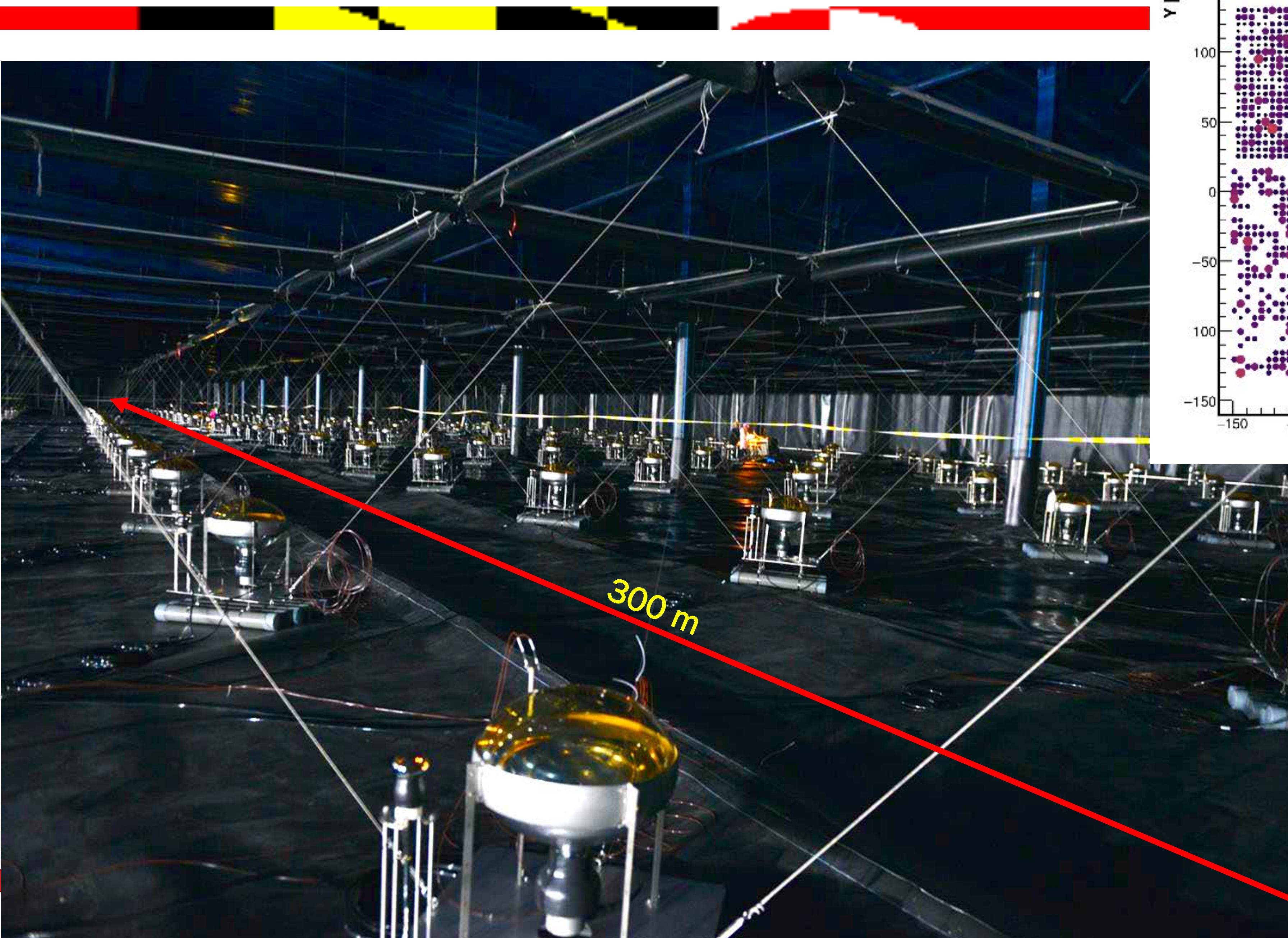
➤ Unit size: $5\text{m}\times 5\text{m}\times 4.4\text{m}$

➤ Two type of PMTs in each pool:

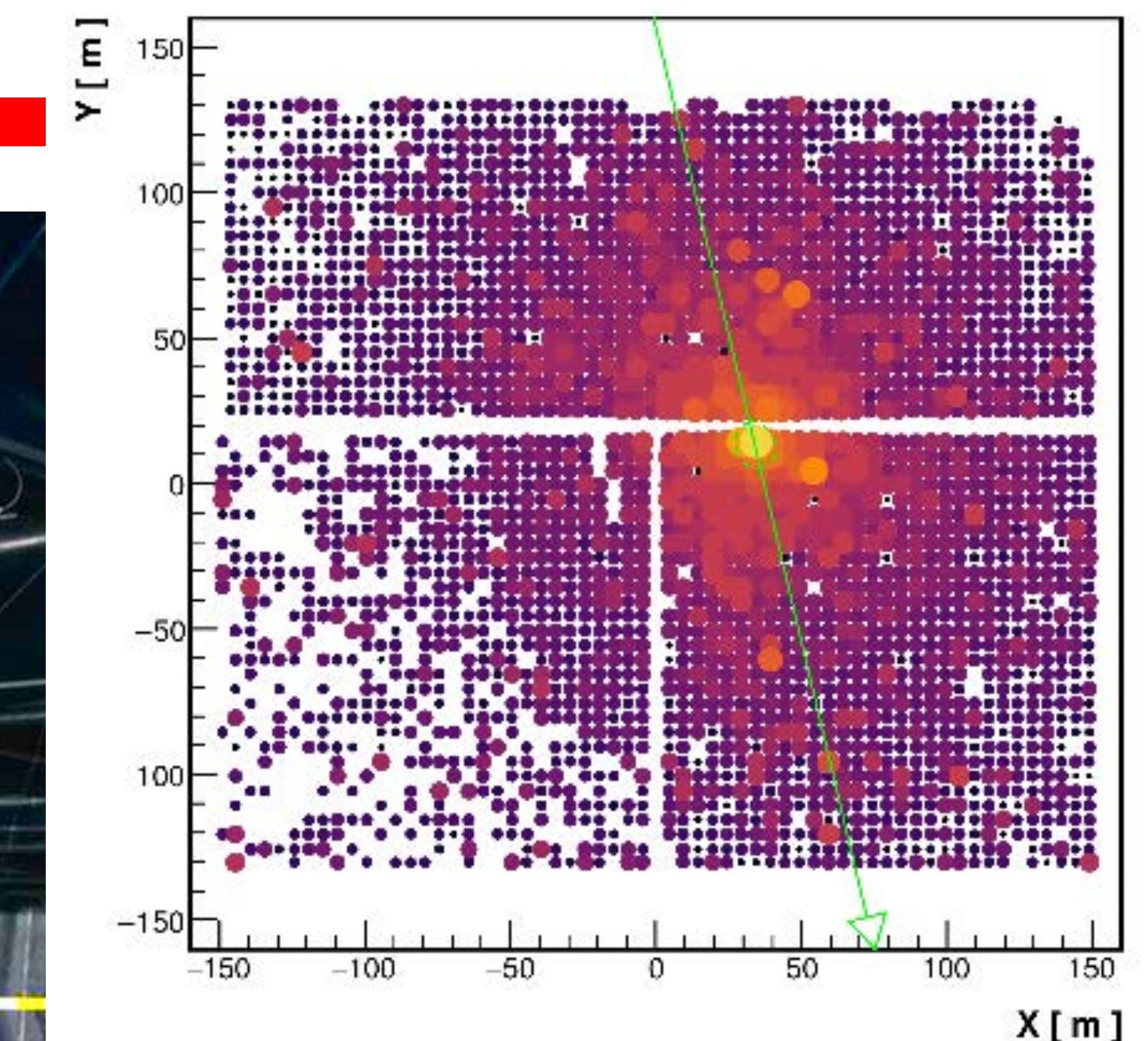
- 8 inches and 1.5 inches for WCDA-1
- 20 inches and 3 inches for WCDA-2 and WCDA-3



Inside of WCDA-3



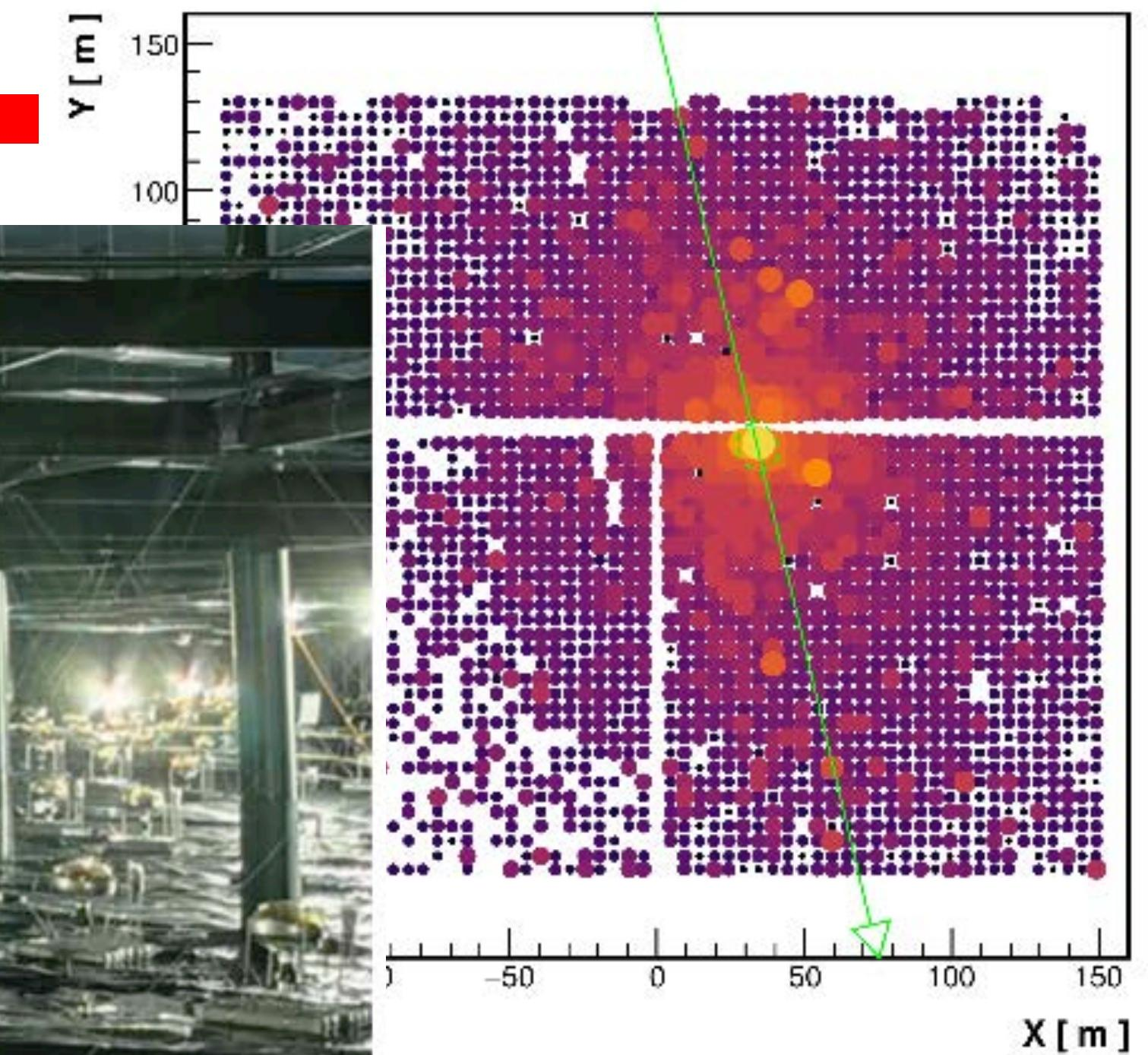
20210511/131236/0.554789897: nTrig=1, 0=37.81±0.02°, φ=103.39±0.02°



- WCDA-1 started operating in April 2019
- WCDA-2 started operating in January 2020
- WCDA-3 started operating in March 2021

Inside of WCDA-3

20210511/131236/0.554789897: nTrig=1, 0=37.81±0.02°, φ=103.39±0.02°



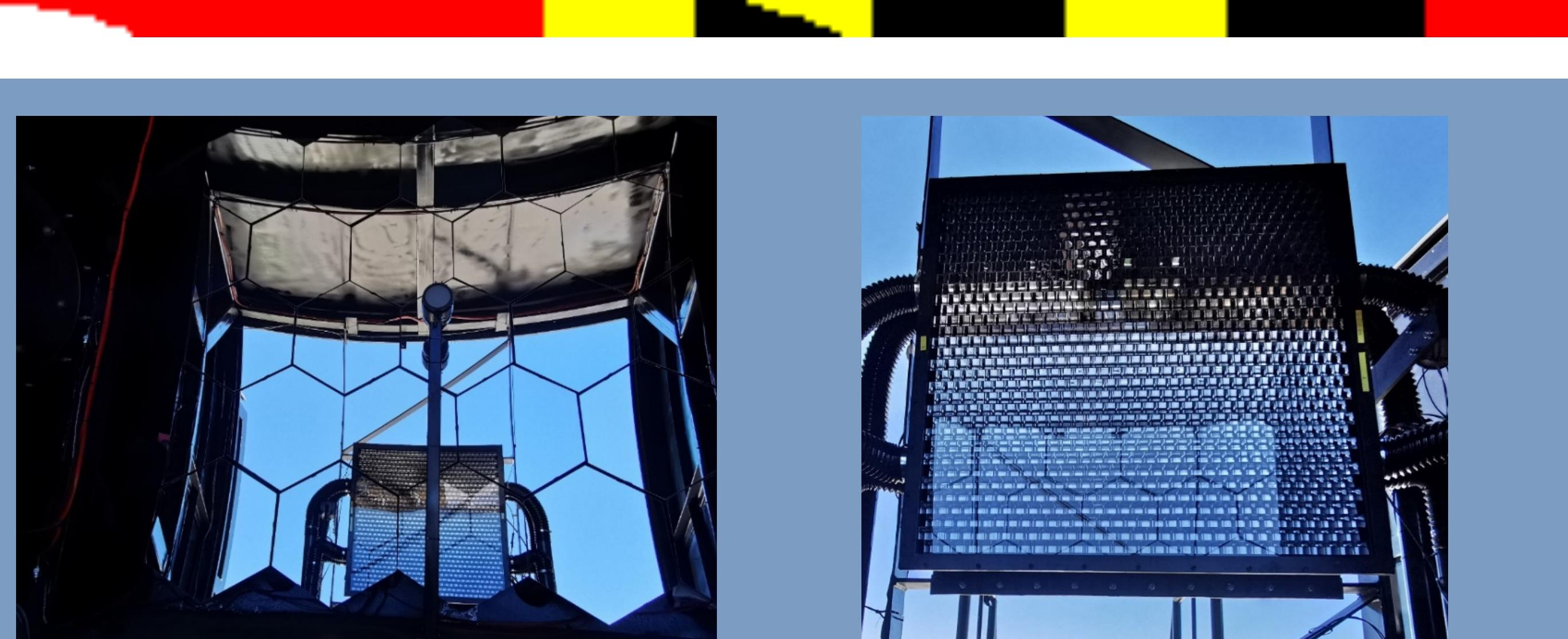
- ❖ WCDA-1 started operating in April 2019
- ❖ WCDA-2 started operating in January 2020
- ❖ WCDA-3 started operating in March 2021



Wide Field of View Cherenkov Telescope (WFCTA)

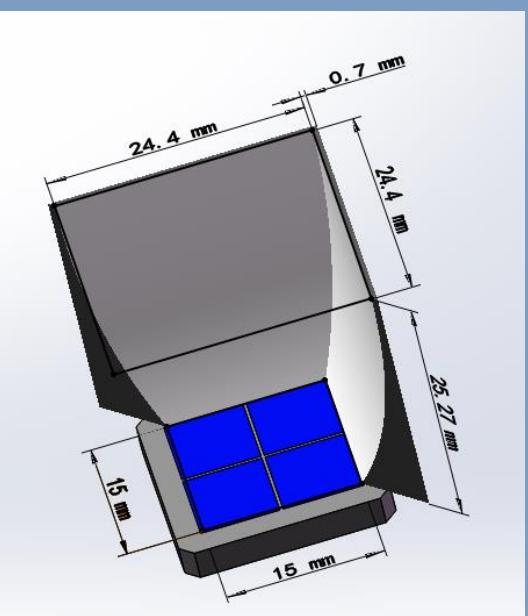
◆ Telescope parameters:

- $\sim 5 \text{ m}^2$ spherical mirror
- Camera: 32×32 SiPMs array
- FOV: $16^\circ \times 16^\circ$
- Pixel size: 0.5°

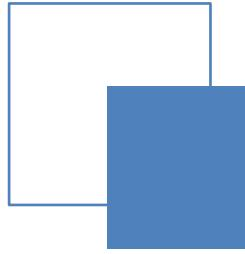


Mirror

SiPM camera

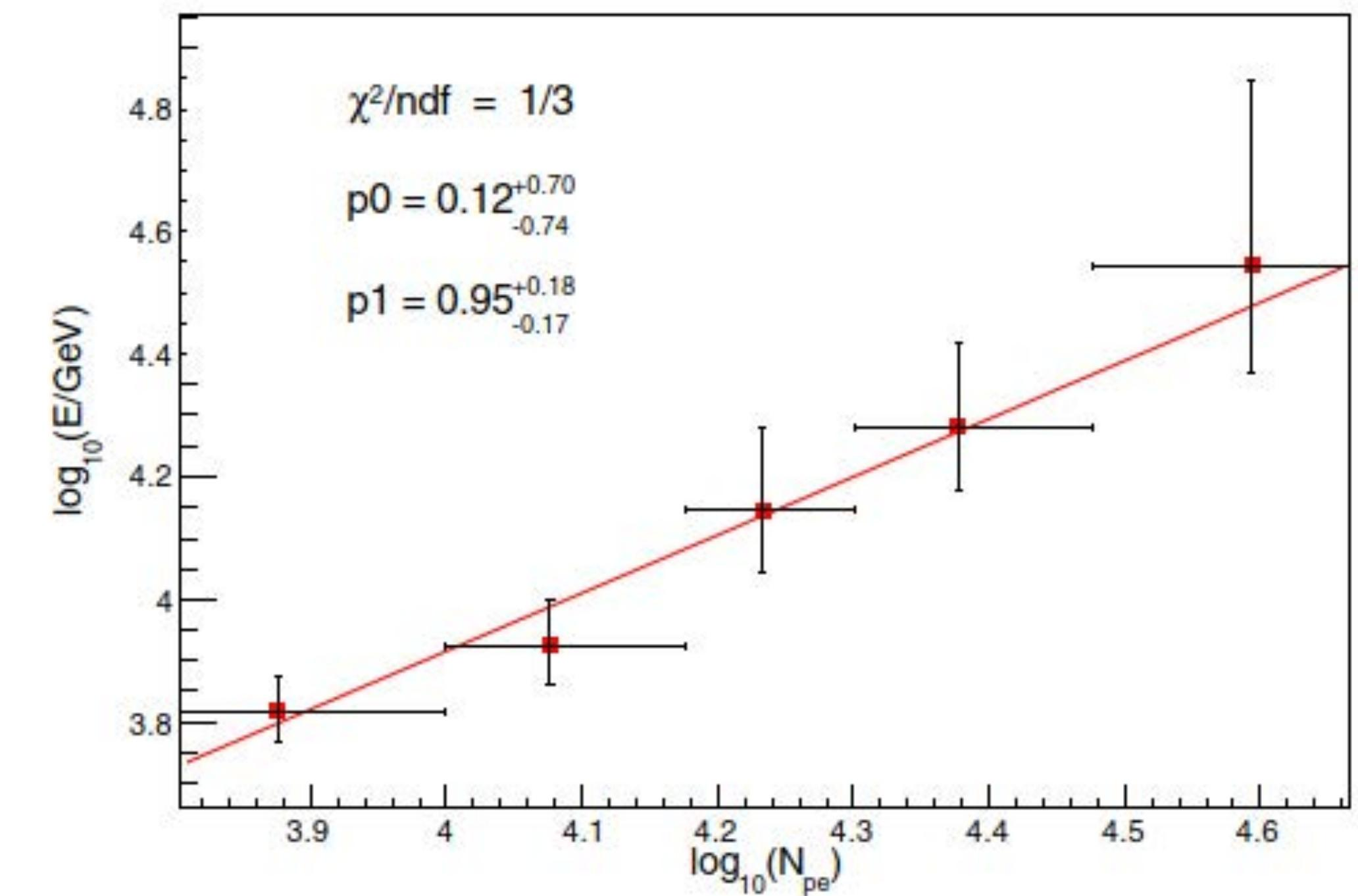


SiPM and Winstone cone



Absolute energy scale with WCDA-1

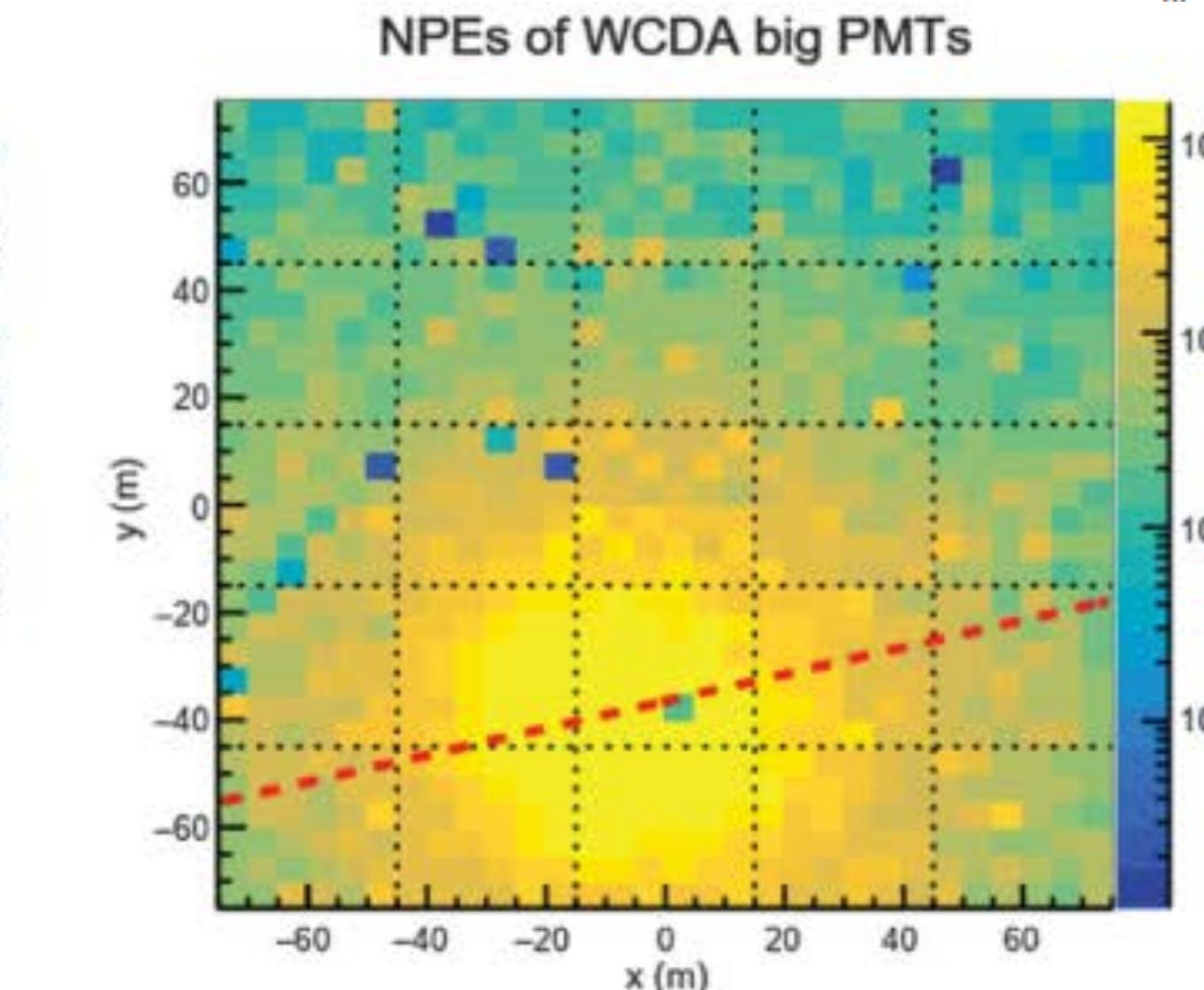
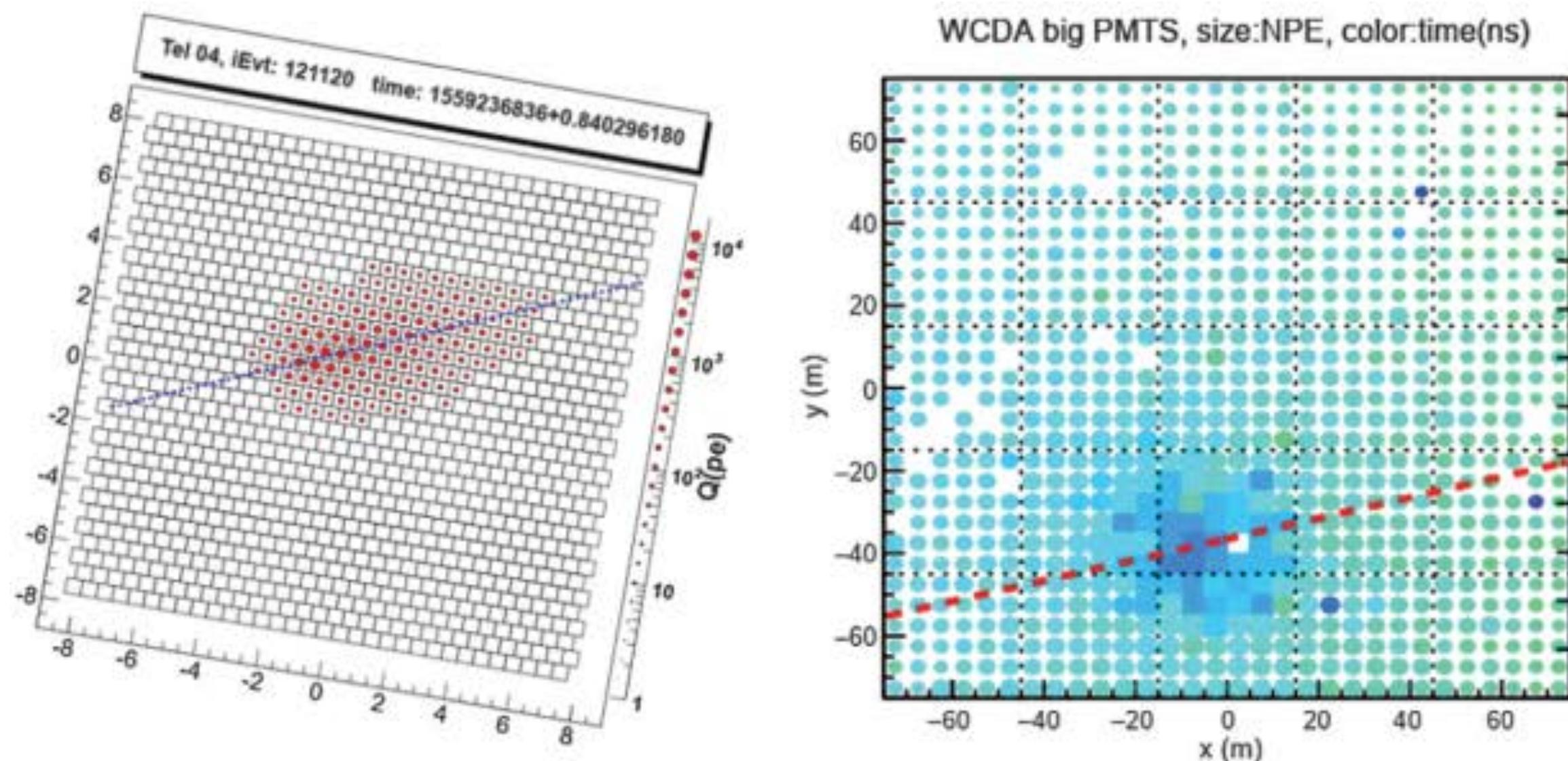
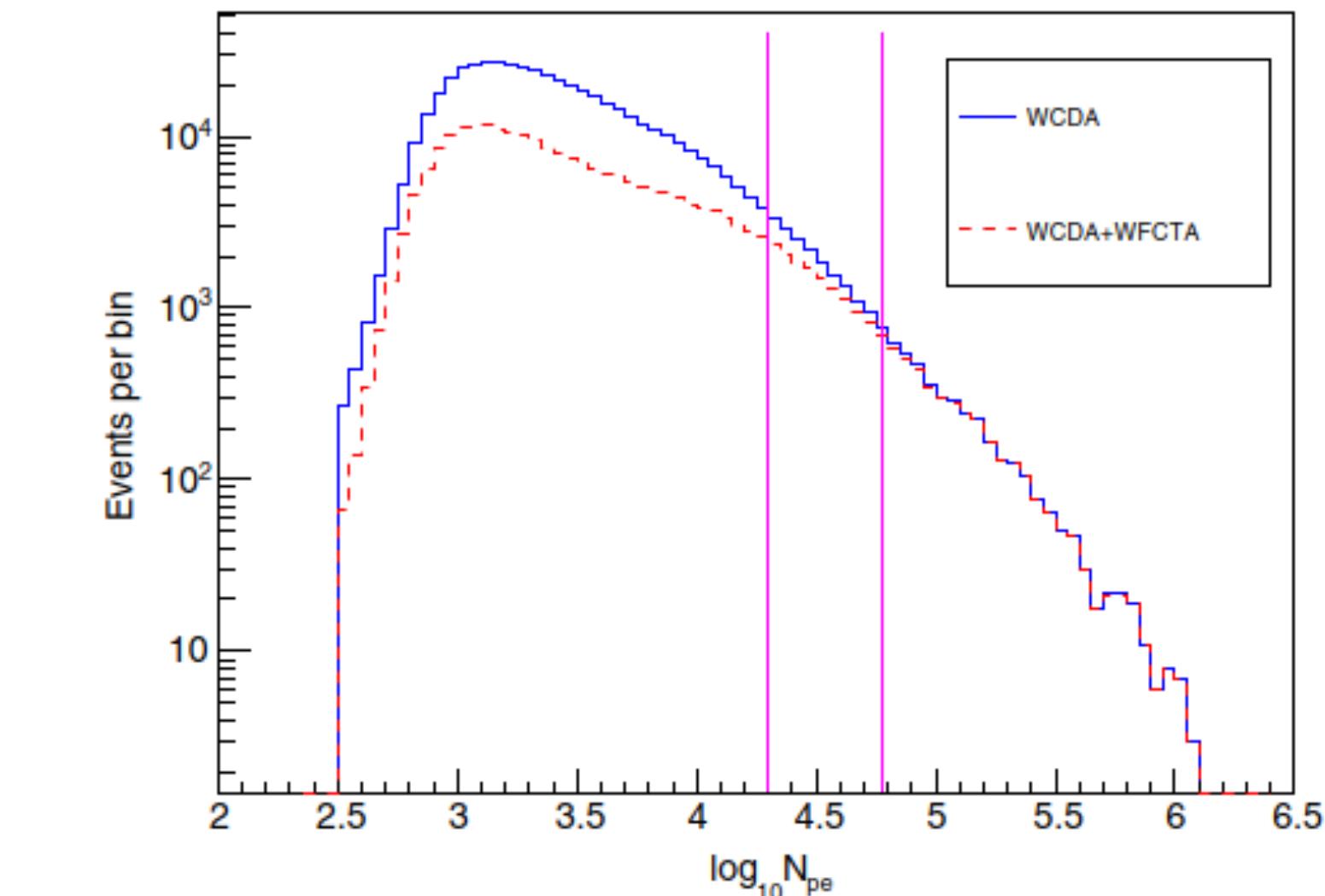
- ◆ In the energy range from 1 TeV to 50 TeV, the cosmic rays are dominated by protons and helium nuclei.
 - ◆ The ratio of protons and helium nuclei can be obtained from CREAM and DAMPE.
 - ◆ The trigger efficiency of WCDA-1 for protons and helium is obtained from simulation.
-
- ◆ System uncertainties:
 - Uncertainty caused by 10% changing of the ratio of protons and helium nuclei is about 3%.
 - Uncertainty from different hadronic models (EPOS-LHC vs. QGSJET-II04) is less than 2%.
 - An uncertainty of 4% is caused by the energy and angular resolution.



$$E(\text{GeV}) = a N_{pe}^b$$
$$a = 1.33^{+5.26}_{-1.06}$$
$$b = 0.95 \pm 0.17$$

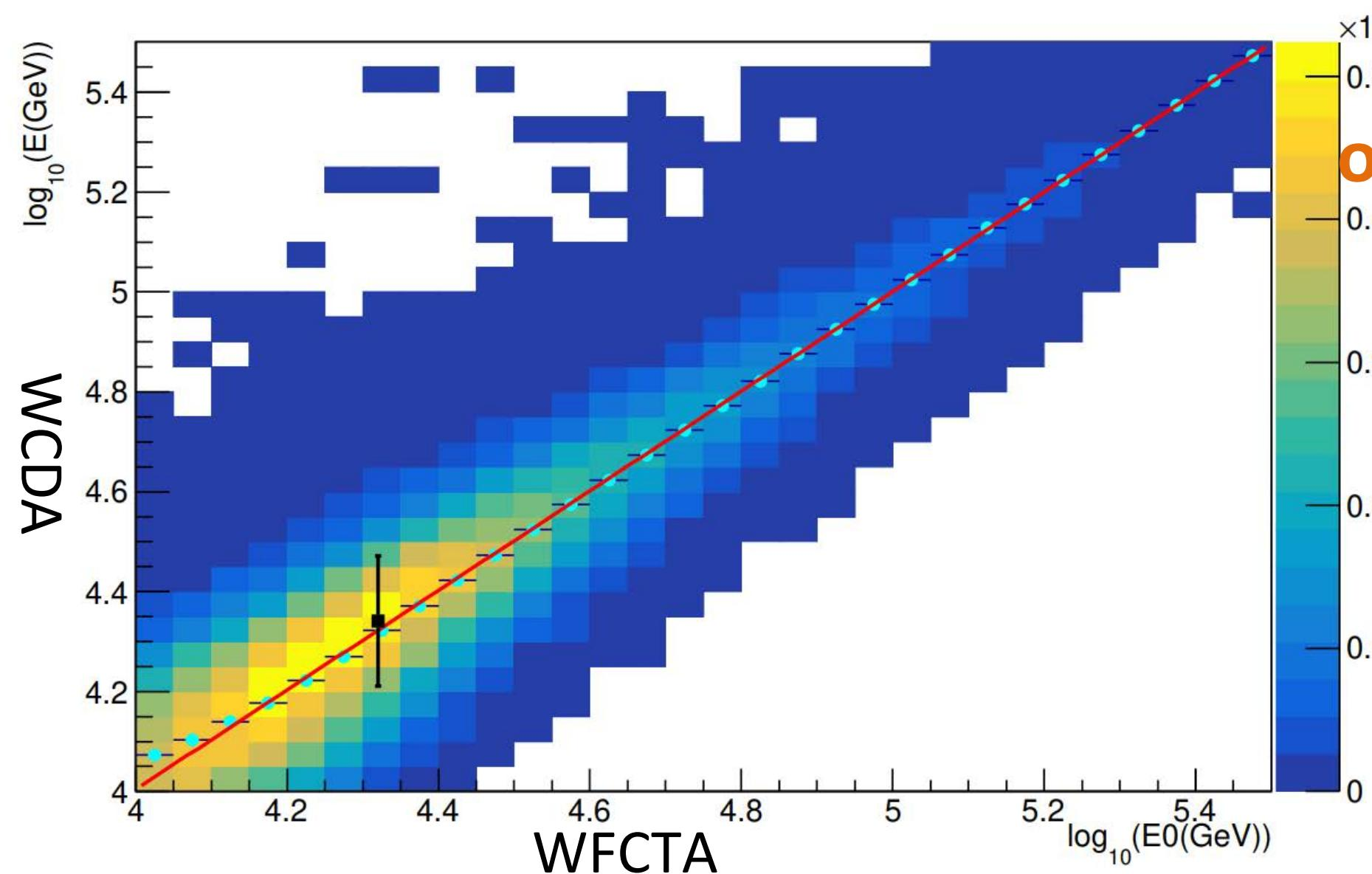
Absolute energy scale propagates from WCDA to WFCTA

- ◆ It is impossible for WFCTA to measure Moon shadow shifts directly.
- ◆ The absolute energy scale obtained by WCDA-1 can be propagated to WFCTA by using common-triggered events.
- ◆ Data Set of WCDA-1+WFCTA:
 - telescope FoV: $22^\circ < \text{Zenith angles} < 38^\circ$
 - $N_{\text{hit}} > 200$
 - $20k < N_{\text{pe}} < 60k$
 - shower cores inside WCDA-1:
 $|\text{core}_x| < 55 \text{ m}, |\text{core}_y| < 55 \text{ m}$



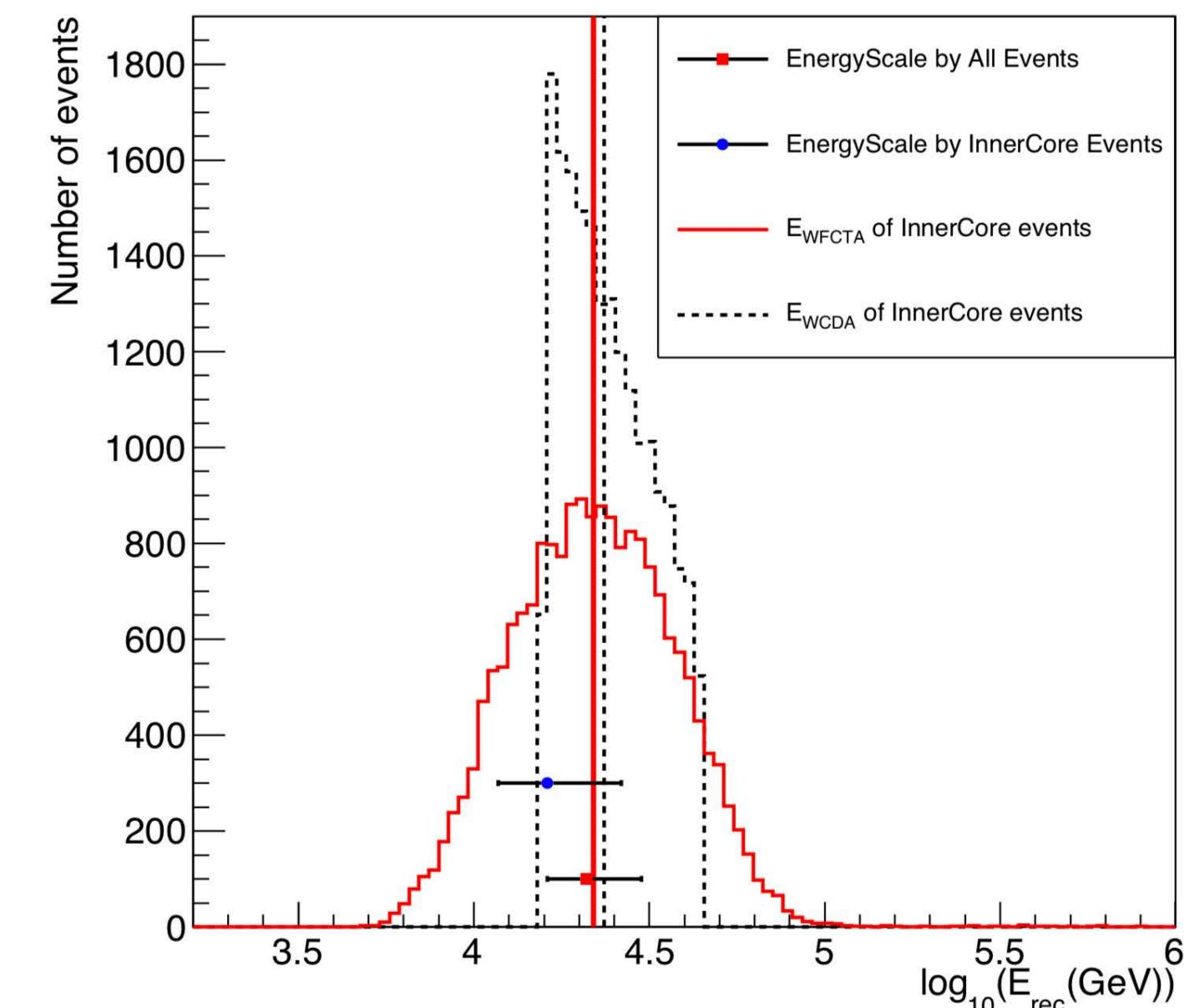
Absolute energy scale of WFCTA

- And then the absolute energy scale obtained by WCDA is propagated to WFCTA by using the common trigger events.
 - The energy reconstructed by WFCTA is 21.9 ± 0.1 TeV;
 - $23.4 \pm 0.1 \pm 1.3$ TeV by the formula of the absolute energy scale.
 - The two energies are consistent with each other within uncertainties.
- It is the first time that Cherenkov telescopes have the absolute energy scale.



WCDA Calibration result (8 months, one pool) :

- ✓ 21.0 ± 6.5 TeV for all events
- ✓ 16.2 ± 6.2 TeV for shower core falling inside WCDA.
- ✓ The uncertainty largely dominated by the low statistics. After 4 years, the uncertainty will be $< 10\%$.



Wide FoV C-Telescope Array (WFCTA)

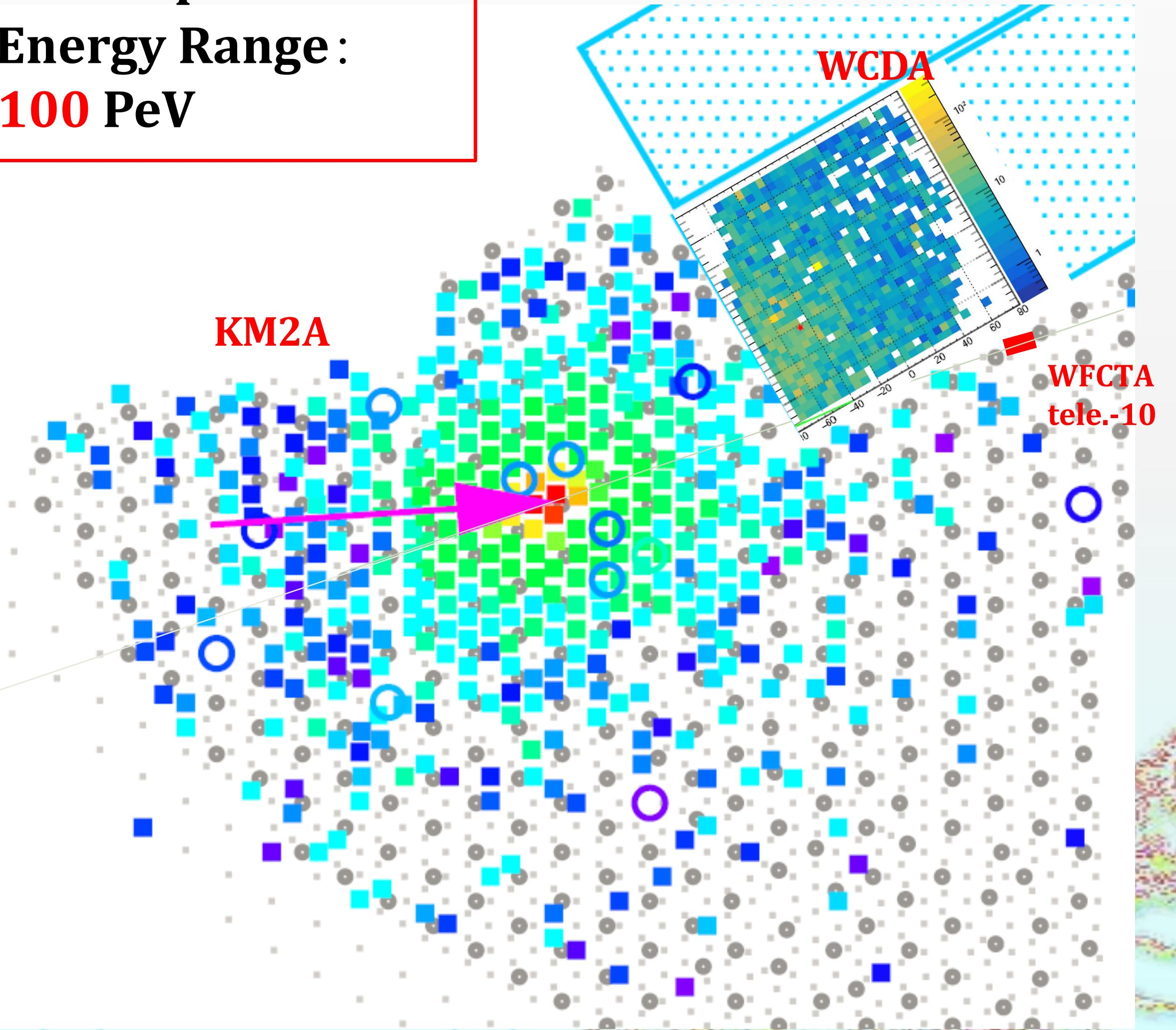
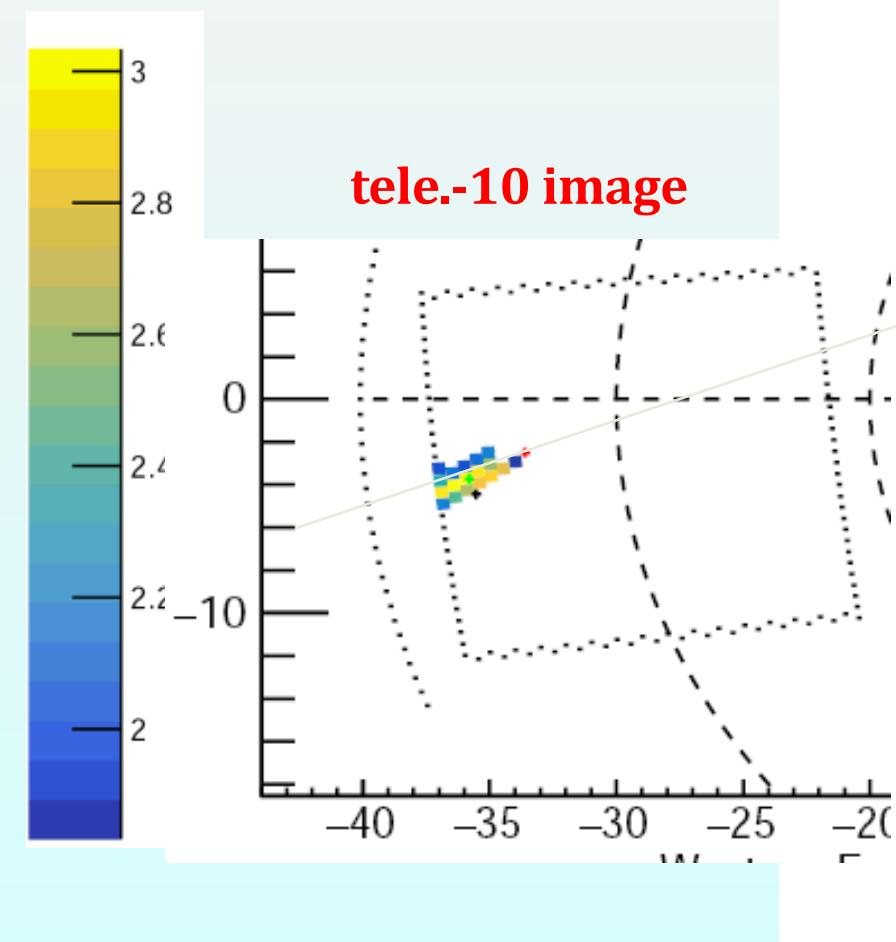
Cross-checking inside Collaboration



- ◆ Telescopes: 18
- ◆ Energy Range:
0.1-100 PeV

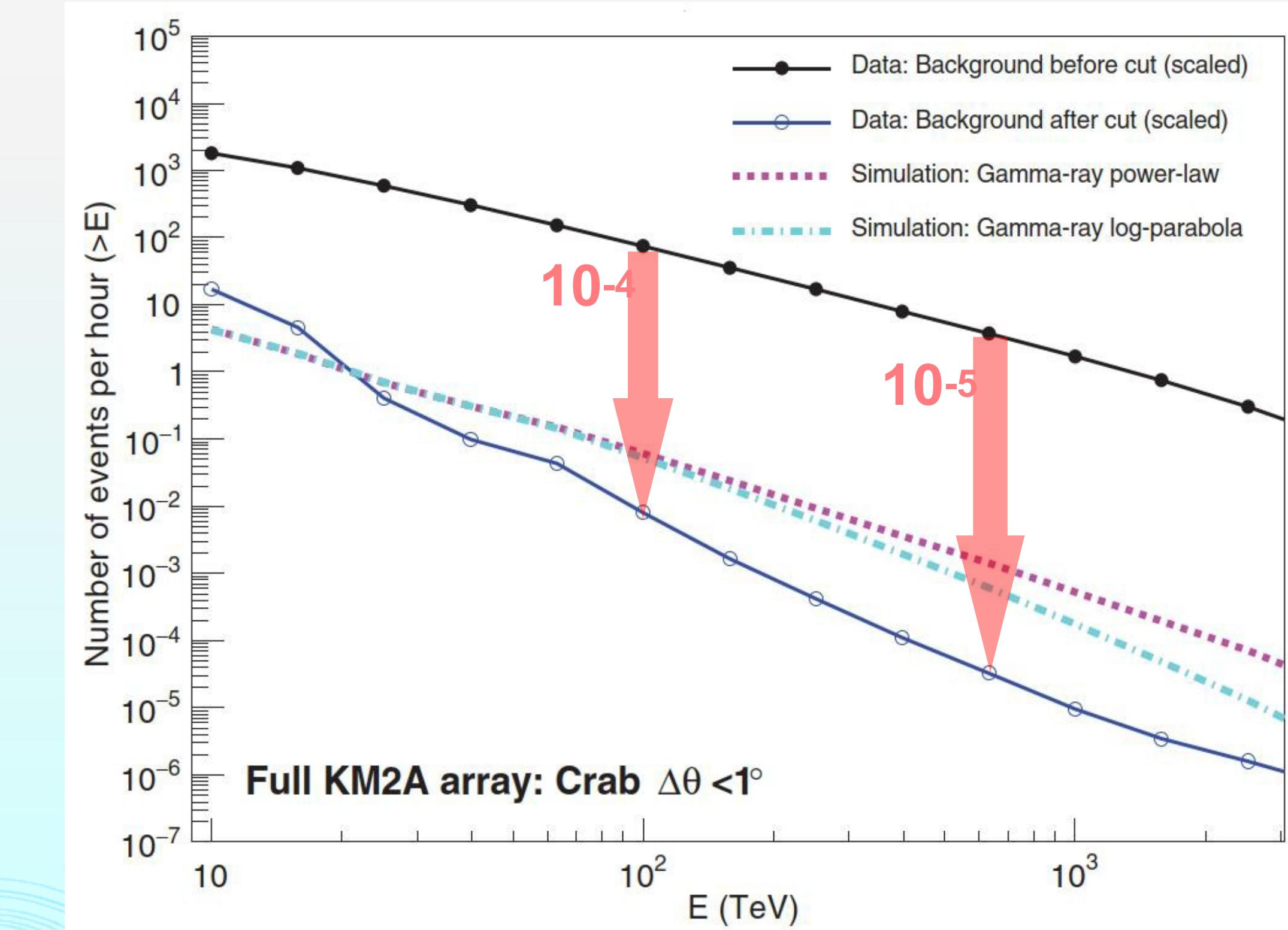
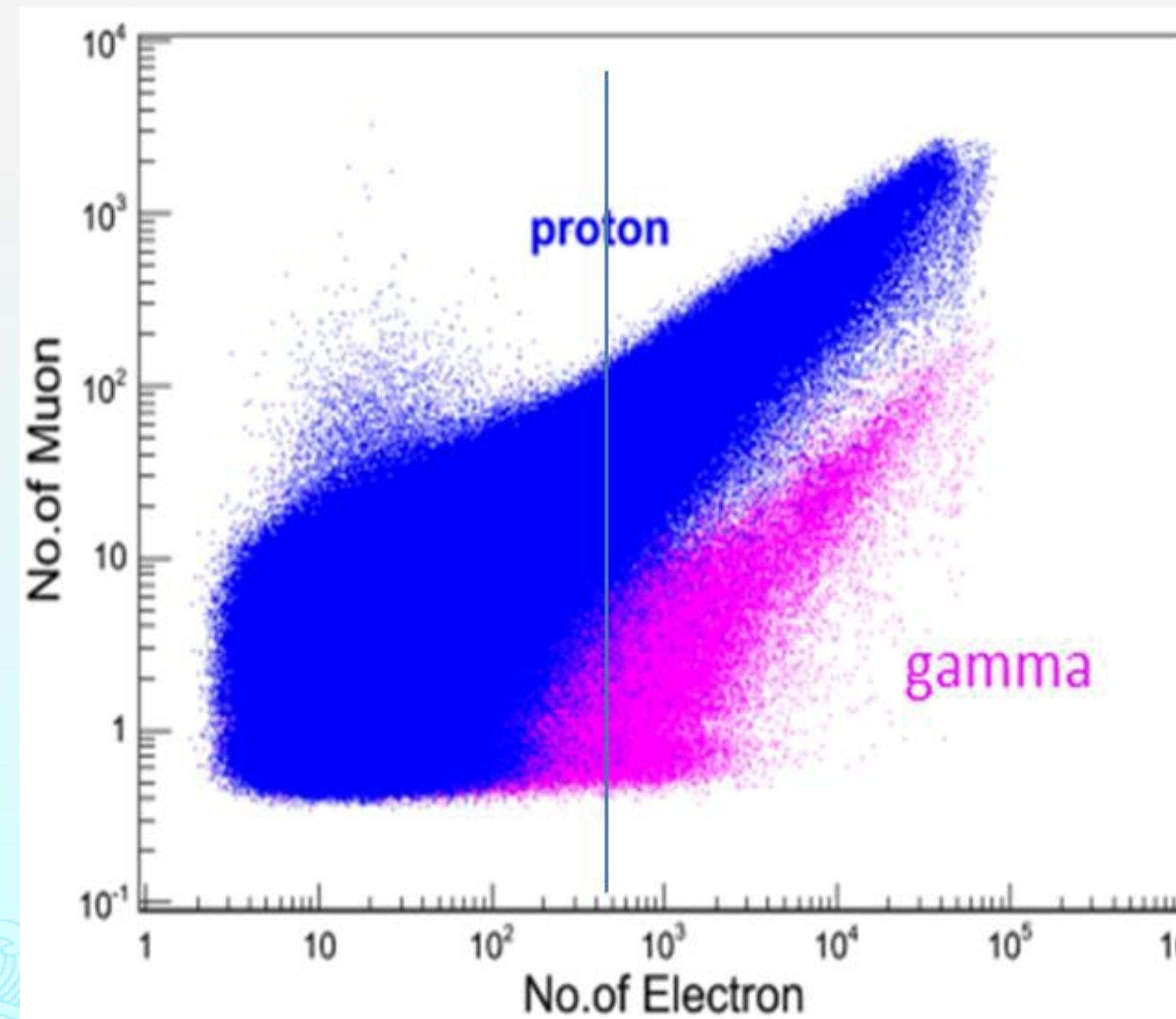
WFCTA measured the event simultaneously
 $L/W \sim 2.6$, $N_{pe} \sim 9100$ in 11 pixels

- ◆ Energy : **0.9 ± 0.2 PeV**
- ◆ KM2A measured the event
 $N_{particle} \sim 4574$ in 395 EDs
- ◆ Energy : **0.9 ± 0.1 PeV**
- ◆ Chance probability: <0.1%
- ◆ $N_{\mu} \sim 15$ in 11 MDs



Background rejection

- Counting number of measured muons in a shower
- Cutting on ratio $N_\mu/N_e < \mathbf{1/230}$
- BG-free ($N_\gamma > 10N_{\text{CR}}$) Photon Counting
for showers $E > 100 \text{ TeV}$ from the Crab

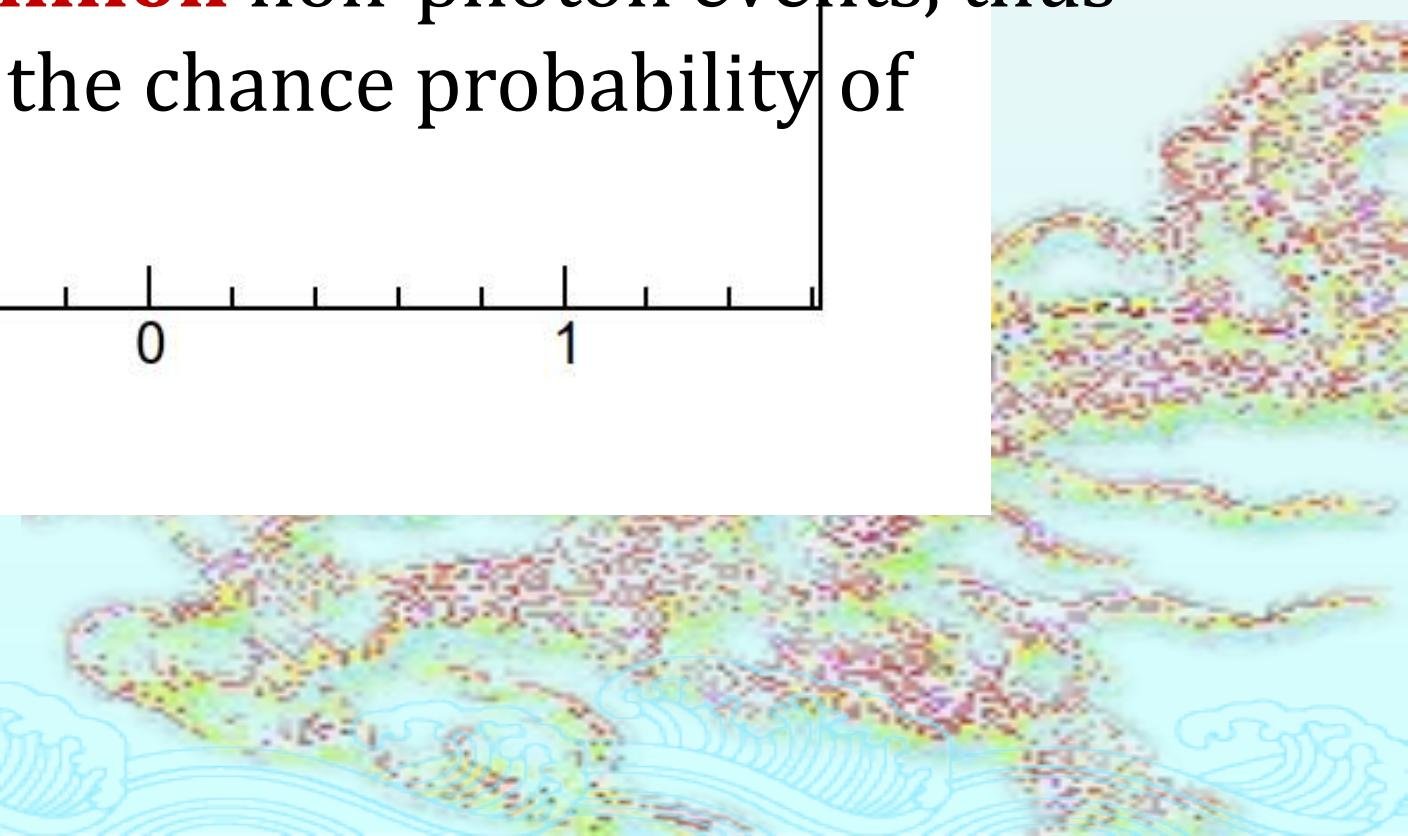
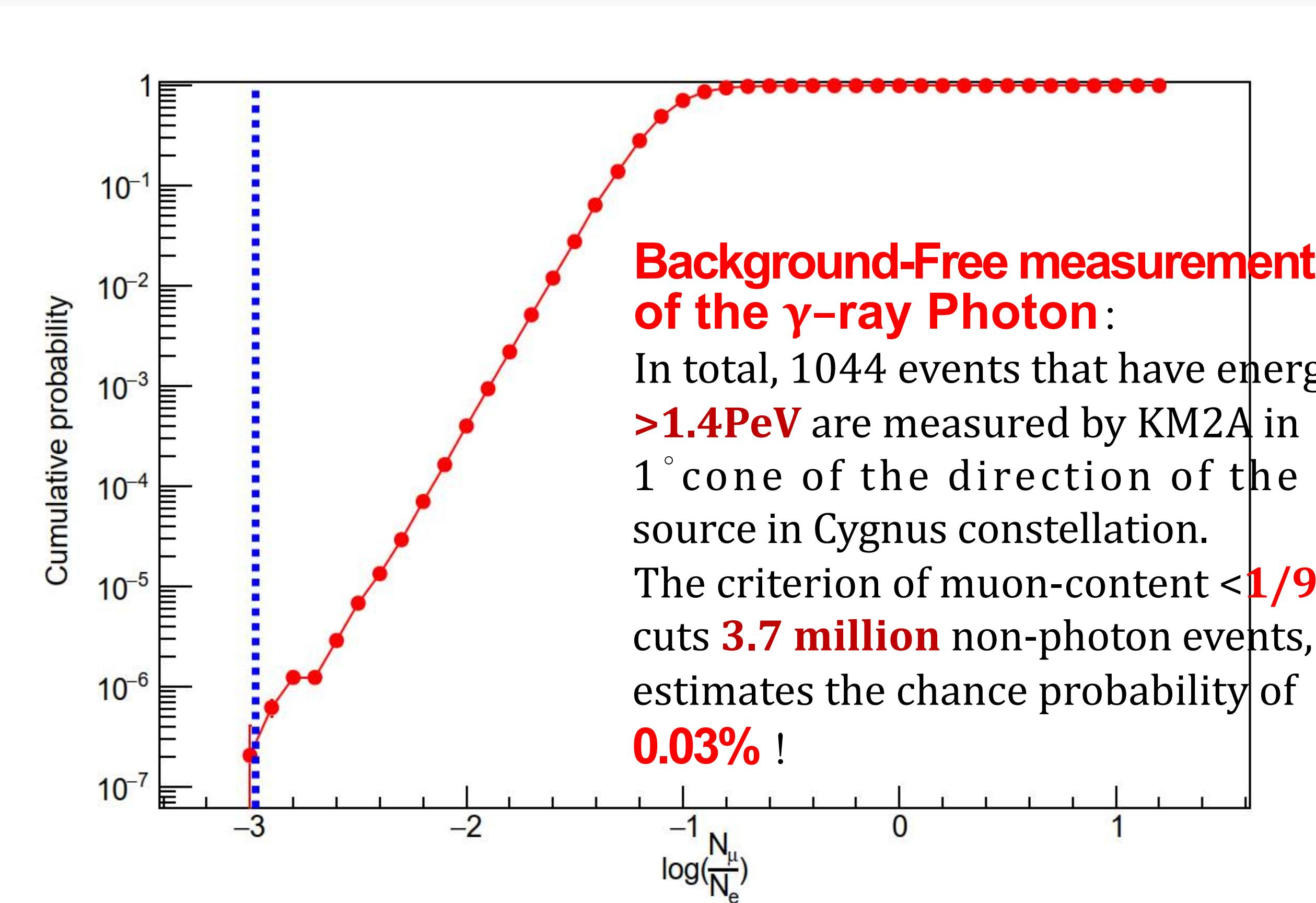
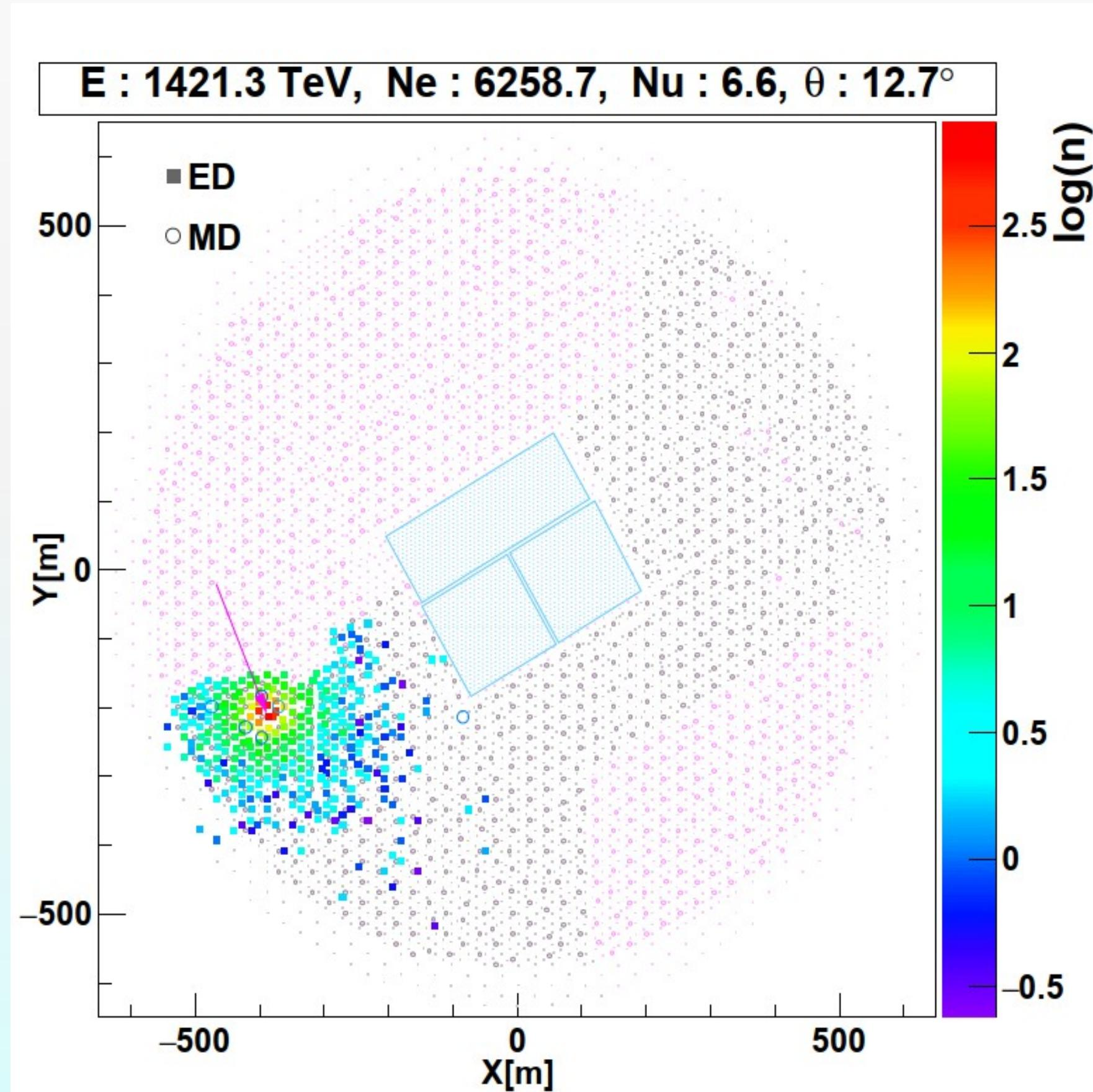


1.4 PeV Photon

from Cygnus Direction Record by KM2A

LHAASO, Nature, 594,

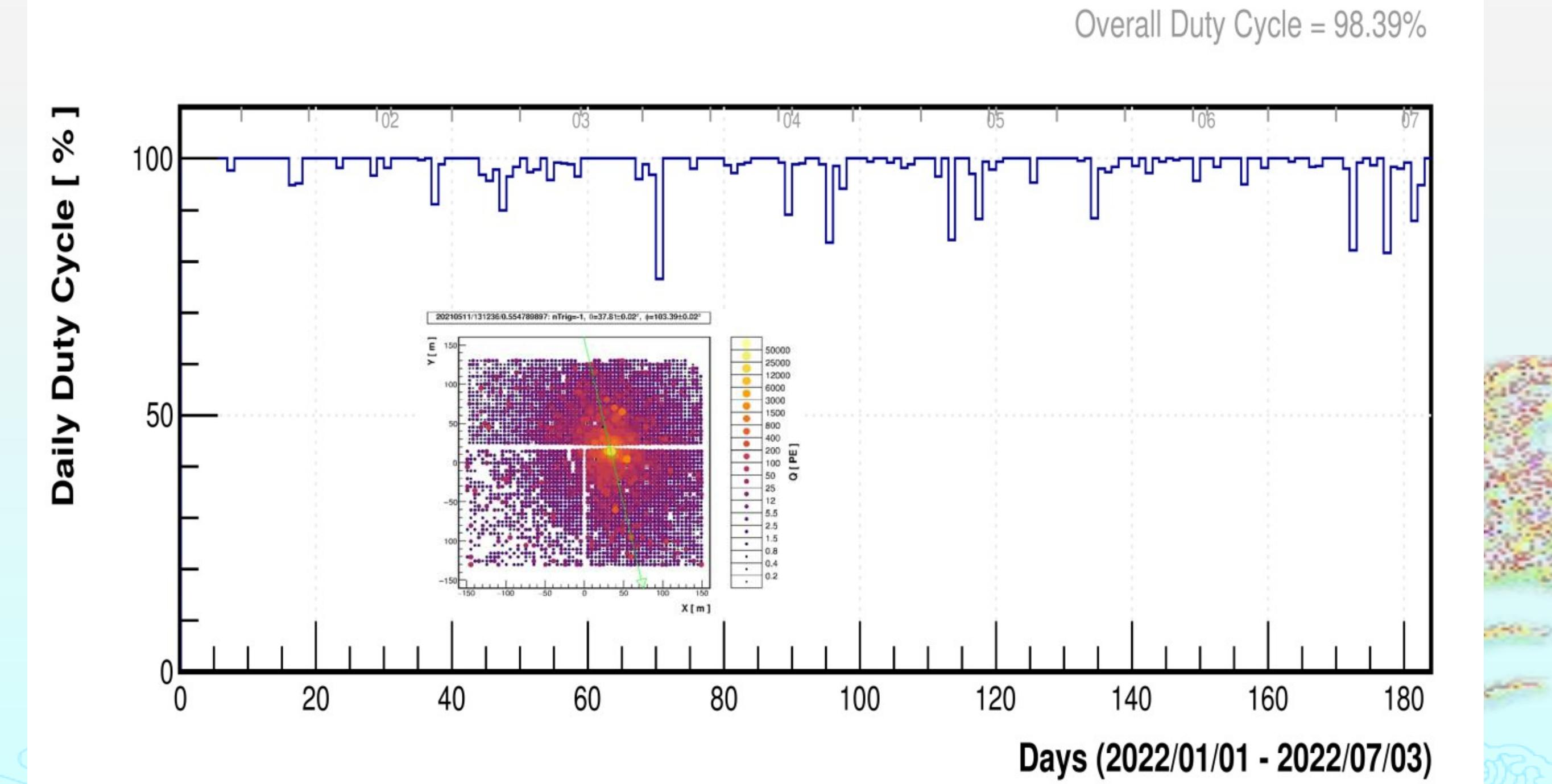
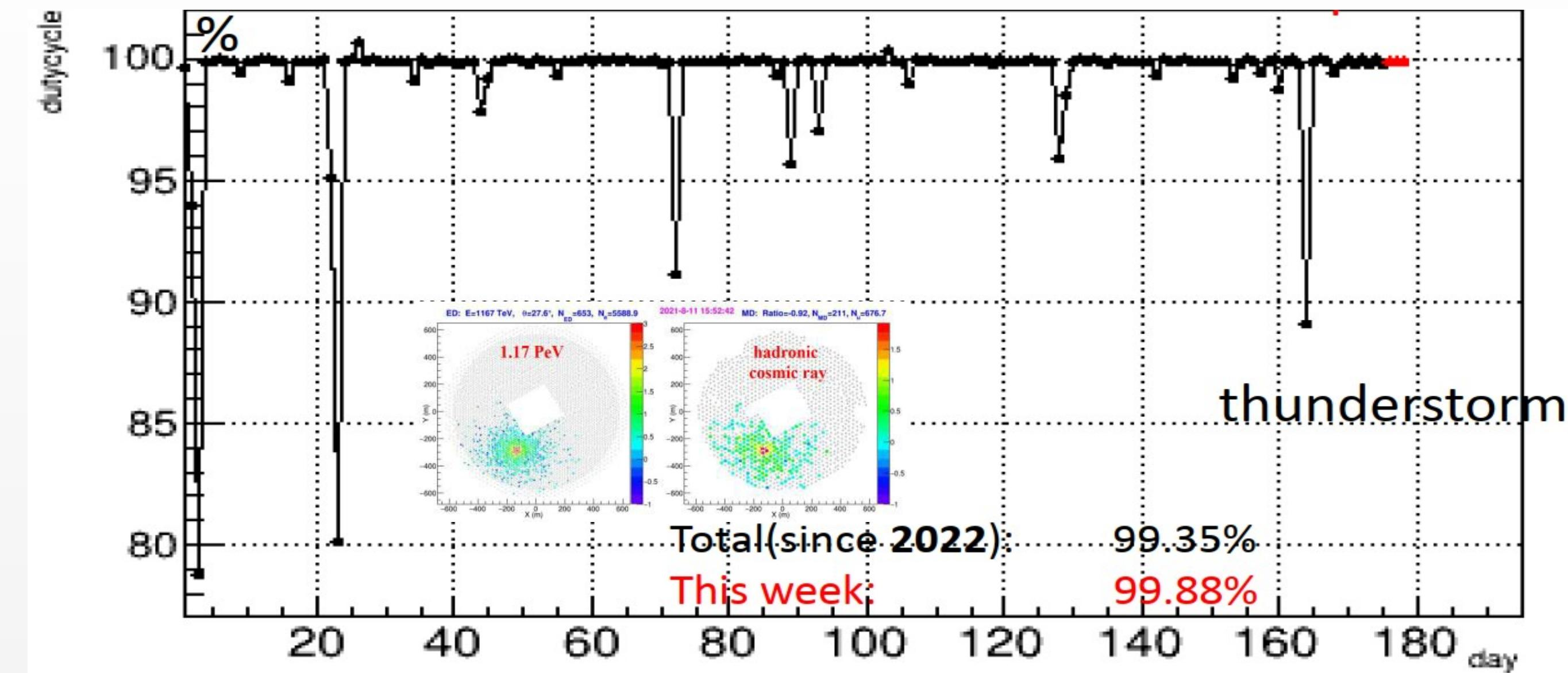
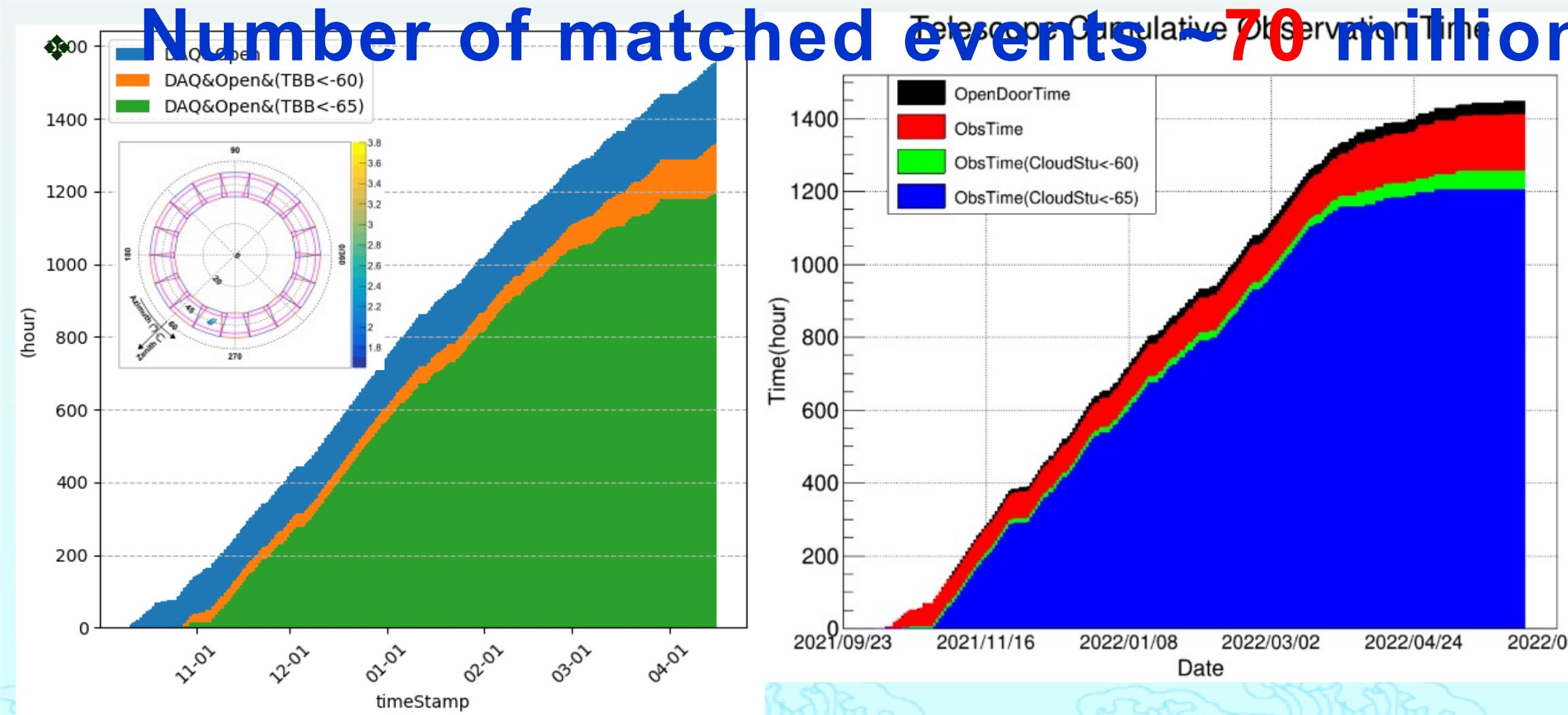
p.33-36, 2021





Operation

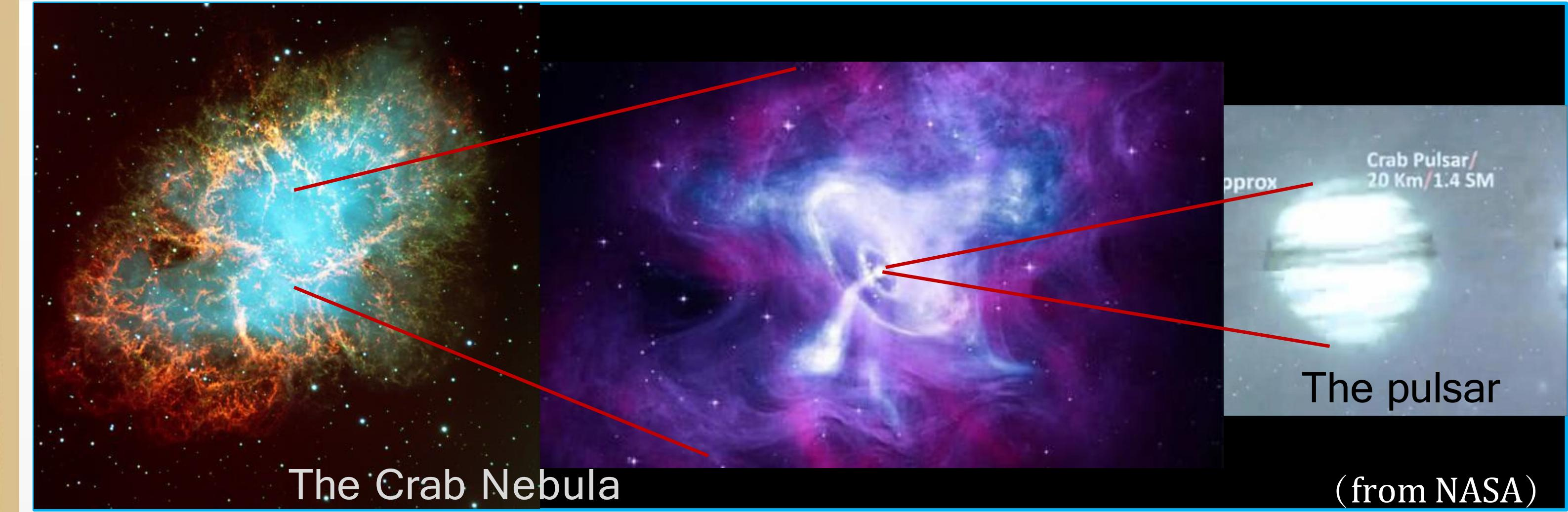
- ❖ The duty cycle of KM2A is >99.4%
- ❖ Event rate 2×10^8 /day
- ❖ The duty cycle of WCDA is 98.4%
- ❖ Event rate 3×10^9 /day
- ❖ Data acquisition time of WFCTA >1400 hrs



Standard candle for γ-ray Observation

高
海

Standard candle for γ-ray Observation

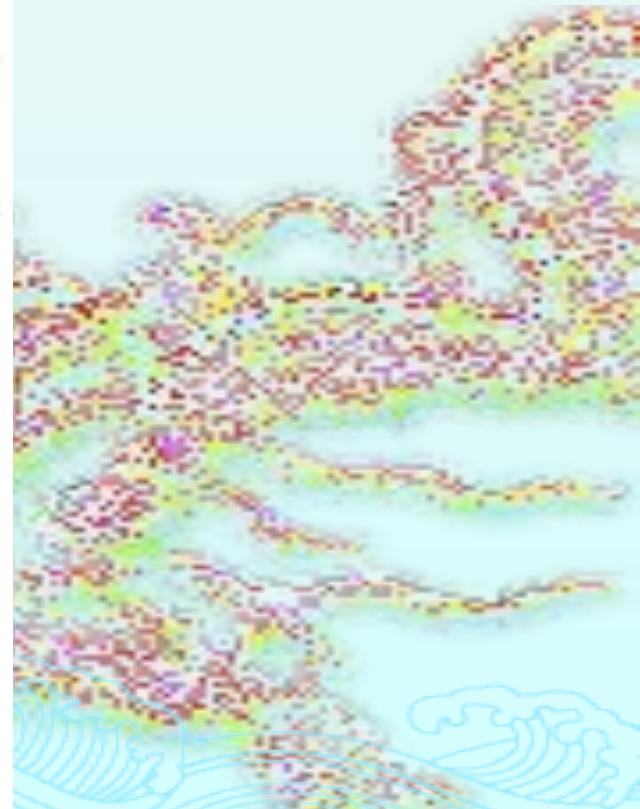
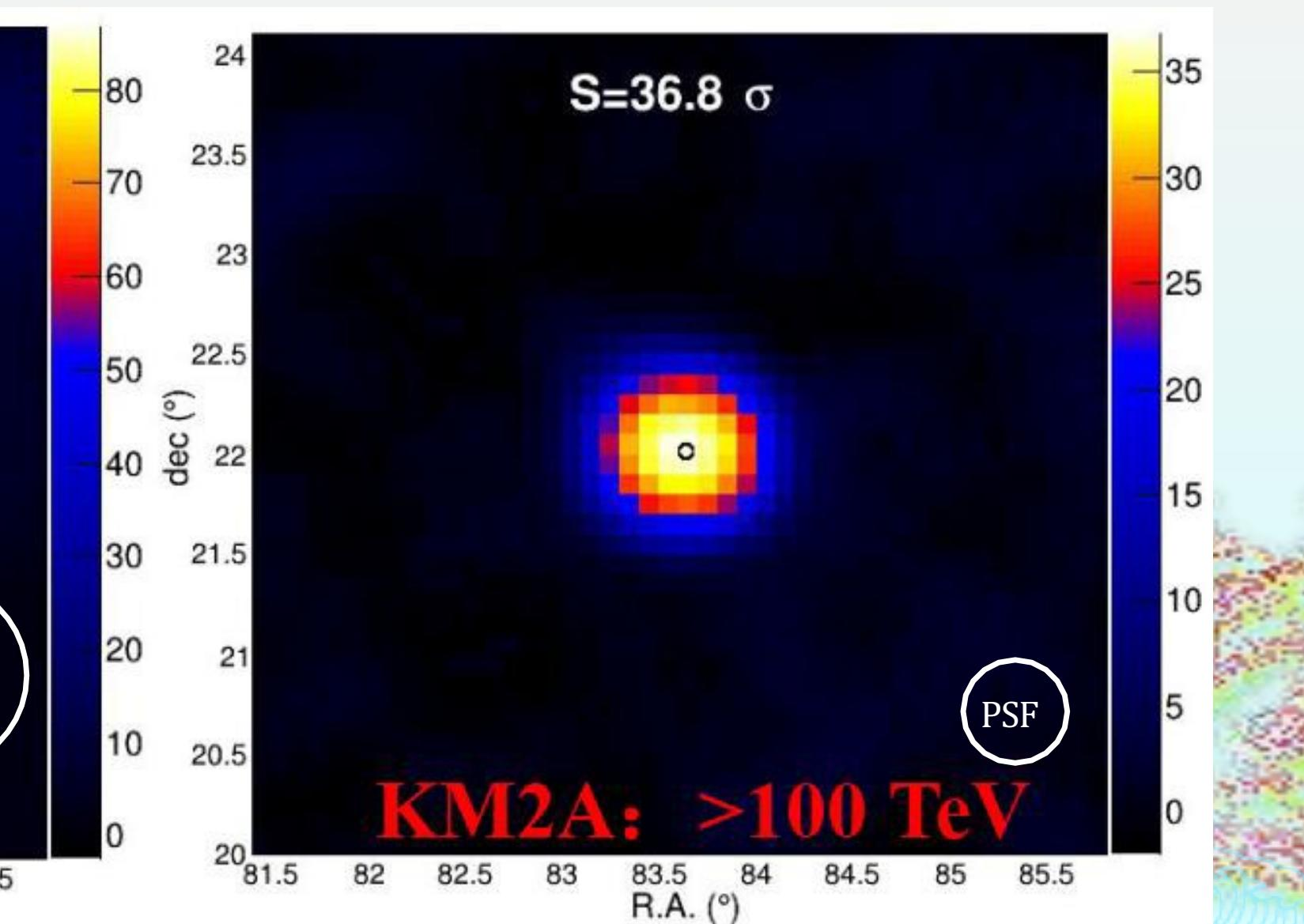
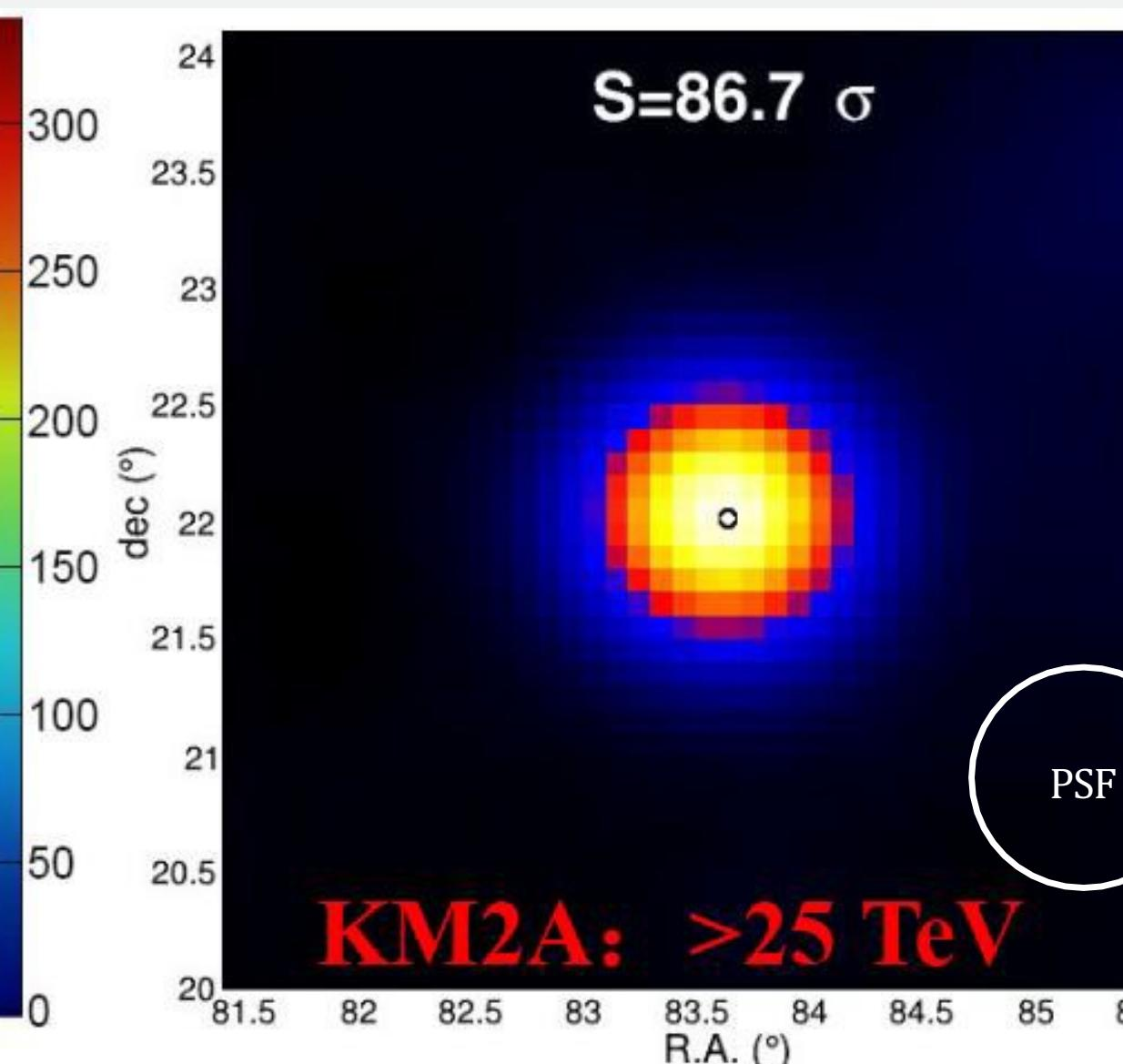
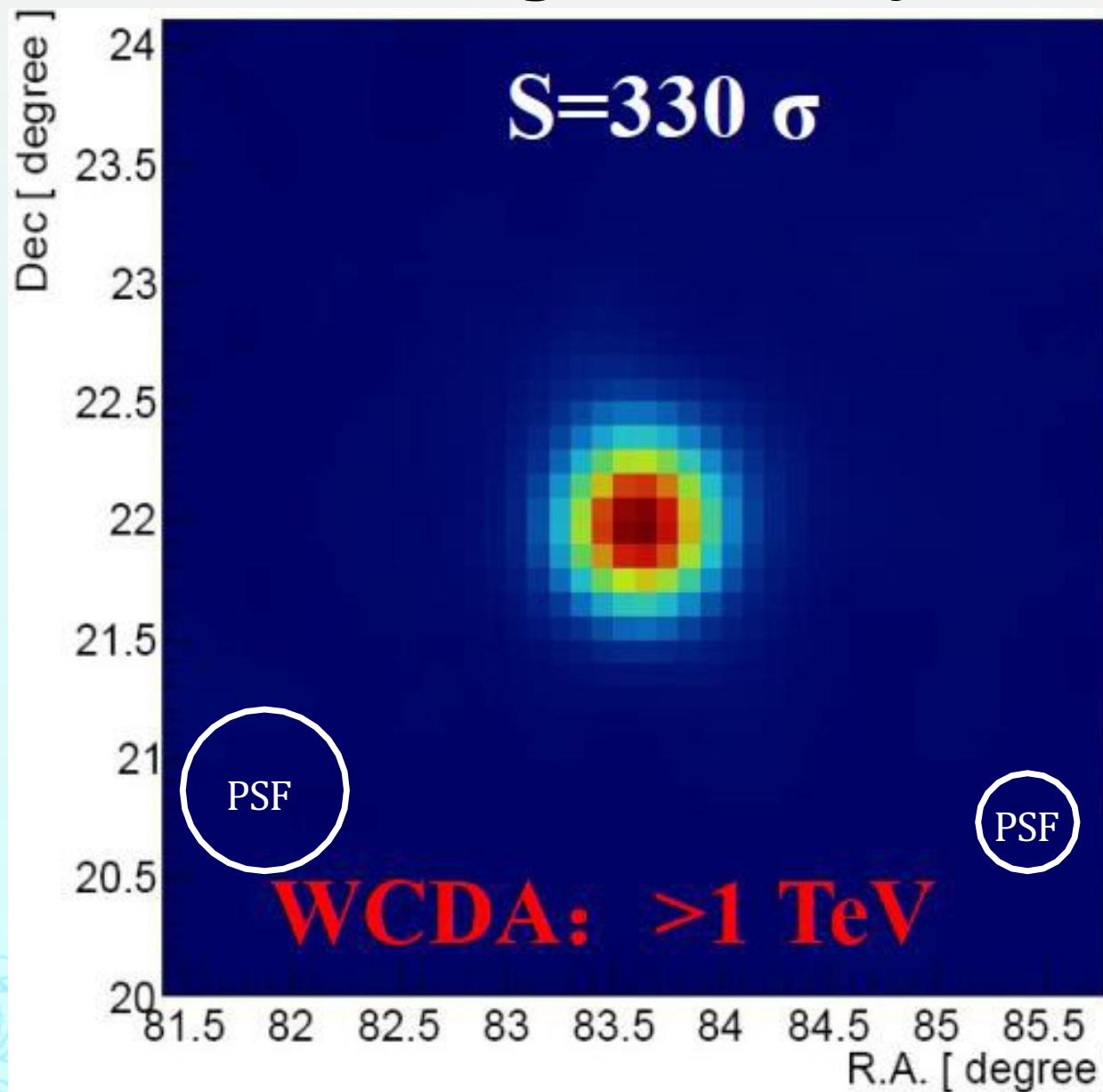


The coverage of 3.5 orders of magnitudes of ener

1 - 12 TeV

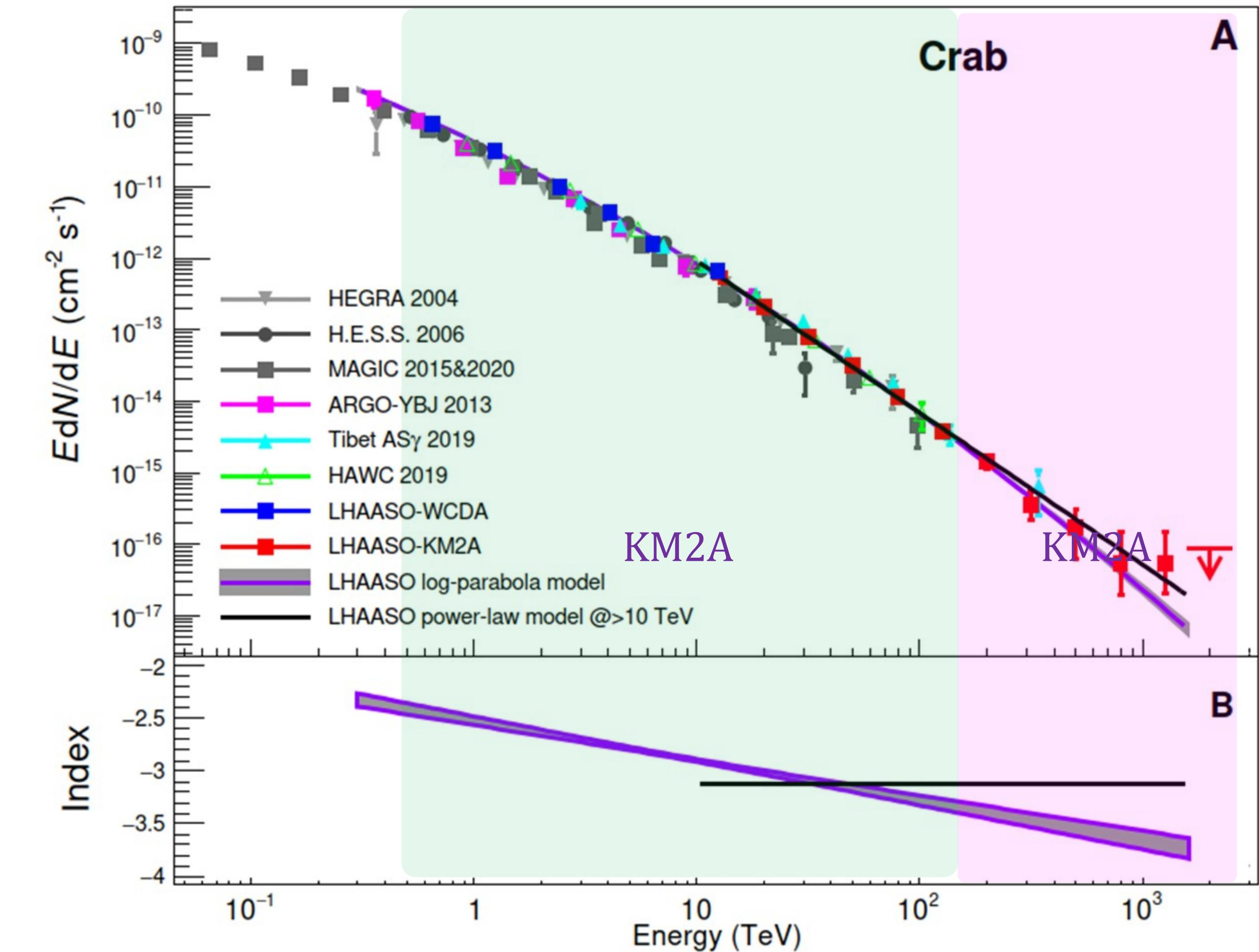
PSF: 0.22°

Pointing accuracy: 0.01°

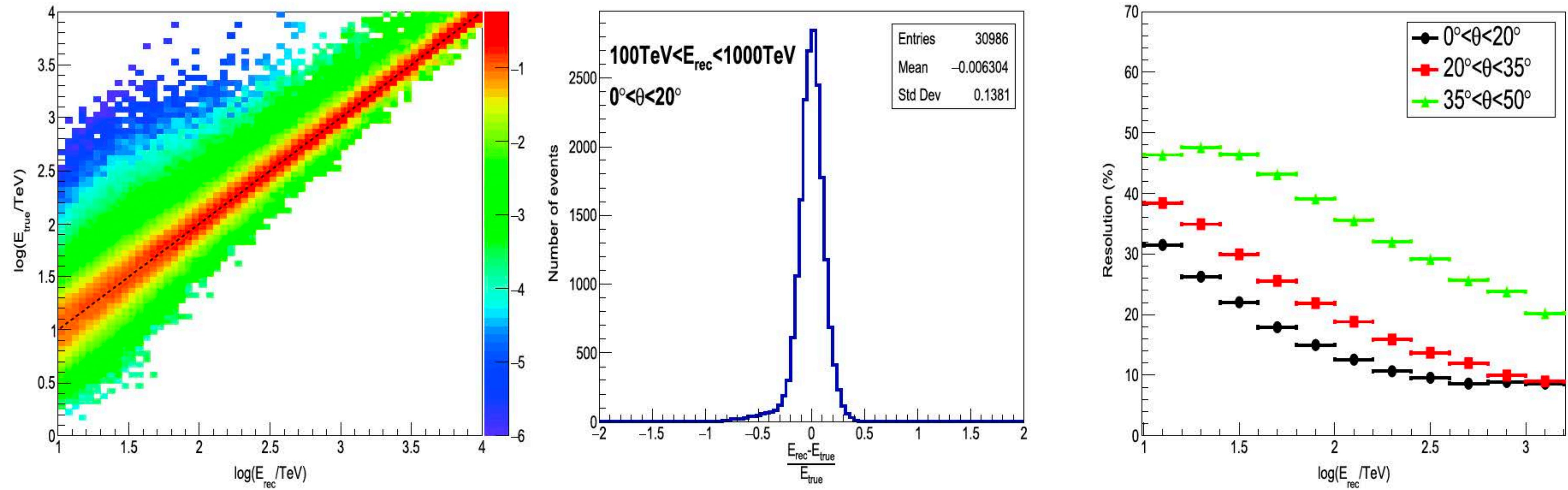


SED of the Crab

- ❖ LHAASO:
 - Covering 3.5 decades of energy
 - Agreeing with other experiments below 100 TeV
 - Self cross-checking between WCDA & KM2A
- ❖ LHAASO-KM2A:
 - Unique UHE SED
 - A PeVatron without ambiguity
 - ❖ Clear origin: a well-known PWN
- ❖ An extreme e-accelerator:
 - 2.3 PeV electrons
 - in ~ 0.025 pc compact region
 - accelerating efficiency of 15% (1000 \times better than SNR shock waves)



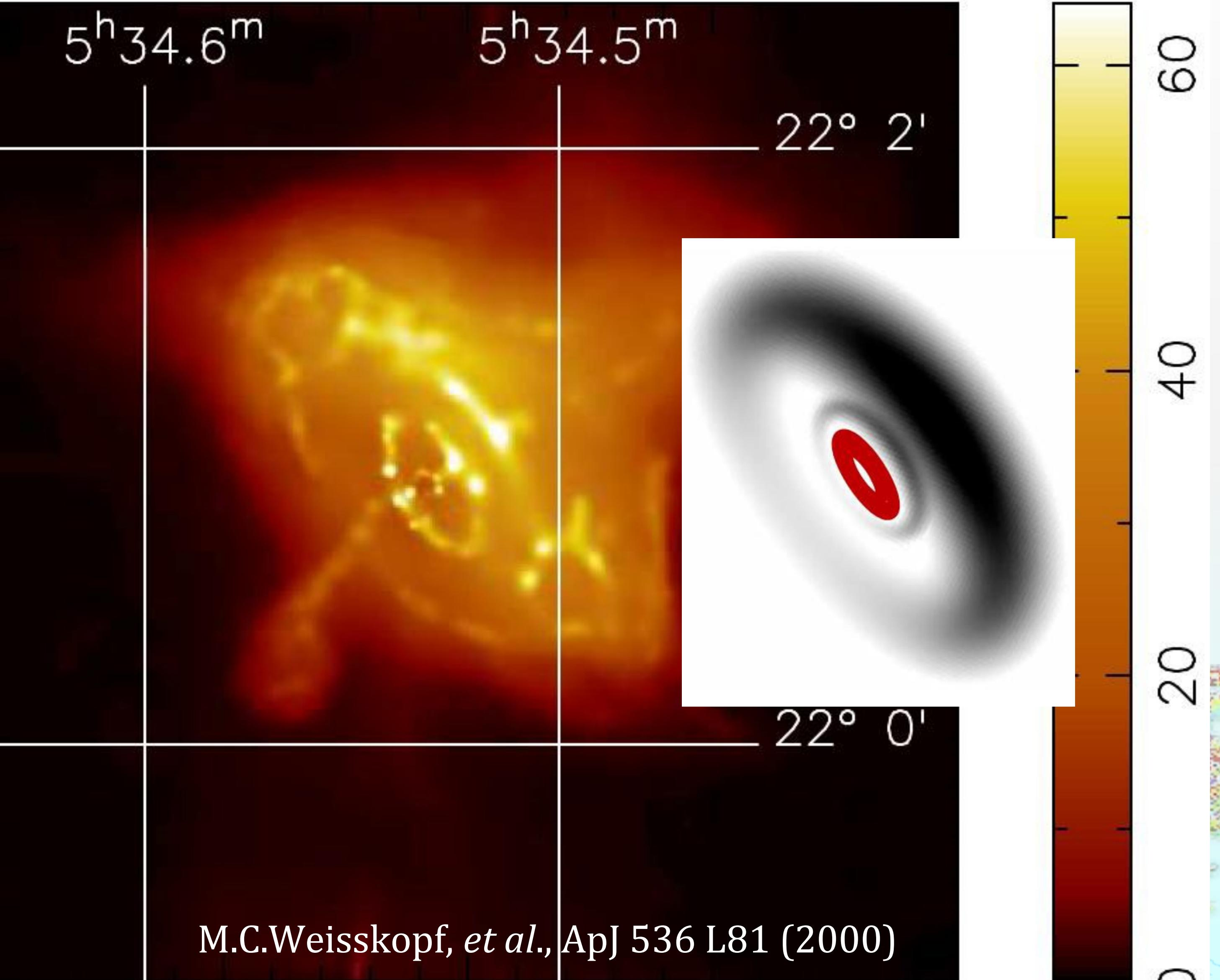
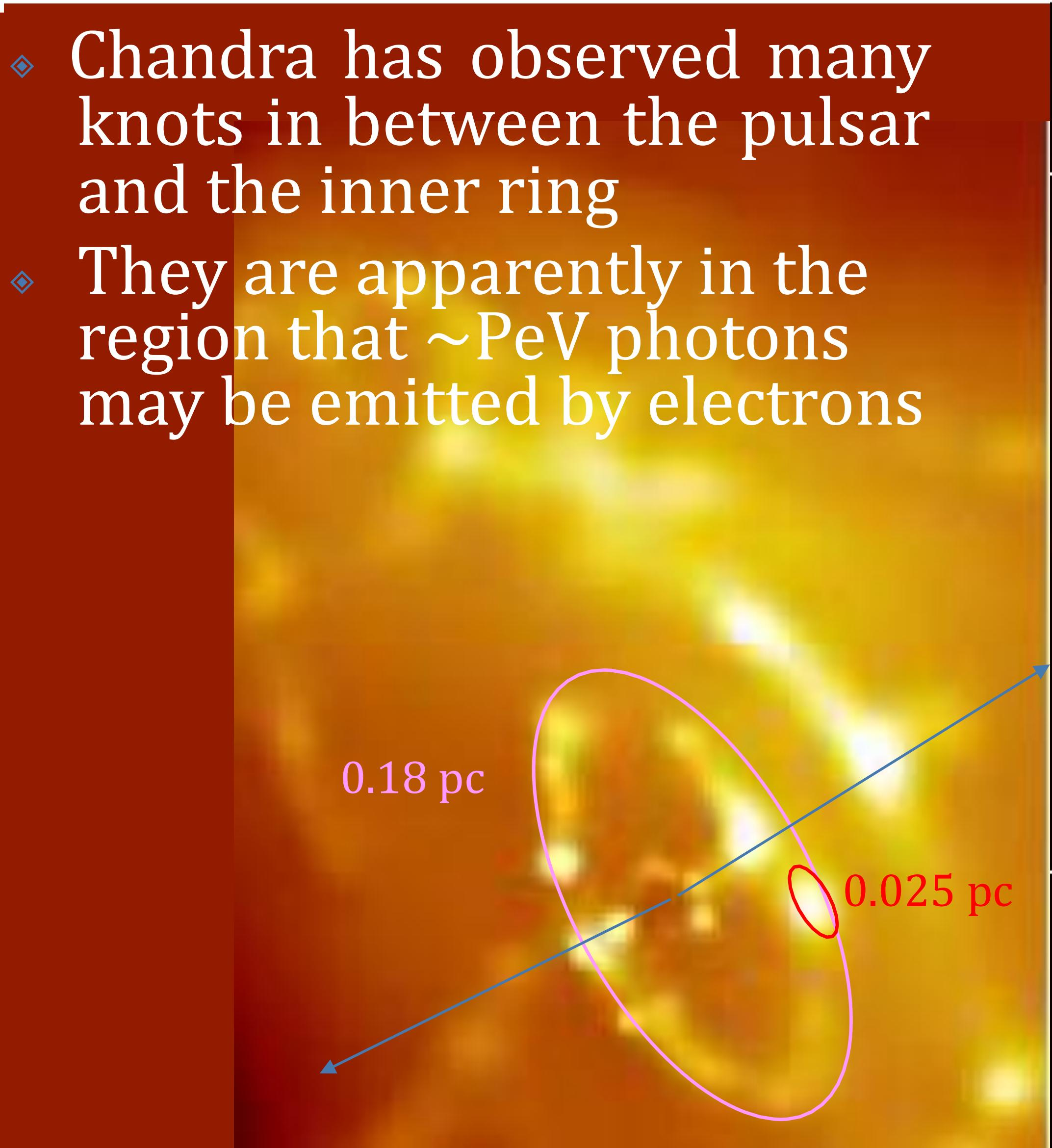
Energy reconstruction of KM2A



- The energy resolution is better than 14% for photons above 100 TeV arriving from a zenith angle of $< 35^\circ$.

Inner ring, jets and knots

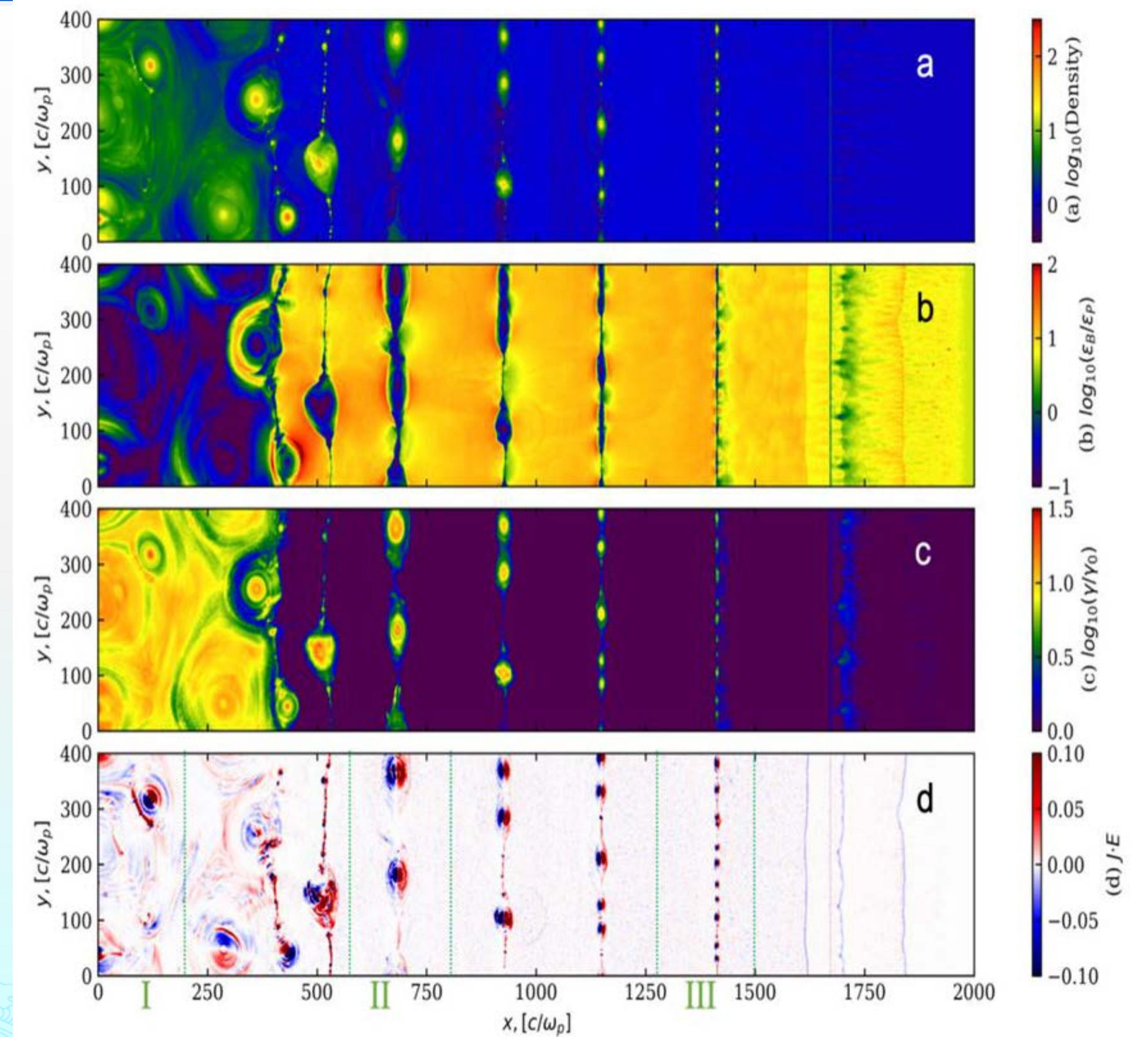
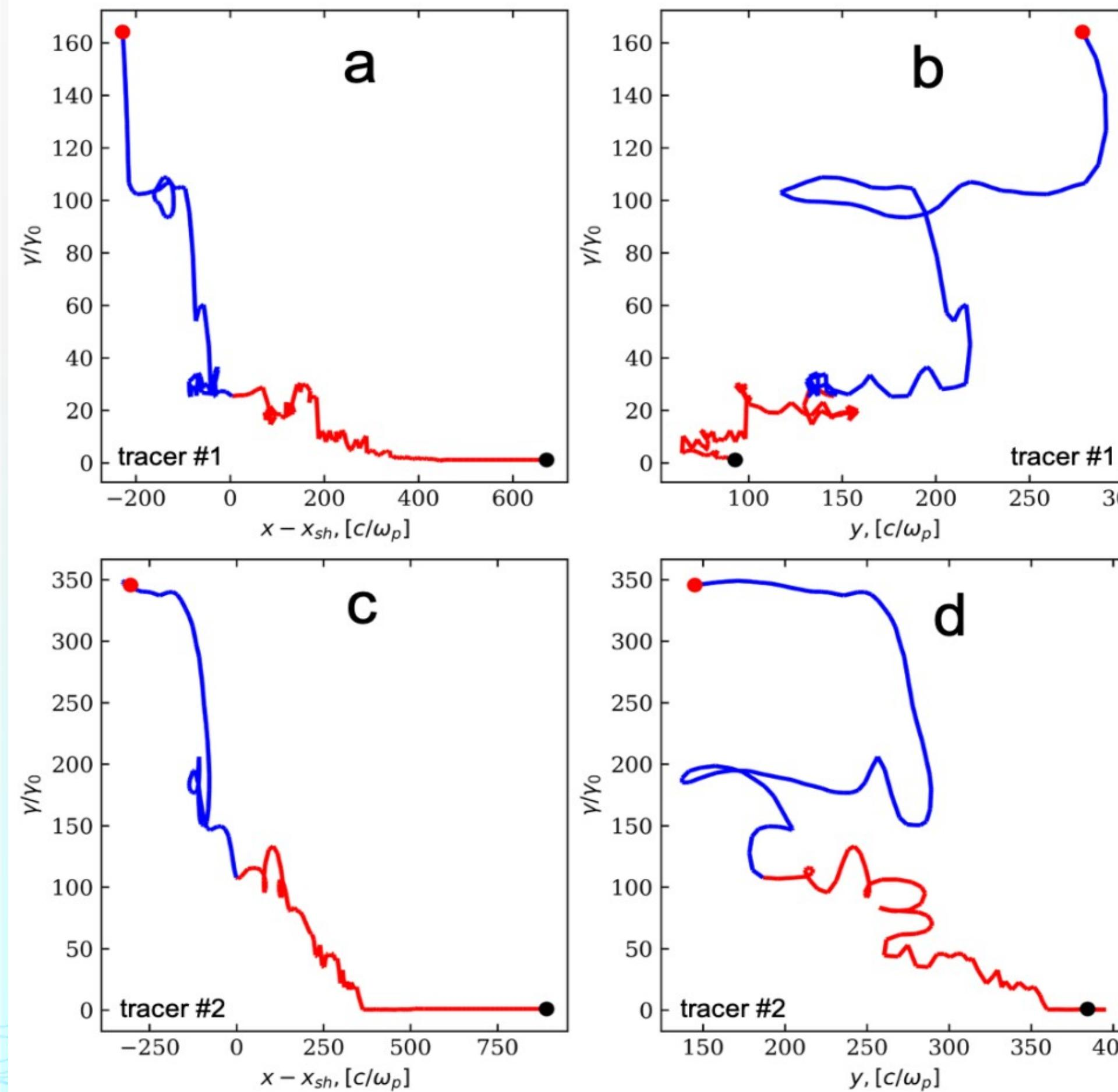
- ◆ Chandra has observed many knots in between the pulsar and the inner ring
- ◆ They are apparently in the region that \sim PeV photons may be emitted by electrons





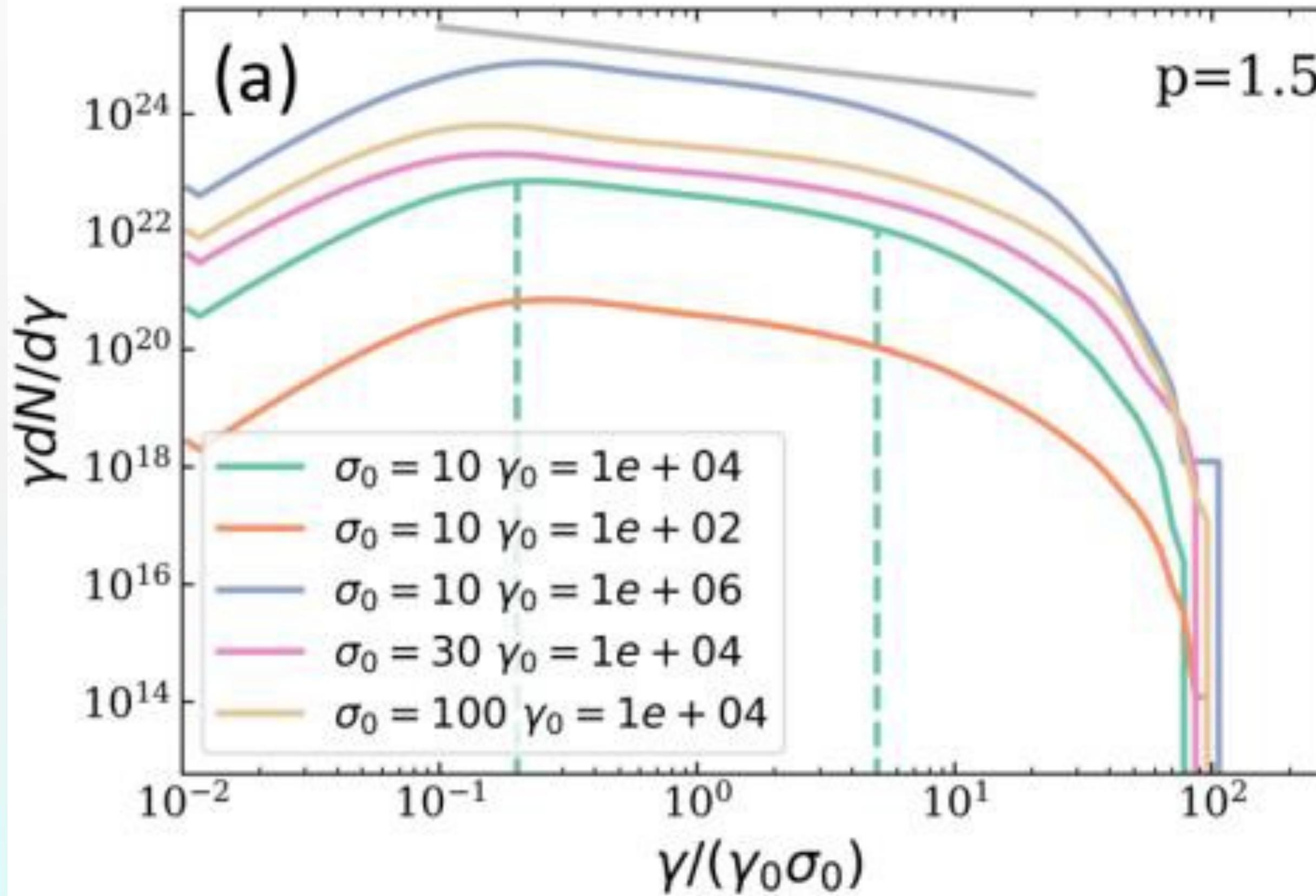
MHD PIC Simulation

Yingchao Lu et al., ApJ 908, 2, 147 (2021)

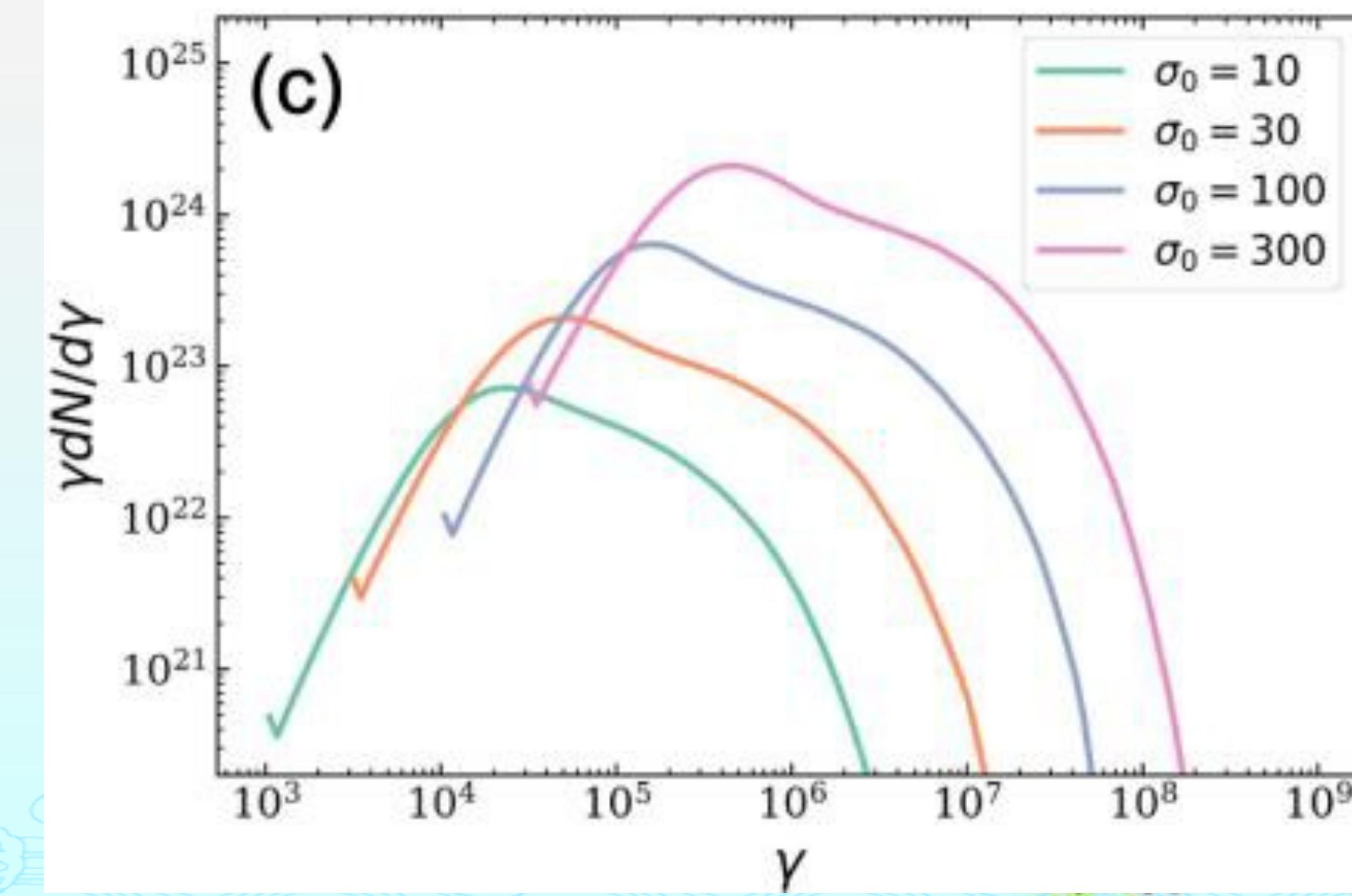
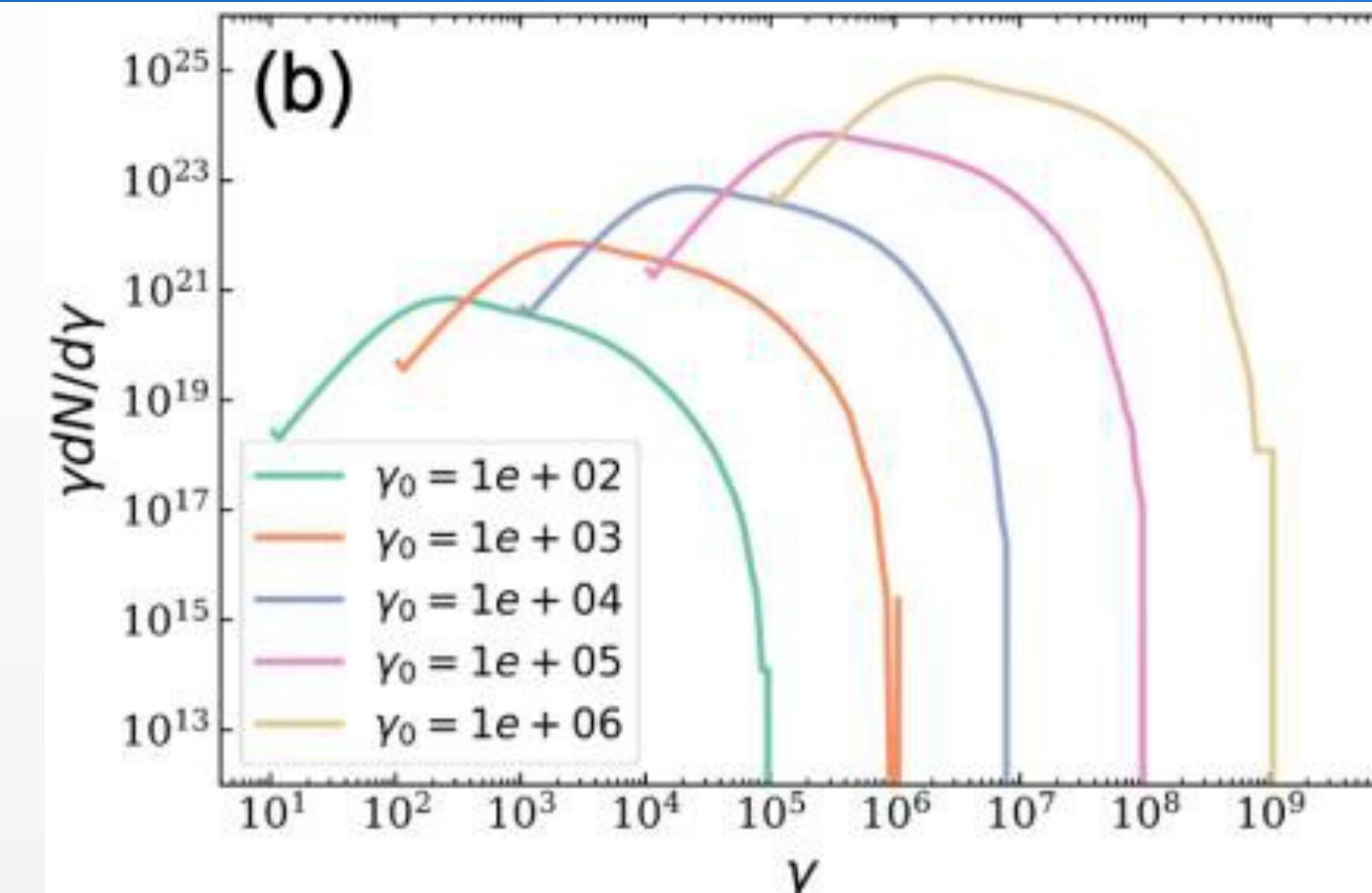


Electron E-Spectrum

Yingchao Lu et al., ApJ 908, 2, 147 (2021)

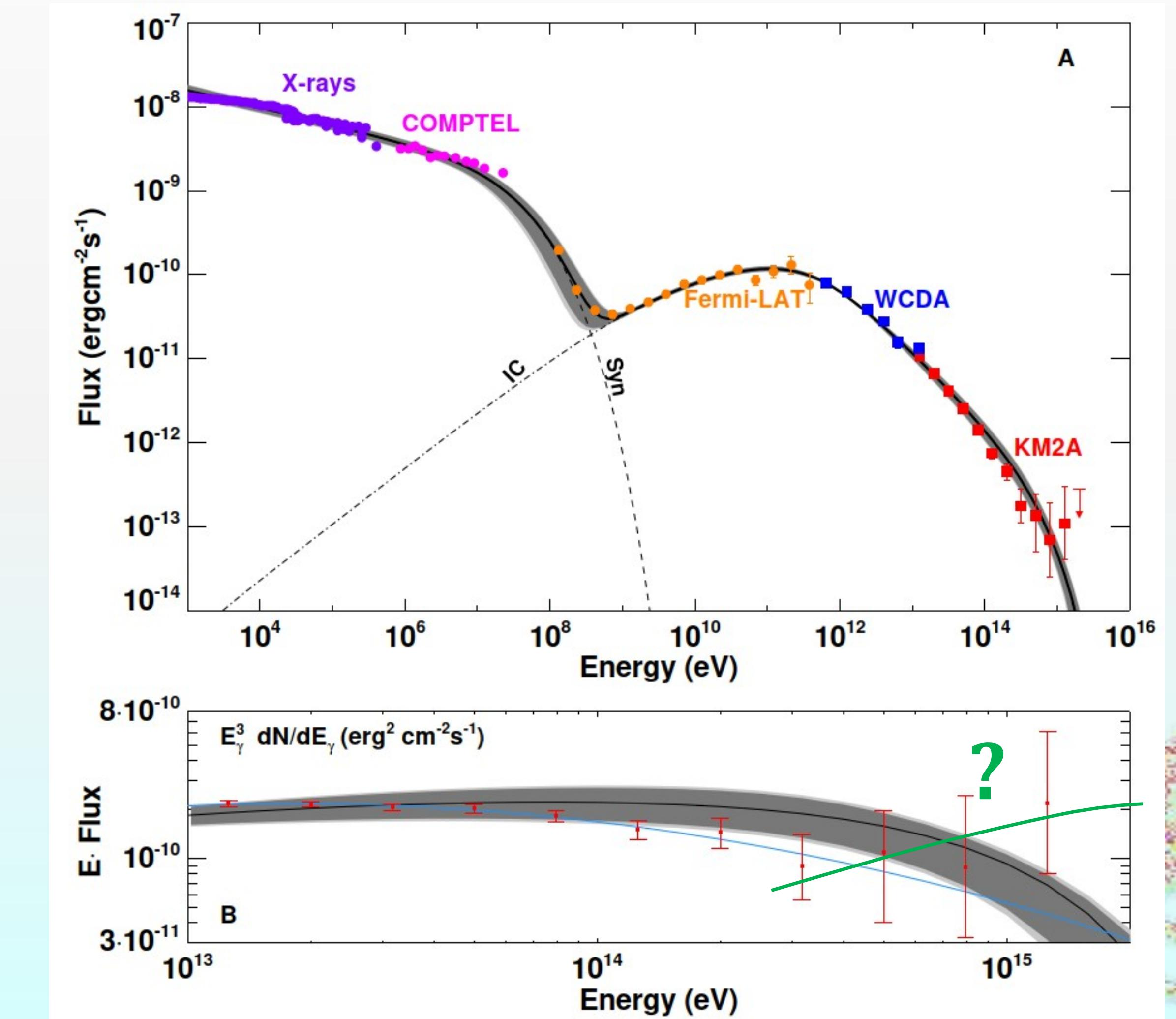


- it seems not impossible to reach 1 PeV, but quite extreme!



SED of the Crab: Extreme E-accelerator
LHAASO, Science, DOI:10.1126/science.abg5137, 2021

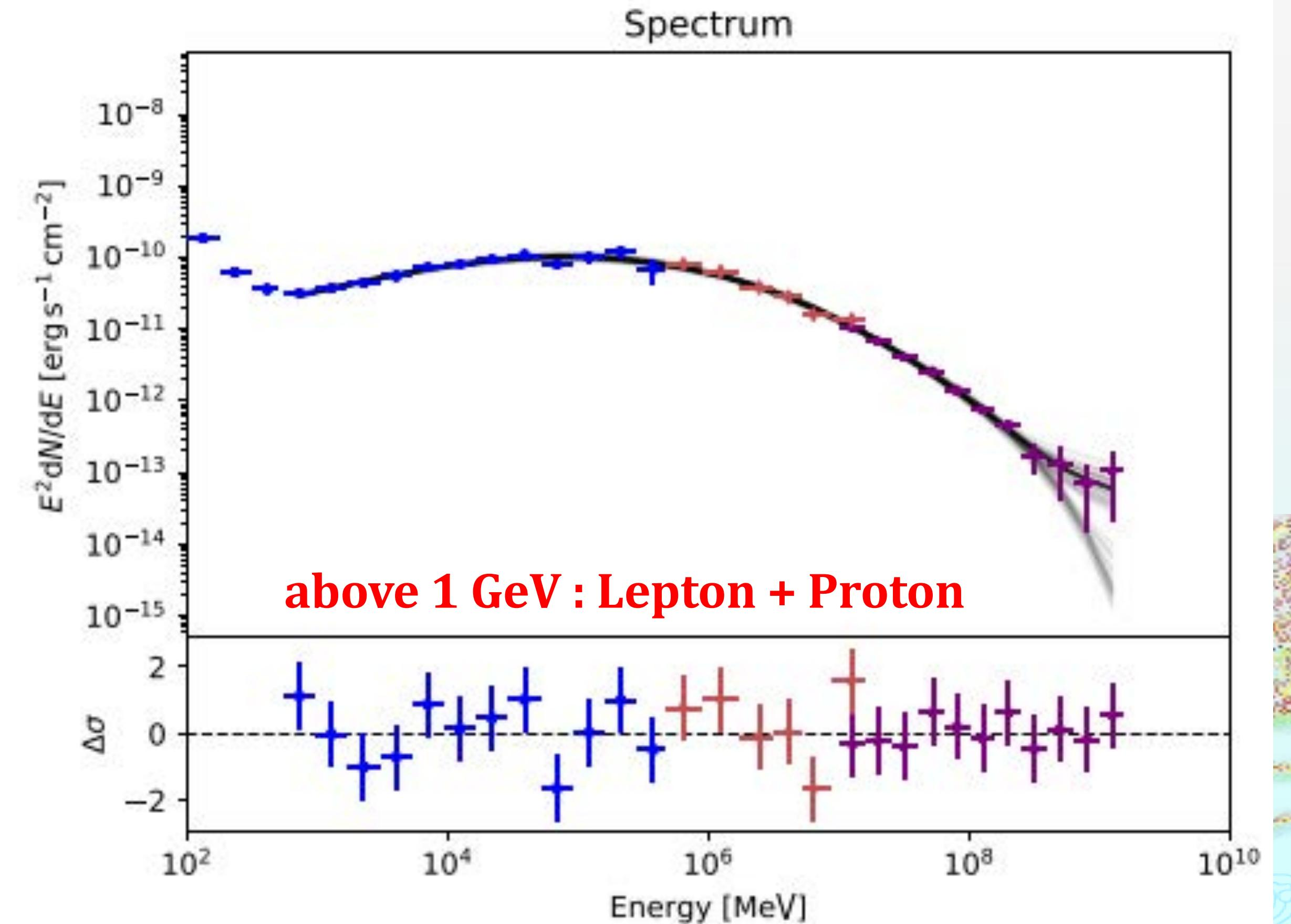
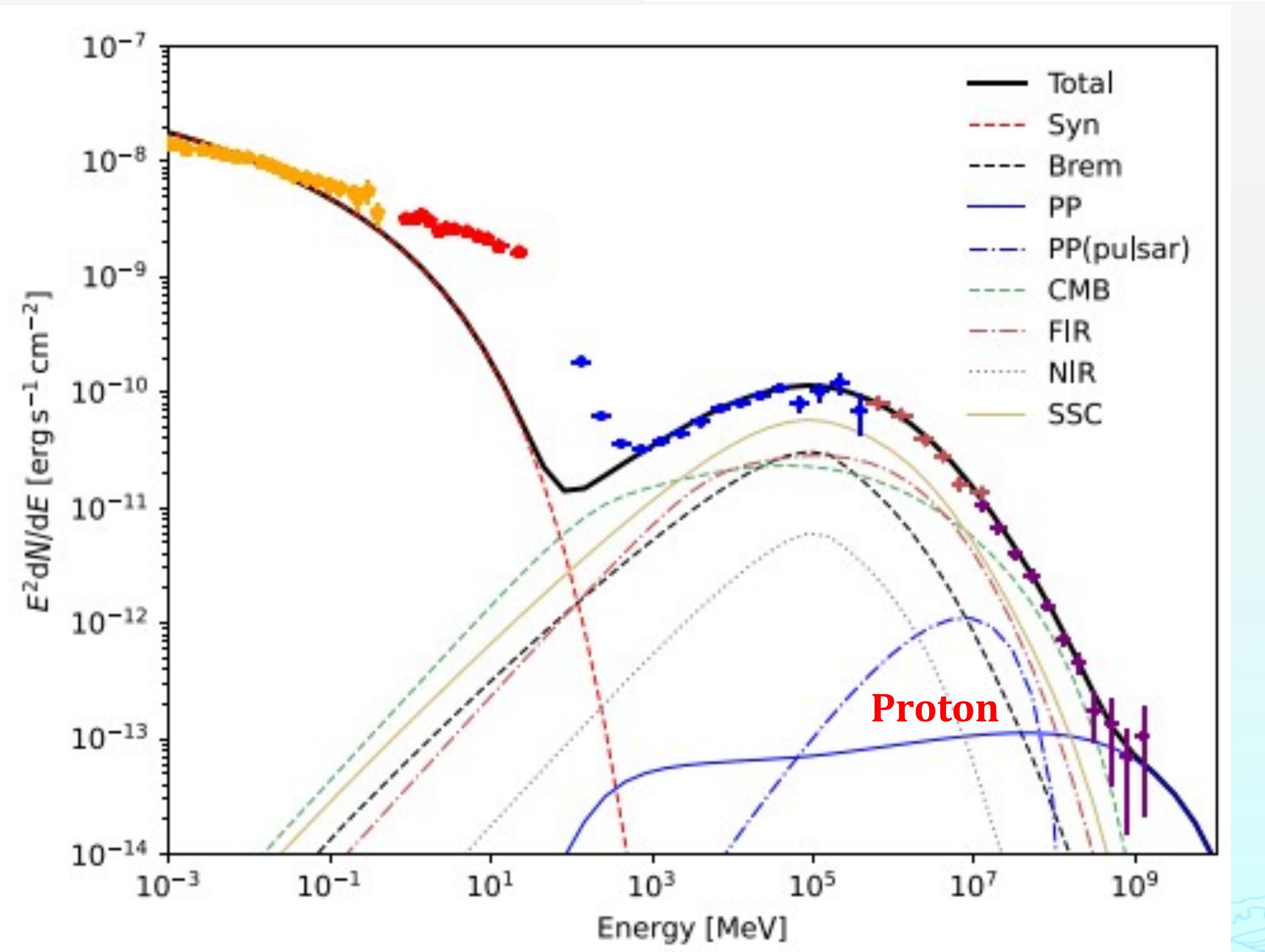
- ◆ Perfect interpretation of one-zone electronic origin up to 50 TeV
- ◆ Reasonable extension up to 1 PeV, with a deviation of **4 σ**
- ◆ Can not rule out proton origin of photons \sim 1.1 PeV, yet



Seems to be a better interpretation

- ❖ Relaxing the tension of 2.3 PeV electron's acceleration
- ❖ Origin of CRs above the knee: a Super-PeVatron

L. Nie et al., ApJ, 924 42, [arXiv:2201.03796](https://arxiv.org/abs/2201.03796)





Discovery in KM2A Survey

Our Galaxy is full of PeVatrons

LHAASO, Nature, 594, p.33-36, 2021

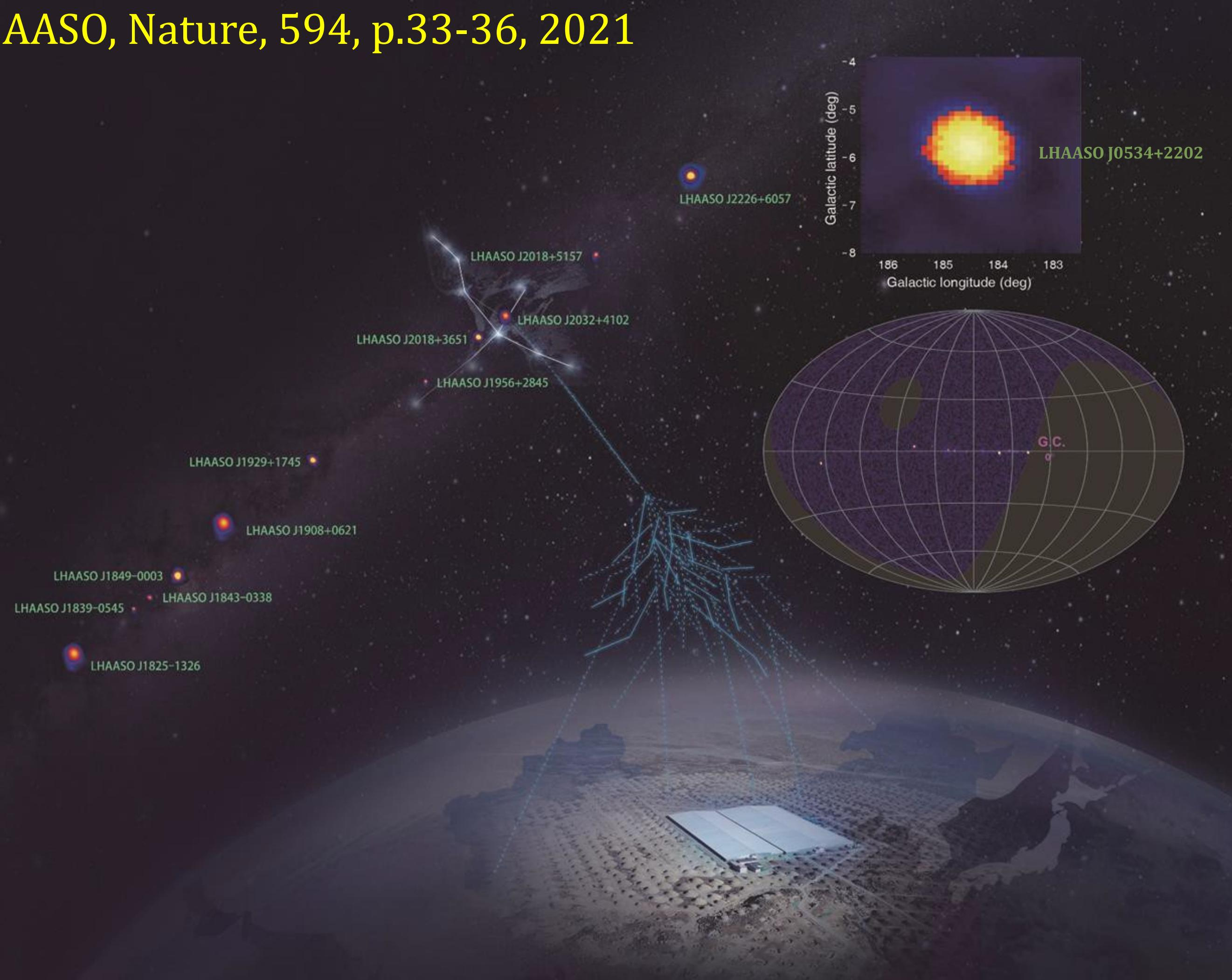


Table 1 | UHE γ -ray sources

Source name	RA ($^{\circ}$)	dec. ($^{\circ}$)	Significance above 100 TeV ($\times\sigma$)	E_{\max} (PeV)	Flux at 100 TeV (CU)
LHAASO J0534+2202	83.55	22.05	17.8	0.88 ± 0.11	1.00(0.14)
LHAASO J1825-1326	276.45	-13.45	16.4	0.42 ± 0.16	3.57(0.52)
LHAASO J1839-0545	279.95	-5.75	7.7	0.21 ± 0.05	0.70(0.18)
LHAASO J1843-0338	280.75	-3.65	8.5	$0.26 - 0.10^{+0.16}$	0.73(0.17)
LHAASO J1849-0003	282.35	-0.05	10.4	0.35 ± 0.07	0.74(0.15)
LHAASO J1908+0621	287.05	6.35	17.2	0.44 ± 0.05	1.36(0.18)
LHAASO J1929+1745	292.25	17.75	7.4	$0.71 - 0.07^{+0.16}$	0.38(0.09)
LHAASO J1956+2845	299.05	28.75	7.4	0.42 ± 0.03	0.41(0.09)
LHAASO J2018+3651	304.75	36.85	10.4	0.27 ± 0.02	0.50(0.10)
LHAASO J2032+4102	308.05	41.05	10.5	1.42 ± 0.13	0.54(0.10)
LHAASO J2108+5157	317.15	51.95	8.3	0.43 ± 0.05	0.38(0.09)
LHAASO J2226+6057	336.75	60.95	13.6	0.57 ± 0.19	1.05(0.16)

12 PeVatrons are discovered

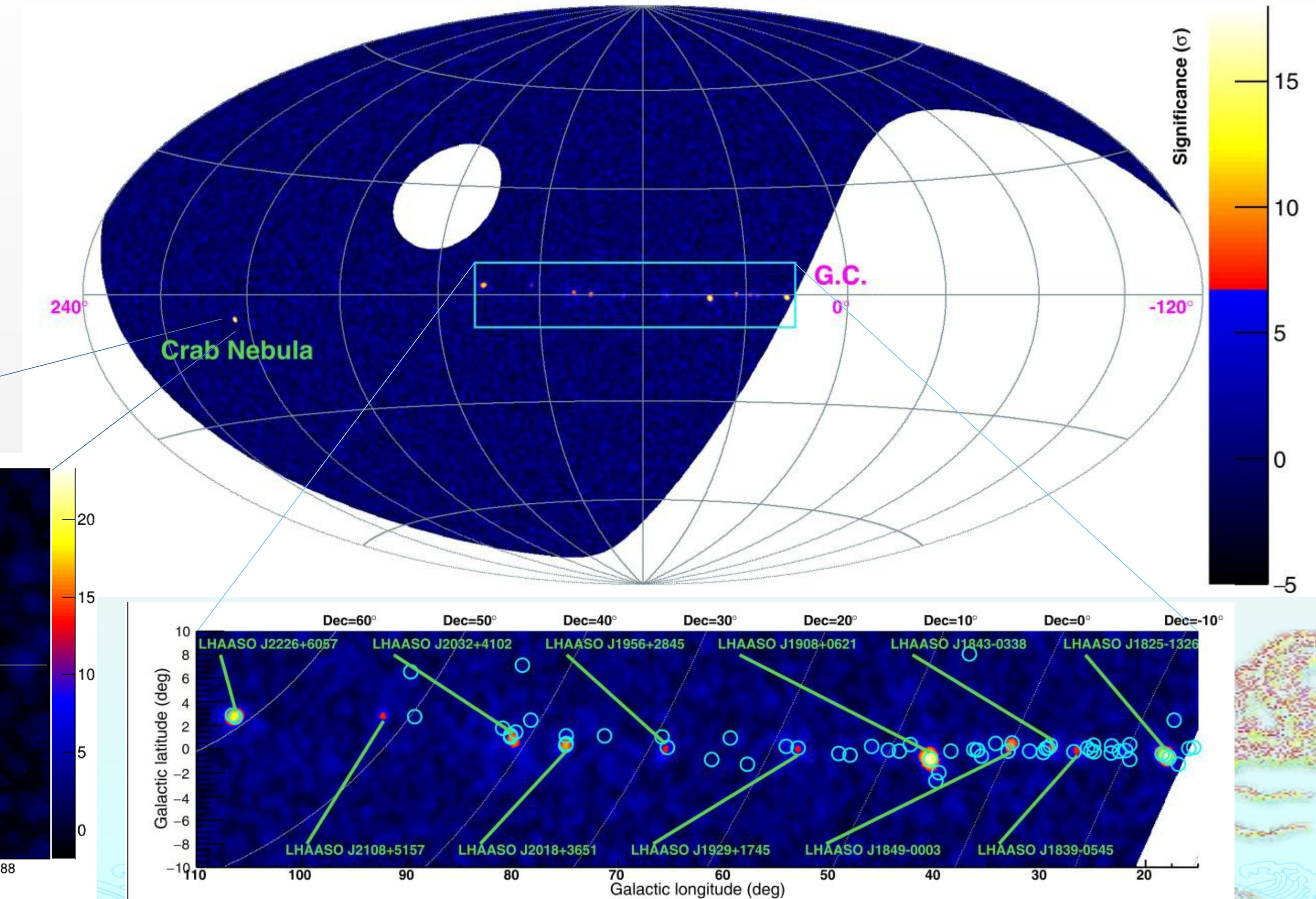
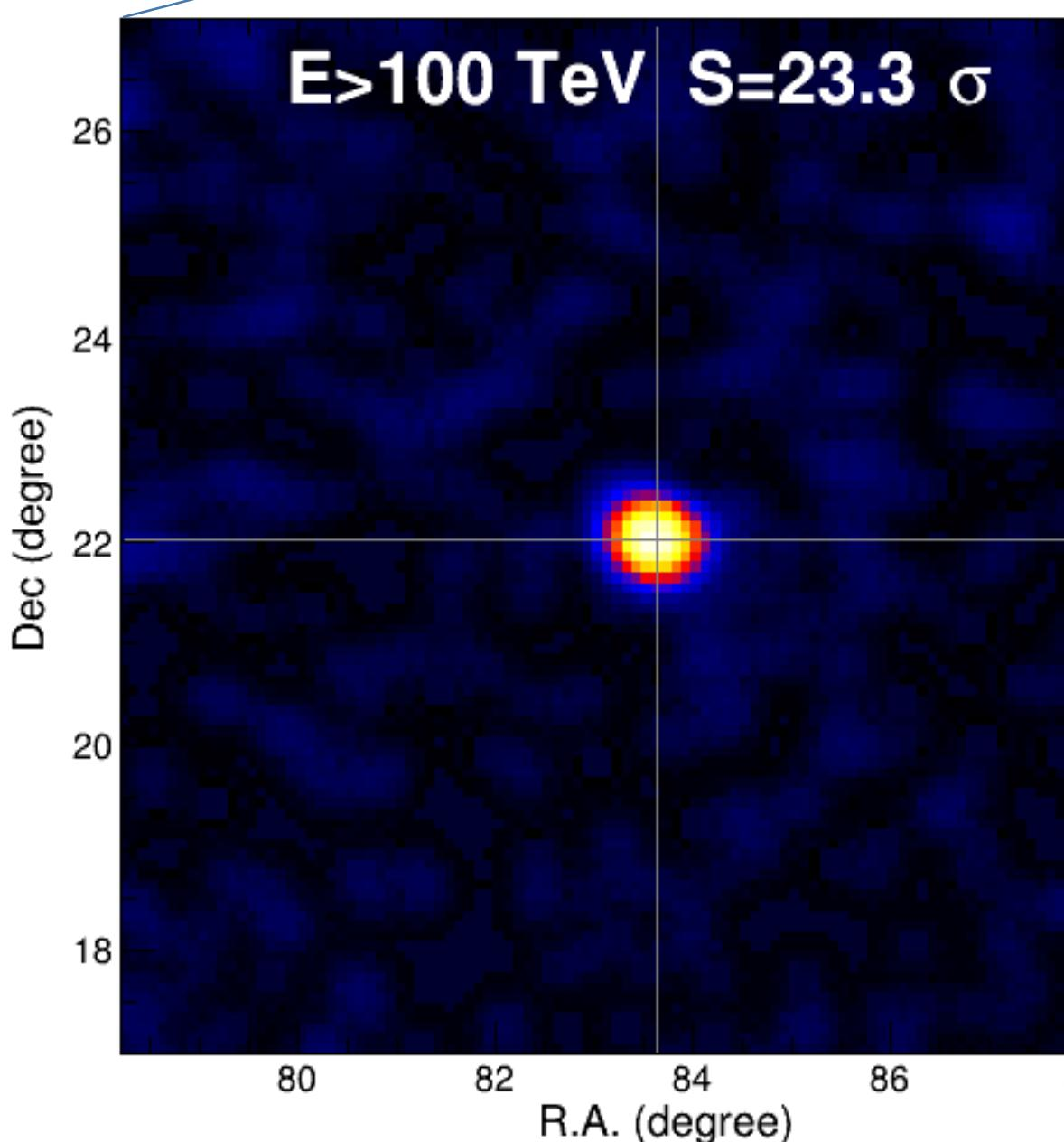
- ◆ High Standard: significance $>7\sigma$
- ◆ BG-free: Cosmic Ray background rejection rate $<10^{-4}$

◆ High Statistics: 530 UHE photons

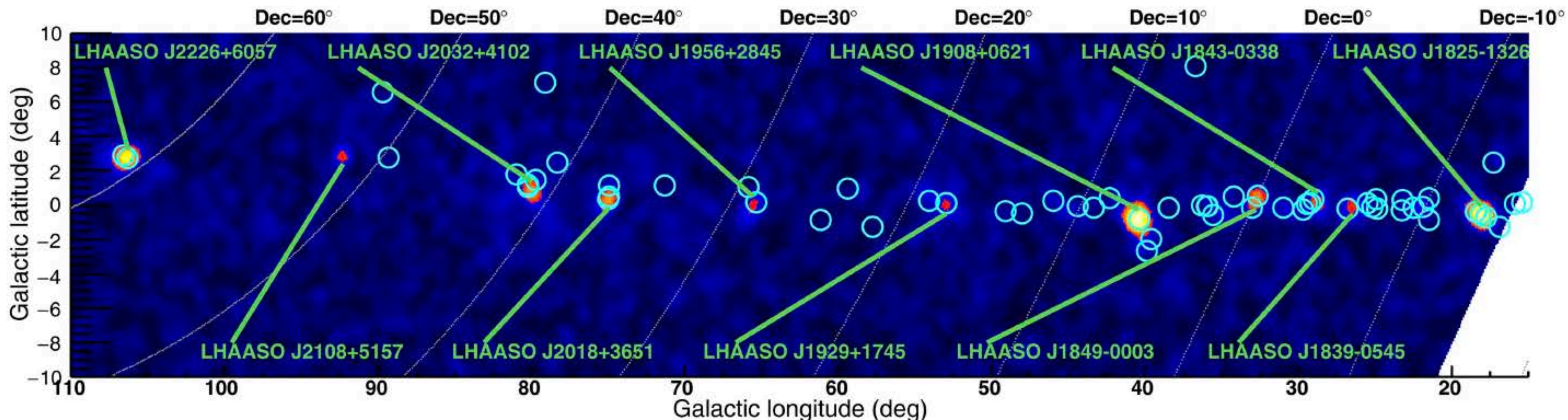
◆ Multiple Type of Sources



UHE γ -ray (0.1-1 PeV) Sky Map



LHAASO sky map ($E > 100\text{TeV}$)



Significance > 7-sigma

Table 1 | UHE γ -ray sources

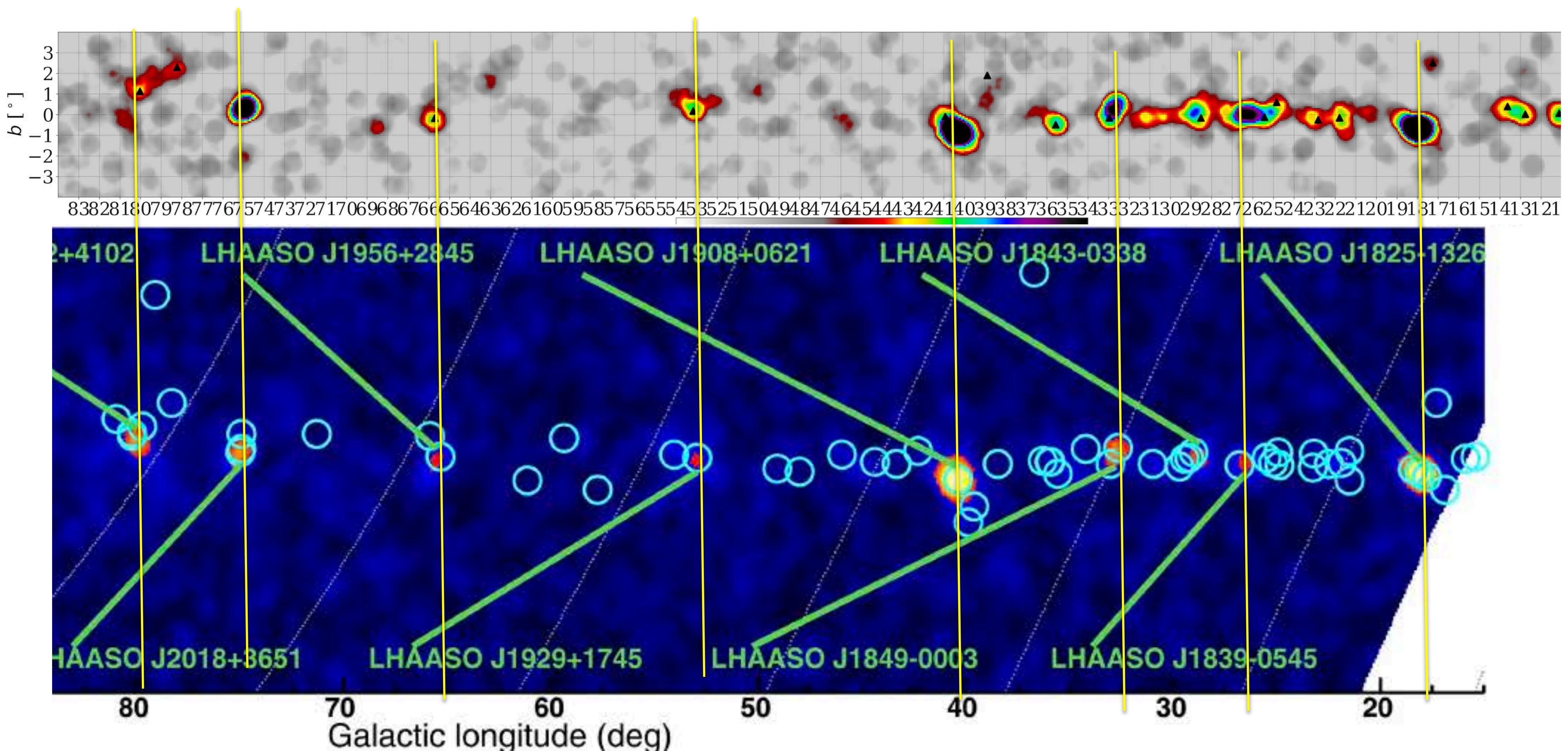
Source name		RA ($^{\circ}$)	dec. ($^{\circ}$)	Significance above 100 TeV ($\times\sigma$)	E_{\max} (PeV)	Flux at 100 TeV (CU)
LHAASO J0534+2202	Crab	83.55	22.05	17.8	0.88 ± 0.11	1.00(0.14)
LHAASO J1825-1326	1825 region	276.45	-13.45	16.4	0.42 ± 0.16	3.57(0.52)
LHAASO J1839-0545		279.95	-5.75	7.7	0.21 ± 0.05	0.70(0.18)
LHAASO J1843-0338		280.75	-3.65	8.5	$0.26 - 0.10^{+0.16}$	0.73(0.17)
LHAASO J1849-0003		282.35	-0.05	10.4	0.35 ± 0.07	0.74(0.15)
LHAASO J1908+0621	MGRO1908	287.05	6.35	17.2	0.44 ± 0.05	1.36(0.18)
LHAASO J1929+1745		292.25	17.75	7.4	$0.71 - 0.07^{+0.16}$	0.38(0.09)
LHAASO J1956+2845		299.05	28.75	7.4	0.42 ± 0.03	0.41(0.09)
LHAASO J2018+3651		304.75	36.85	10.4	0.27 ± 0.02	0.50(0.10)
LHAASO J2032+4102	Cygnus OB	308.05	41.05	10.5	1.42 ± 0.13	0.54(0.10)
LHAASO J2108+5157		317.15	51.95	8.3	0.43 ± 0.05	0.38(0.09)
LHAASO J2226+6057	Boomerang	336.75	60.95	13.6	0.57 ± 0.19	1.05(0.16)

Celestial coordinates (RA, dec.); statistical significance of detection above 100 TeV (calculated using a point-like template for the Crab Nebula and LHAASO J2108+5157 and 0.3° extension templates for the other sources); the corresponding differential photon fluxes at 100 TeV; and detected highest photon energies. Errors are estimated as the boundary values of the area that contains $\pm 34.14\%$ of events with respect to the most probable value of the event distribution. In most cases, the distribution is a Gaussian and the error is 1σ .

Extended Data Table 2 | List of energetic astrophysical objects possibly associated with each LHAASO source

LHAASO Source	Possible Origin	Type	Distance (kpc)	Age (kyr) ^a	L_s (erg/s) ^b	Potential TeV Counterpart ^c
LHAASO J0534+2202	PSR J0534+2200	PSR	2.0	1.26	4.5×10^{38}	Crab, Crab Nebula
LHAASO J1825-1326	PSR J1826-1334	PSR	3.1 ± 0.2^d	21.4	2.8×10^{36}	HESS J1825-137, HESS J1826-130,
	PSR J1826-1256	PSR	1.6	14.4	3.6×10^{36}	2HWC J1825-134
LHAASO J1839-0545	PSR J1837-0604	PSR	4.8	33.8	2.0×10^{36}	2HWC J1837-065, HESS J1837-069,
	PSR J1838-0537	PSR	1.3^e	4.9	6.0×10^{36}	HESS J1841-055
LHAASO J1843-0338	SNR G28.6-0.1	SNR	9.6 ± 0.3^f	< 2 ^f	—	HESS J1843-033, HESS J1844-030, 2HWC J1844-032
LHAASO J1849-0003	PSR J1849-0001	PSR	7 ^g	43.1	9.8×10^{36}	HESS J1849-000, 2HWC J1849+001
	W43	YMC	5.5^h	—	—	
LHAASO J1908+0621	SNR G40.5-0.5	SNR	3.4^i	$\sim 10 - 20^j$	—	MGRO J1908+06, HESS J1908+063,
	PSR 1907+0602	PSR	2.4	19.5	2.8×10^{36}	ARGO J1907+0627, VER J1907+062,
	PSR 1907+0631	PSR	3.4	11.3	5.3×10^{35}	2HWC 1908+063
LHAASO J1929+1745	PSR J1928+1746	PSR	4.6	82.6	1.6×10^{36}	2HWC J1928+177, 2HWC J1930+188,
	PSR J1930+1852	PSR	6.2	2.9	1.2×10^{37}	HESS J1930+188, VER J1930+188
	SNR G54.1+0.3	SNR	$6.3^{+0.8}_{-0.7}{}^d$	$1.8 - 3.3^k$	—	
LHAASO J1956+2845	PSR J1958+2846	PSR	2.0	21.7	3.4×10^{35}	2HWC J1955+285
	SNR G66.0-0.0	SNR	2.3 ± 0.2^d	—	—	
LHAASO J2018+3651	PSR J2021+3651	PSR	$1.8^{+1.7}_{-1.4}{}^l$	17.2	3.4×10^{36}	MGRO J2019+37, VER J2019+368,
	Sh 2-104	H II/YMC	$3.3 \pm 0.3^m / 4.0 \pm 0.5^n$	—	—	VER J2016+371
LHAASO J2032+4102	Cygnus OB2	YMC	1.40 ± 0.08^o	—	—	TeV J2032+4130, ARGO J2031+4157,
	PSR 2032+4127	PSR	1.40 ± 0.08^o	201	1.5×10^{35}	MGRO J2031+41, 2HWC J2031+415,
	SNR G79.8+1.2	SNR candidate	—	—	—	VER J2032+414
LHAASO J2108+5157	—	—	—	—	—	—
LHAASO J2226+6057	SNR G106.3+2.7	SNR	0.8^p	$\sim 10^p$	—	VER J2227+608, Boomerang Nebula
	PSR J2229+6114	PSR	0.8^p	$\sim 10^p$	2.2×10^{37}	

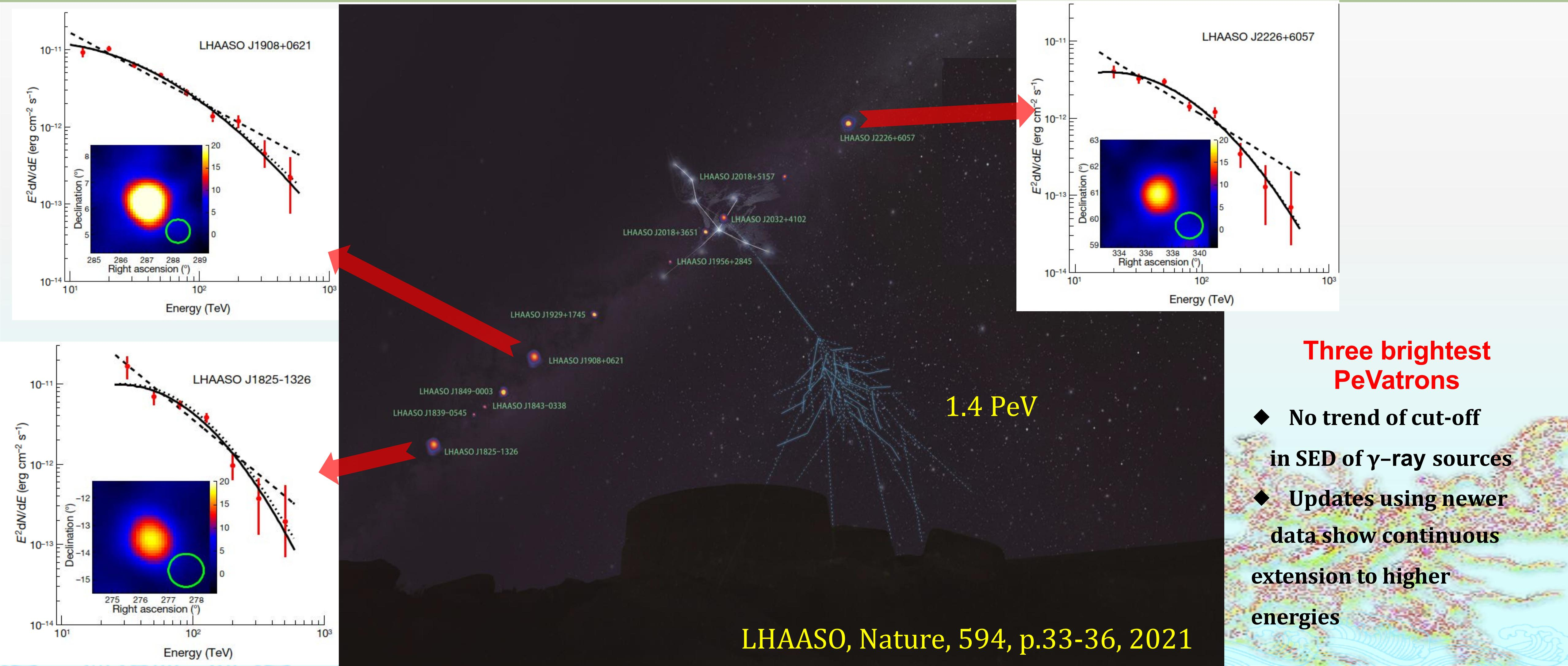
HAWC LHAASO Comparison

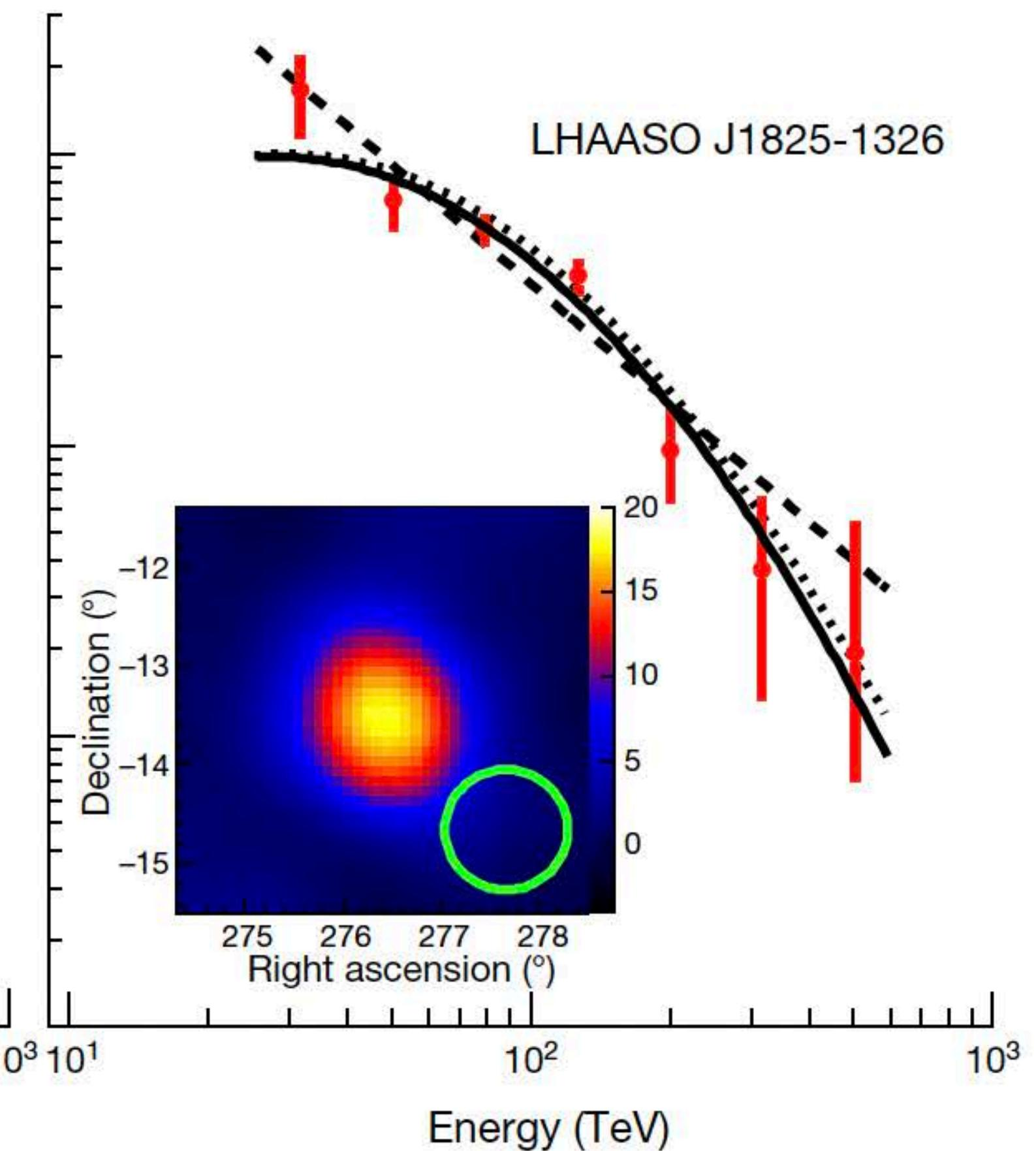
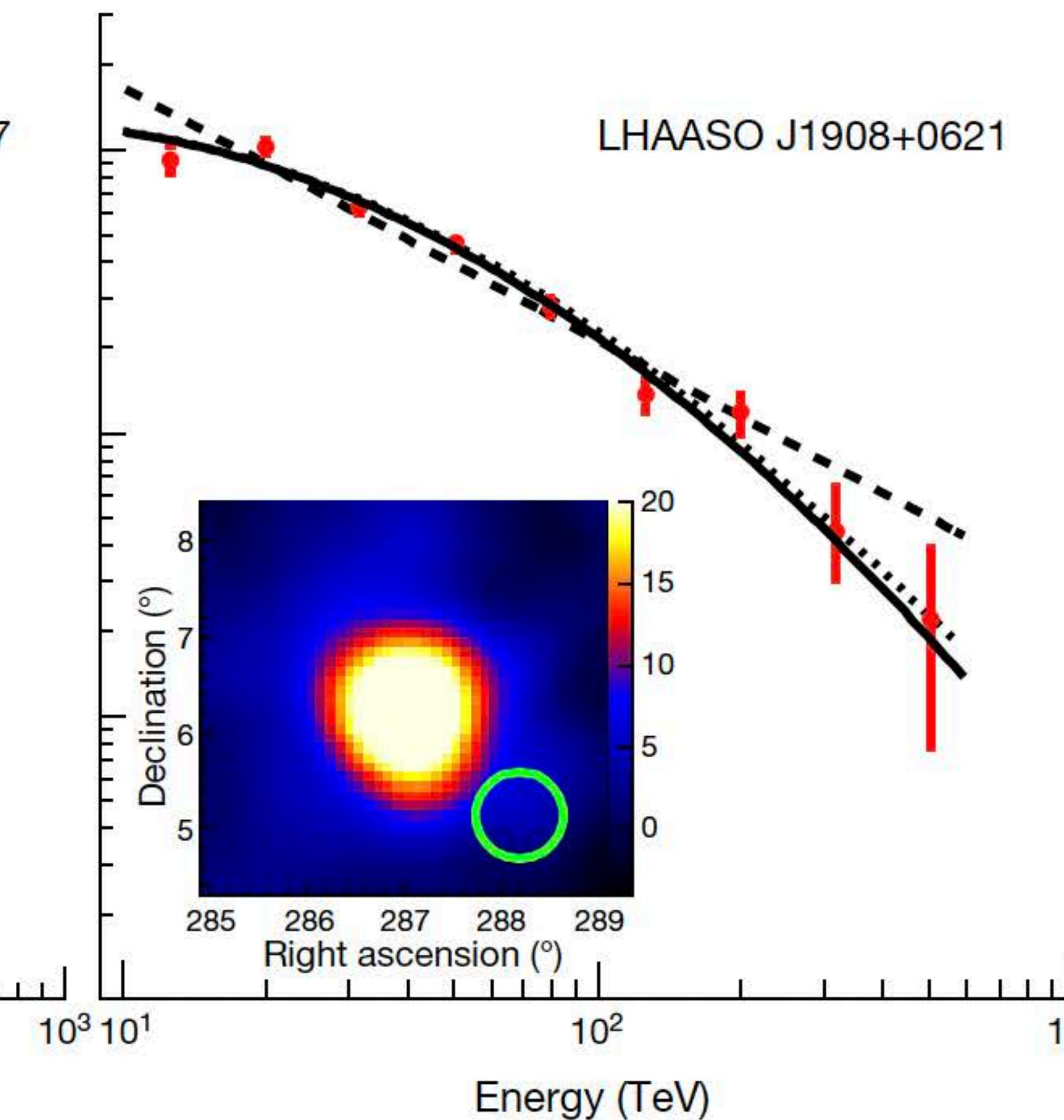
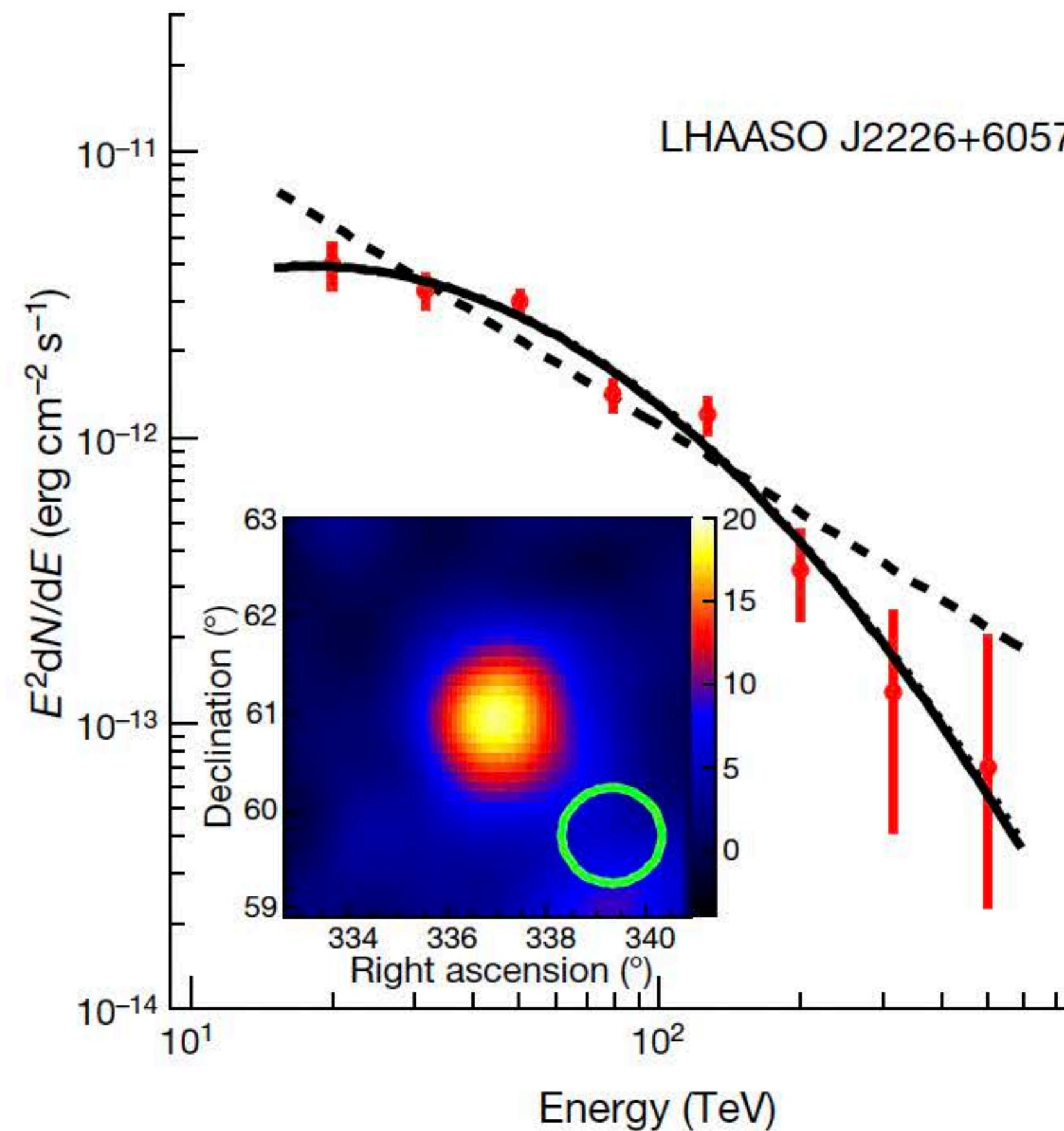




KM2A Survey

Do not observe clear cut-off up to ~ 1 PeV

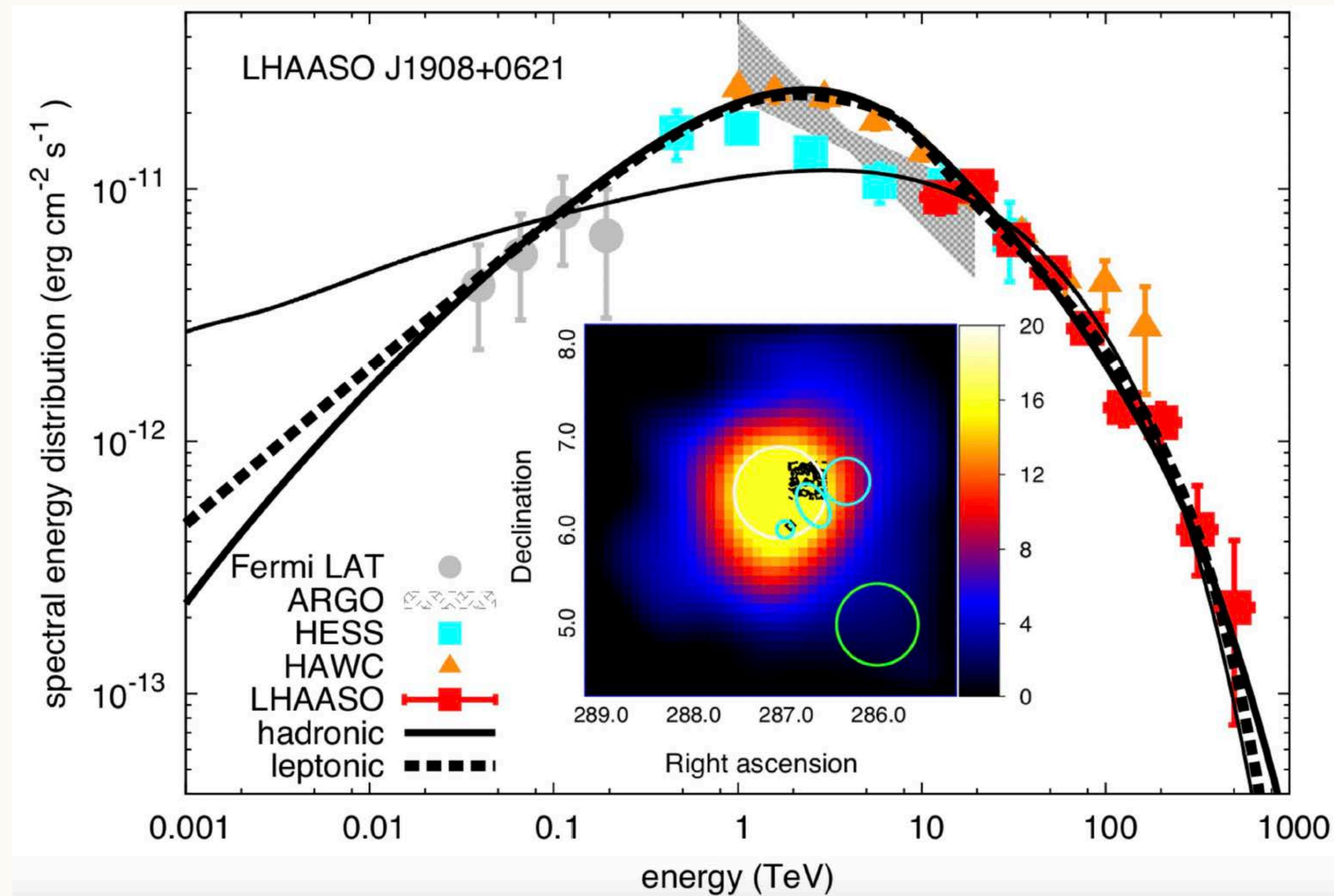




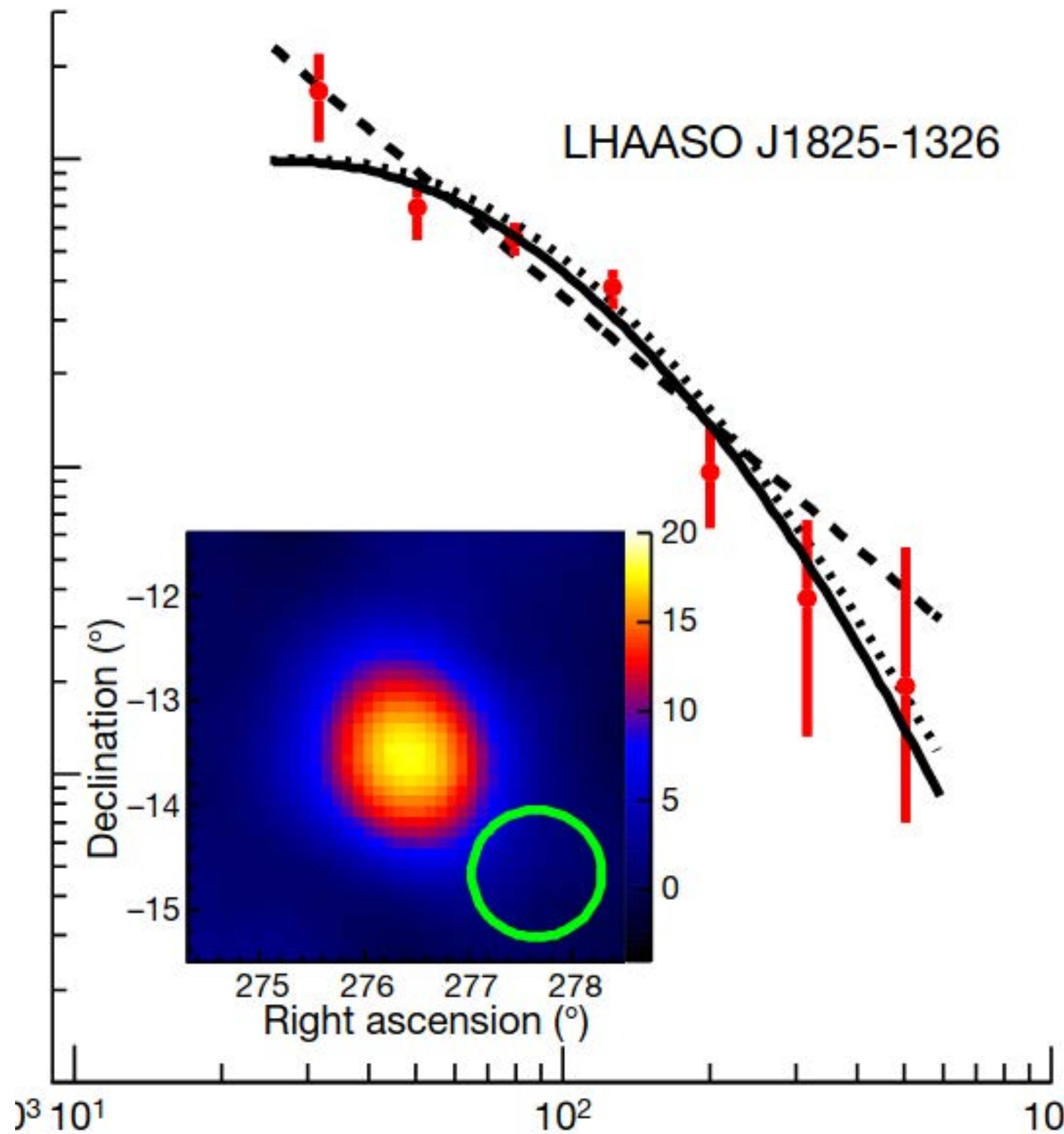
E_{max} (PeV) 0.57 ± 0.19

0.44 ± 0.55

0.42 ± 0.16



LHAASO J1825-1326



>100 TeV:
sign=16.4 σ (Extension=0.3°)
R.A.=276.45°
Decl.-13.45°

The 68% contamination angle is 0.62°
for LHAASO J1825-1326

[2021Natur.594...33C](#)

HESS J1825-137

PSR B1823-13 (PSR J1826-1334)

RA: 18 h 26 m 13.06 s

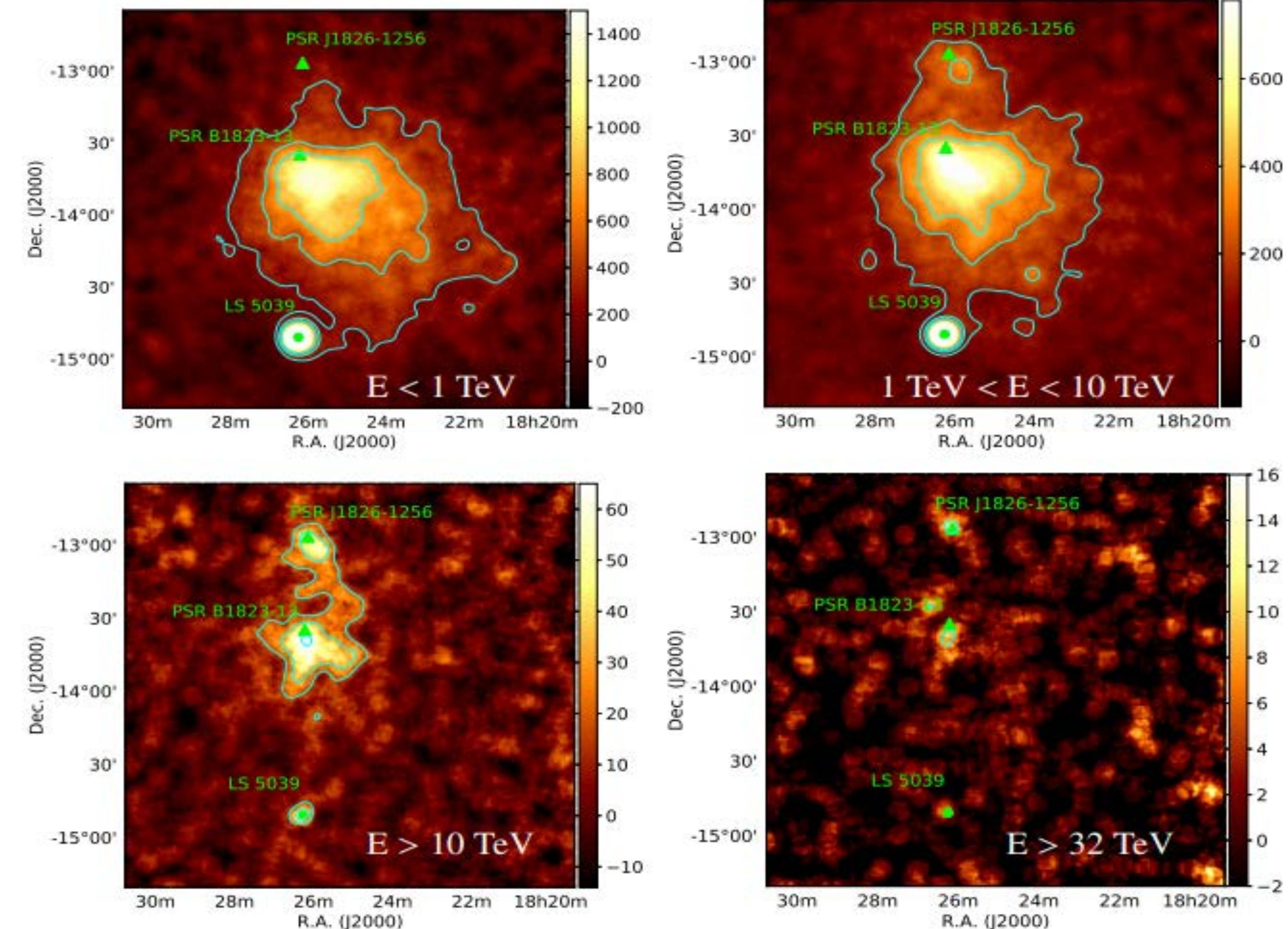
Dec: $-13^{\circ} 34'48.1''$

Age $\tau = 2.14 \times 10^4$ yr

$\dot{E} = 2.8 \times 10^{36}$ erg s $^{-1}$

period $P = 0.1015$ s

Distance: ~ 4 kpc



H.E.S.S. Collaboration 2019

HESS J1826-130

The Fermi/LAT detected the radio-quiet
 γ -ray pulsar PSR J1826 – 1256

RA: 276.54°

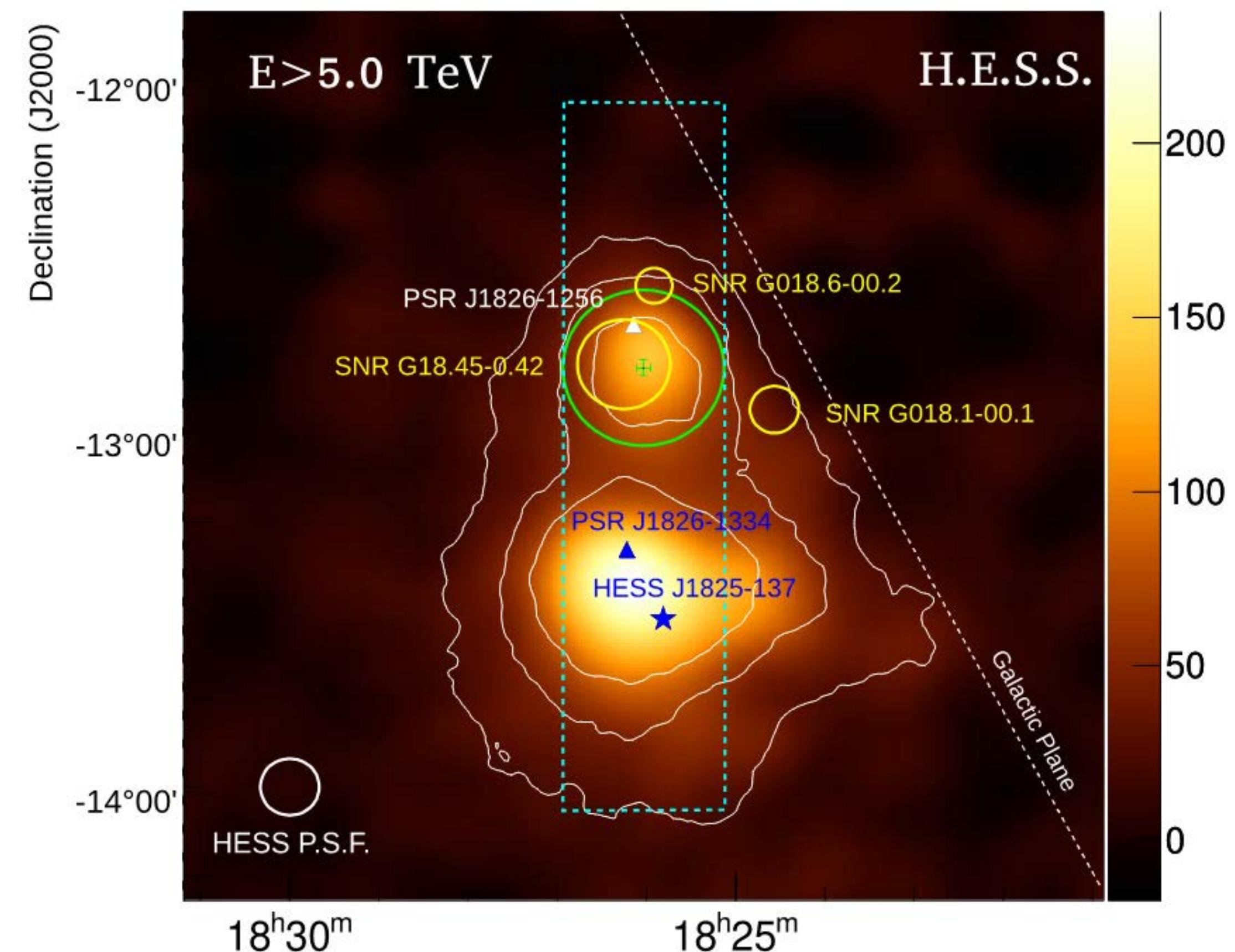
Dec: -12.94°

Age $\tau = 1.44 \times 10^4$ yr

$\dot{E} = 3.6 \times 10^{36}$ erg s $^{-1}$

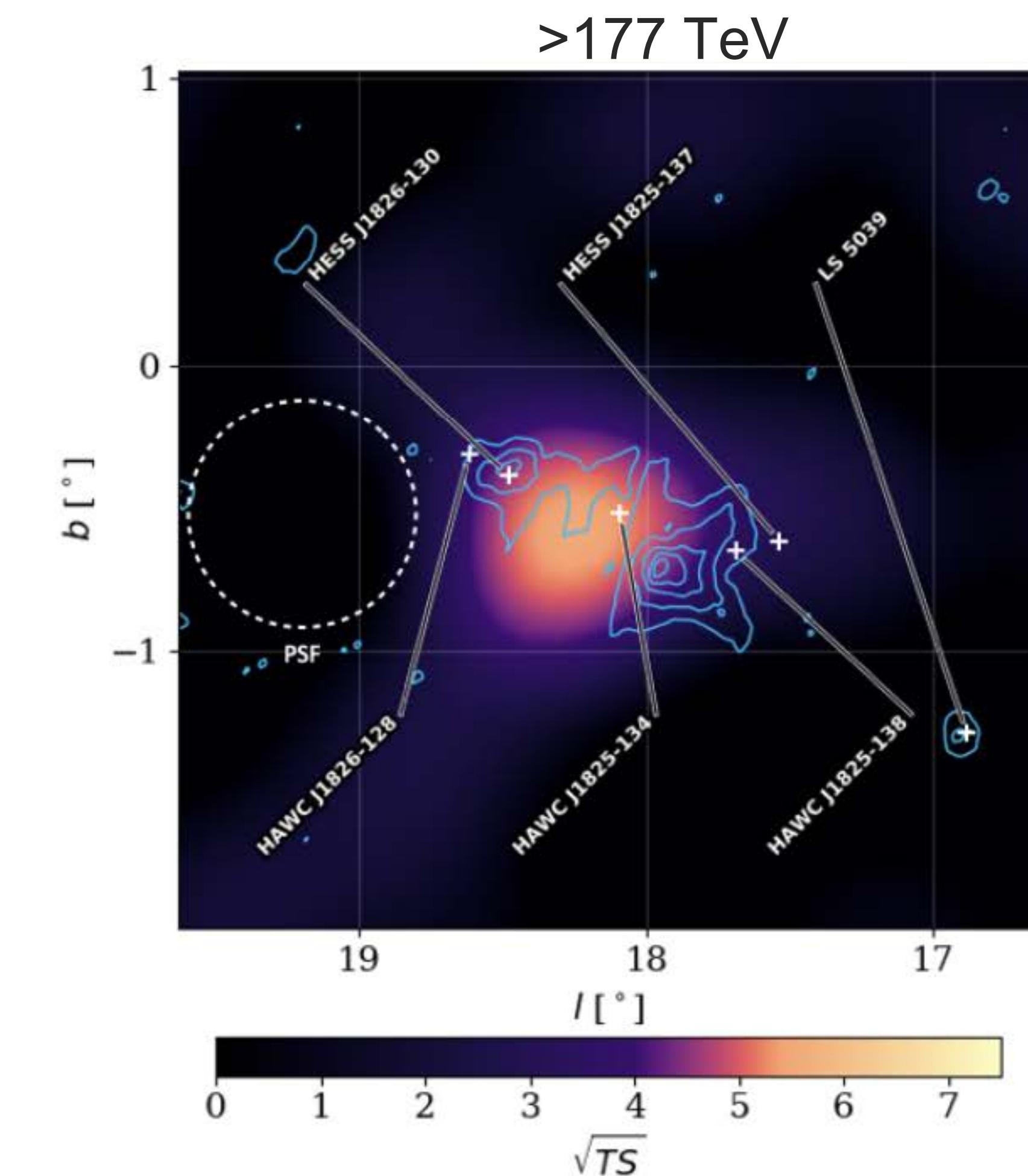
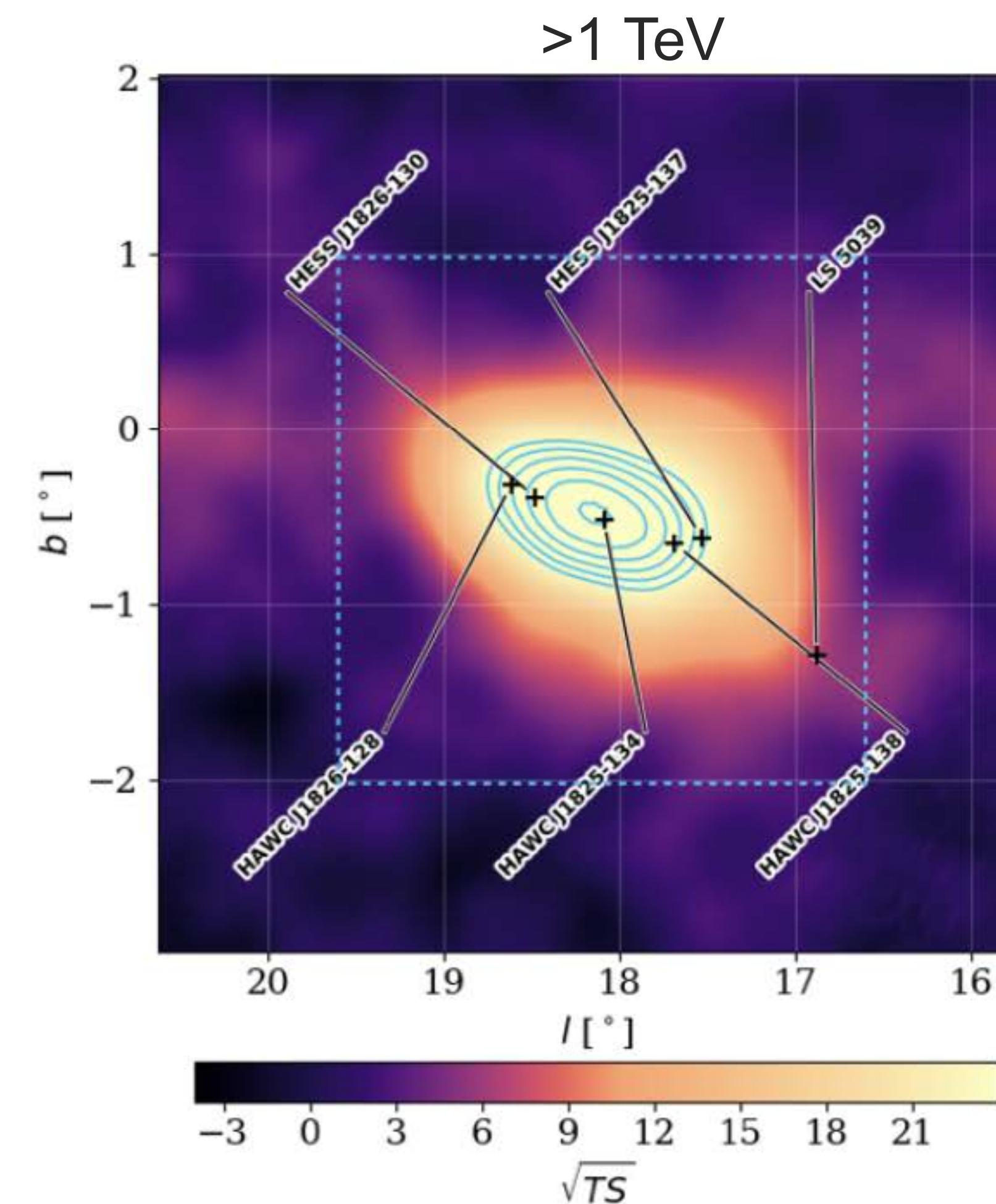
PSR J1826-1256 to HESS J1825-137

Distance: 0.64°



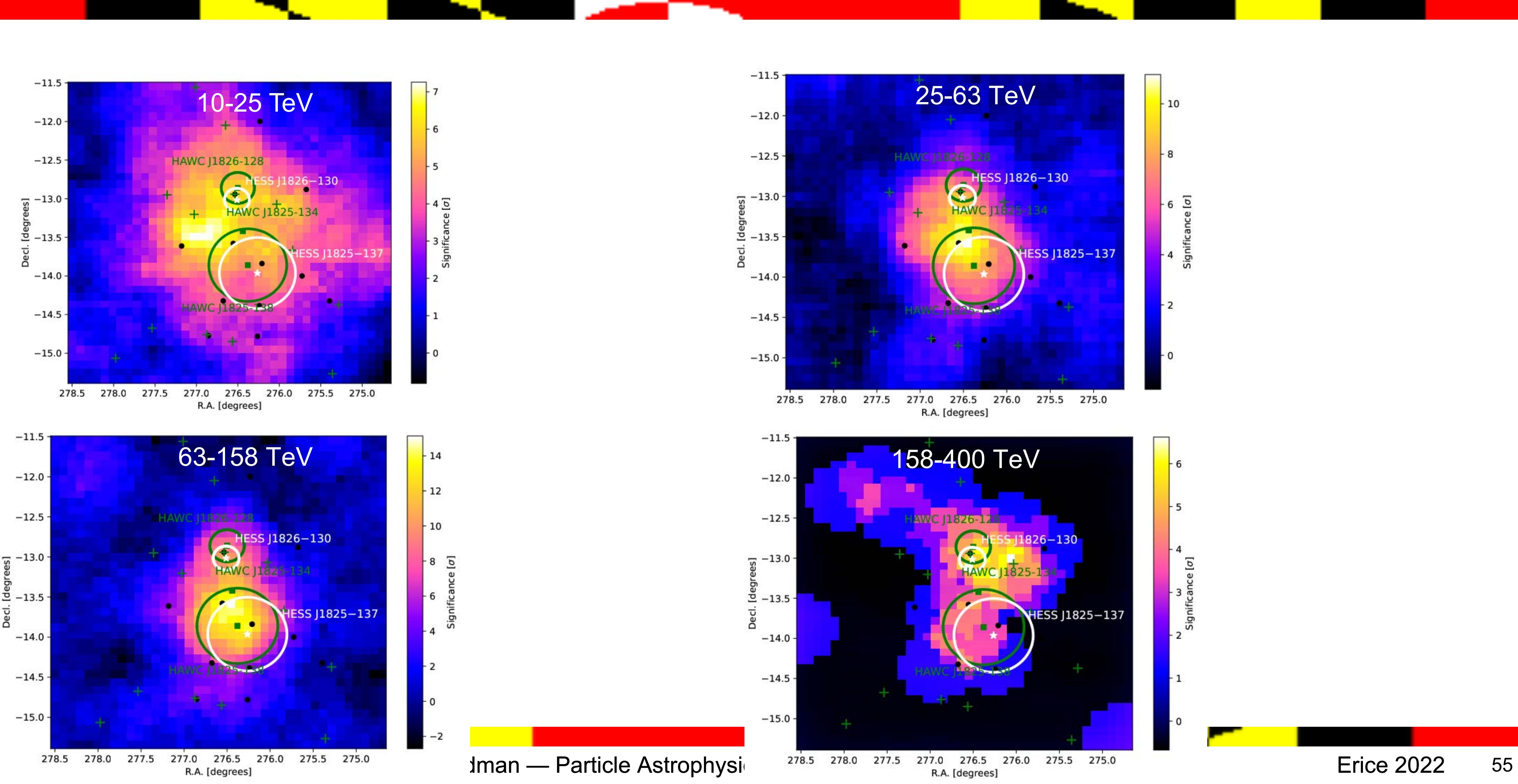
H.E.S.S. Collaboration
2020

eHWC J1825-134

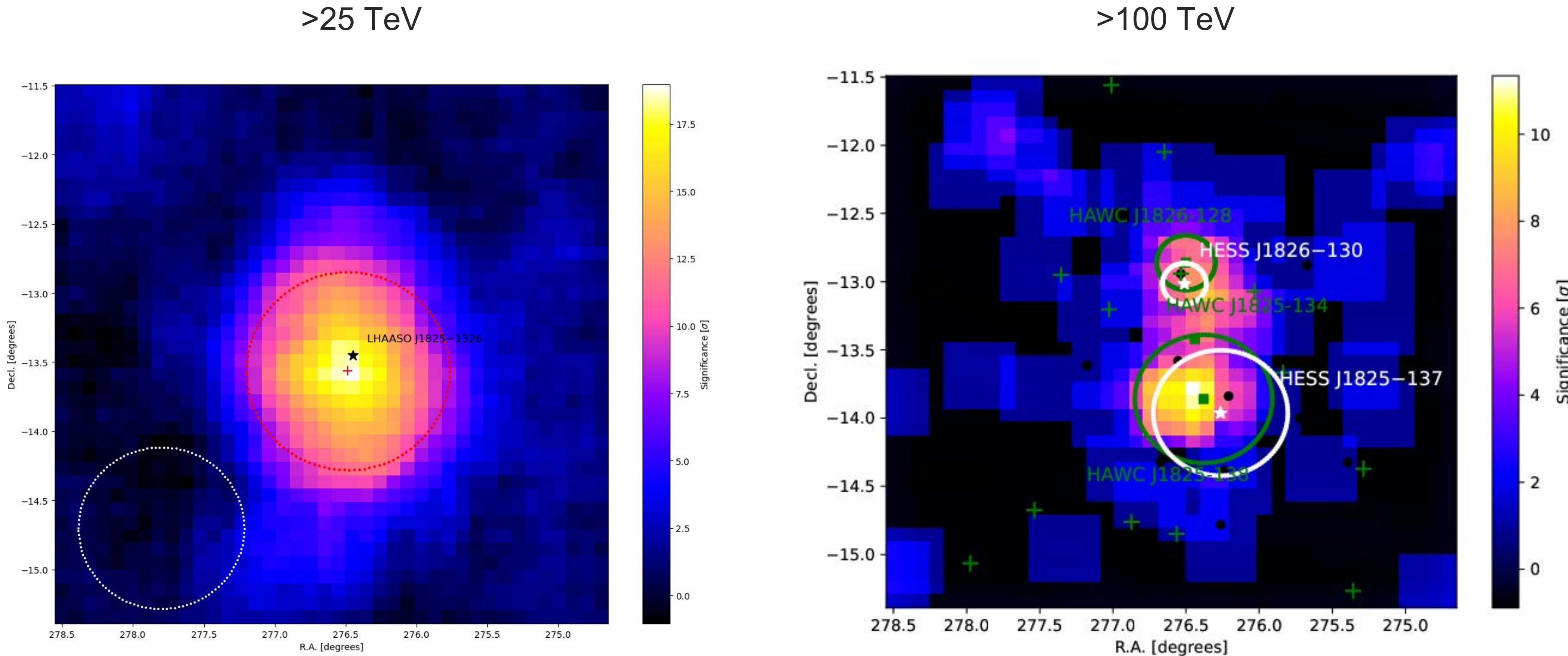


Albert et al. 2021

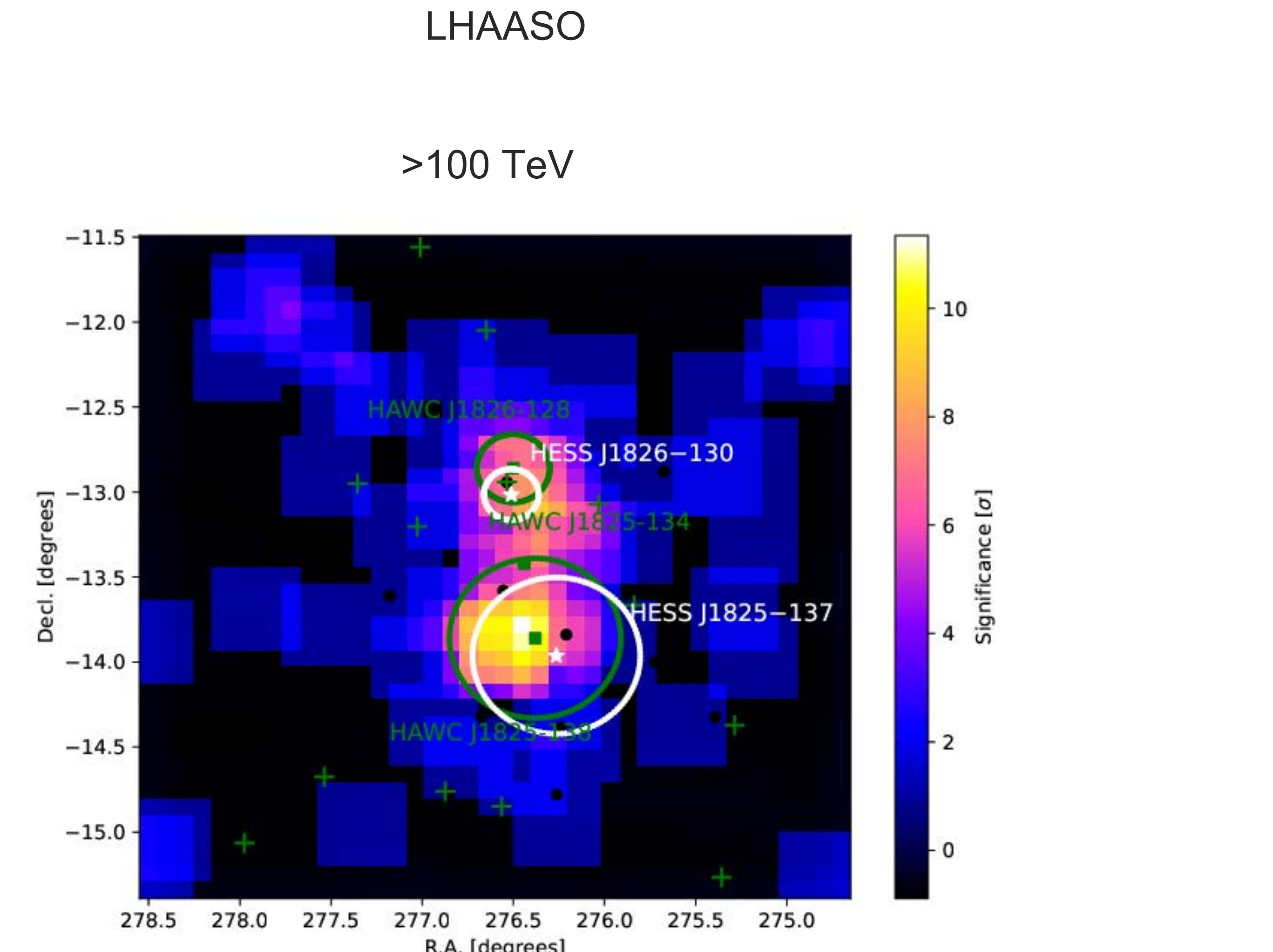
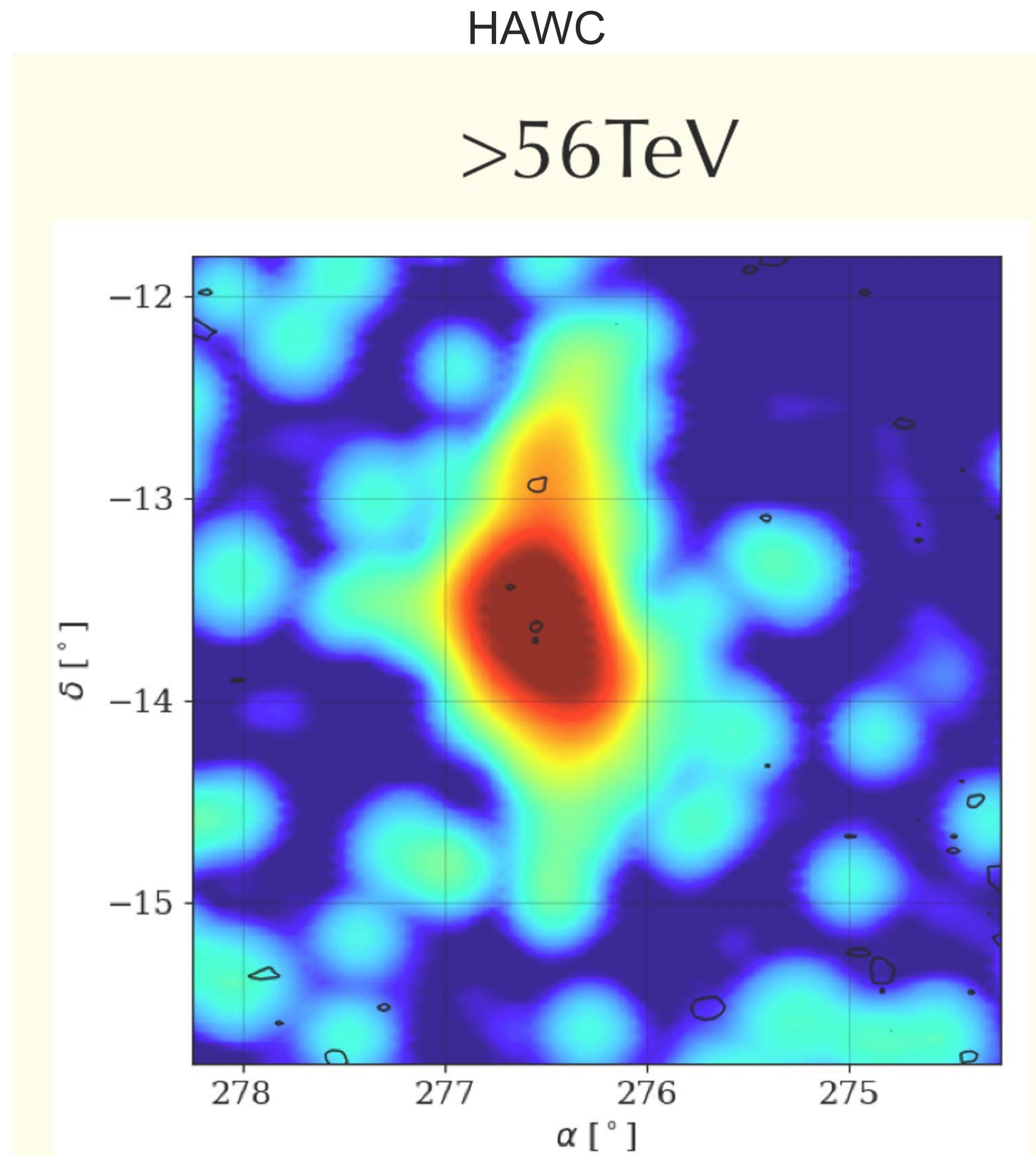
J1825-134 Energy dependent morphology



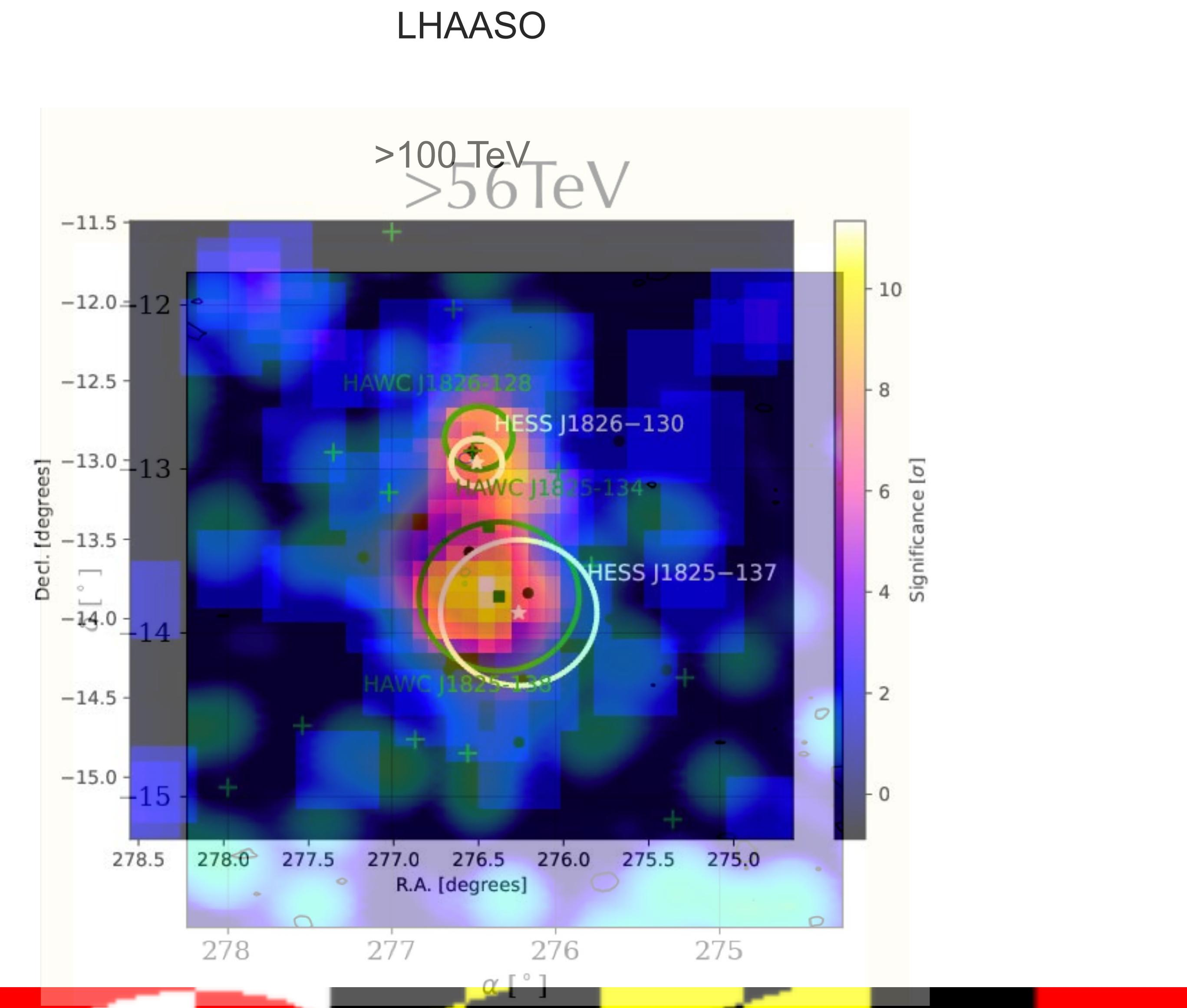
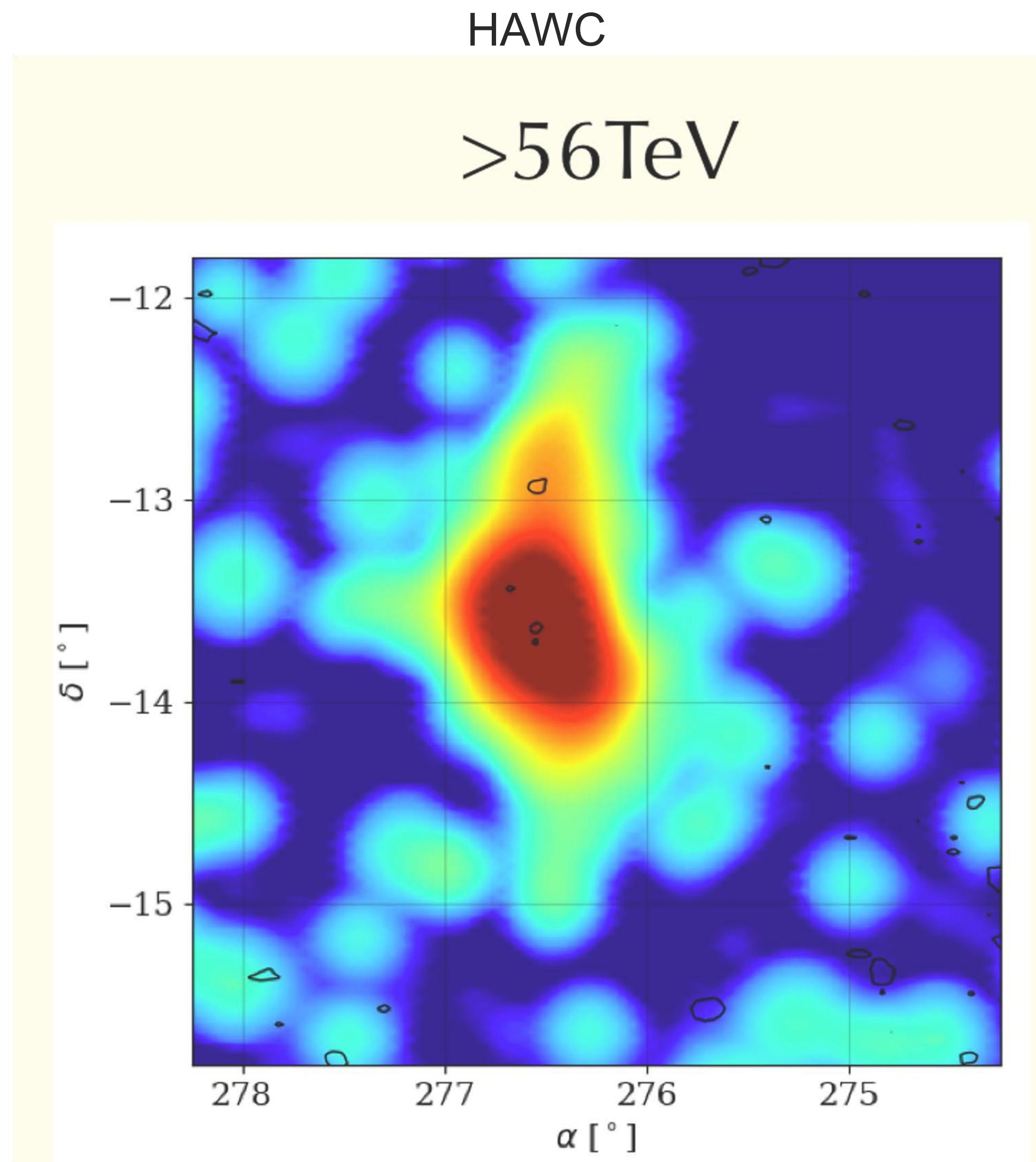
J1825-134 >25 TeV & >100 TeV morphology



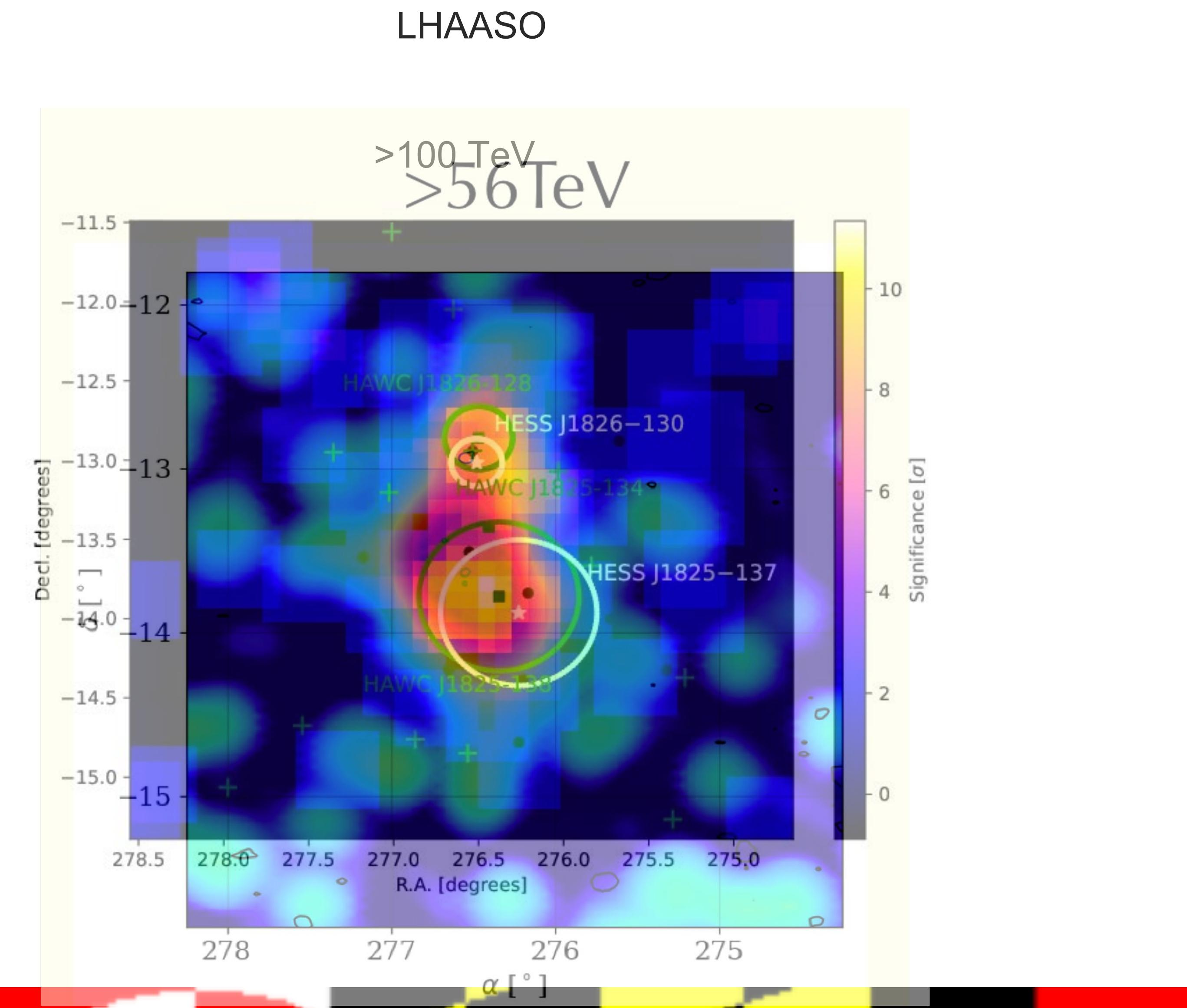
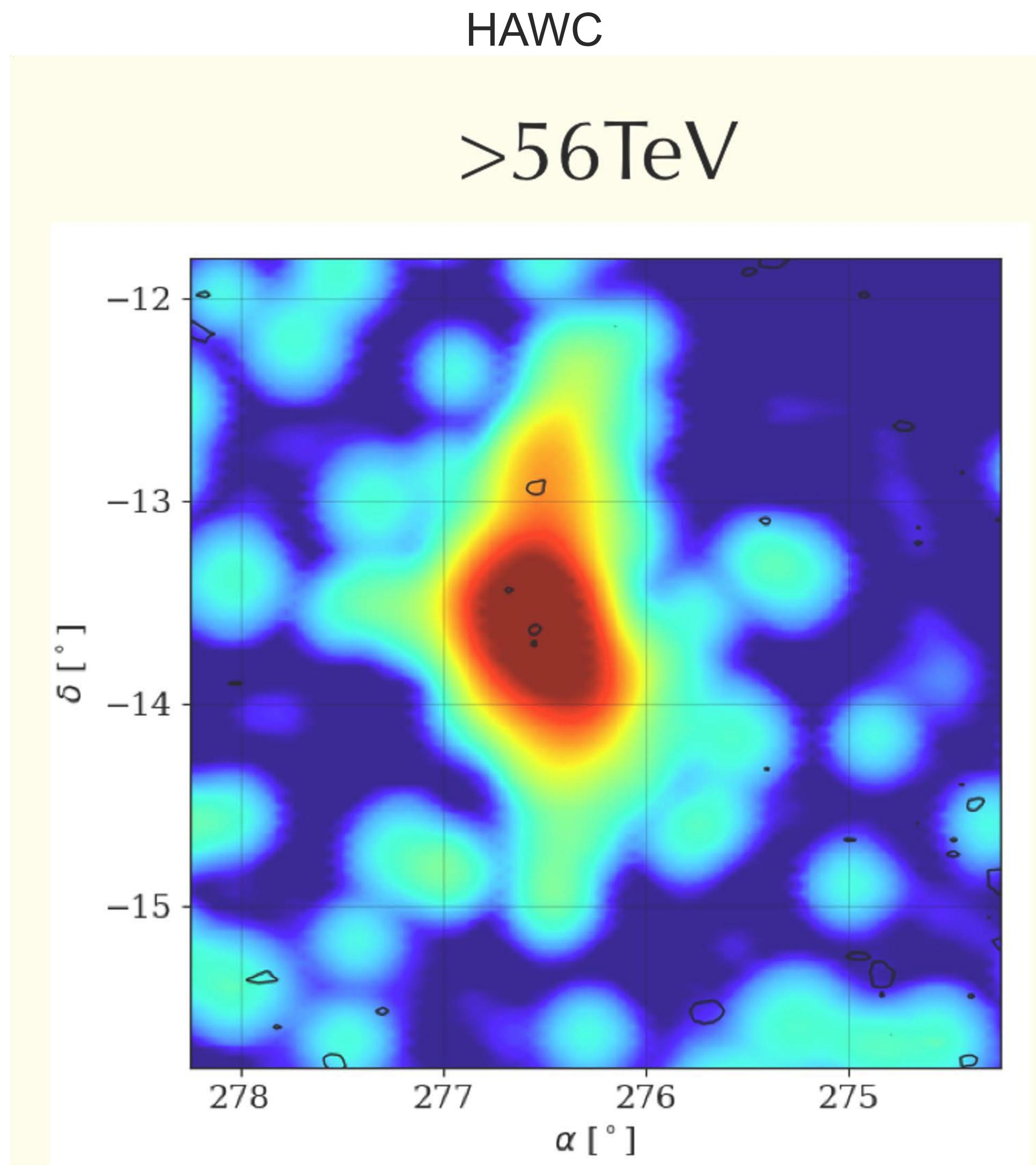
J1825-134 >25 TeV & >100 TeV morphology



J1825-134 >56 TeV & >100 TeV morphology



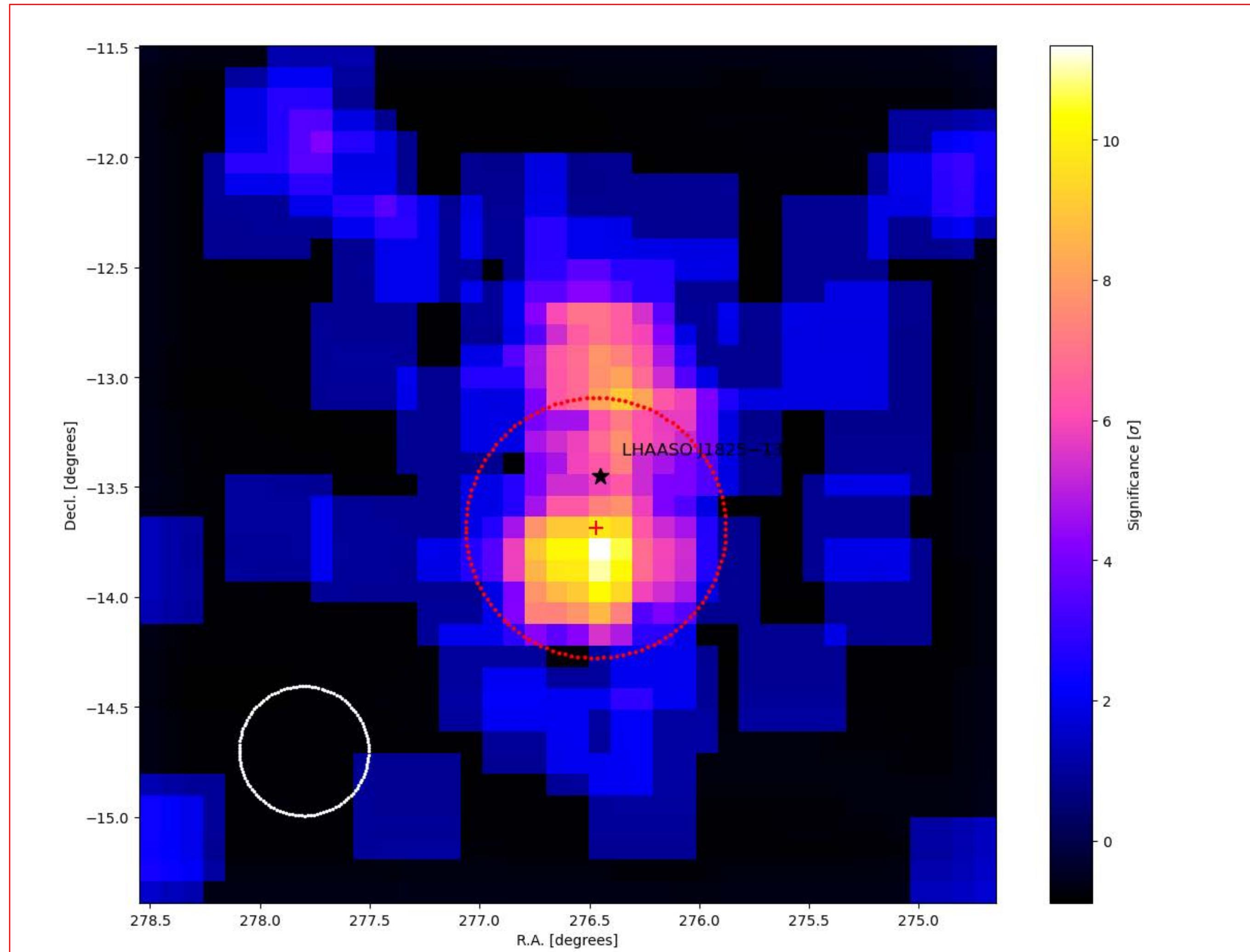
J1825-134 >56 TeV & >100 TeV morphology



>100 TeV morphology

sign=16.4 σ
Extension=0.3°
R.A.=276.45°
Decl.-13.45°

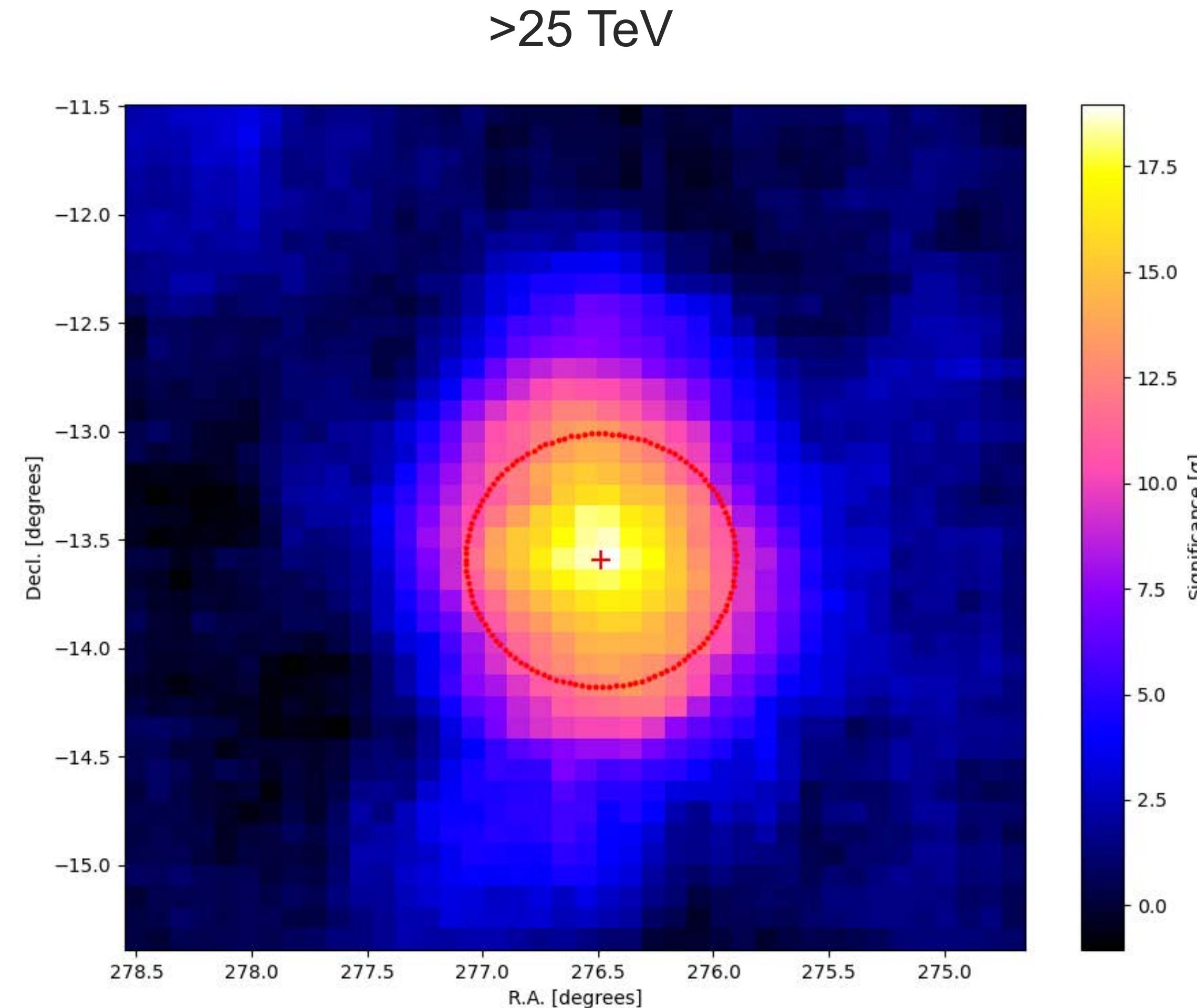
sign=15.0 σ
Extension=0.34
ra = 276.47° +0.12° -0.15°
dec = -13.69° +0.33° -0.18°



Morphology test: point-like source

ra = $276.49^\circ \pm 0.03^\circ$
Dec = $-13.59^\circ \pm 0.04^\circ$
PSF(σ)= 0.387°

-loglikelihood:
 $L_0=1684.56$
 $L_1=1470.97$
TS: 427.18



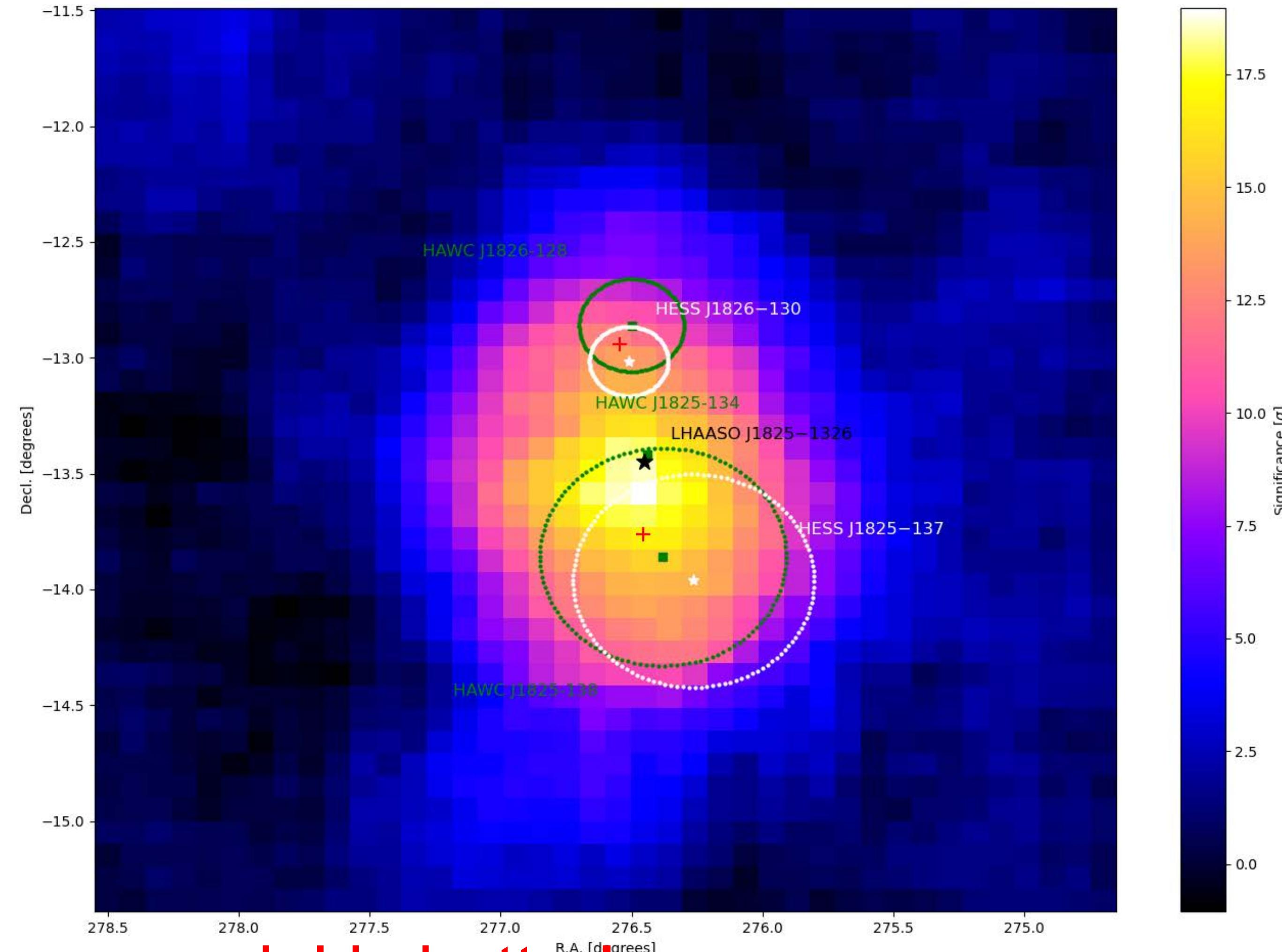
Morphology test: two point-like sources

$\text{ra} = 276.46^\circ \pm 0.04^\circ$
 $\text{Dec} = -13.76^\circ \pm 0.05^\circ \pm 0.06^\circ$

$\text{ra} = 276.54^\circ \pm 0.06^\circ$
 $\text{Dec} = -12.94^\circ \pm 0.10^\circ \pm 0.11^\circ$

-loglikelihood:
 $L_0=1684.56$
 $L_1=1454.14$
 $TS_2\text{pts}=33.67$

$TS_{\text{ext}} < TS_{\text{2pts}}$



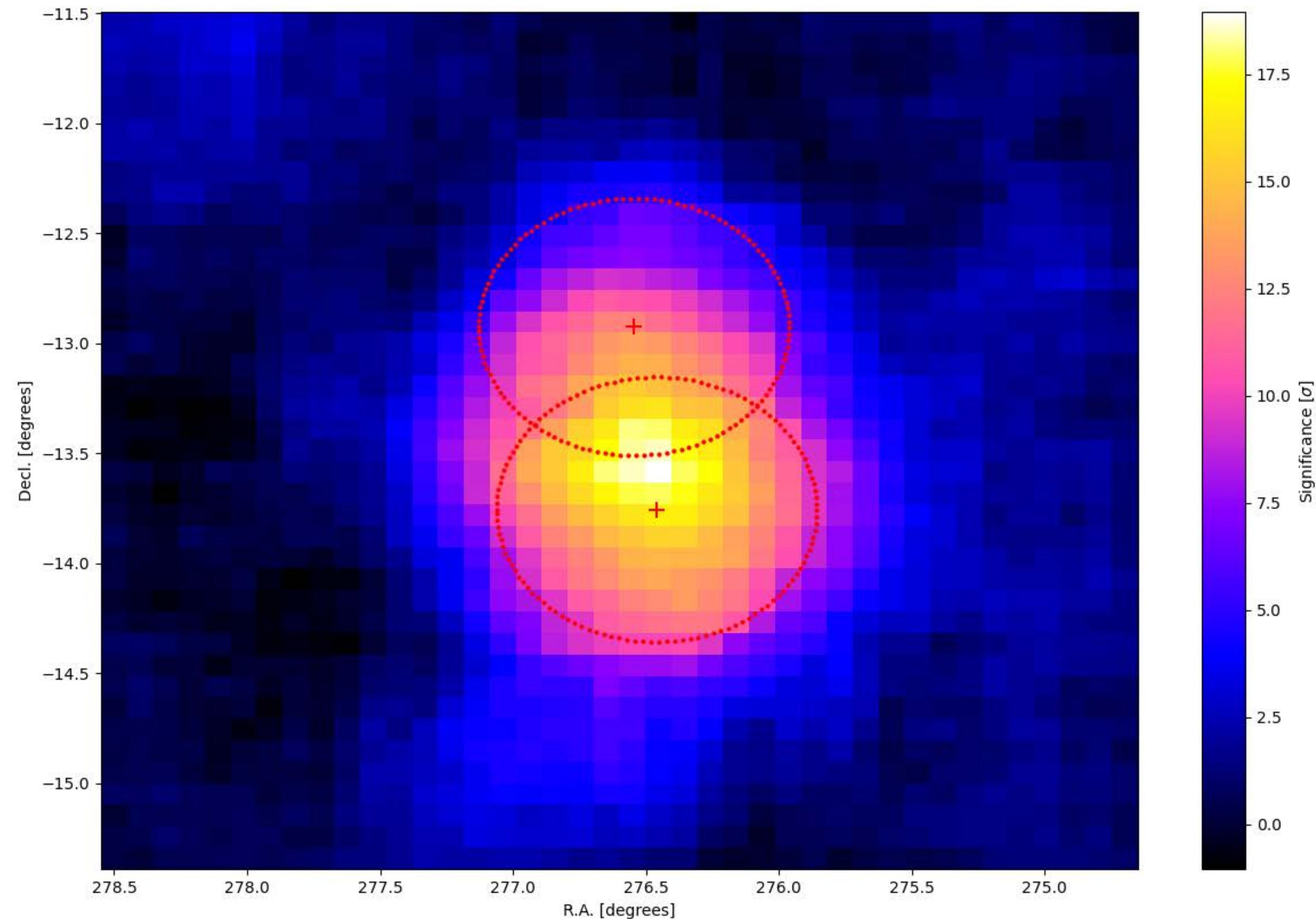
Two sources model is better!

Morphology test: 2-D Gaussian+PS

TS_ext=0.68
sigma_ul=0.33°
(95%)

TS_ext=0.41
sigma_ul=0.25°(95%)

Two point-like sources!



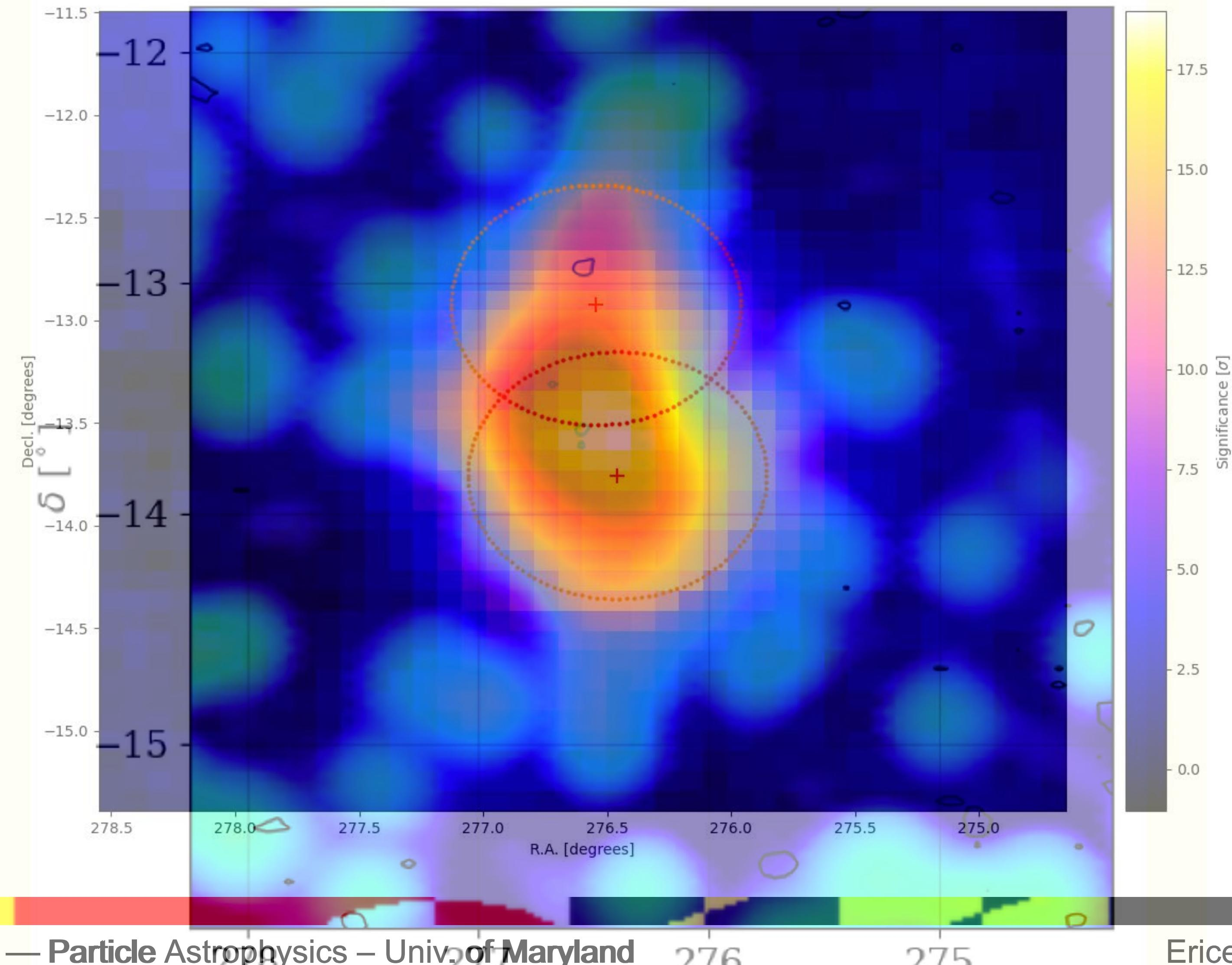
Morphology test: 2-D Gaussian+PS

>56 TeV

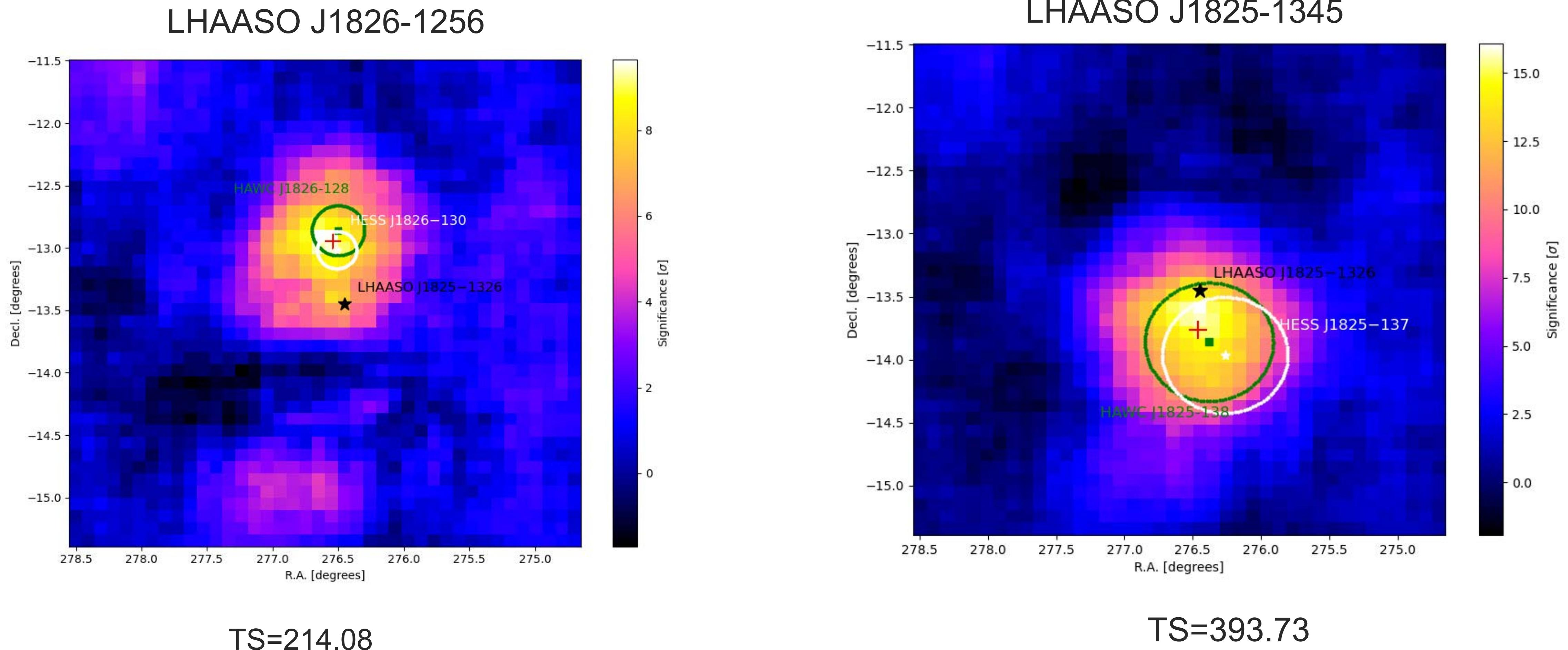
TS_ext=0.68
sigma_ul=0.33°
(95%)

TS_ext=0.41
sigma_ul=0.25°(95%)

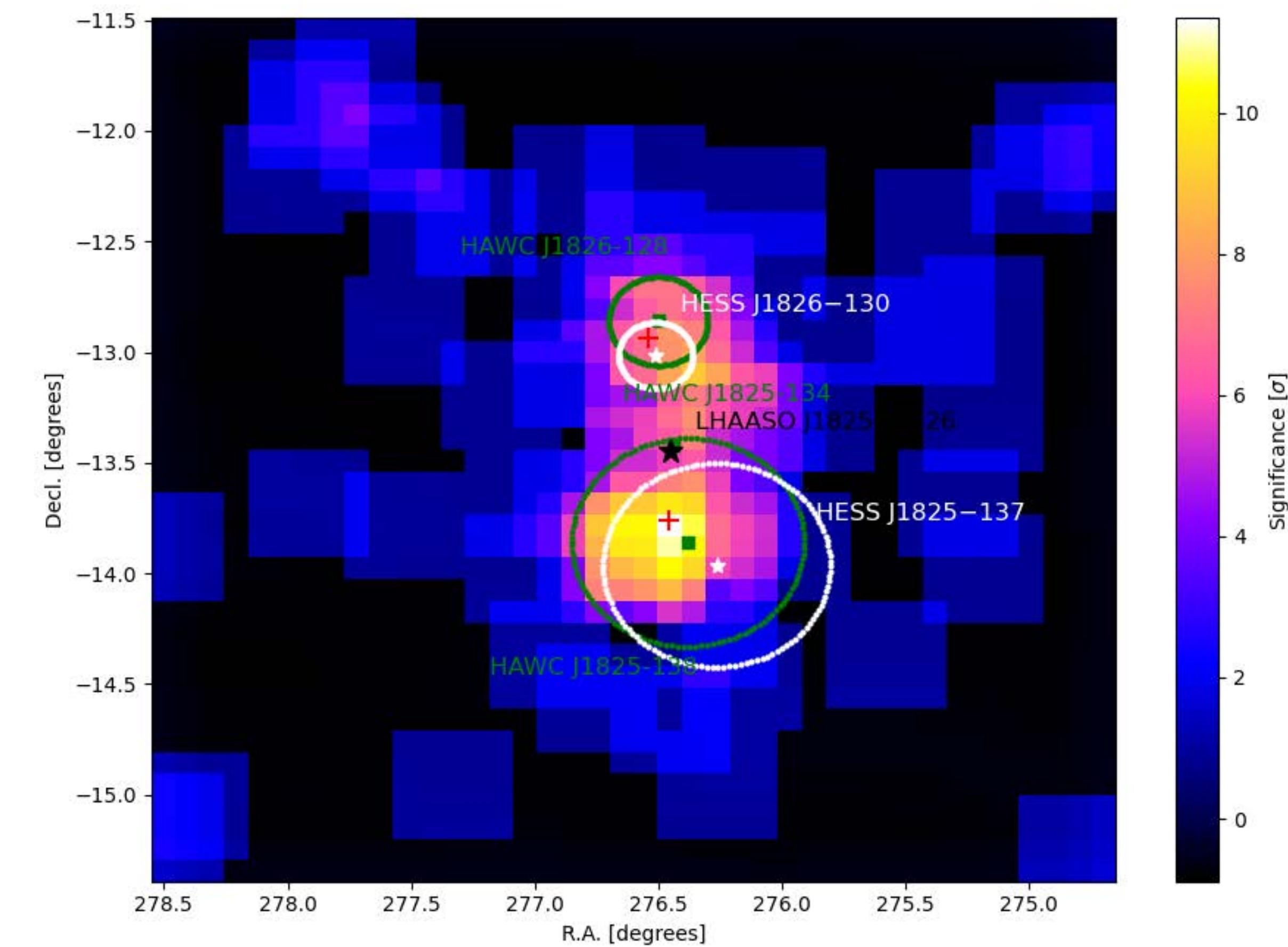
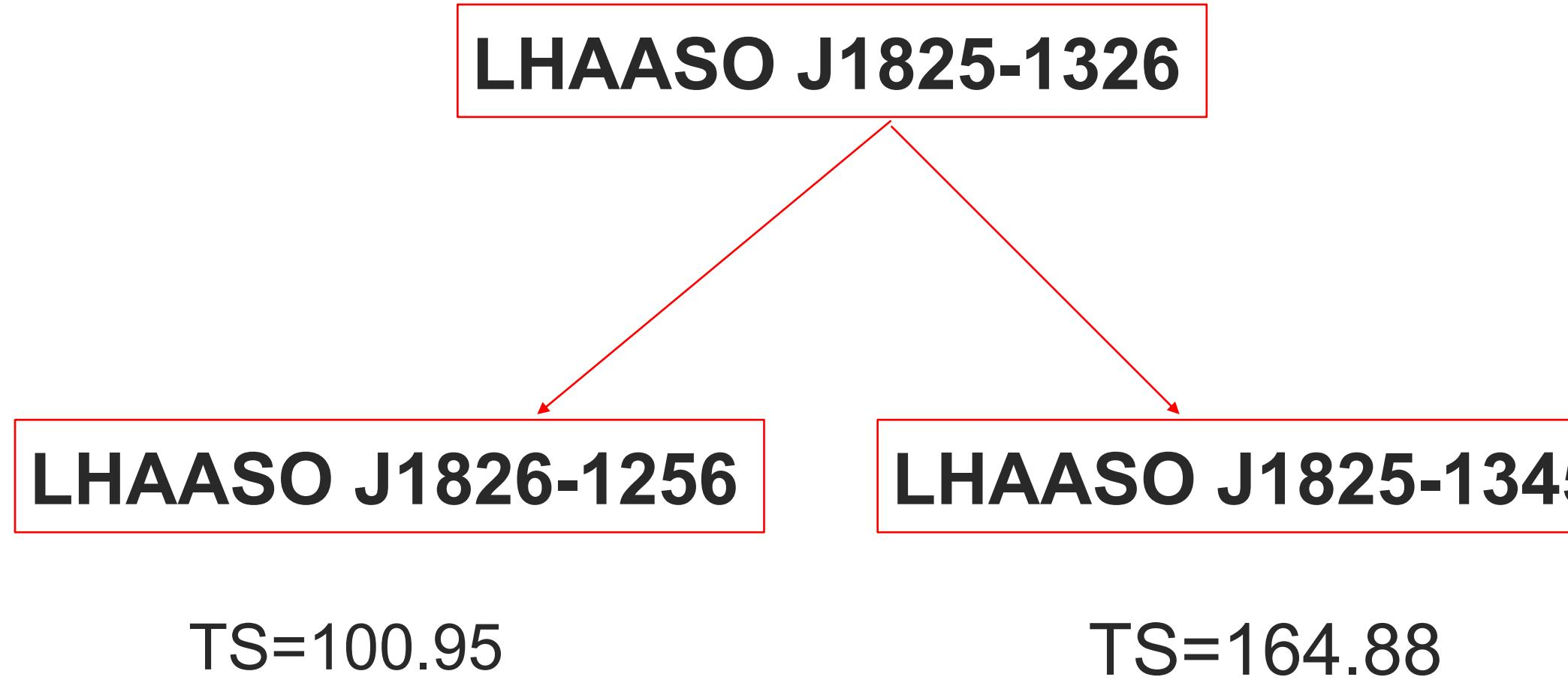
Two point-like sources!



LHAASO J1826-1256 & J1825-1345(>25 TeV)



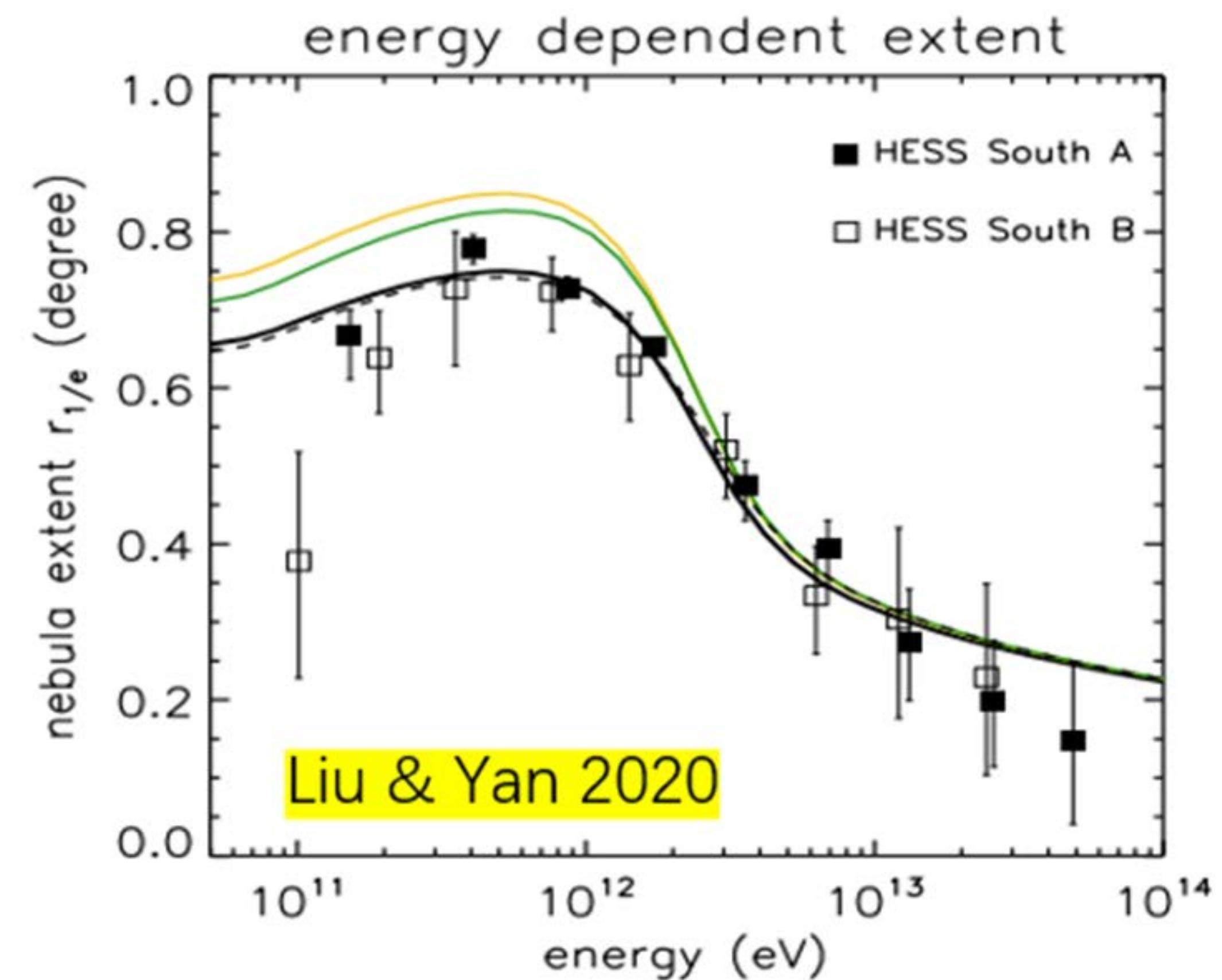
LHAASO J1826-1256 & J1825-1345(>100 TeV)



Summary

Two UHE sources:
LHAASO J1825-1345 & LHAASO J1826-1256
Associated with HESS and observation,

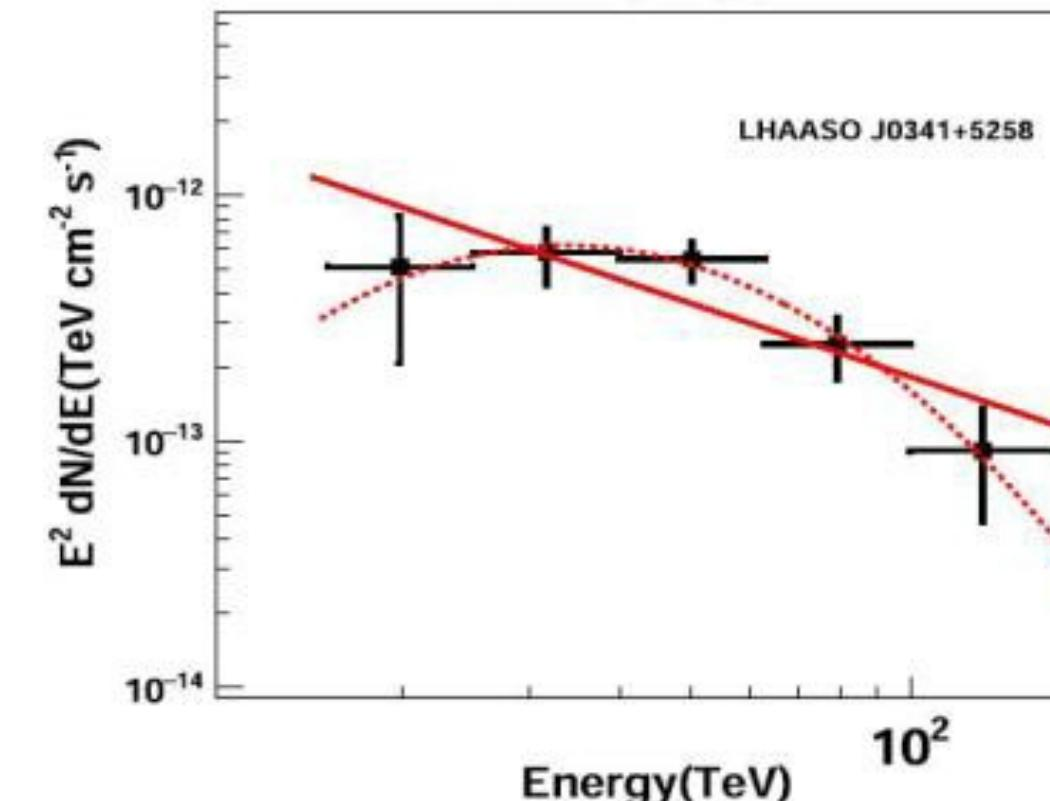
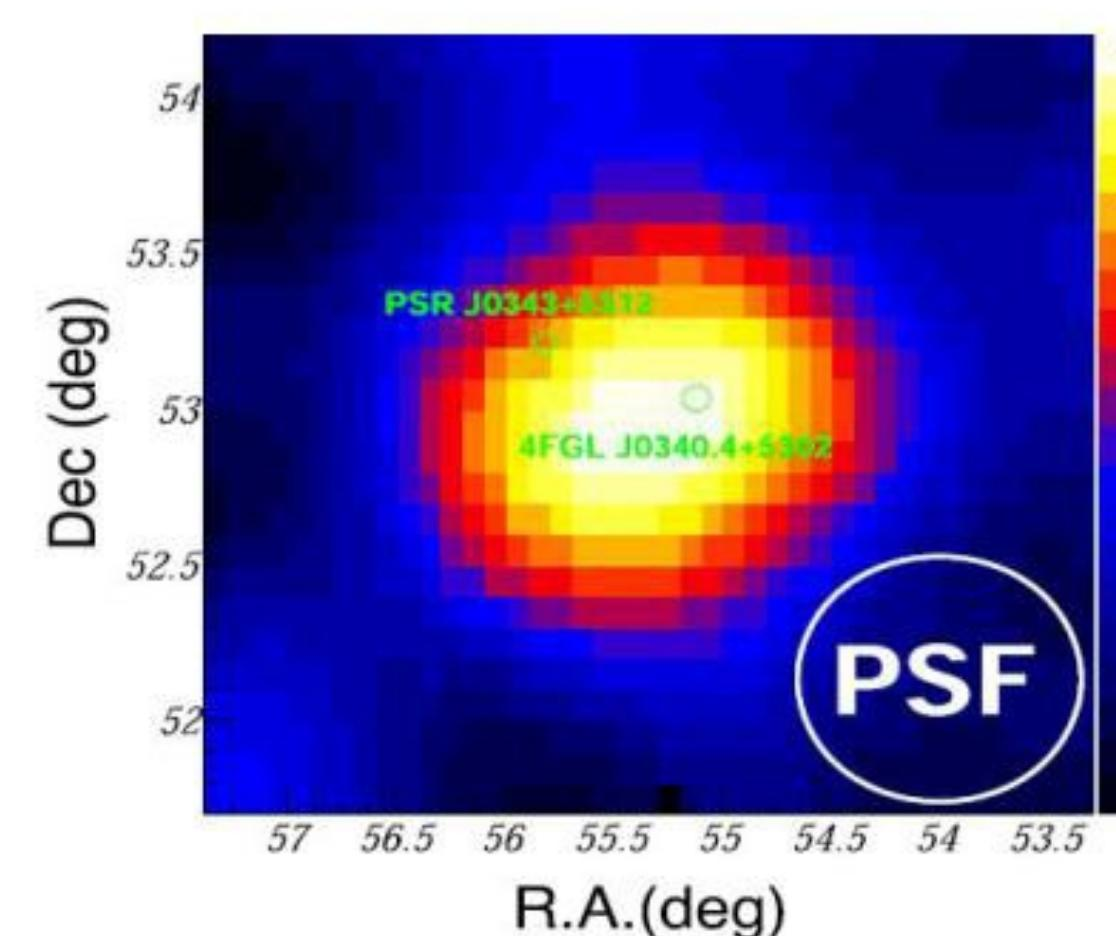
HESS J1825-137



New Source Discovery

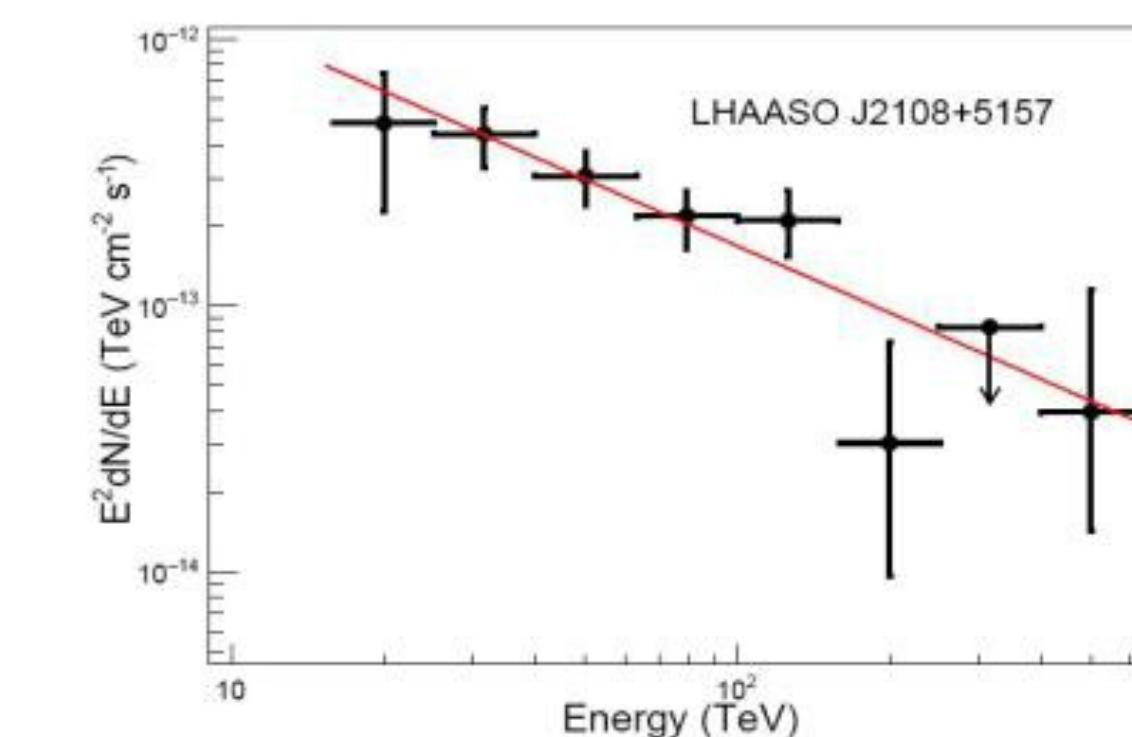
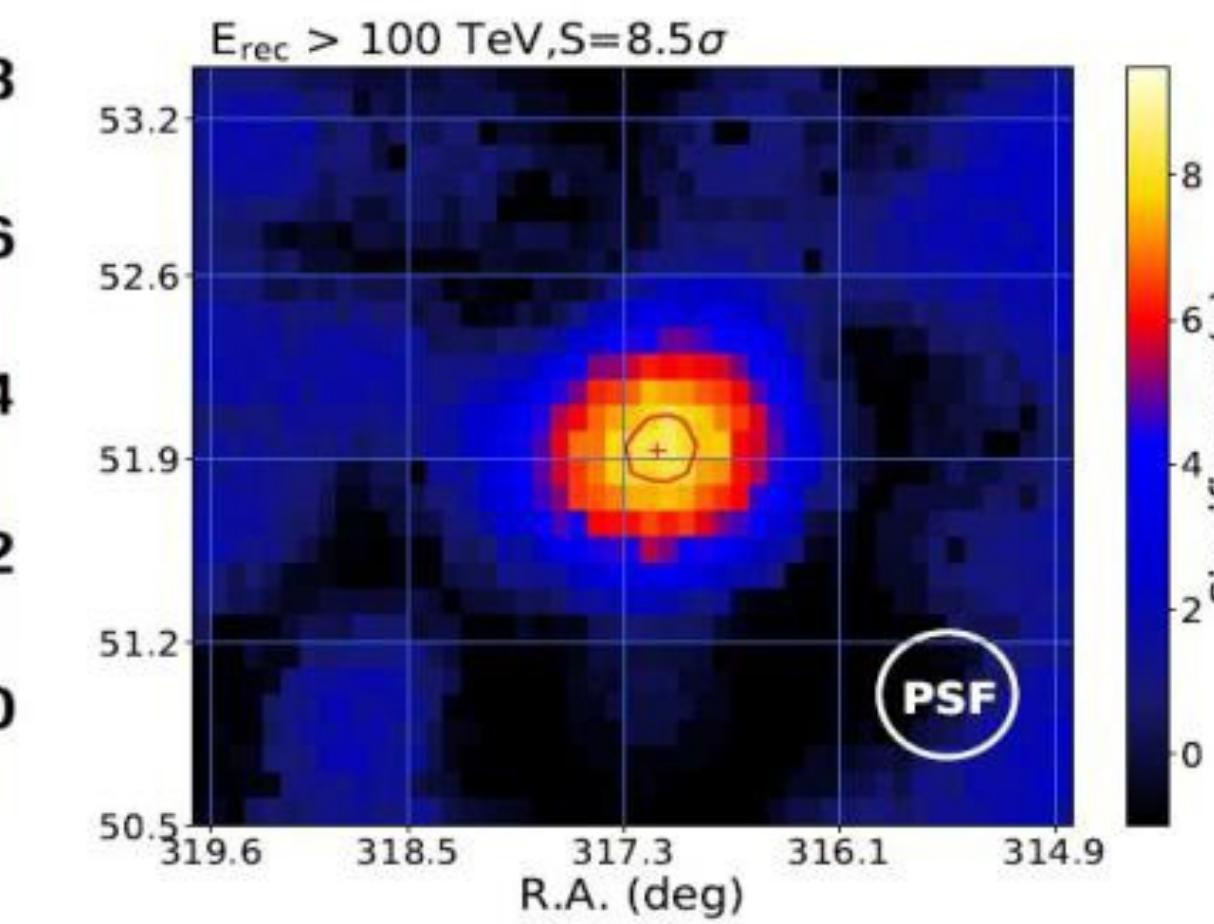
- ❖ WCDA has accumulated data for 16 months
- ❖ KM2A for 12 months
- ❖ LHAASO catalog Ver-1 will be published soon with many new VHE/UHE sources discovered

LHAASO J0341+5258



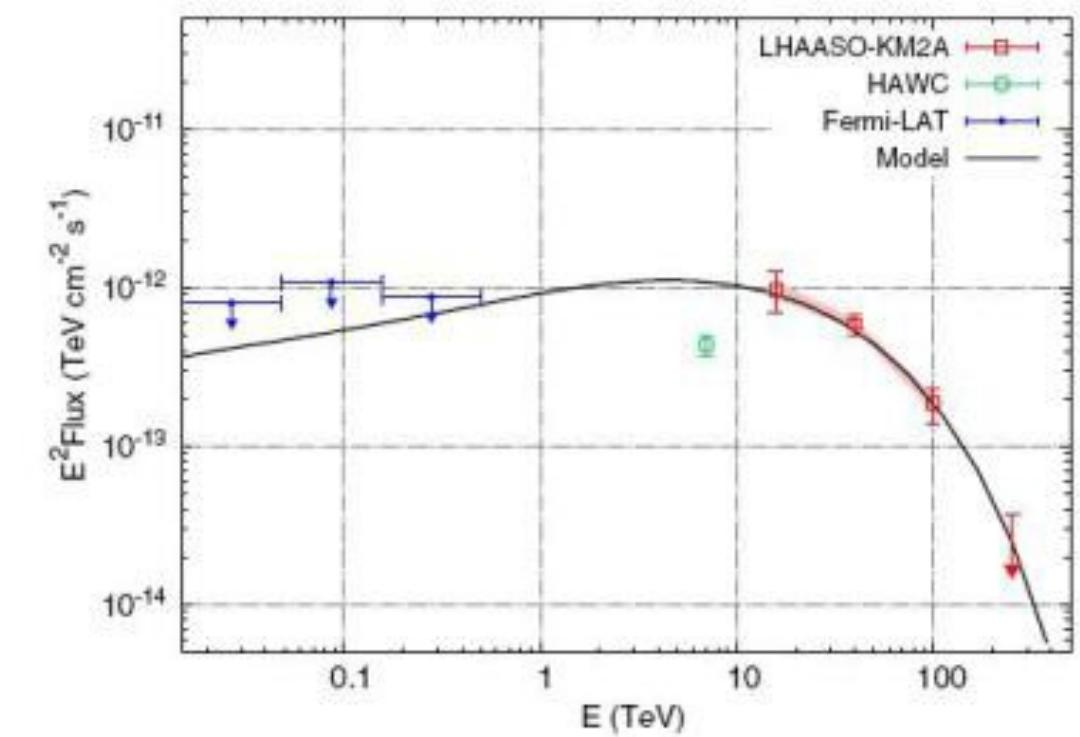
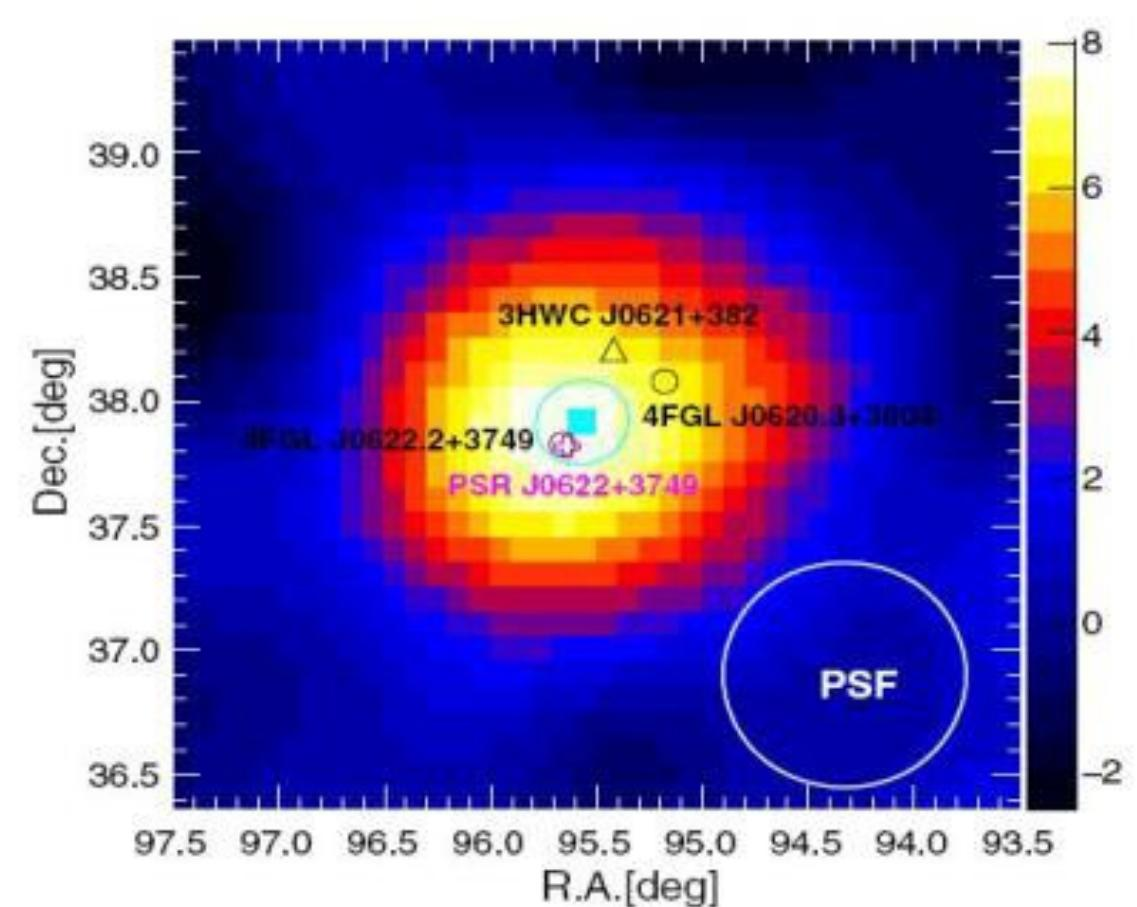
ApJL 917:L4 (2021)

LHAASO J2108+5157



ApJL 919:L22 (2021)

Halo of PSR J0622 + 3749



PRL 126:241103 (2021)



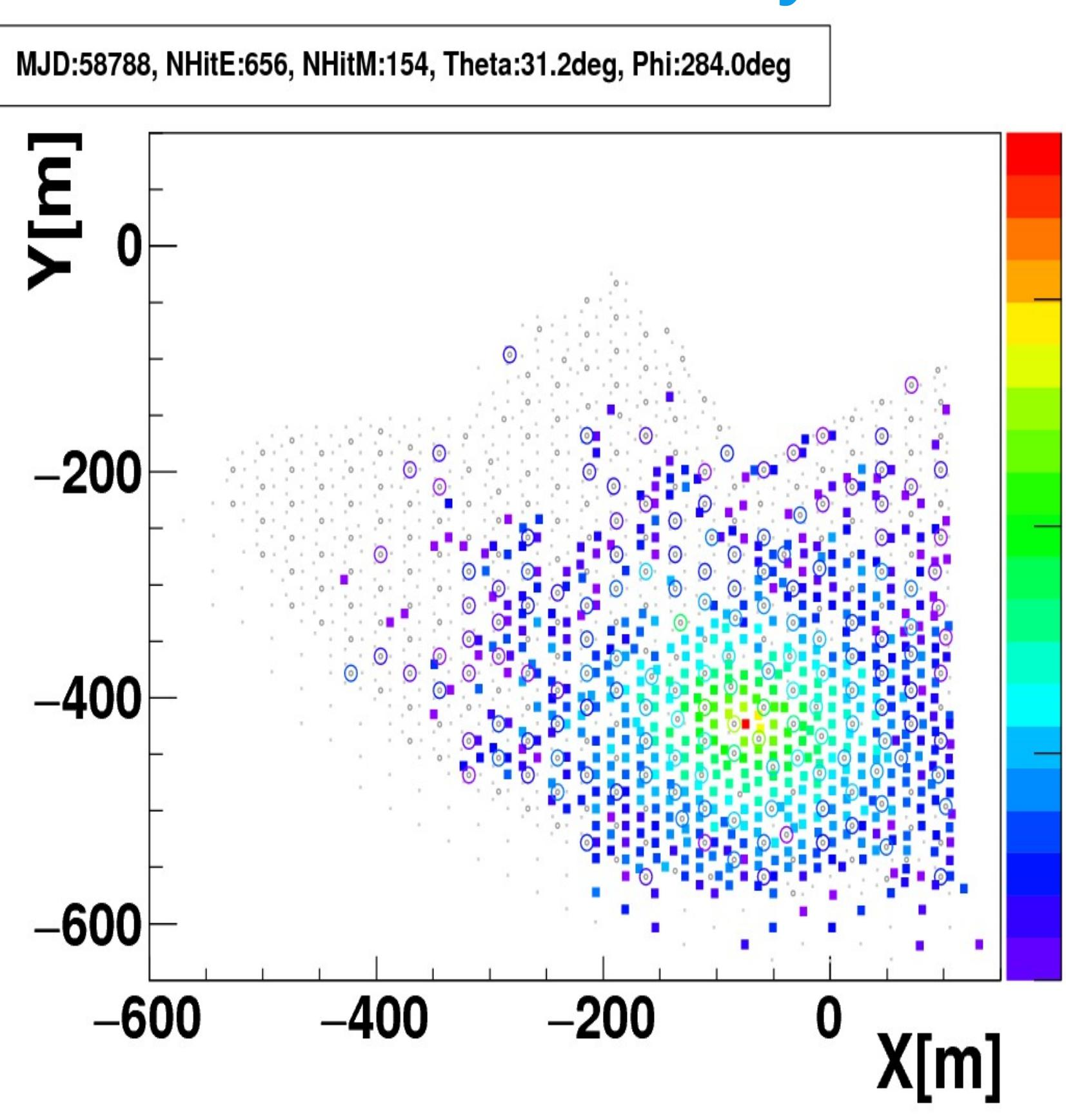
KM2A

Selection of γ -rays out of CR background

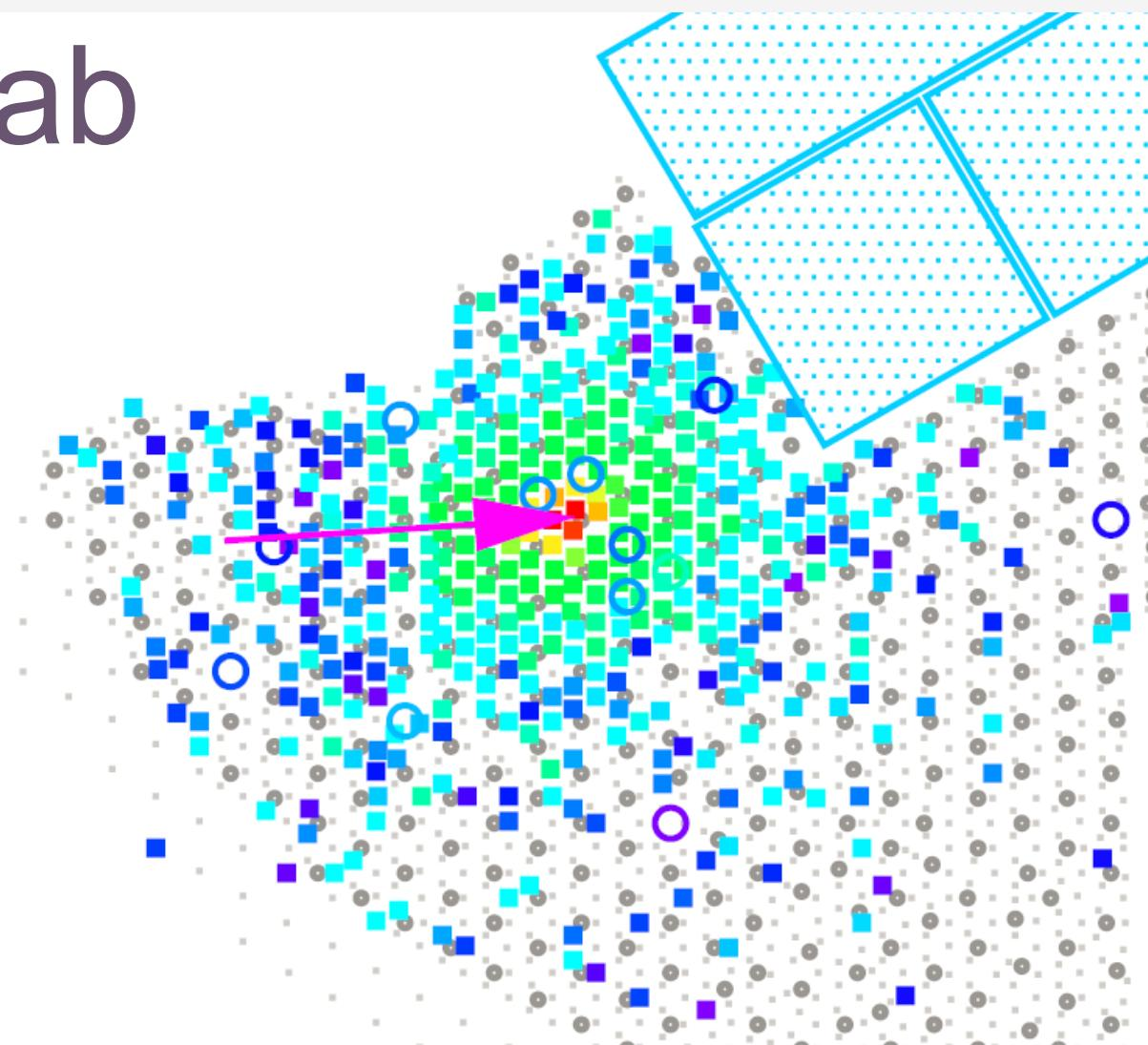
Active Area for Muons vs. Array Area: 4%

~1 PeV CR event: many muons

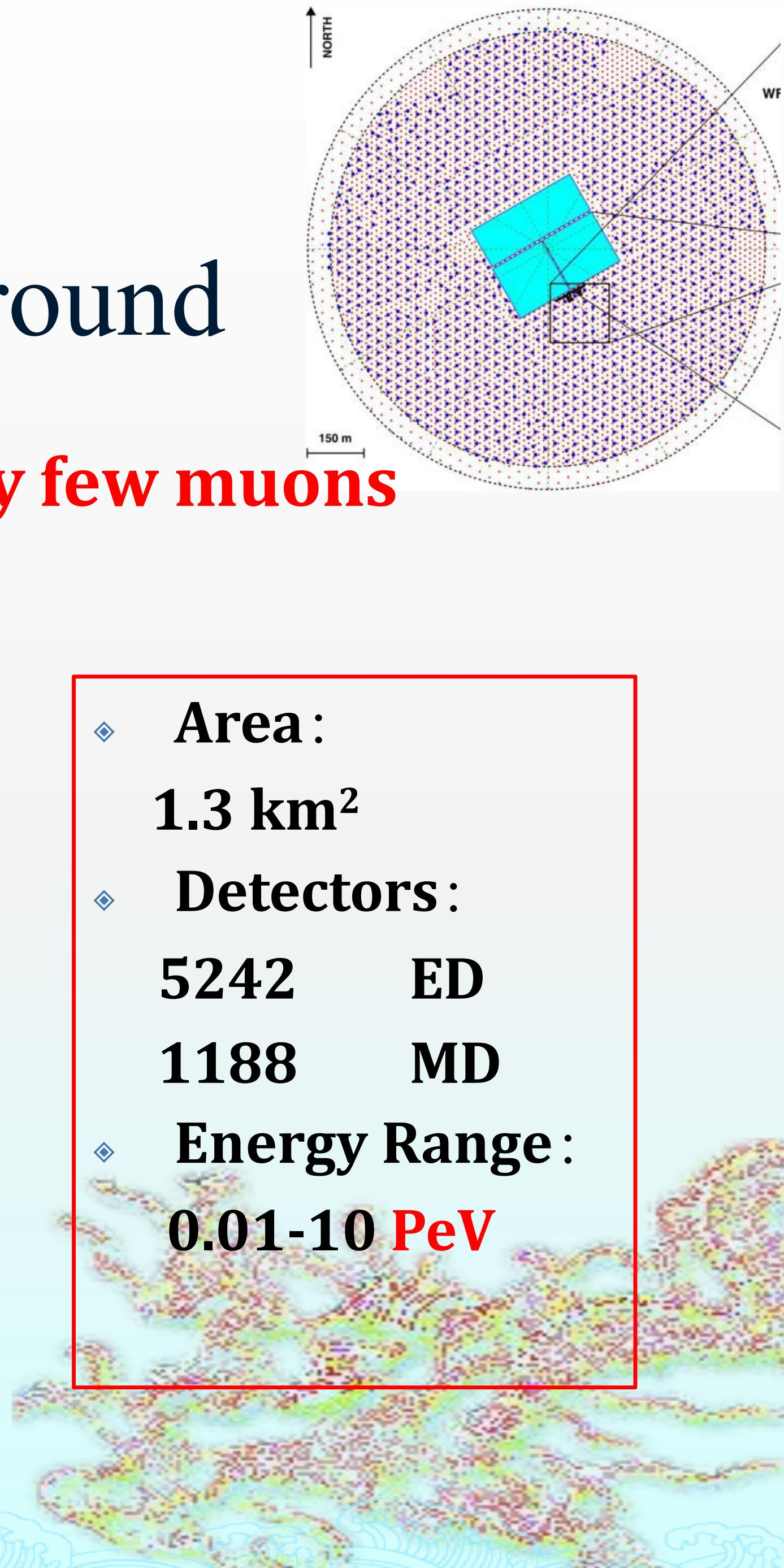
~ 1 PeV γ -ray event : very few muons



**~1 PeV from the
Crab**



- ❖ **Area :**
1.3 km²
- ❖ **Detectors :**
5242 ED
1188 MD
- ❖ **Energy Range :**
0.01-10 PeV

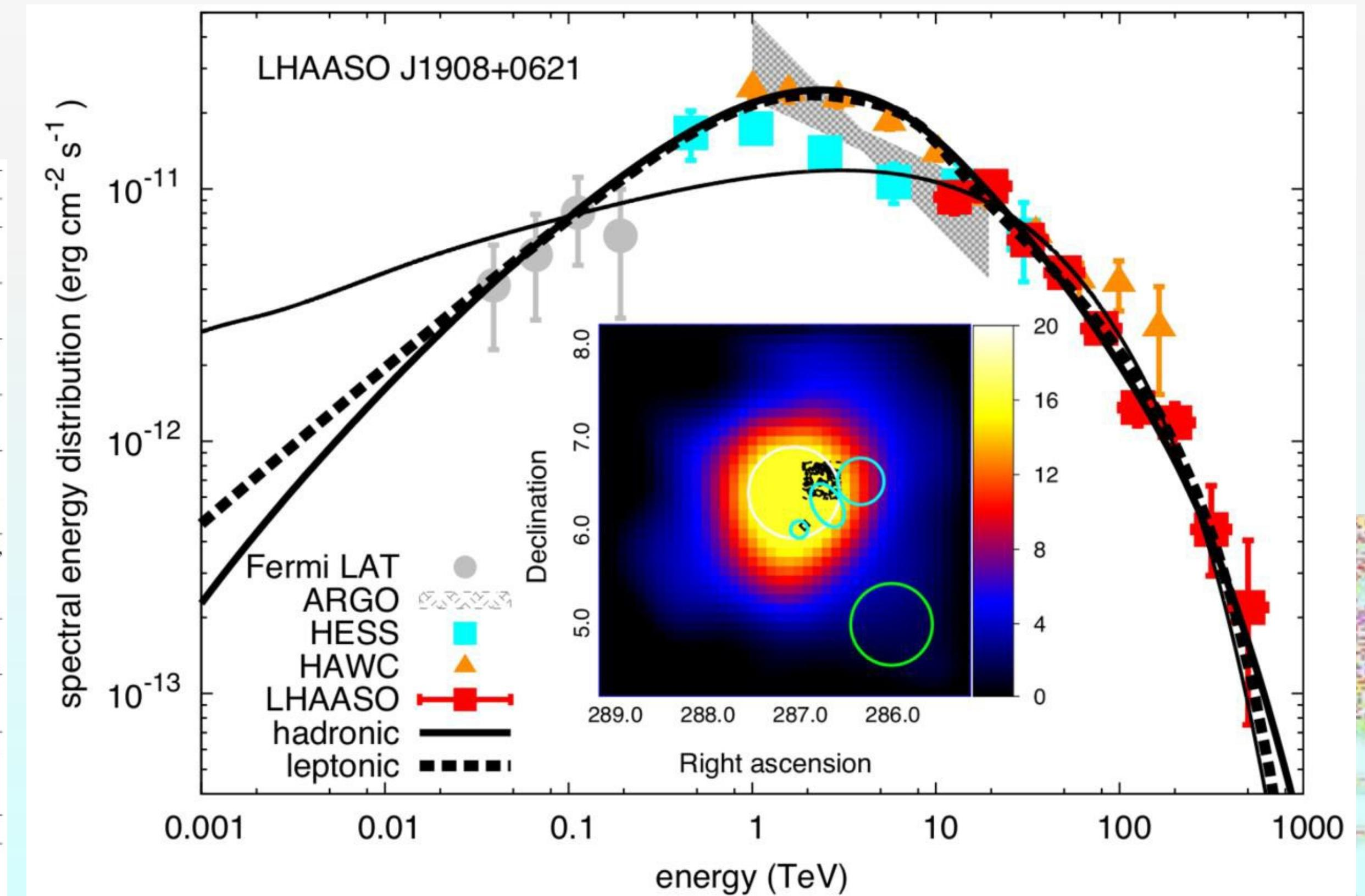


Discovery Using KM2A Onset of UHE γ -ray Astronomy

$E > 0.1 \text{ PeV}$: all types of candidates

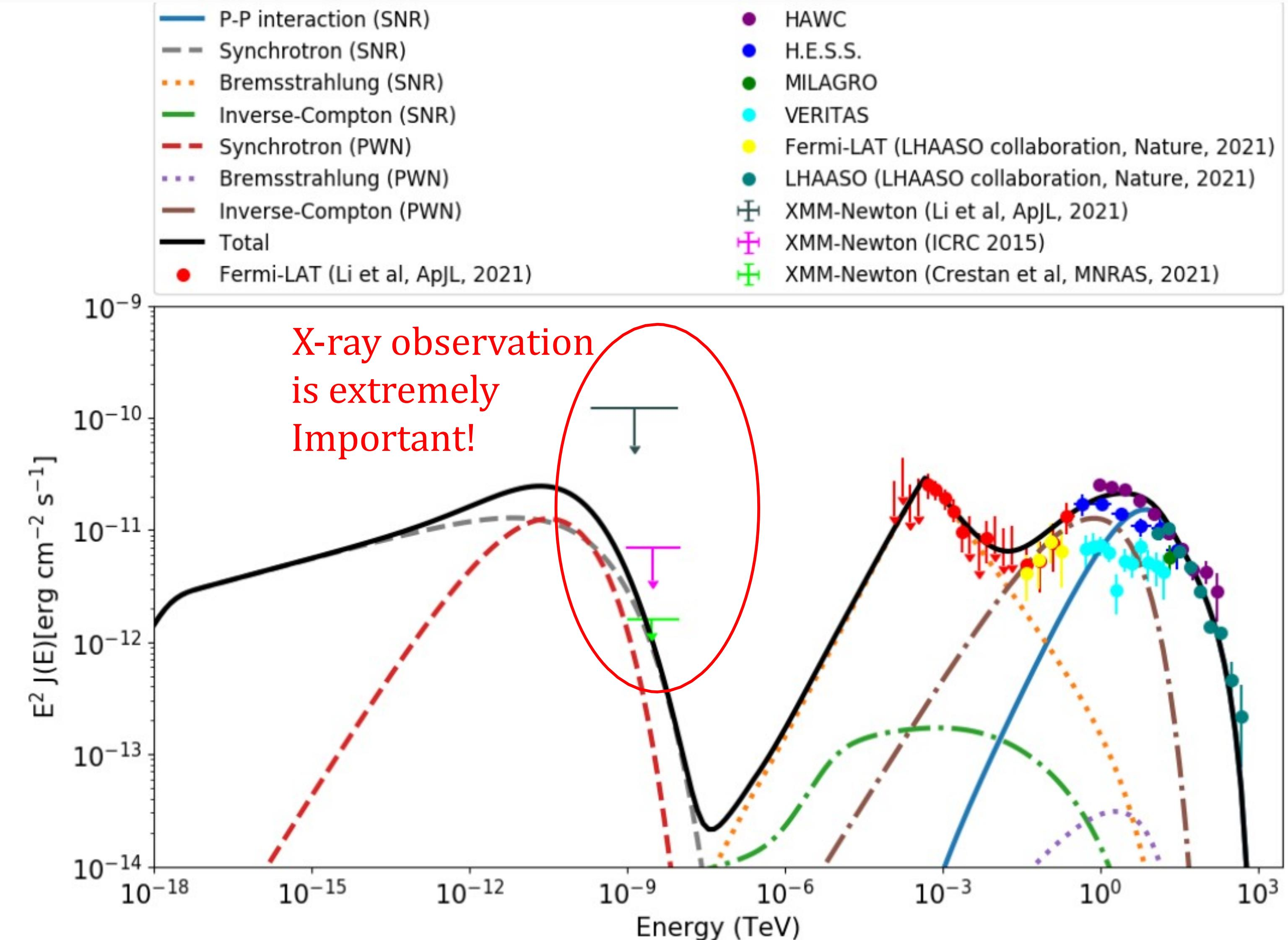
- ◆ Spectroscopy: 15% resolution
- ◆ Morphology: 0.25° PSF

LHAASO Source	Possible Origin	Type	Distance (kpc)	Age (kyr) ^a	L_s (erg/s) ^b	Potential TeV Counterpart ^c
LHAASO J0534+2202	PSR J0534+2200	PSR	2.0	1.26	4.5×10^{38}	Crab, Crab Nebula
LHAASO J1825-1326	PSR J1826-1334	PSR	3.1 ± 0.2^d	21.4	2.8×10^{36}	HESS J1825-137, HESS J1826-130,
	PSR J1826-1256	PSR	1.6	14.4	3.6×10^{36}	2HWC J1825-134
LHAASO J1839-0545	PSR J1837-0604	PSR	4.8	33.8	2.0×10^{36}	2HWC J1837-065, HESS J1837-069,
	PSR J1838-0537	PSR	1.3^e	4.9	6.0×10^{36}	HESS J1841-055
LHAASO J1843-0338	SNR G28.6-0.1	SNR	9.6 ± 0.3^f	$< 2^f$	—	HESS J1843-033, HESS J1844-030,
LHAASO J1849-0003	PSR J1849-0001	PSR	7 ^g	43.1	9.8×10^{36}	HESS J1849-000, 2HWC J1849+001
	W43	YMC	5.5^h	—	—	
LHAASO J1908+0621	SNR G40.5-0.5	SNR	3.4 ⁱ	$\sim 10 - 20^j$	—	MGRO J1908+06, HESS J1908+063,
	PSR 1907+0602	PSR	2.4	19.5	2.8×10^{36}	ARGO J1907+0627, VER J1907+062,
	PSR 1907+0631	PSR	3.4	11.3	5.3×10^{35}	2HWC 1908+063
LHAASO J1929+1745	PSR J1928+1746	PSR	4.6	82.6	1.6×10^{36}	2HWC J1928+177, 2HWC J1930+188,
	PSR J1930+1852	PSR	6.2	2.9	1.2×10^{37}	HESS J1930+188, VER J1930+188
	SNR G54.1+0.3	SNR	$6.3^{+0.8}_{-0.7}^d$	$1.8 - 3.3^k$	—	
LHAASO J1956+2845	PSR J1958+2846	PSR	2.0	21.7	3.4×10^{35}	2HWC J1955+285
	SNR G66.0-0.0	SNR	2.3 ± 0.2^d	—	—	
LHAASO J2018+3651	PSR J2021+3651	PSR	$1.8^{+1.7}_{-1.4}^l$	17.2	3.4×10^{36}	MGRO J2019+37, VER J2019+368,
	Sh 2-104	H II/YMC	$3.3 \pm 0.3^m / 4.0 \pm 0.5^n$	—	—	VER J2016+371
LHAASO J2032+4102	Cygnus OB2	YMC	1.40 ± 0.08^o	—	—	TeV J2032+4130, ARGO J2031+4157,
	PSR 2032+4127	PSR	1.40 ± 0.08^o	201	1.5×10^{35}	MGRO J2031+41, 2HWC J2031+415,
	SNR G79.8+1.2	SNR candidate	—	—	—	VER J2032+414
LHAASO J2108+5157	—	—	—	—	—	
LHAASO J2226+6057	SNR G106.3+2.7	SNR	0.8^p	$\sim 10^p$	—	VER J2227+608, Boomerang Nebula
	PSR J2229+6114	PSR	0.8^p	$\sim 10^p$	2.2×10^{37}	



LHAASO J1908+0621

- ❖ Multi Wavelength analysis reveals more exciting features
- ❖ Hadronic process dominates the UHE emission ?
- ❖ SNRs may be still strong candidates for PeVatrons



Exploring Lorentz Invariance Violation

In the superluminal LIV

$$\gamma \rightarrow e^- e^+$$

$$\alpha_0 \leq \frac{4m_e^2}{E_\gamma^2 - 4m_e^2},$$

$$E_{LIV}^{(1)} \geq 9.57 \times 10^{23} \text{ eV} \left(\frac{E_\gamma}{\text{TeV}} \right)^3,$$

$$E_{LIV}^{(2)} \geq 9.78 \times 10^{17} \text{ eV} \left(\frac{E_\gamma}{\text{TeV}} \right)^2.$$

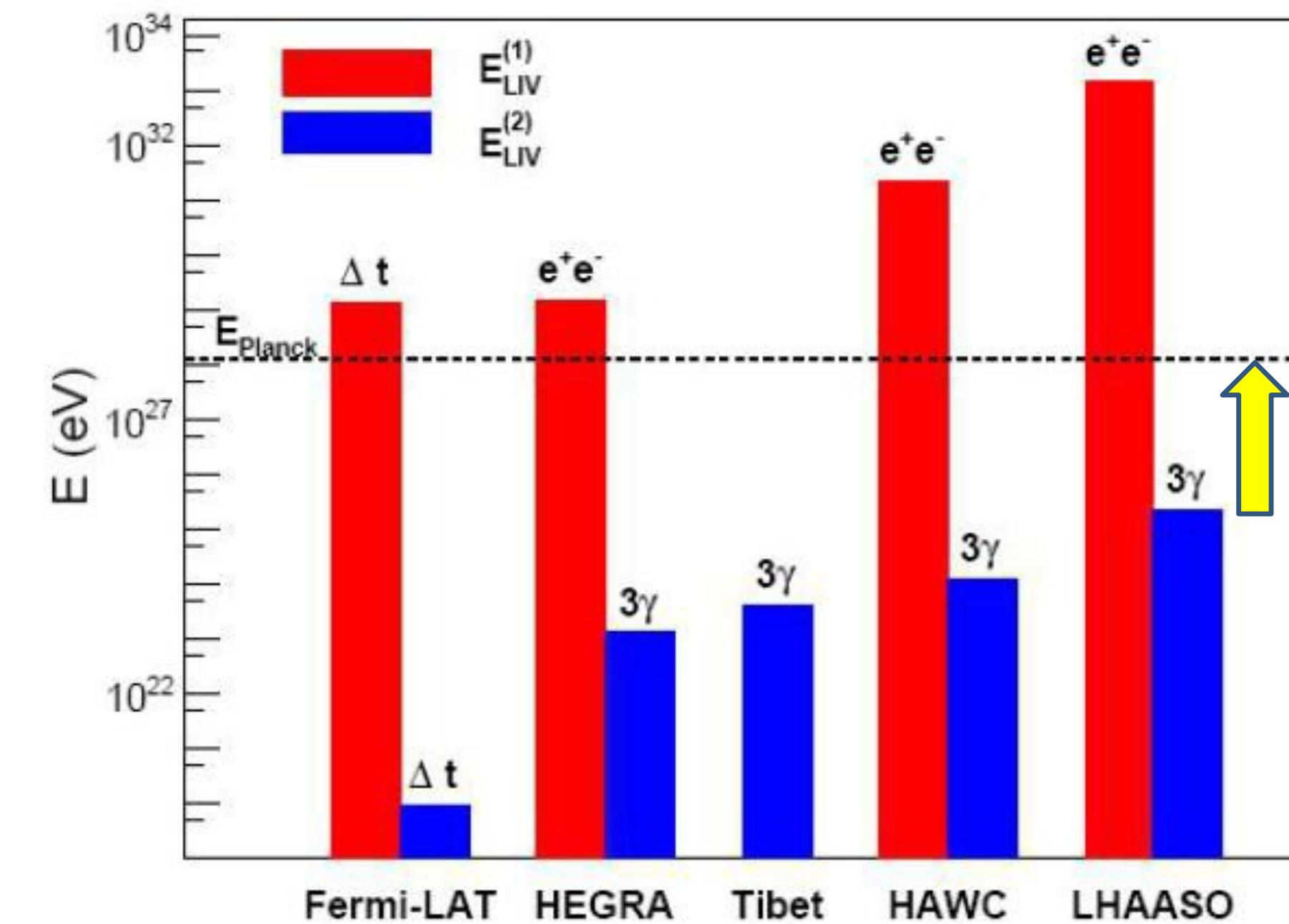
$$\gamma \rightarrow 3\gamma$$

$$\Gamma_{\gamma \rightarrow 3\gamma} = 5 \times 10^{-14} \frac{E_\gamma^{19}}{m_e^8 E_{LIV}^{(2)10}},$$

$$E_{LIV}^{(2)} > 3.33 \times 10^{19} \text{ eV} \left(\frac{L}{\text{kpc}} \right)^{0.1} \left(\frac{E_\gamma}{\text{TeV}} \right)^{1.9}.$$

New CLs method

Source	L (kpc)	E_{\max} (PeV)	$E_{\text{cut}}^{95\%}$ (PeV)
J0534+2202	2.0	0.88	$0.75^{+0.043}_{-0.043}$
J2032+4102	1.4	1.42	$1.14^{+0.06}_{-0.06}$



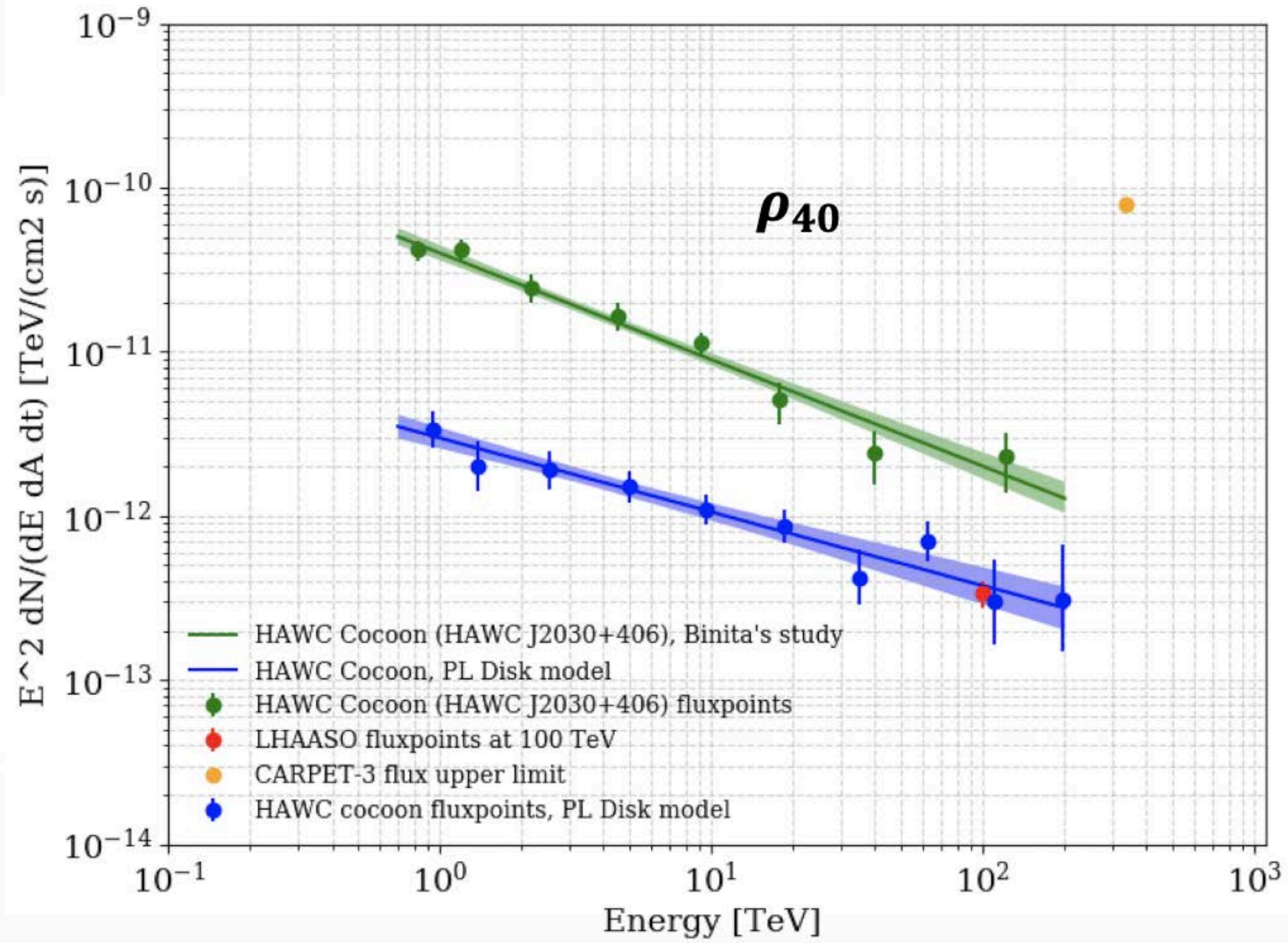
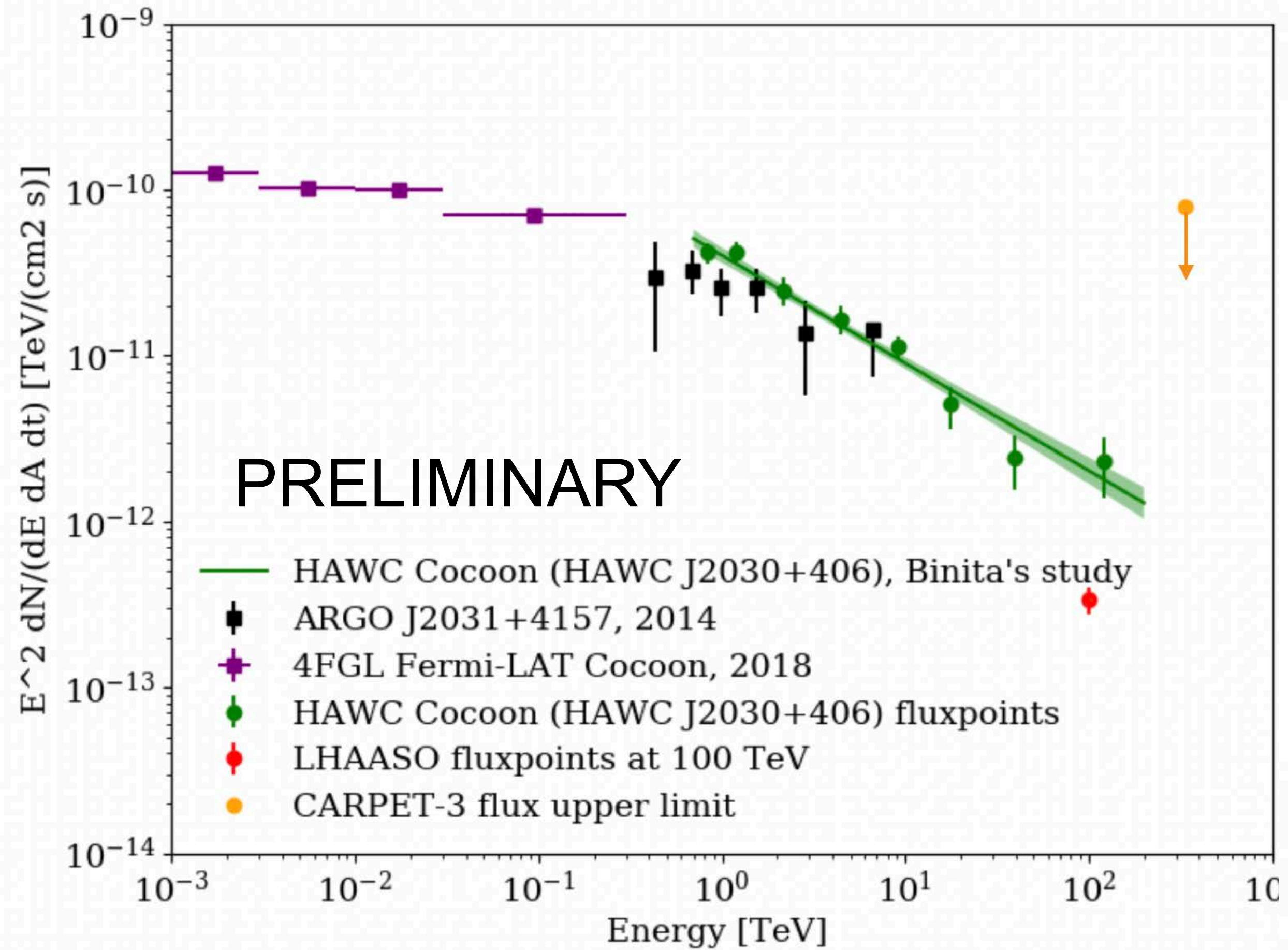
3 orders of magnitudes below the Planck-scale

Summary

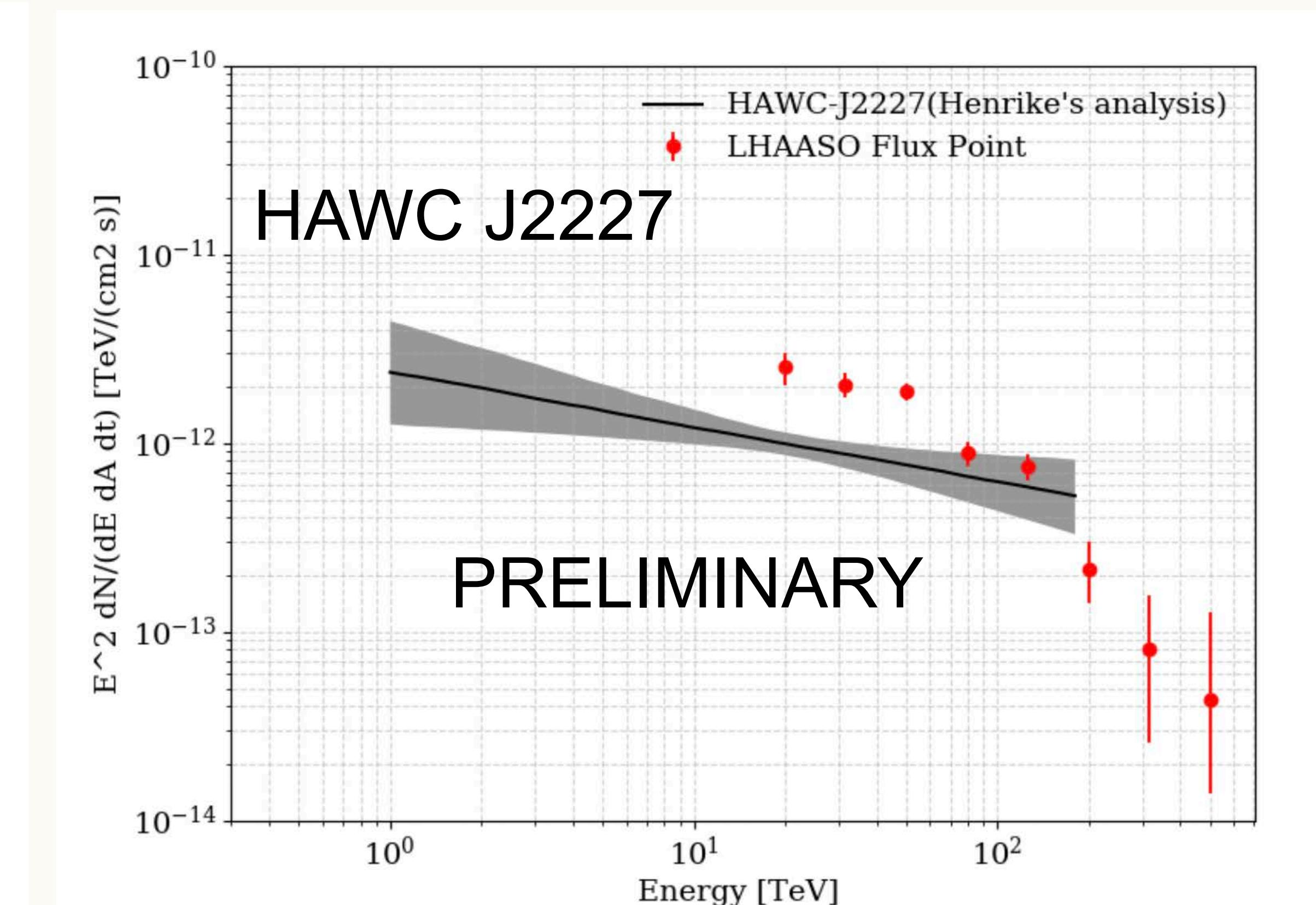
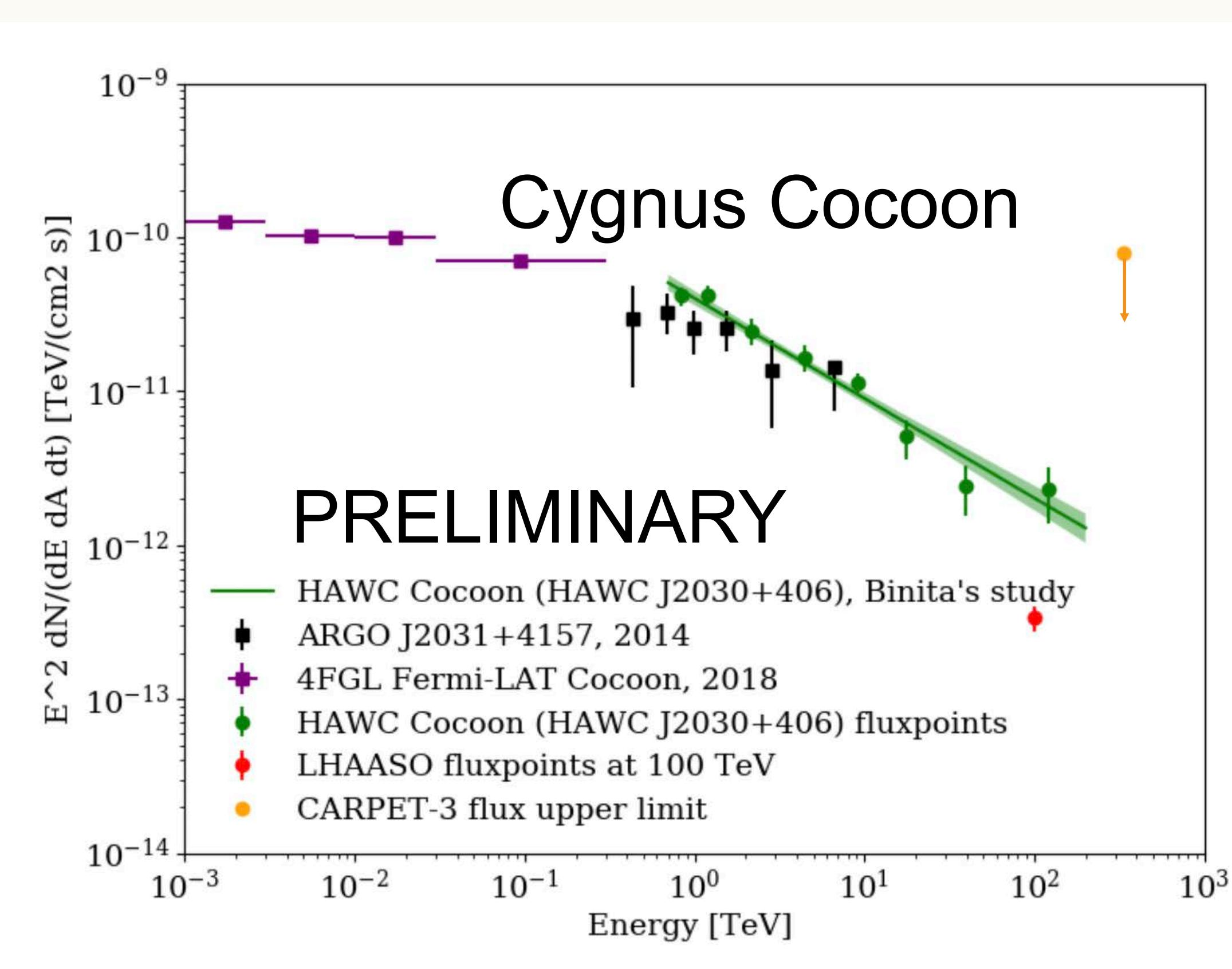
- ❖ LHAASO is completely built, and in full operation since July 2021
- ❖ Open-up “**UHE (>0.1 PeV) Astronomy**”
 - ① 12 PeVatrons are discovered in our galaxy
 - ② A photon at 1.4 PeV is recorded toward Cygnus constellation
- ❖ First Discoveries:
 - ① Our galaxy is full of **PeVatrons** accelerating particles over 1 PeV
 - ② Potential **CR origins**: many type of candidates
 - ③ The Crab: extreme e-PeVatron emitting 1.1 PeV γ posing challenges
 - ④ Many new sources are discovered
- ❖ Fundamental rules, e.g. LIV, are tested in extreme condition
- ❖ Precision Measurements of individual species CRs around knees will be measured at first time

Some comparisons

Cygnus Cocoon

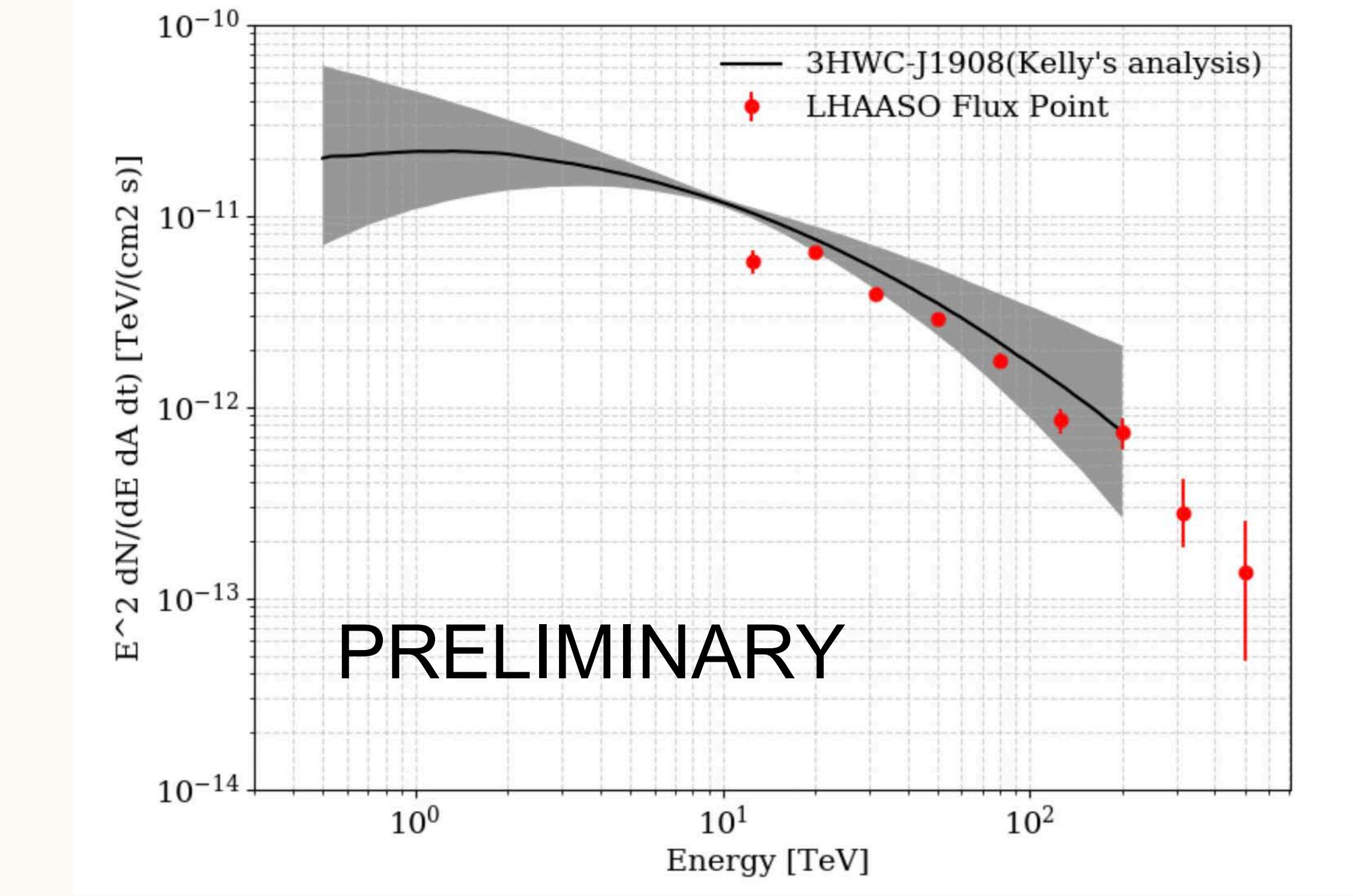
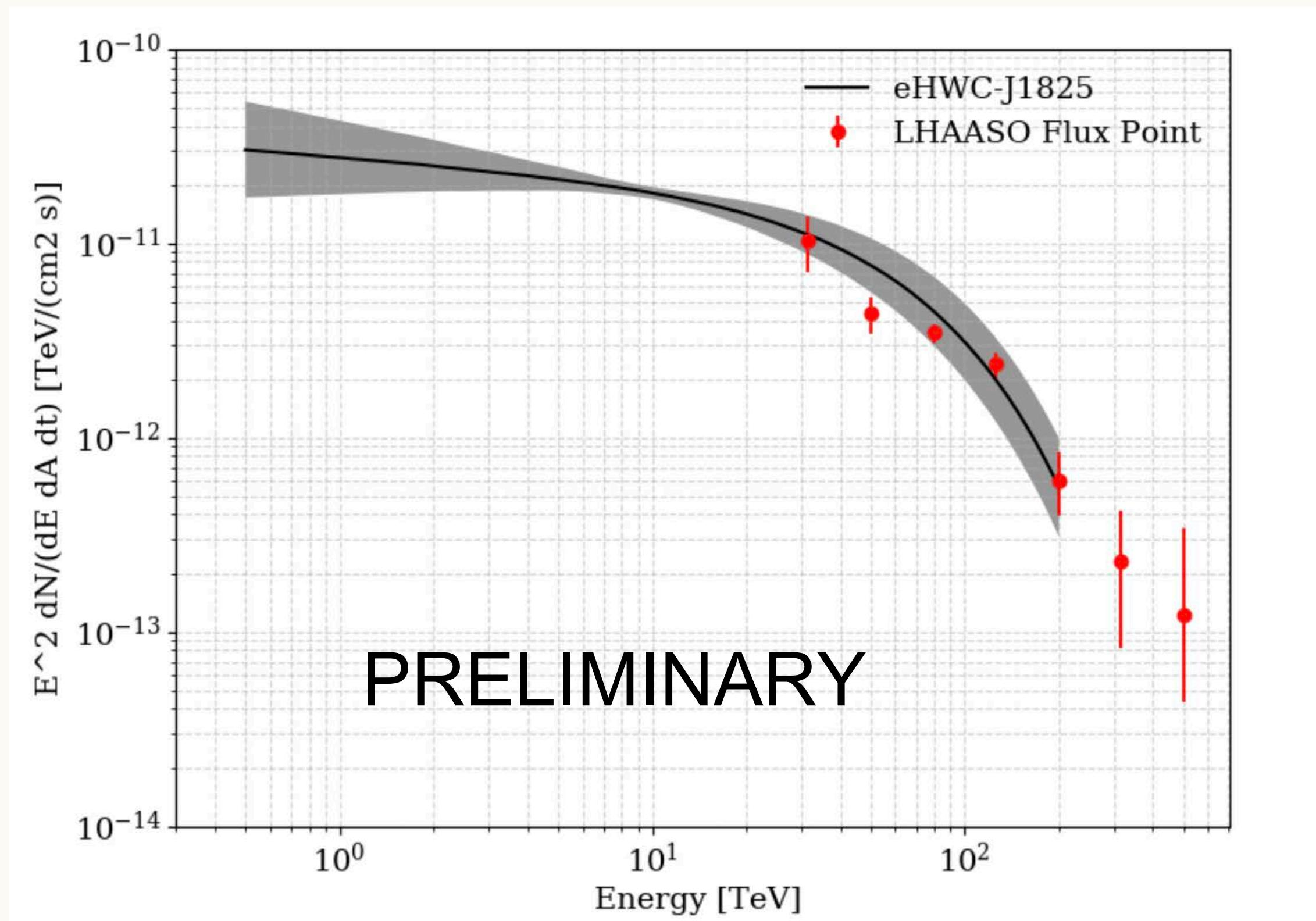


Some comparisons



HAWC + VERITAS joint analysis

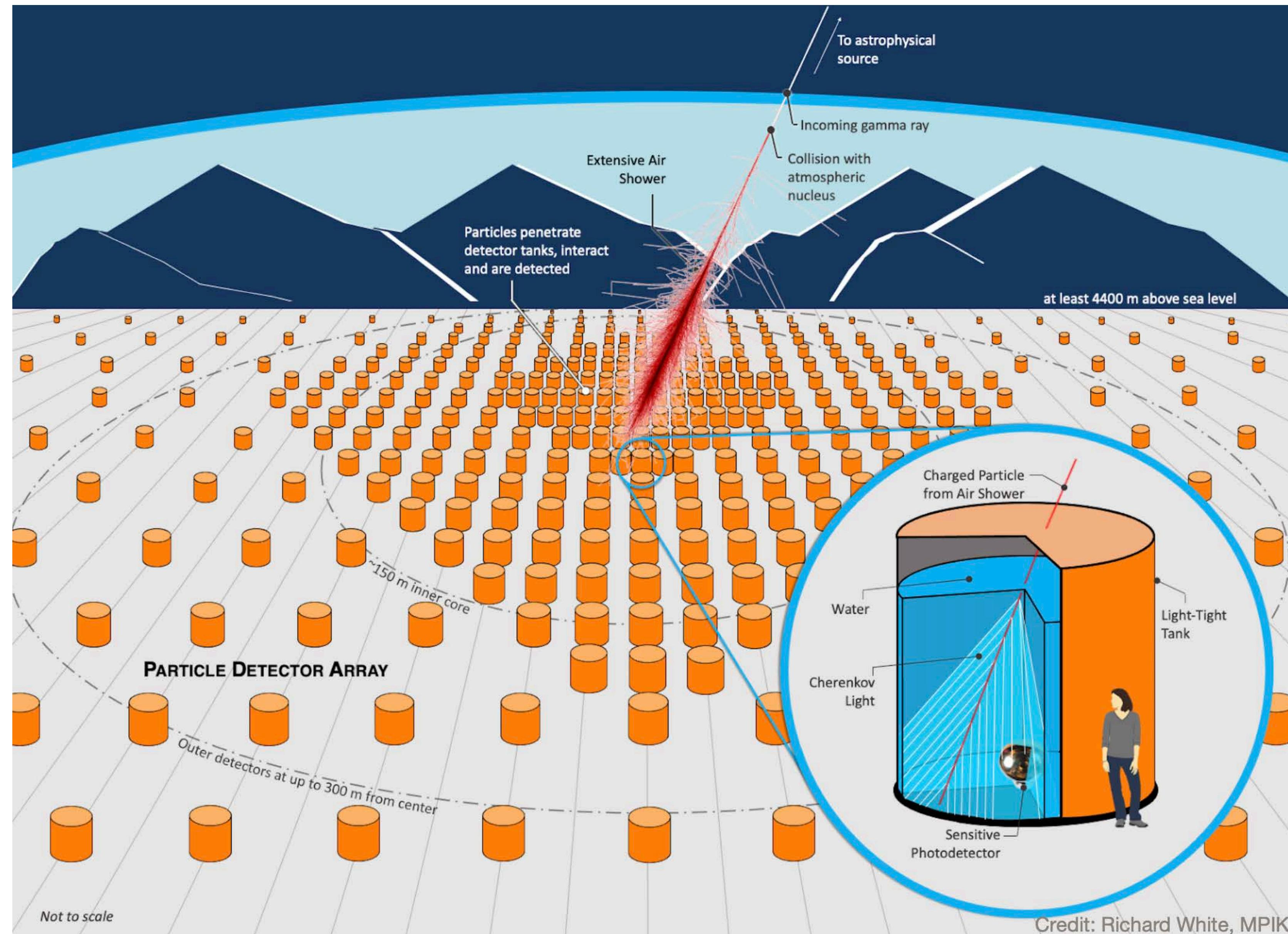
Some comparisons



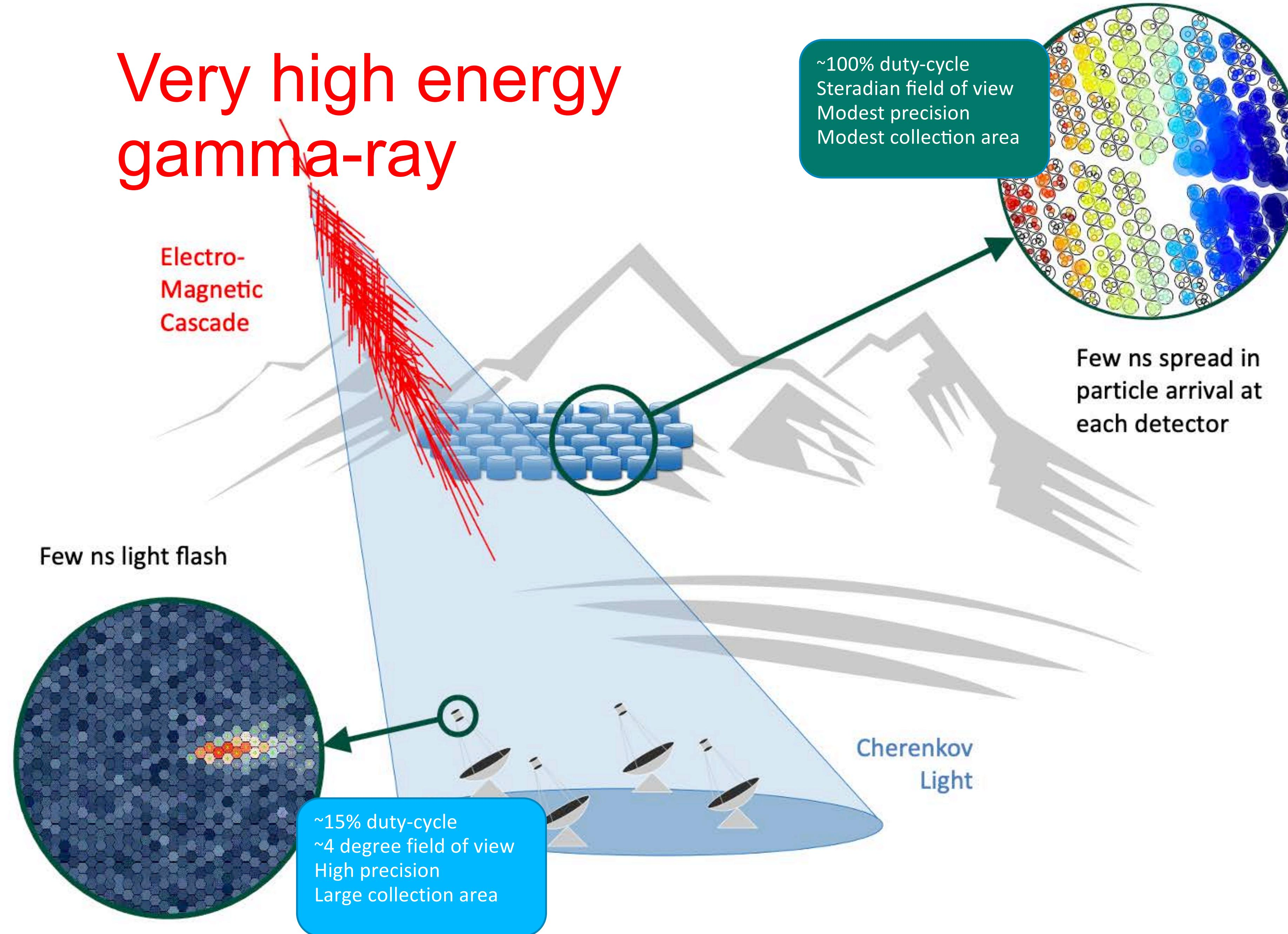
The Future



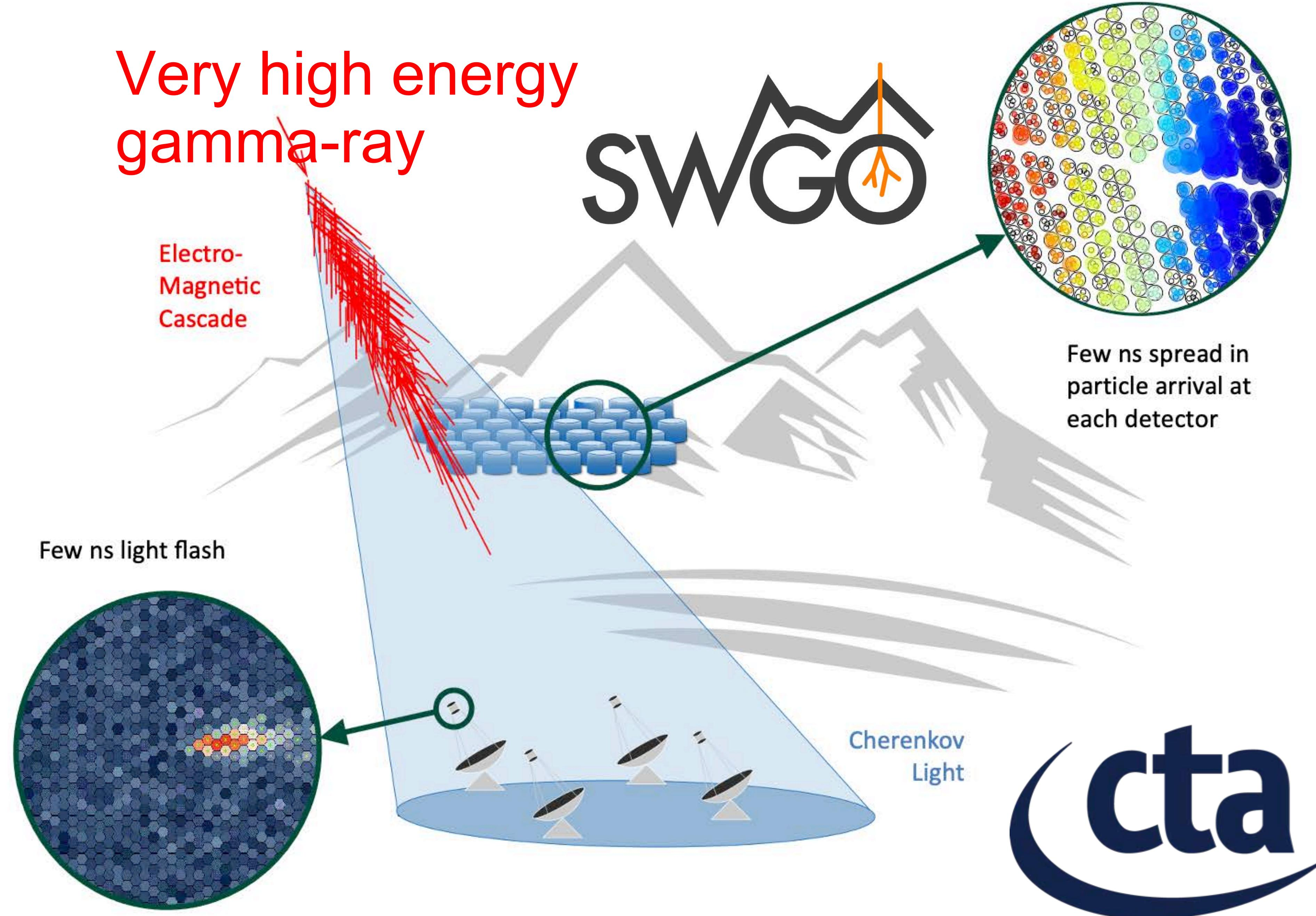
The Southern Wide-field Gamma-ray Observatory

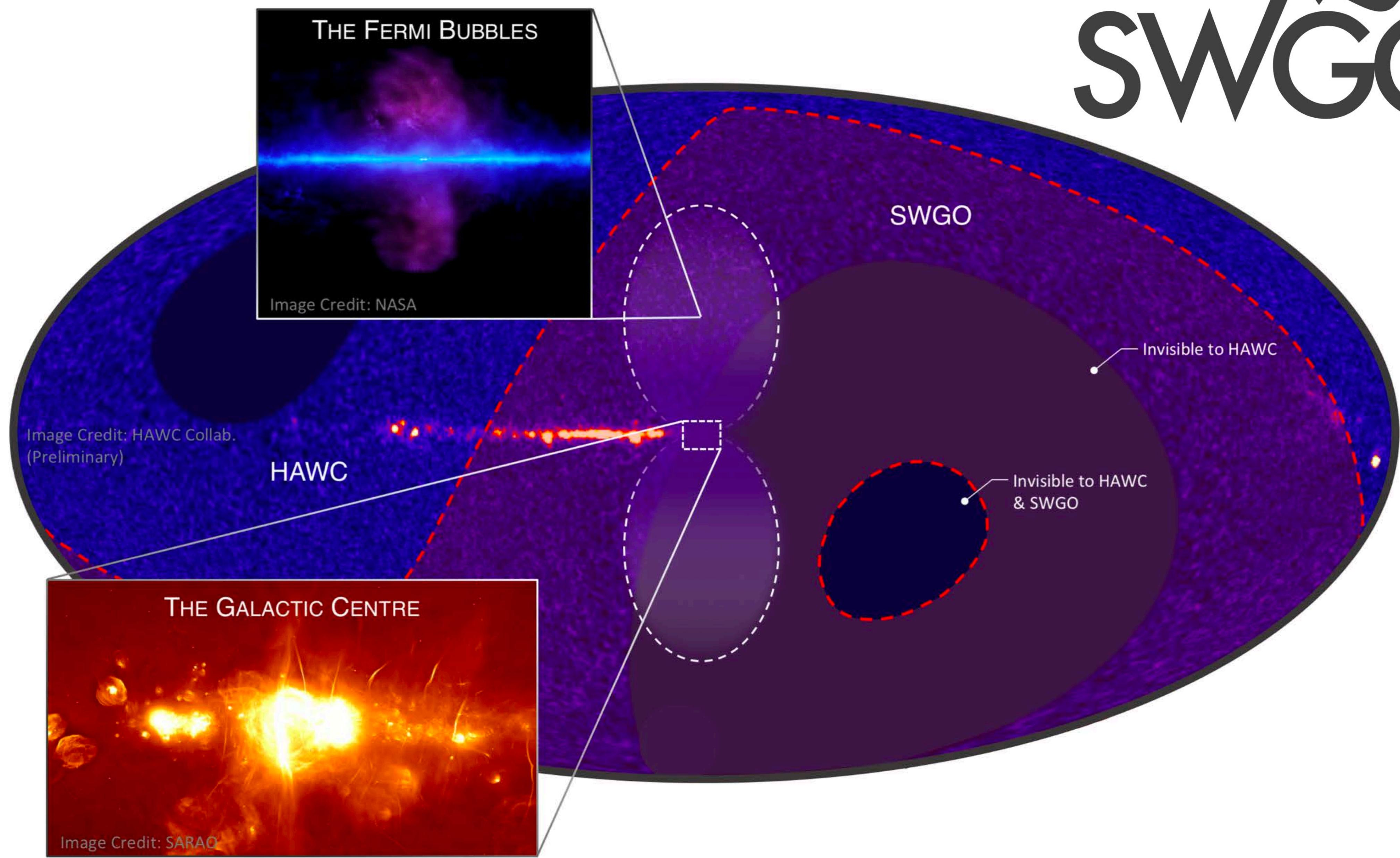


Very high energy gamma-ray



Very high energy gamma-ray





Status & Plan



SWGO R&D Phase Milestones	
M1	R&D Phase Plan Established
M2	Science Benchmarks Defined
M3	Reference Configuration & Options Defined
M4	Site Shortlist Complete
M5	Candidate Configurations Defined
M6	Performance of Candidate Configurations Evaluated
M7	Preferred Site Identified
M8	Design Finalised
M9	Construction & Operation Proposal Complete

- ◎ SWGO partners
 - 47 institutes in 12 countries*
 - + supporting scientists

R&D Phase

Kick off meeting Nov 2019

Expected completion 2023

Site and Design Choices
made

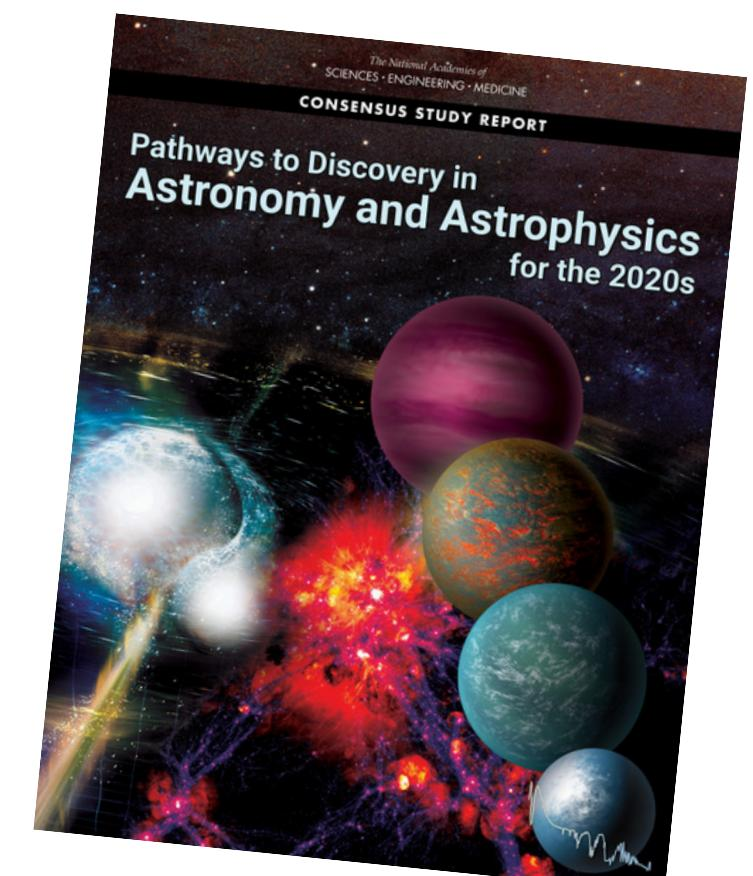
Then:

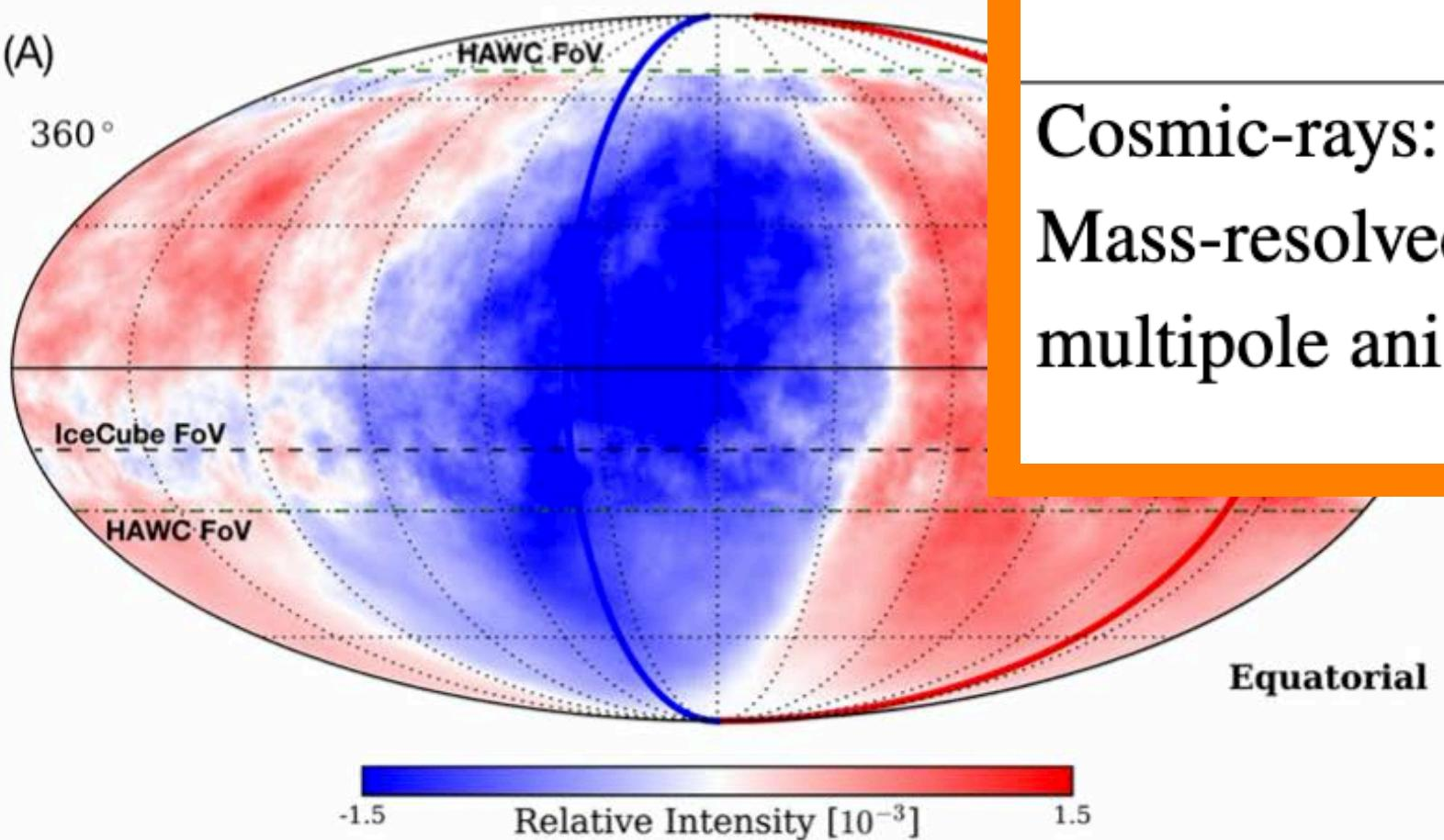
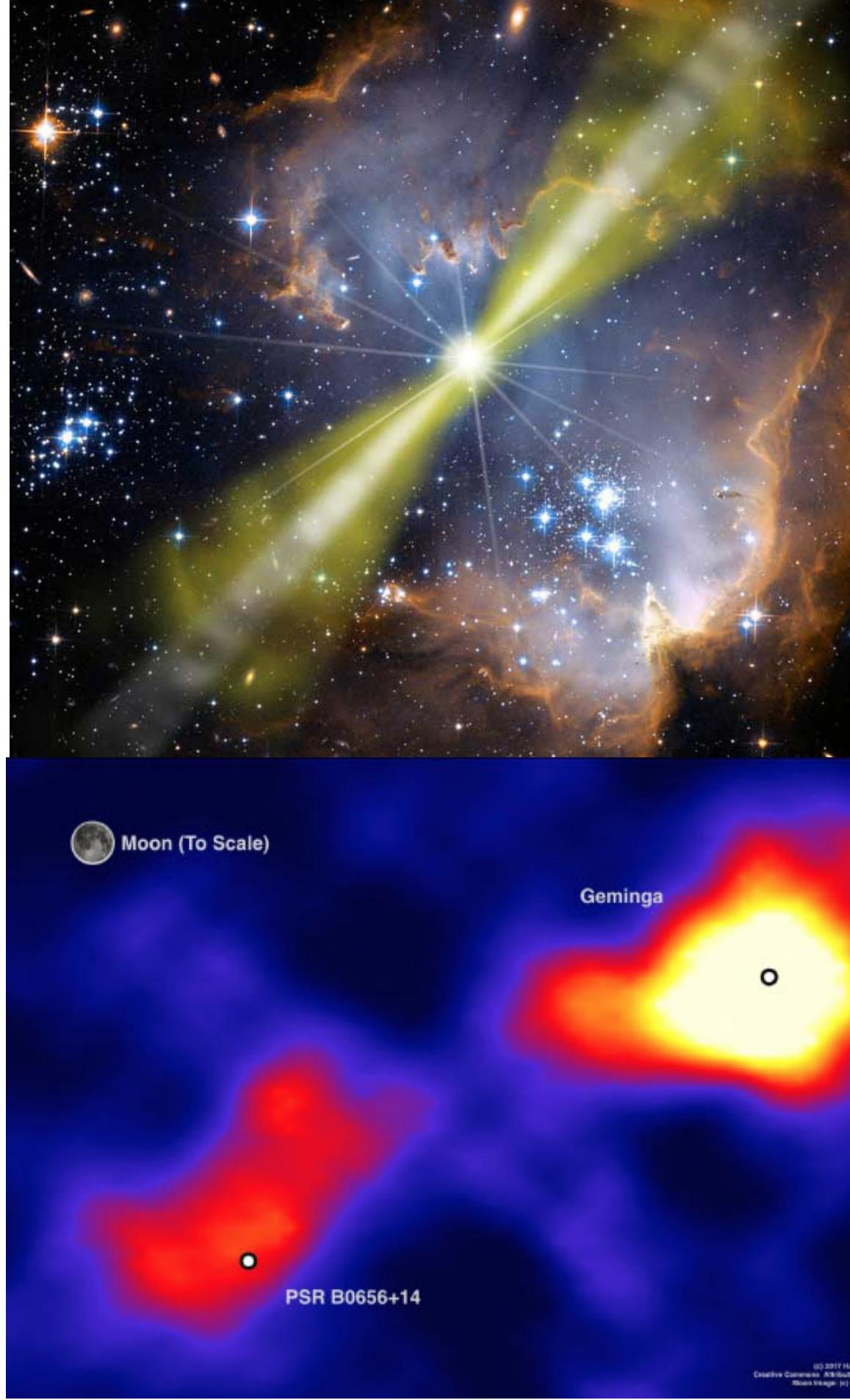
Preparatory Phase

Detailed construction
planning

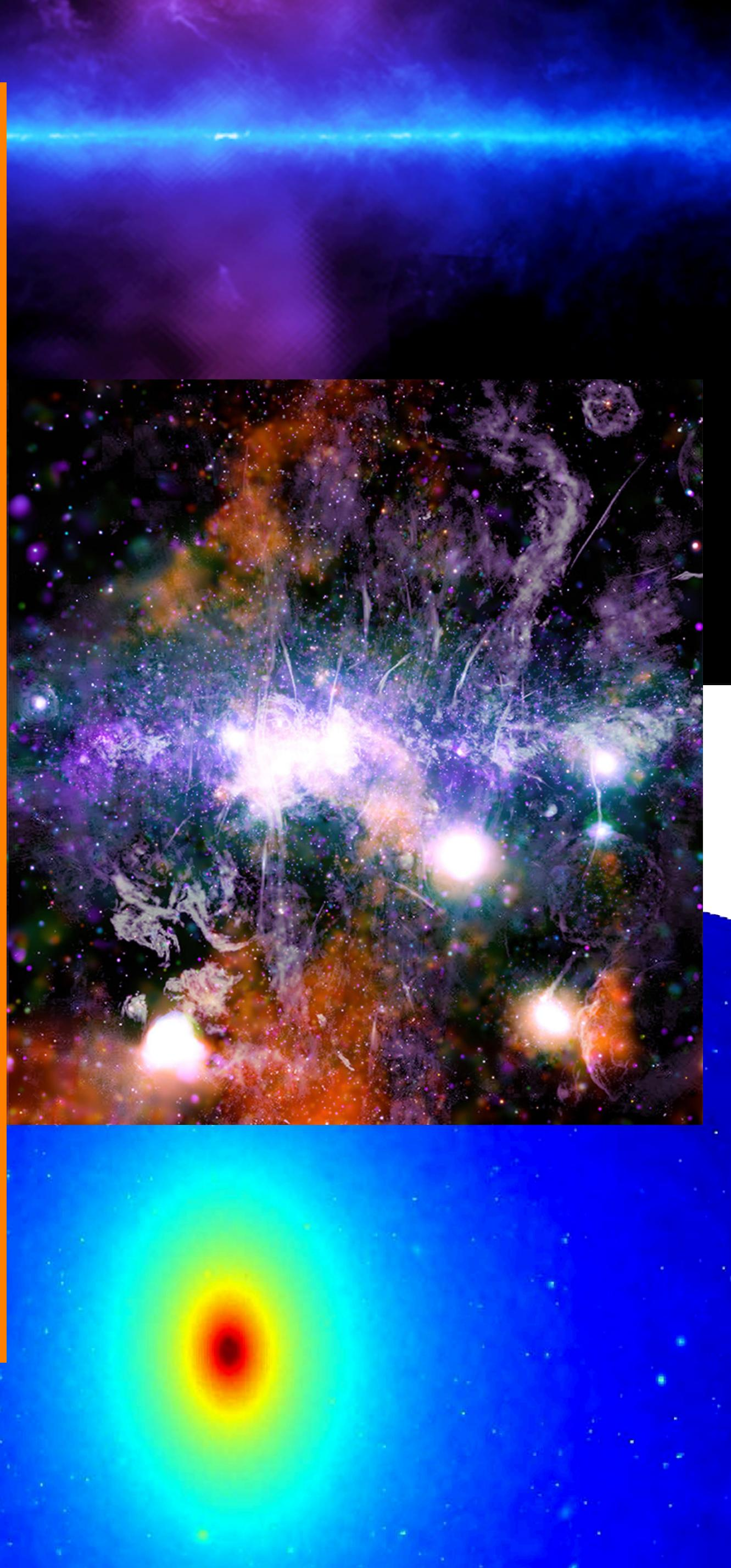
Engineering Array

(Full) Construction Phase
2026+

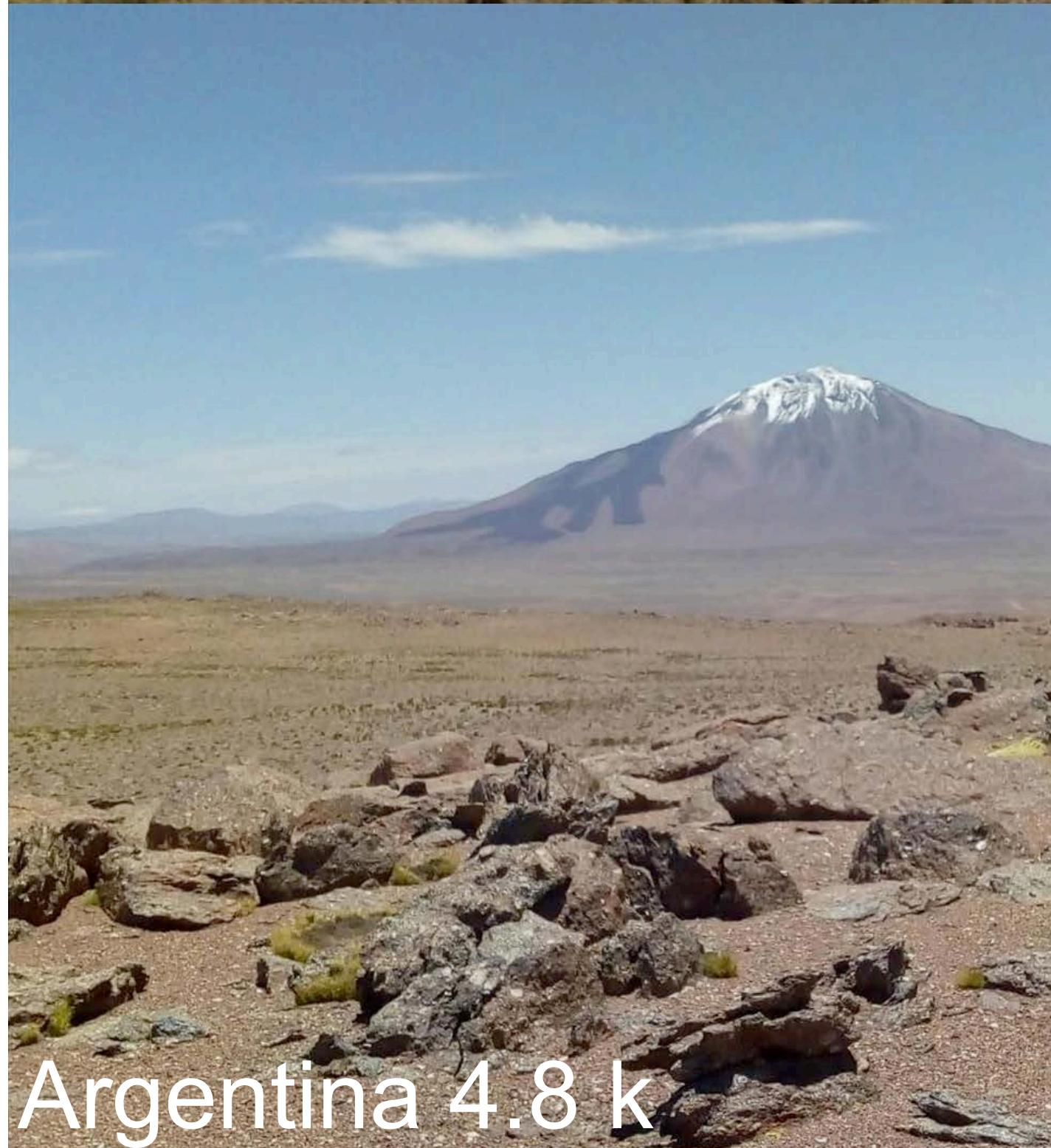




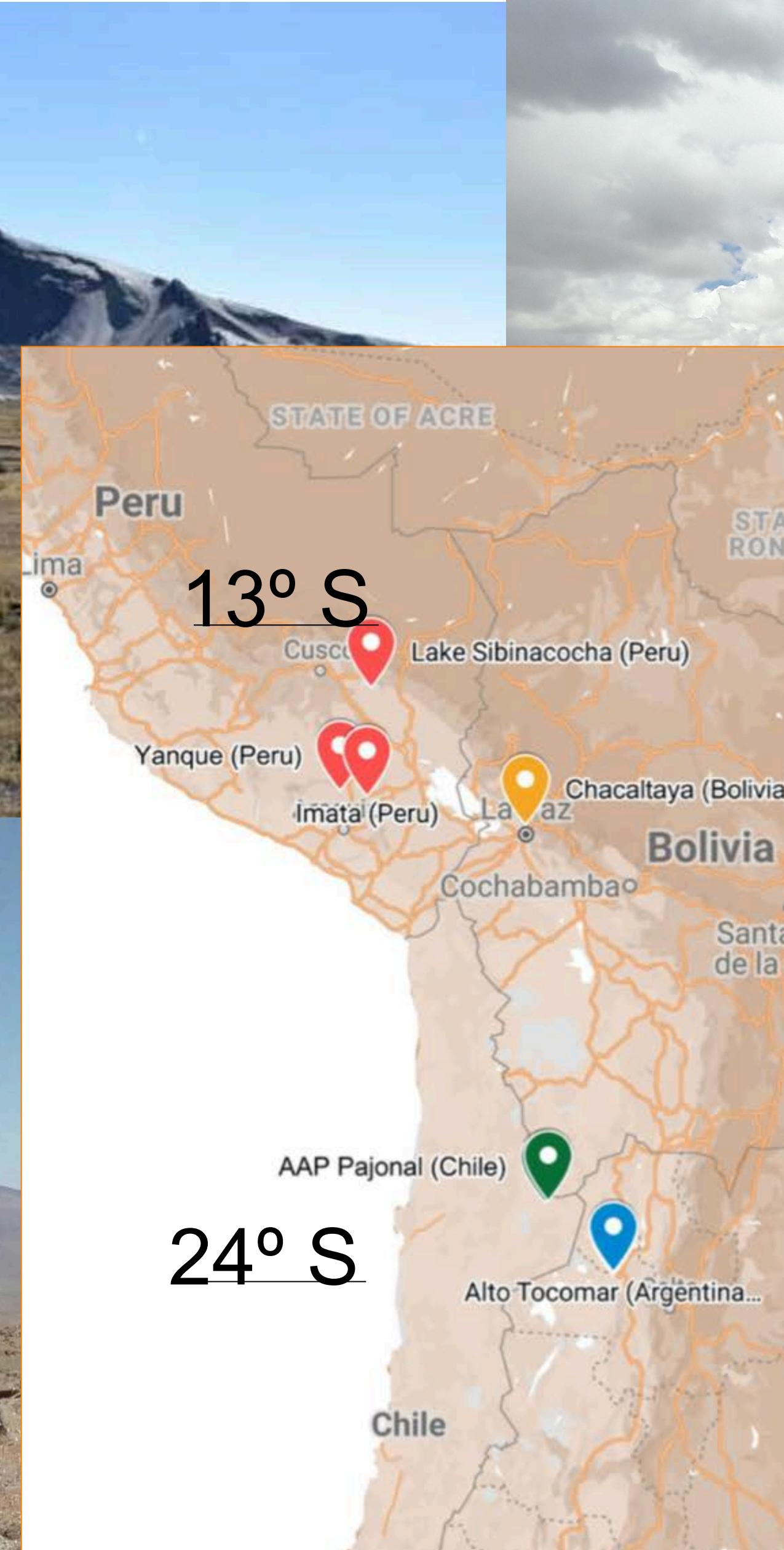
Science Case	Design Drivers
Transient Sources: Gamma-ray Bursts	Low-energy sensitivity & Site altitude ^a
Galactic Accelerators: PeVatron Sources	High-energy sensitivity & Energy resolution ^b
Galactic Accelerators: PWNe and TeV Halos	Extended source sensitivity & Angular resolution ^c
Diffuse Emission: Fermi Bubbles	Background rejection
Fundamental Physics: Dark Matter from GC Halo	Mid-range energy sensitivity Site latitude ^d
Cosmic-rays: Mass-resolved dipole / multipole anisotropy	Muon counting capability ^e



Bolivia 4.7k



Argentina 4.8 k



13° S

24° S

Chile 4.8 k

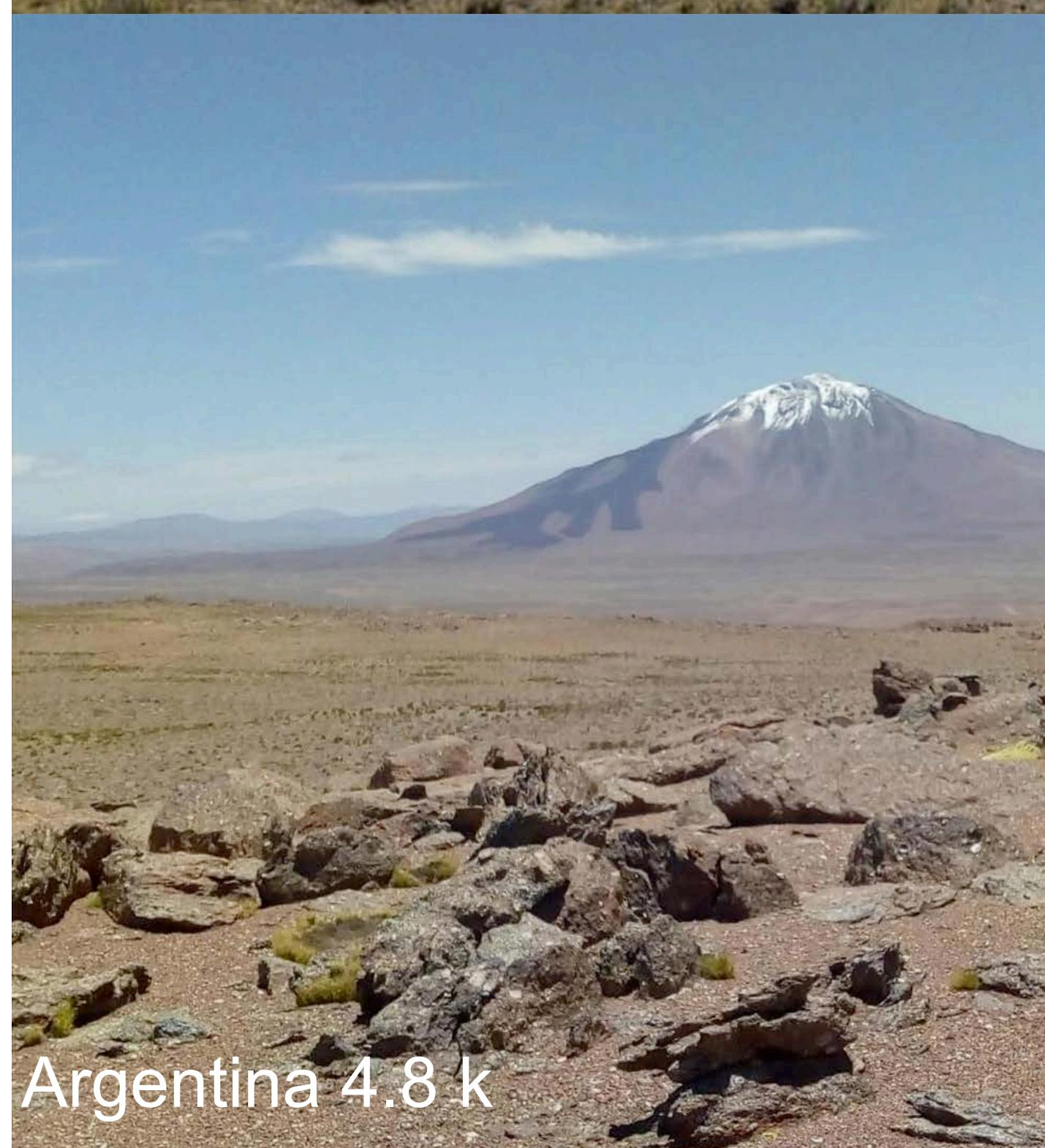


Peru 4.9 k

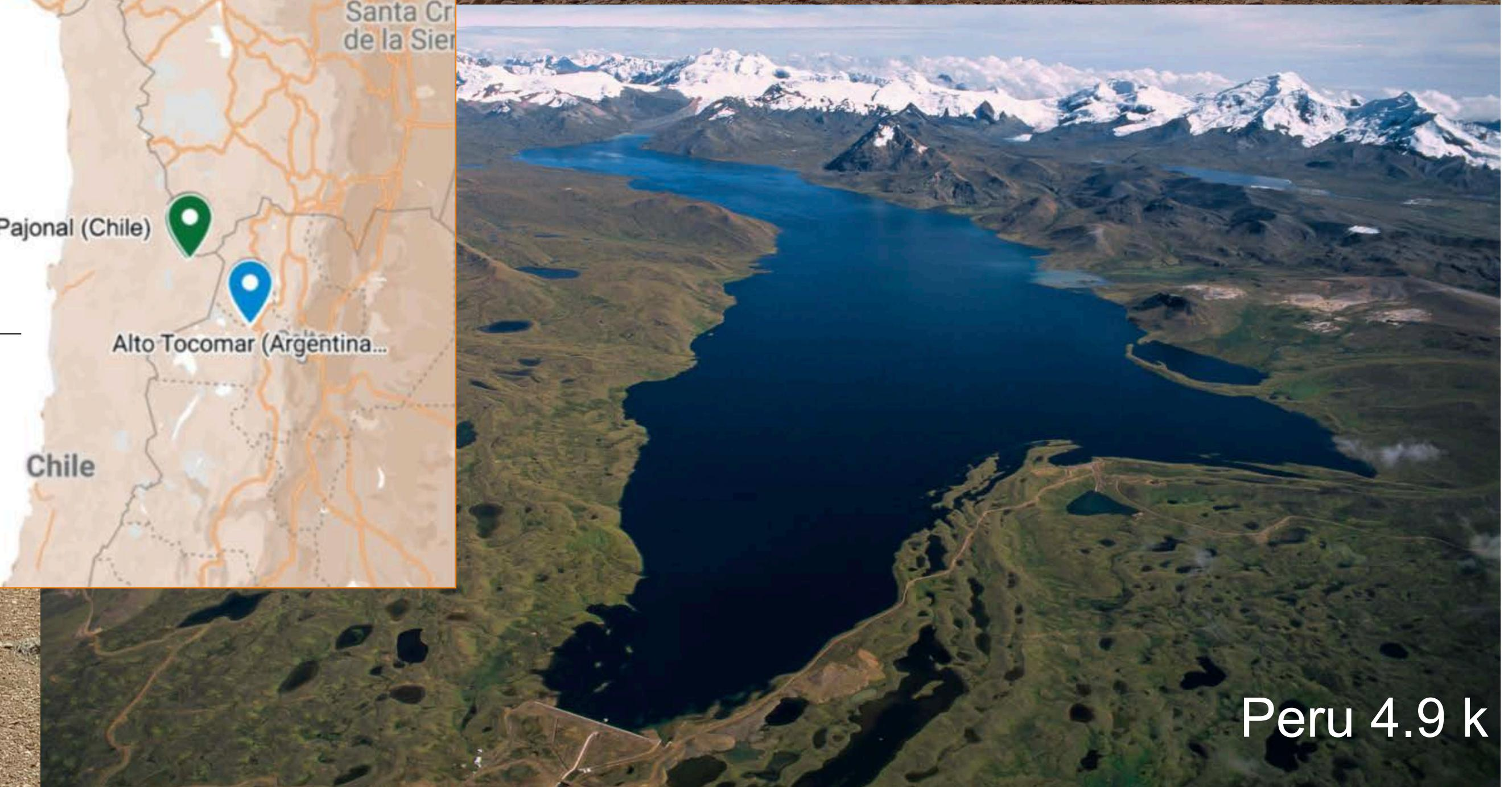
Bolivia 4.7k



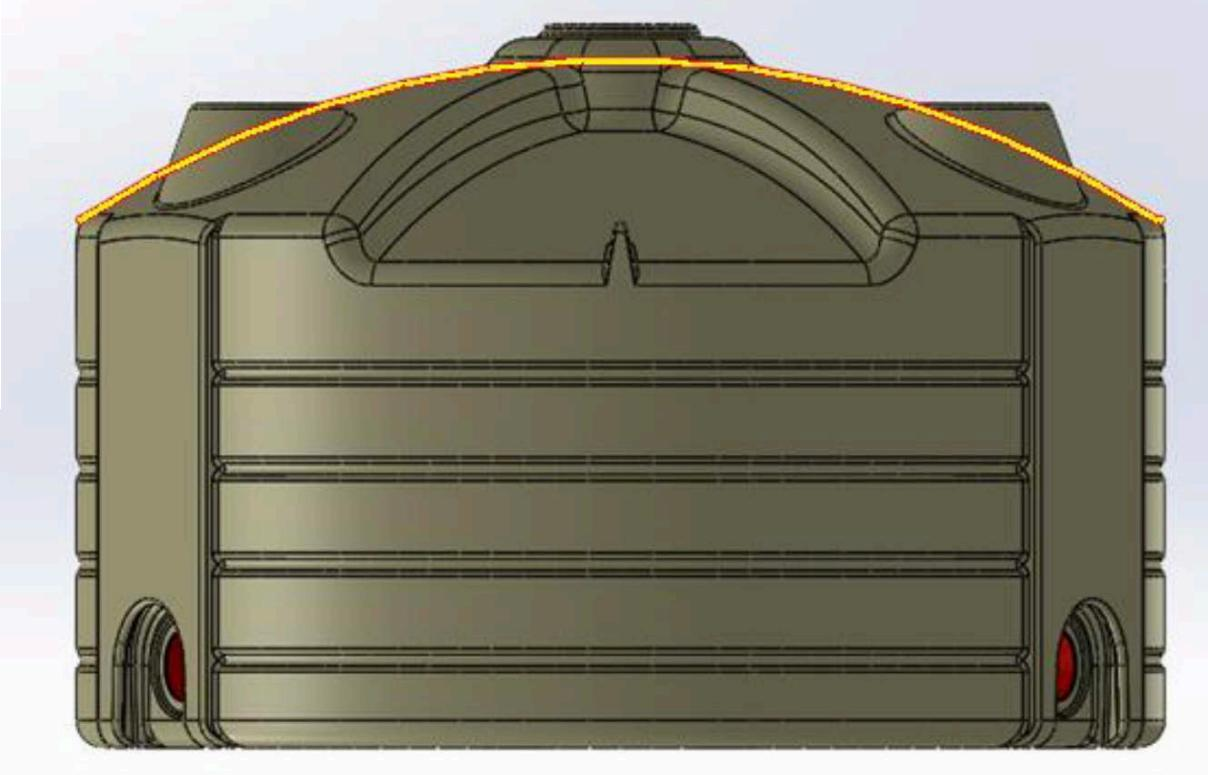
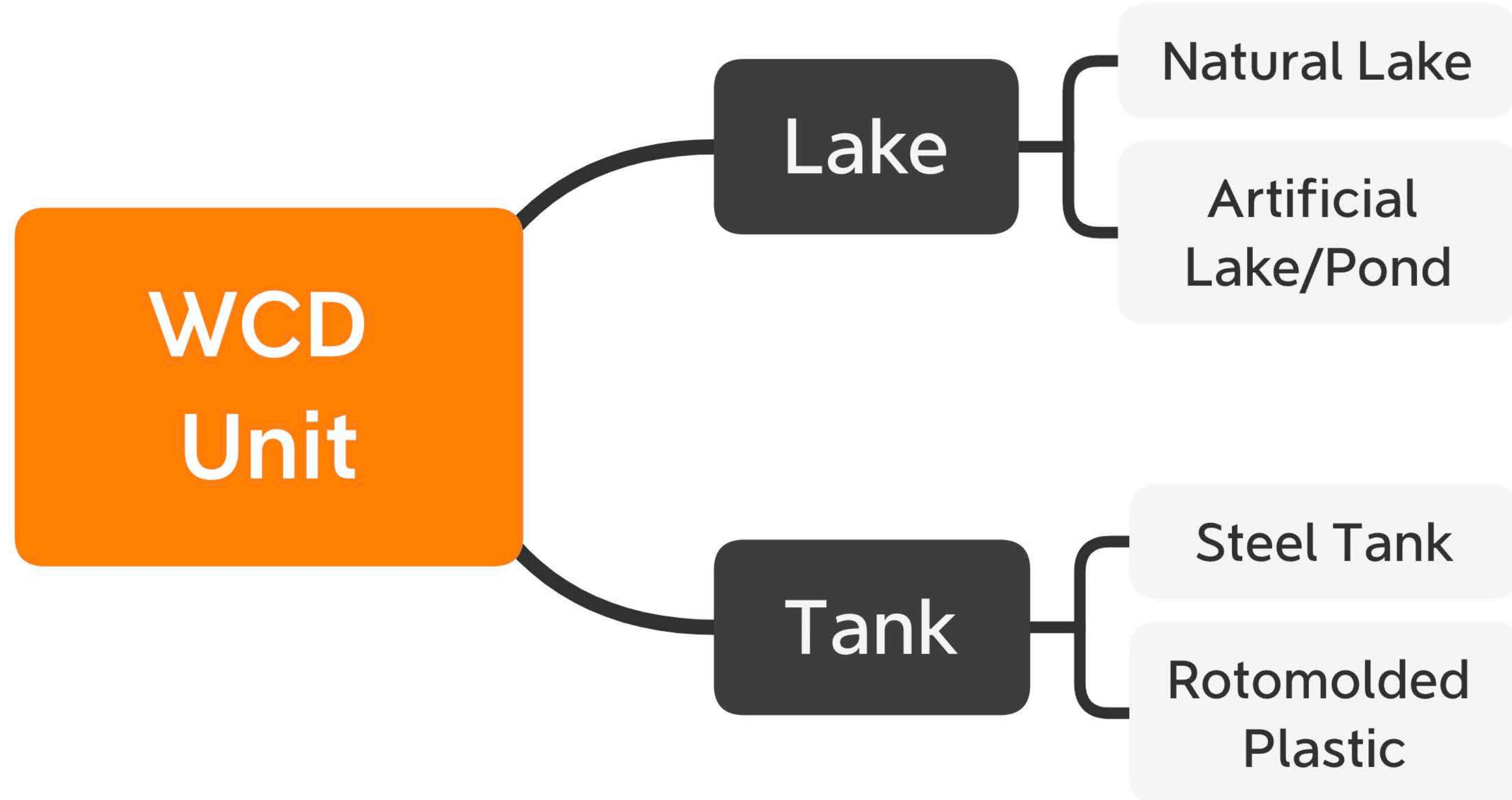
Chile 4.8 k

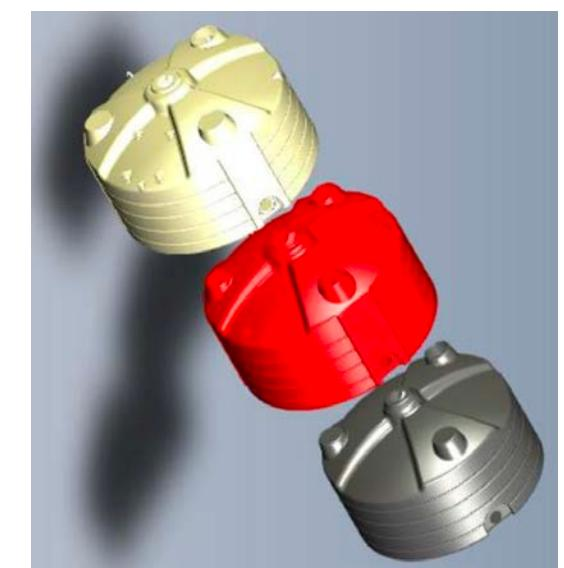
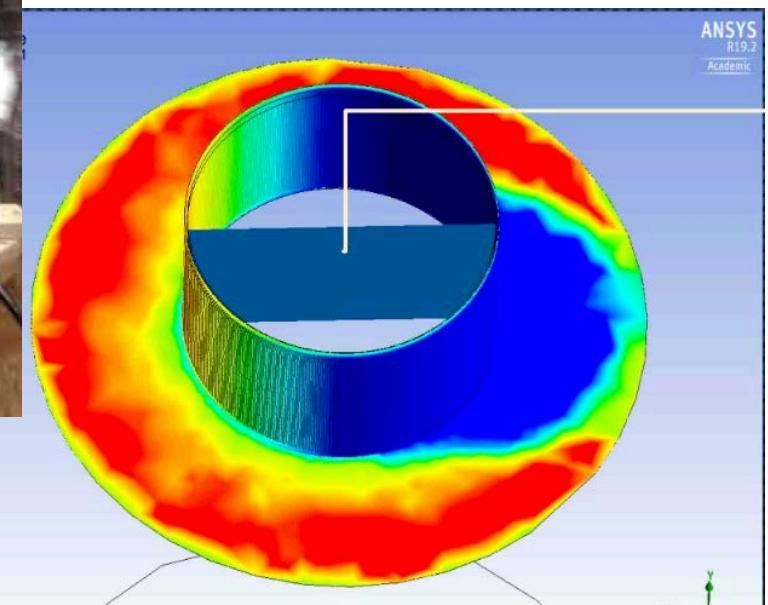
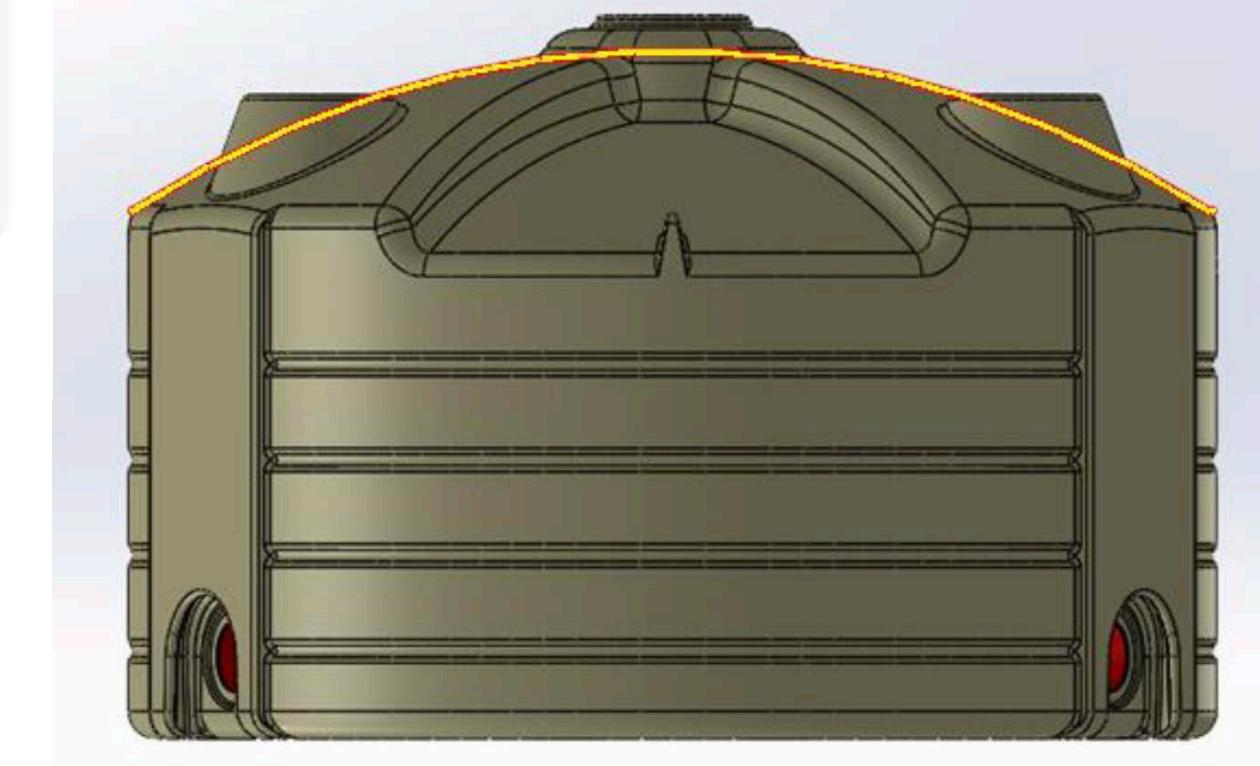
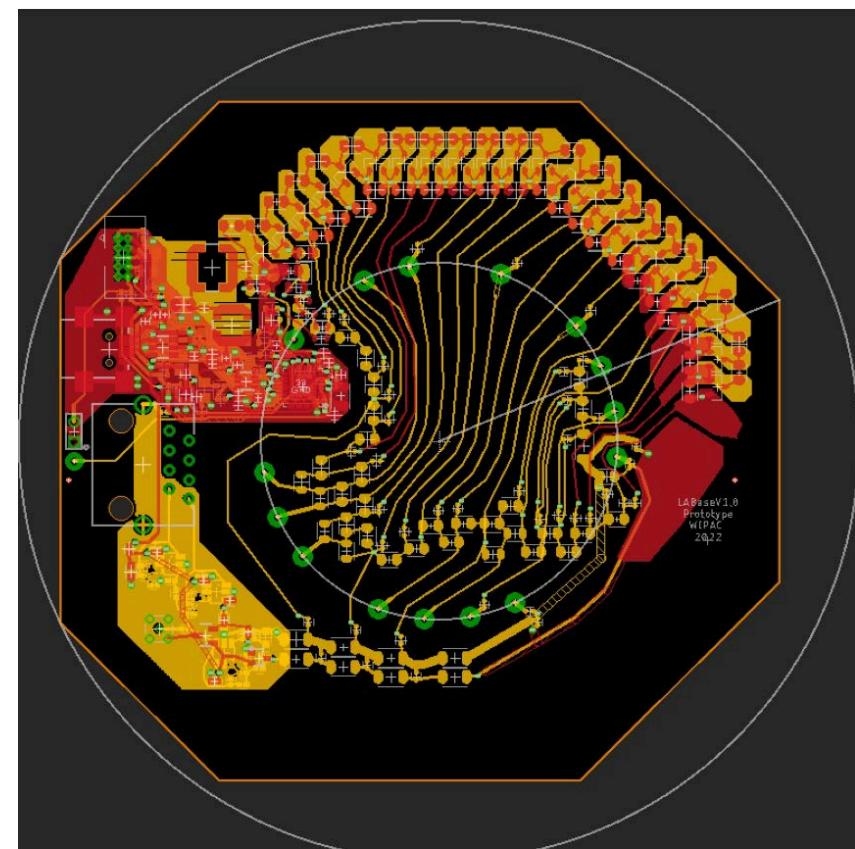


Argentina 4.8 k

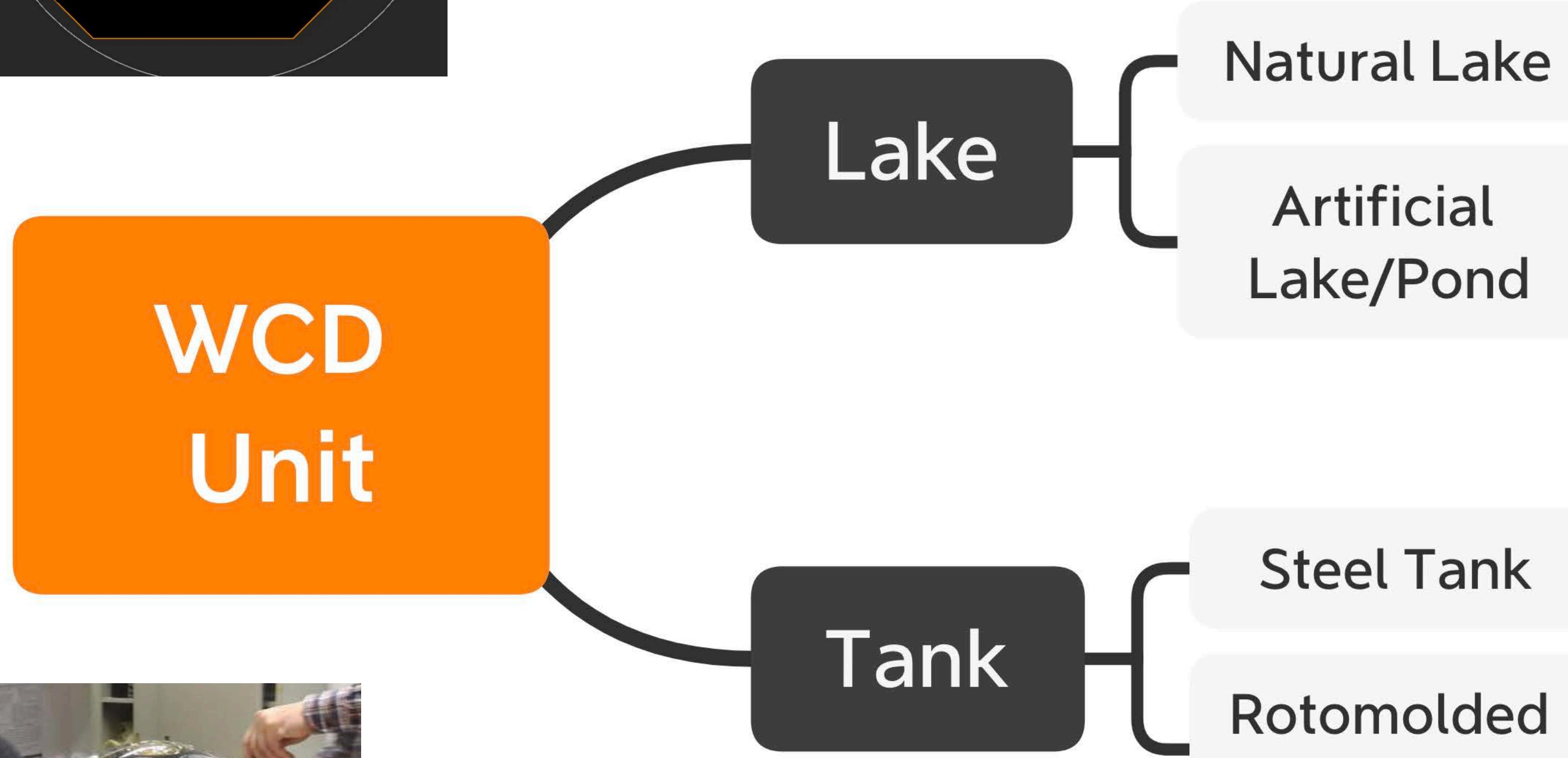


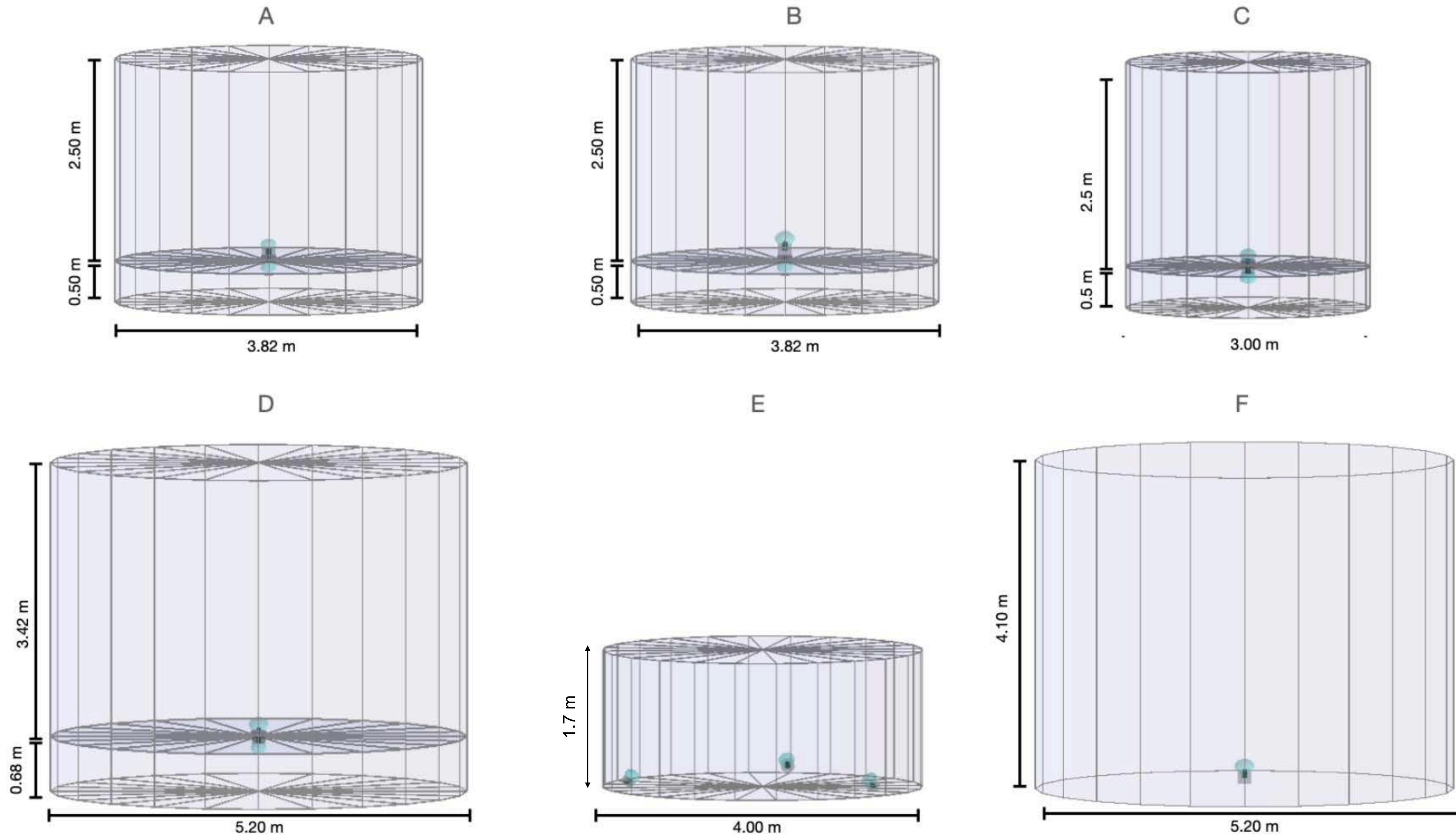
Peru 4.9 k

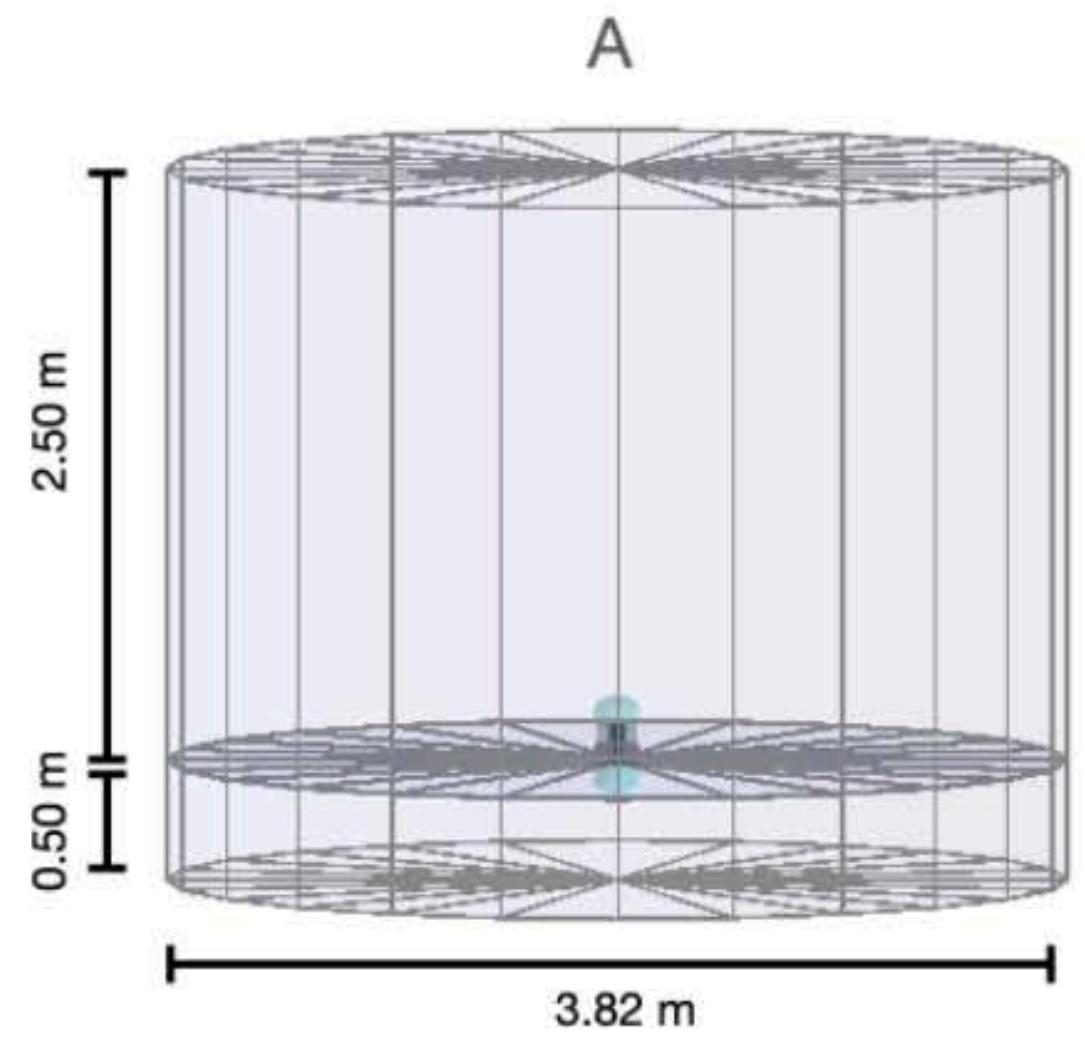




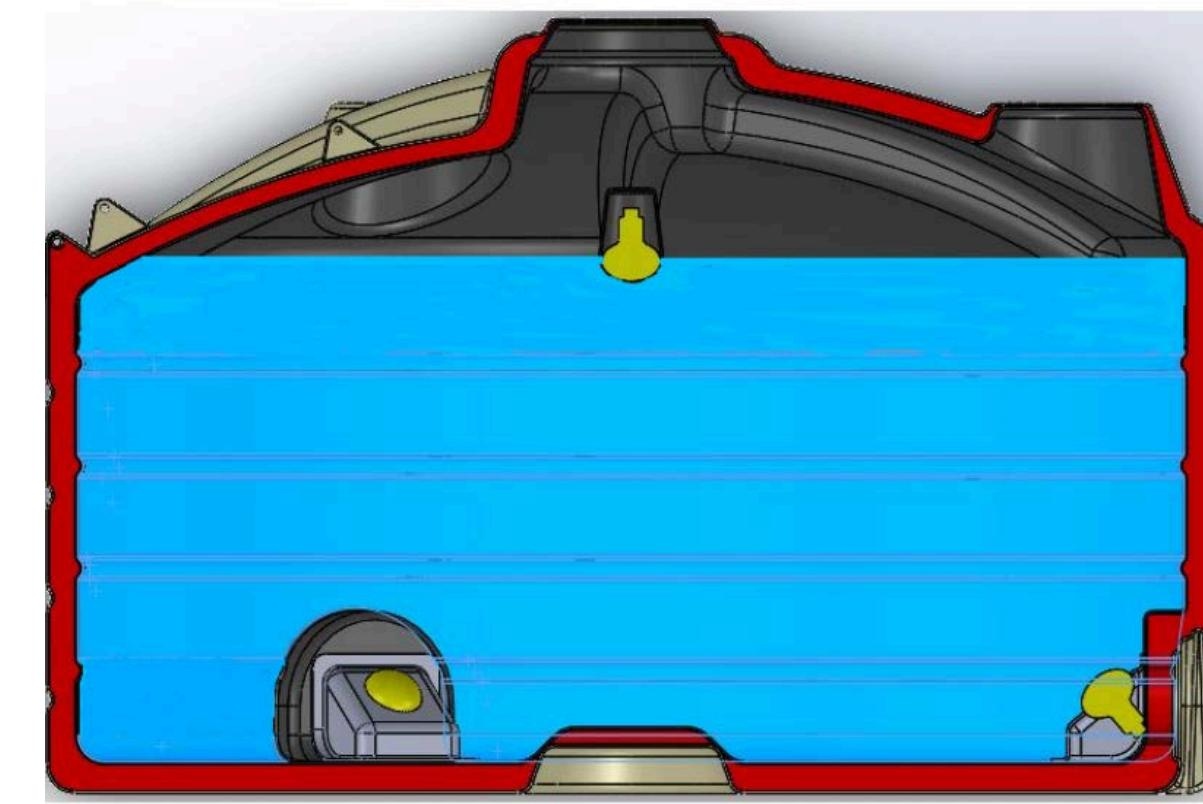
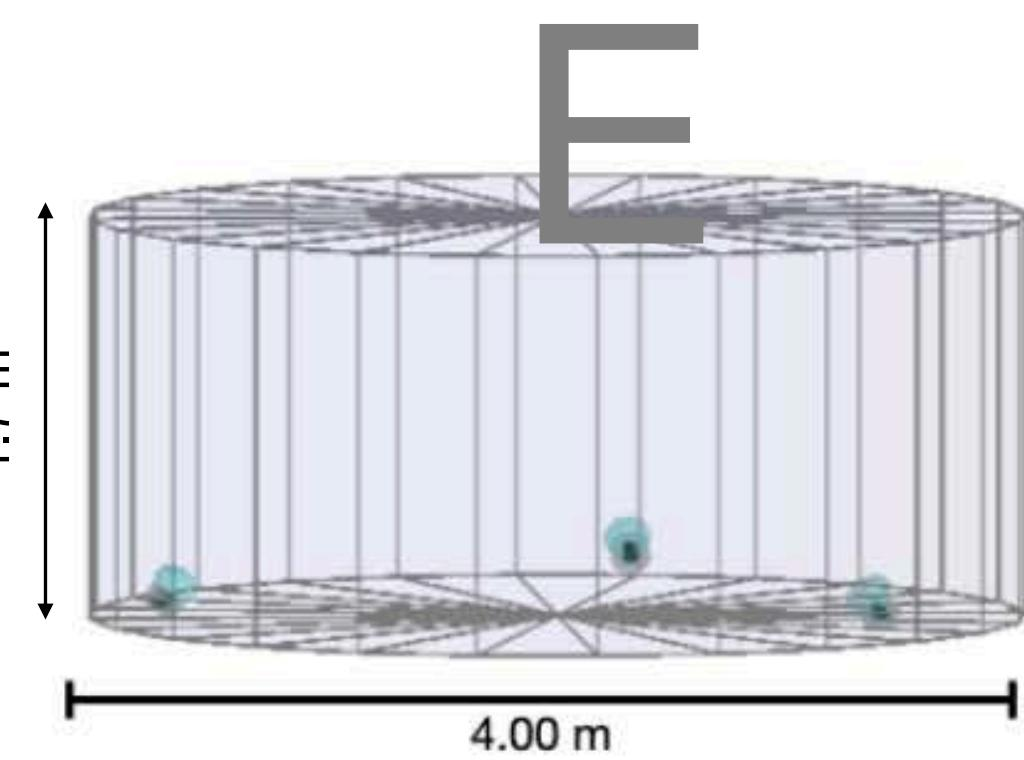
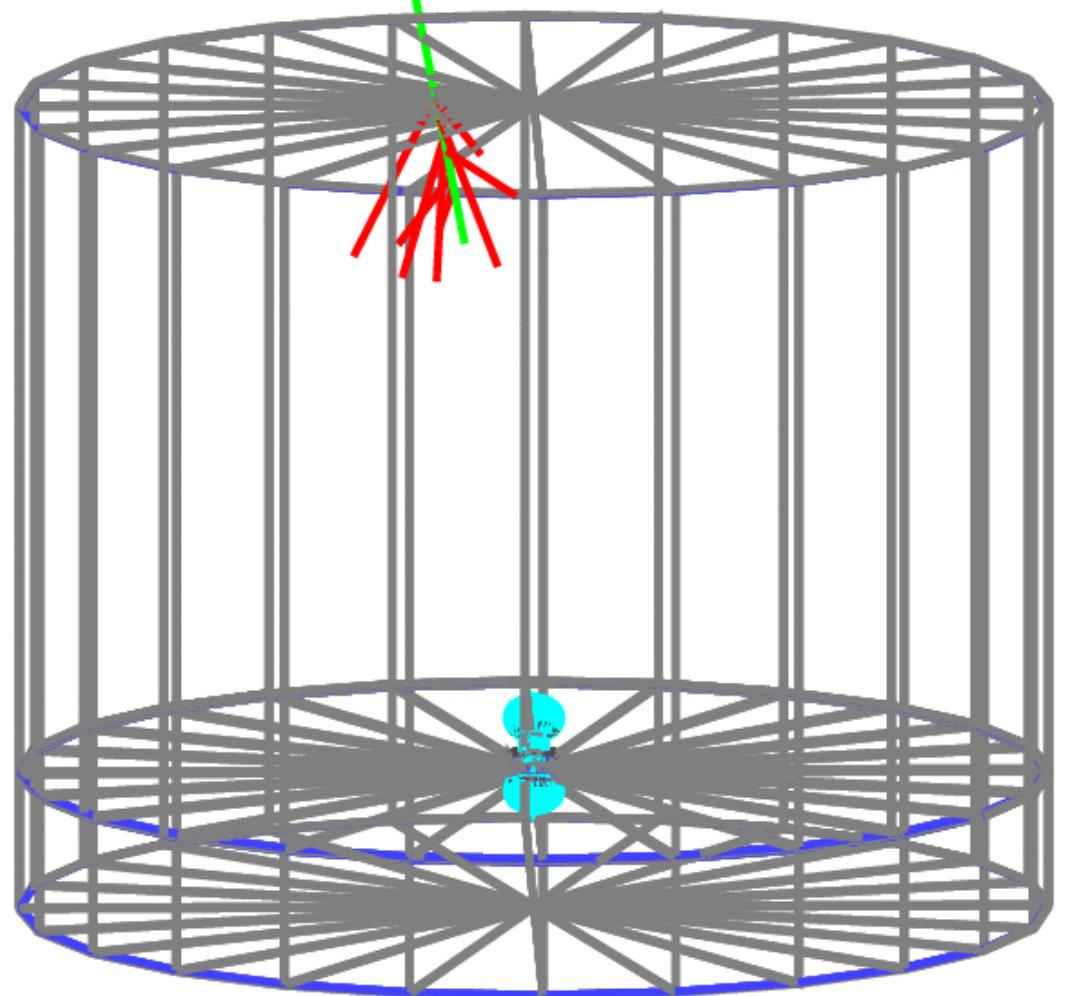
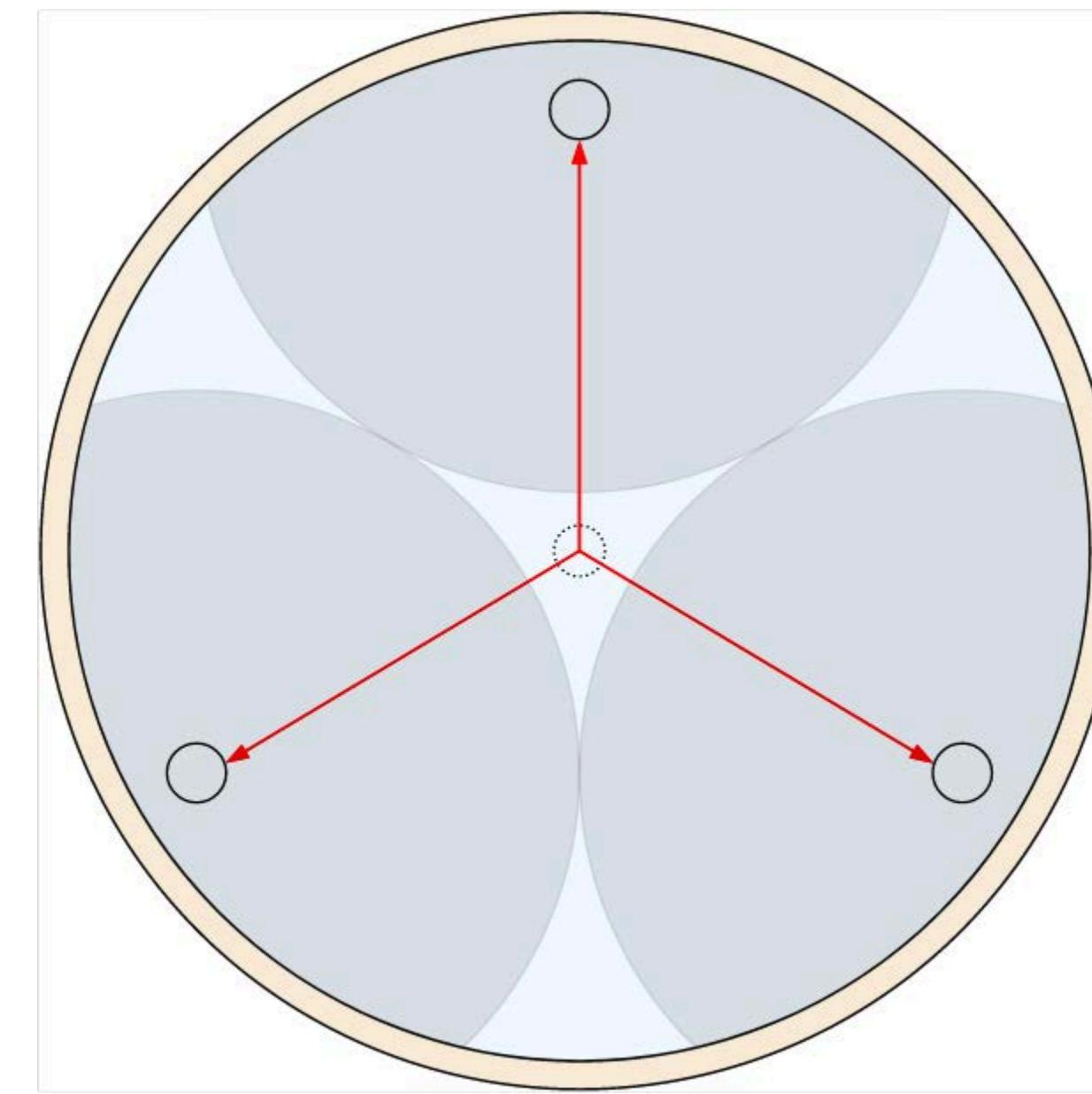
*cooperation with KM3NeT,
MoU in prep.

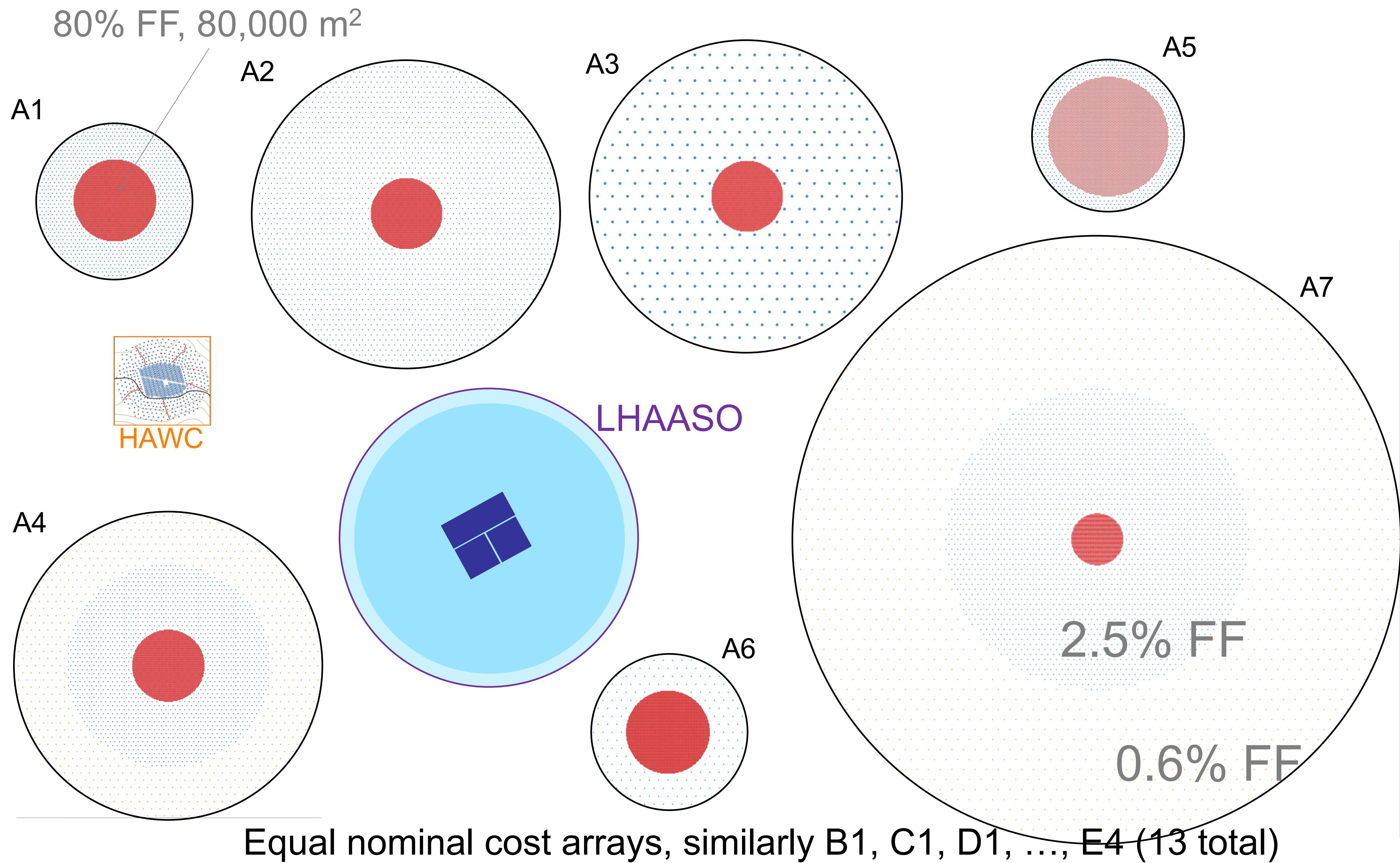






Muon identification a key element of background rejection – two approaches under evaluation

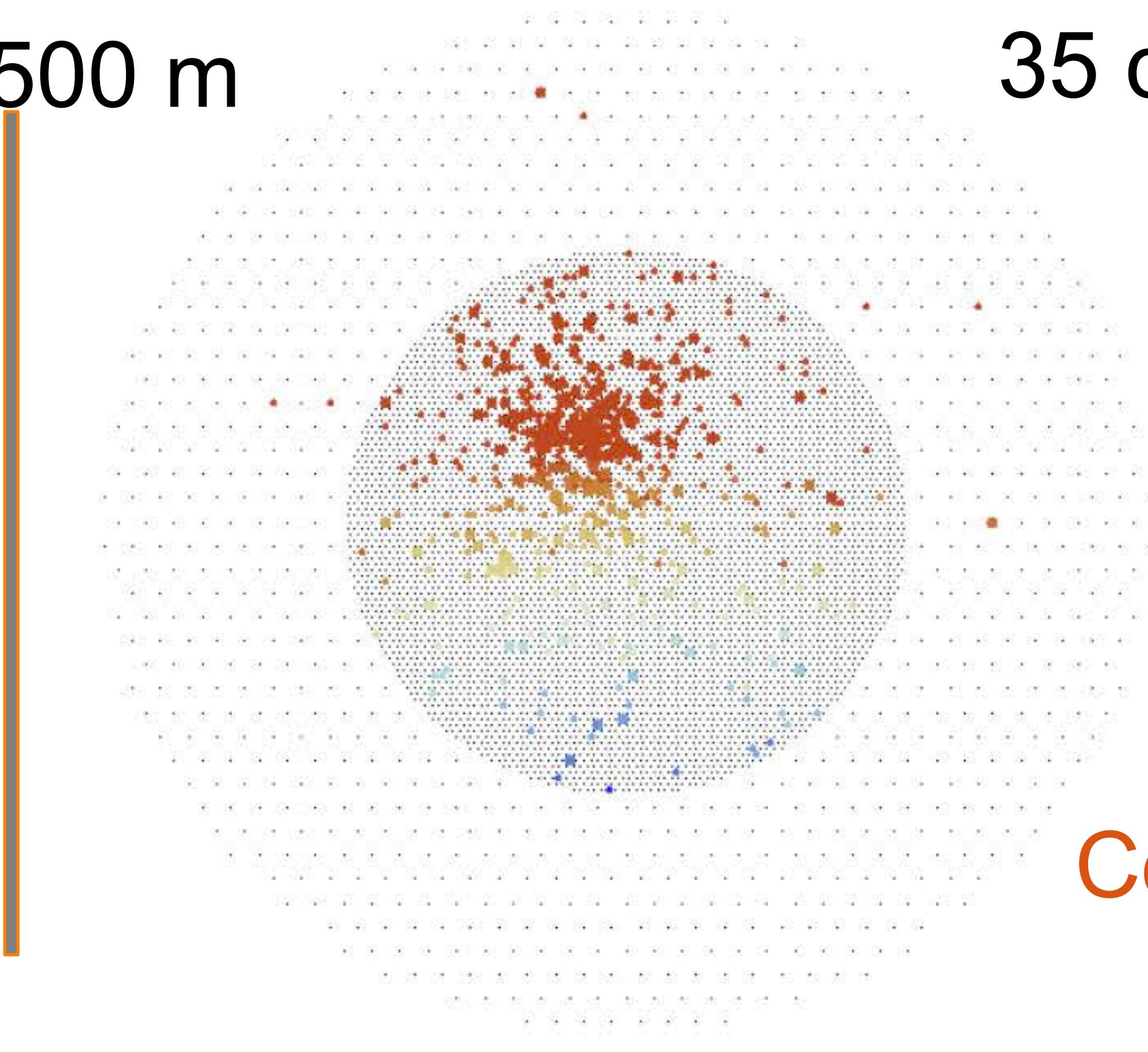




A1

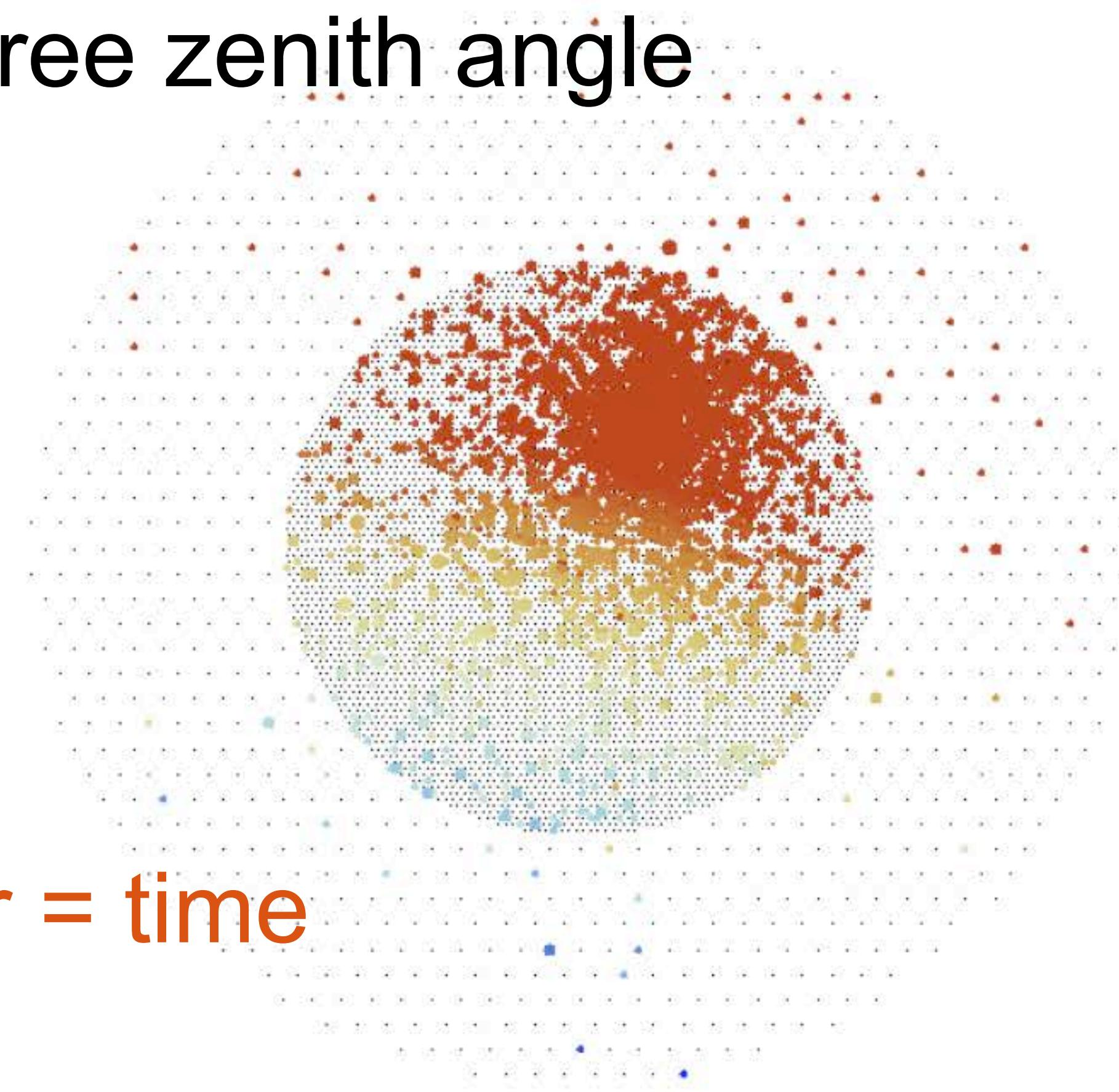
600 GeV

500 m



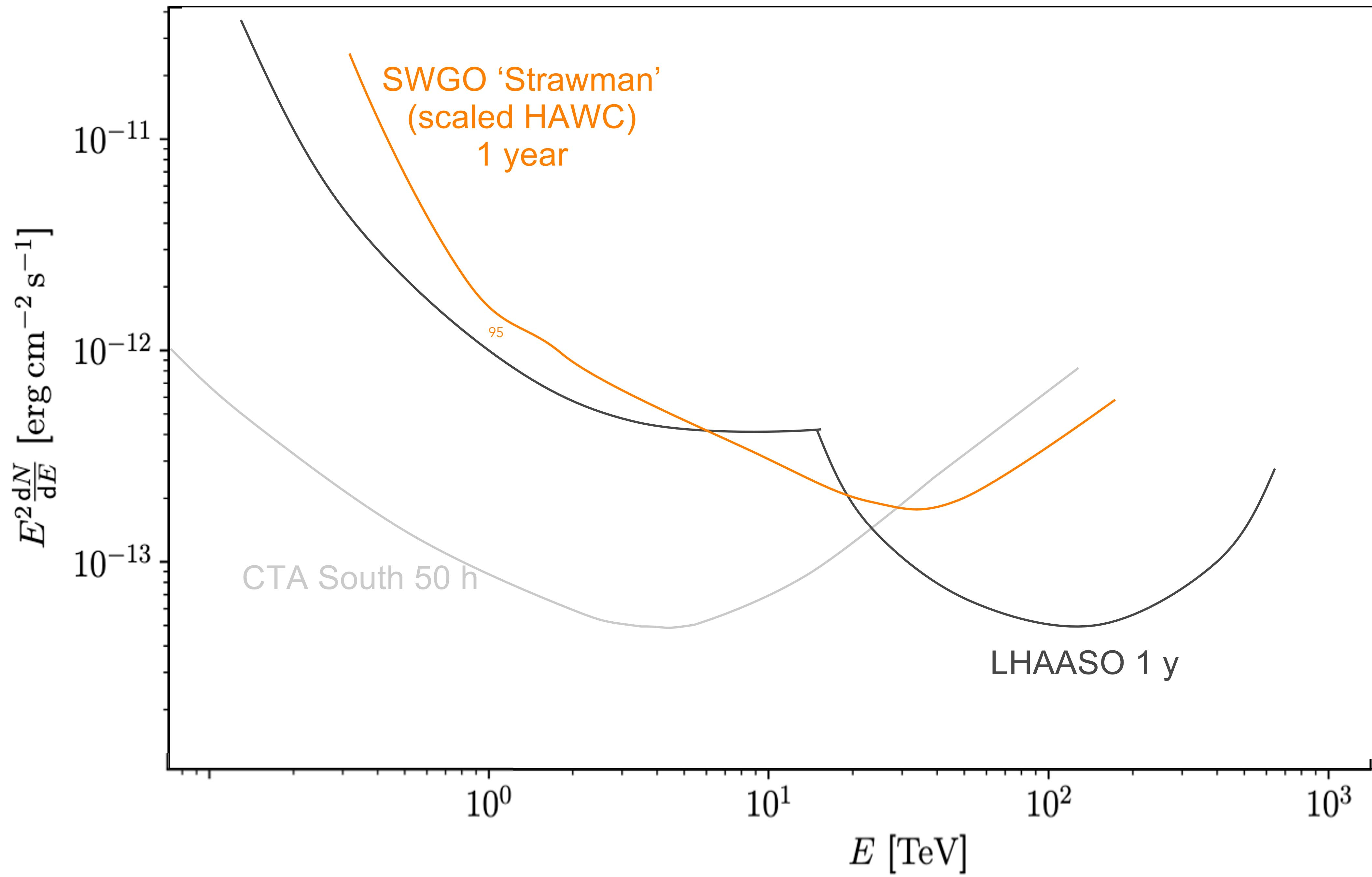
35 degree zenith angle

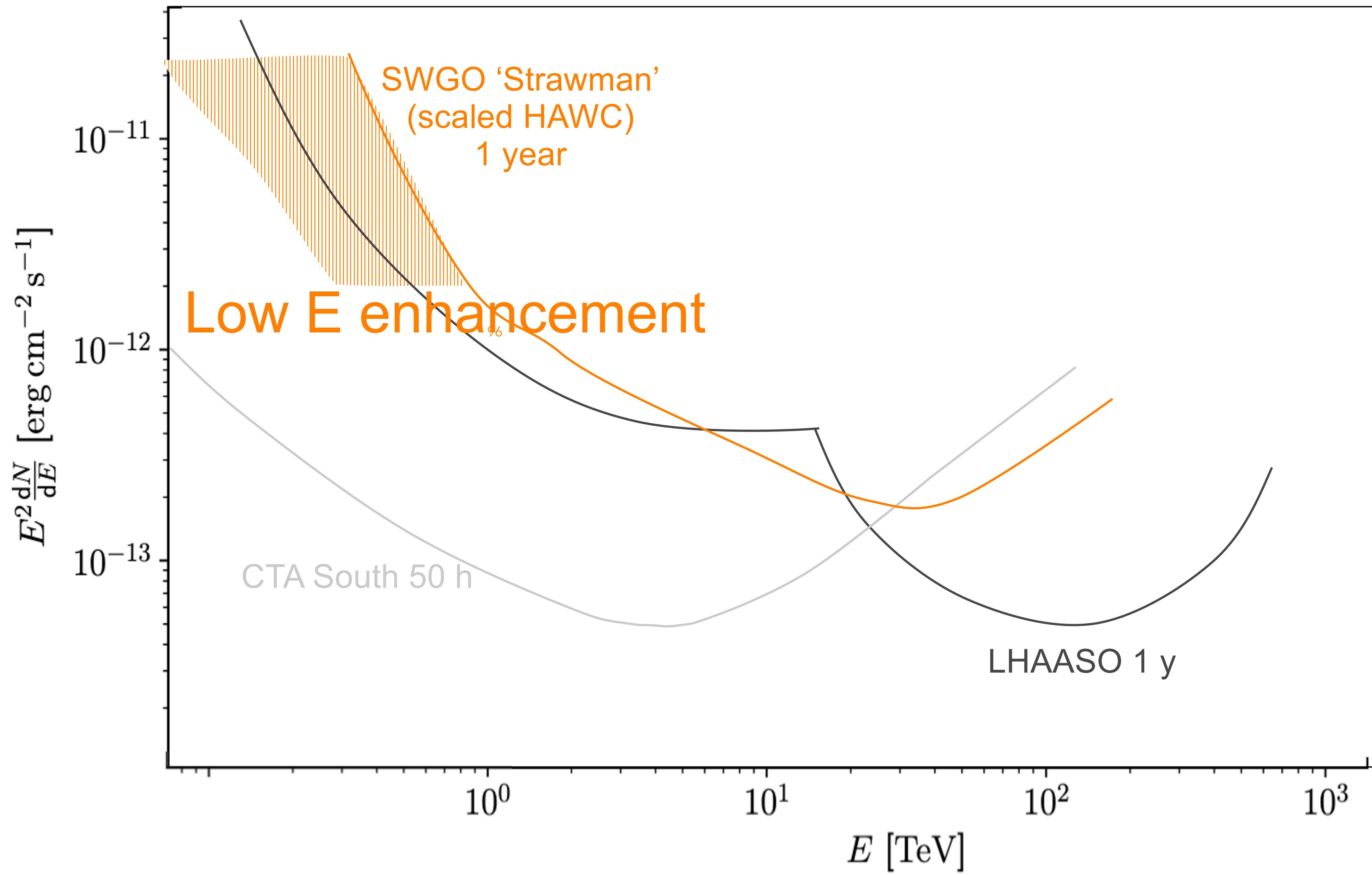
14 TeV

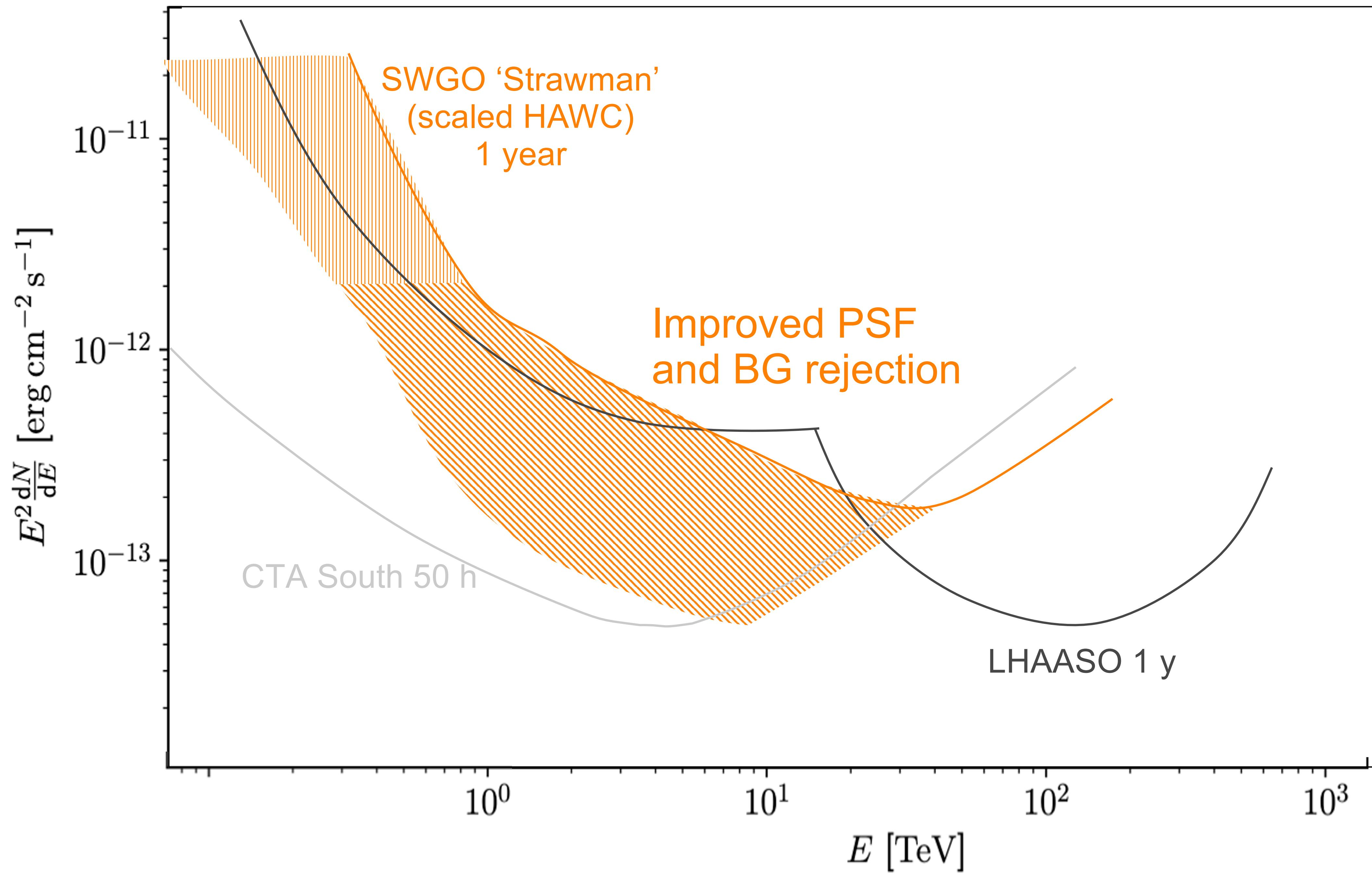


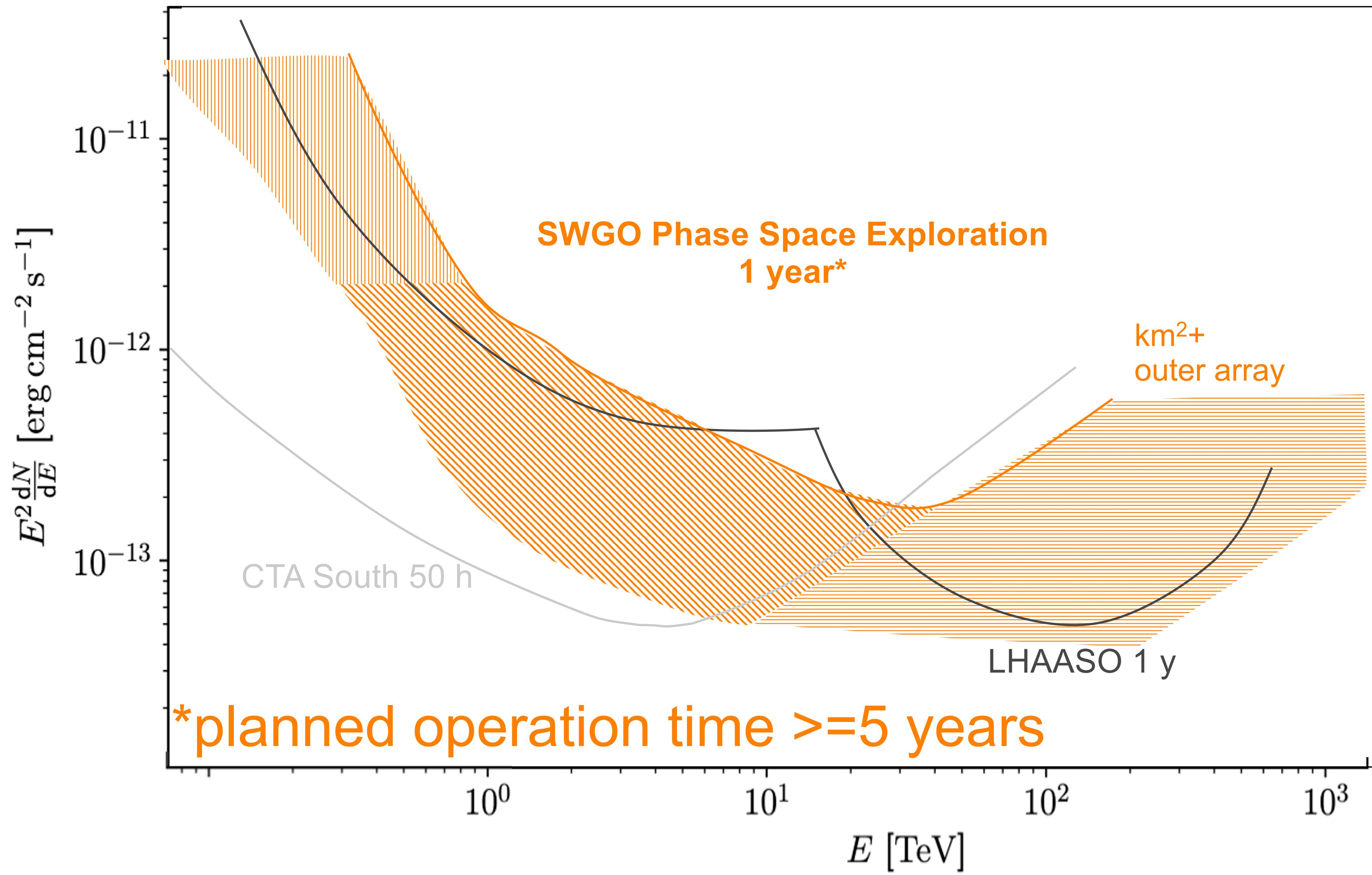
Color = time

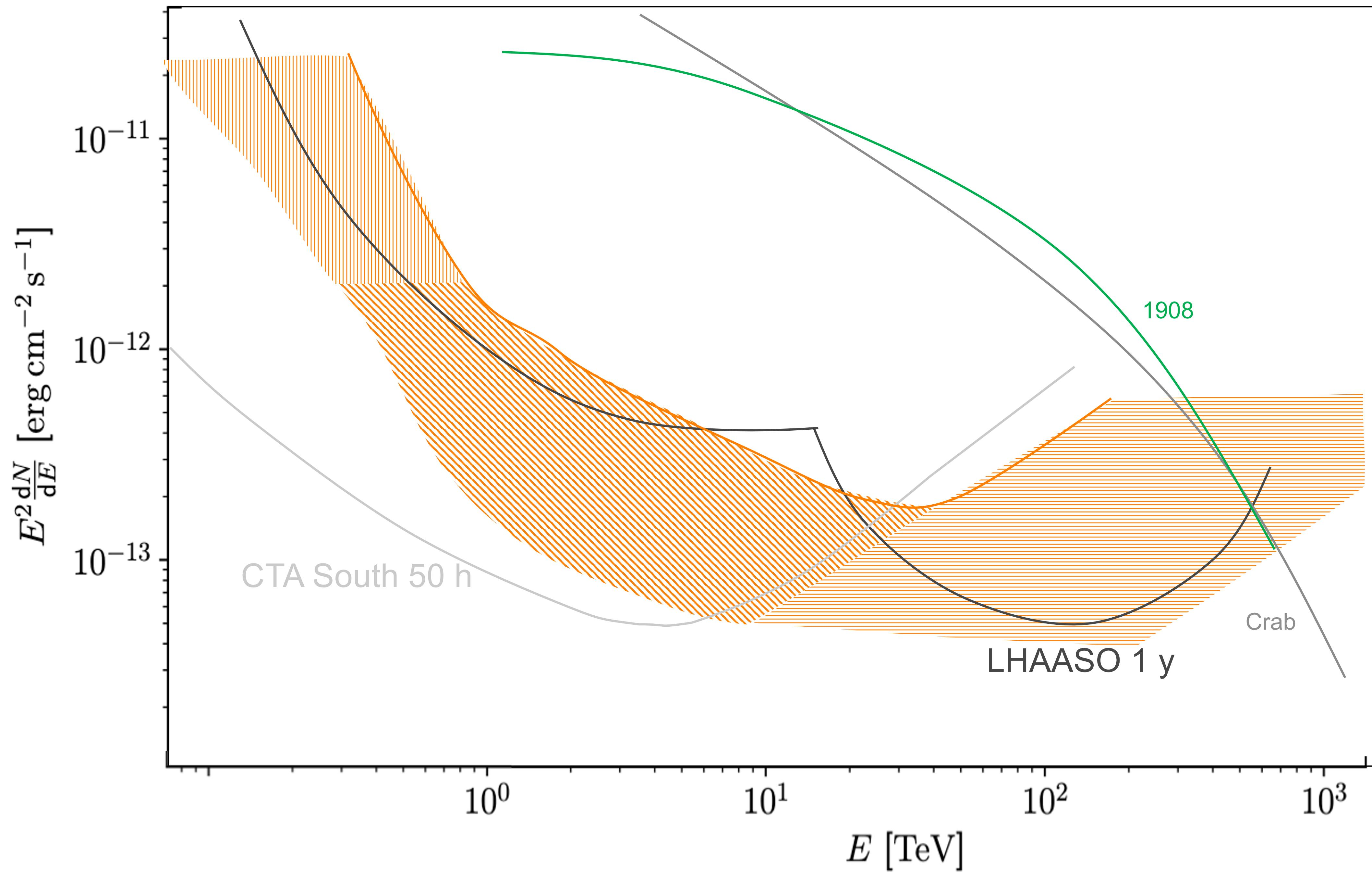
- ◎ Larger detector array and increased altitude w.r.t. HAWC
 - Very precise measurements possible even below 1 TeV

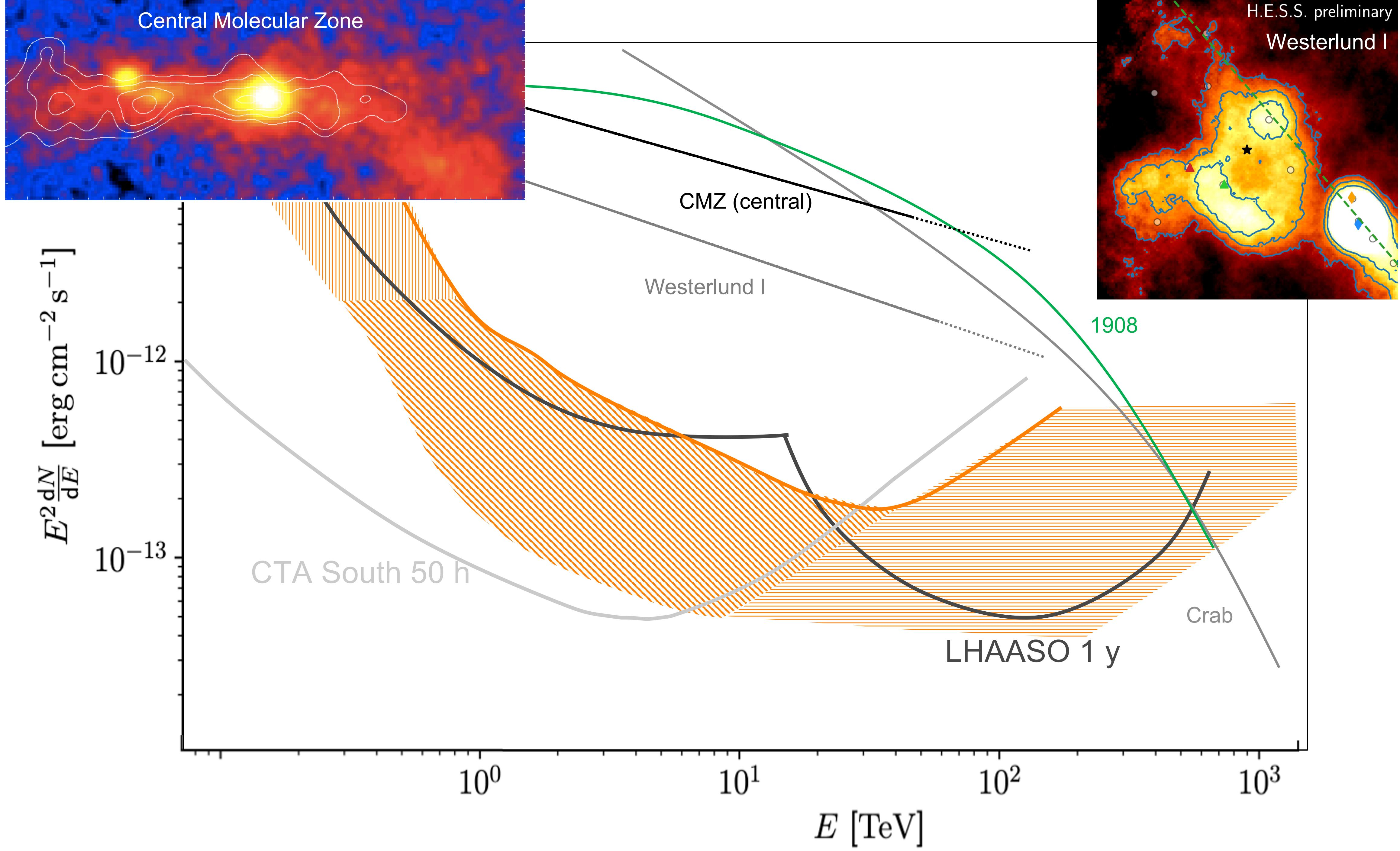




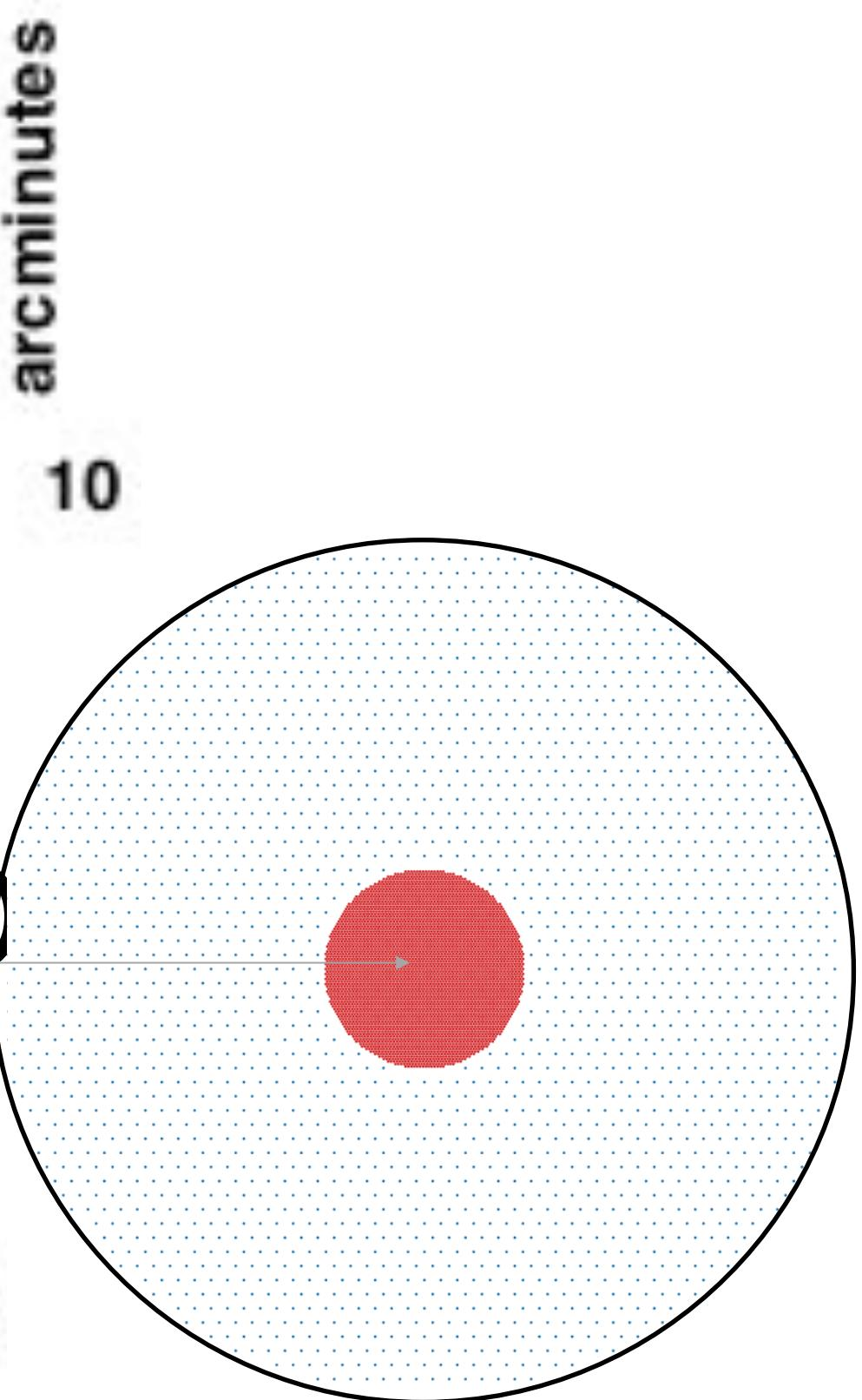
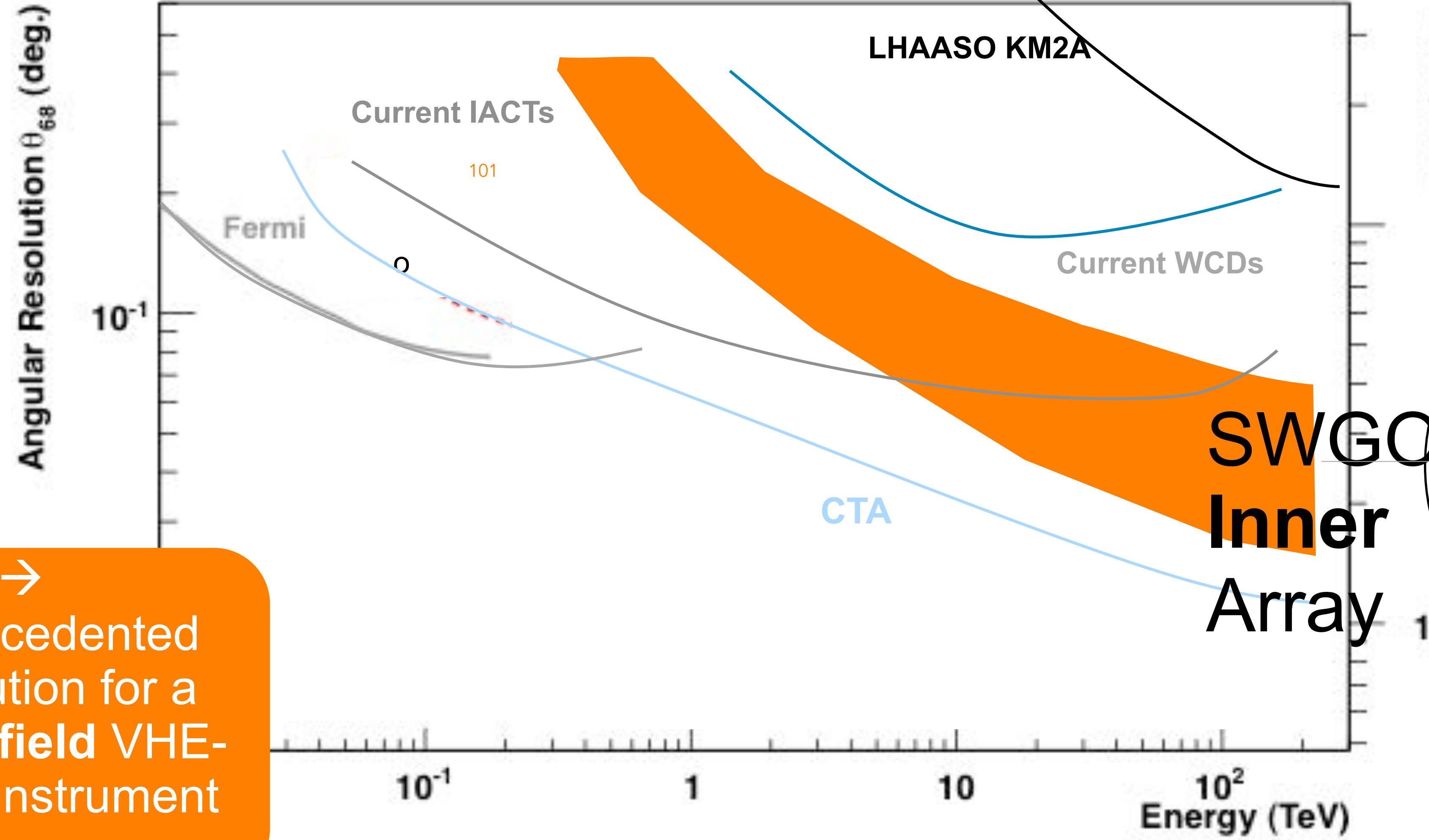








Resolution?



Neutrino Synergy

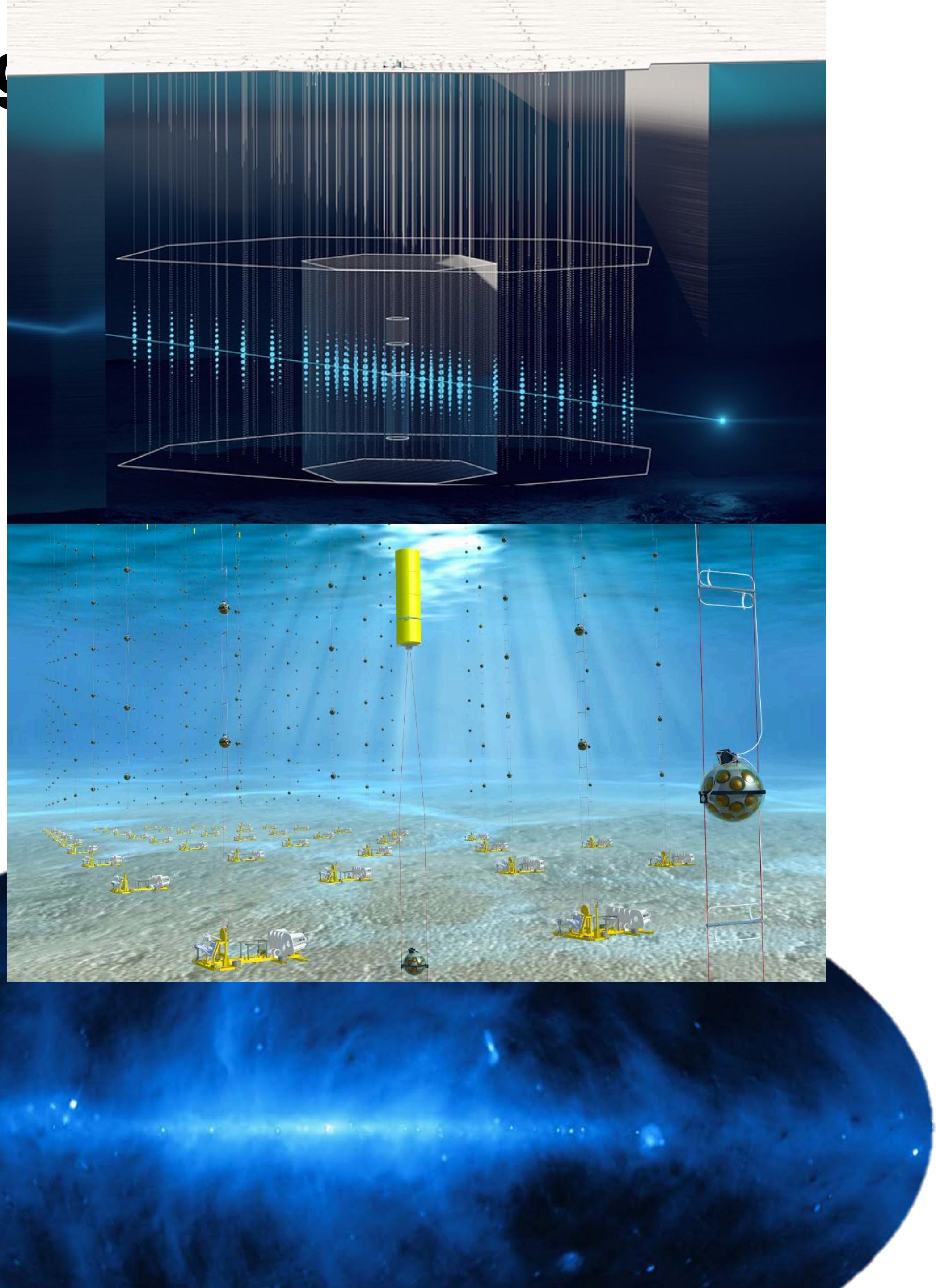
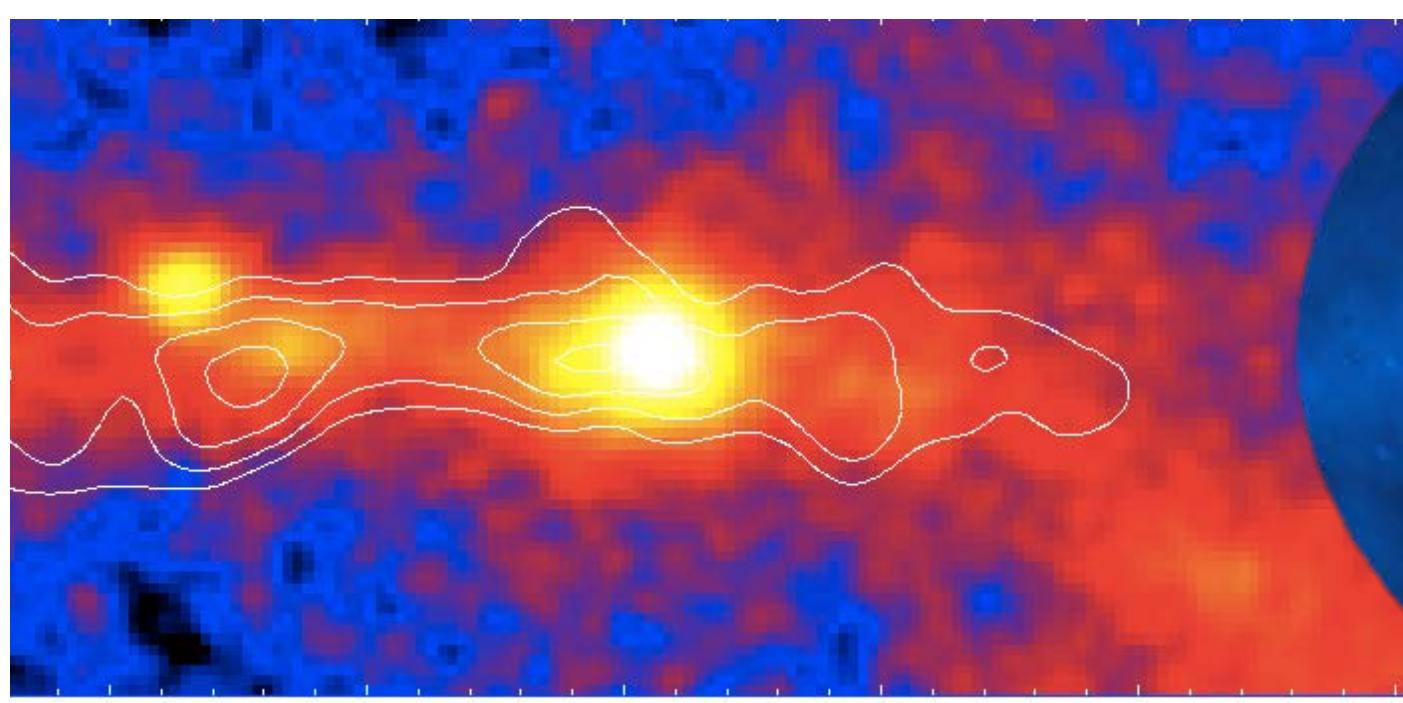
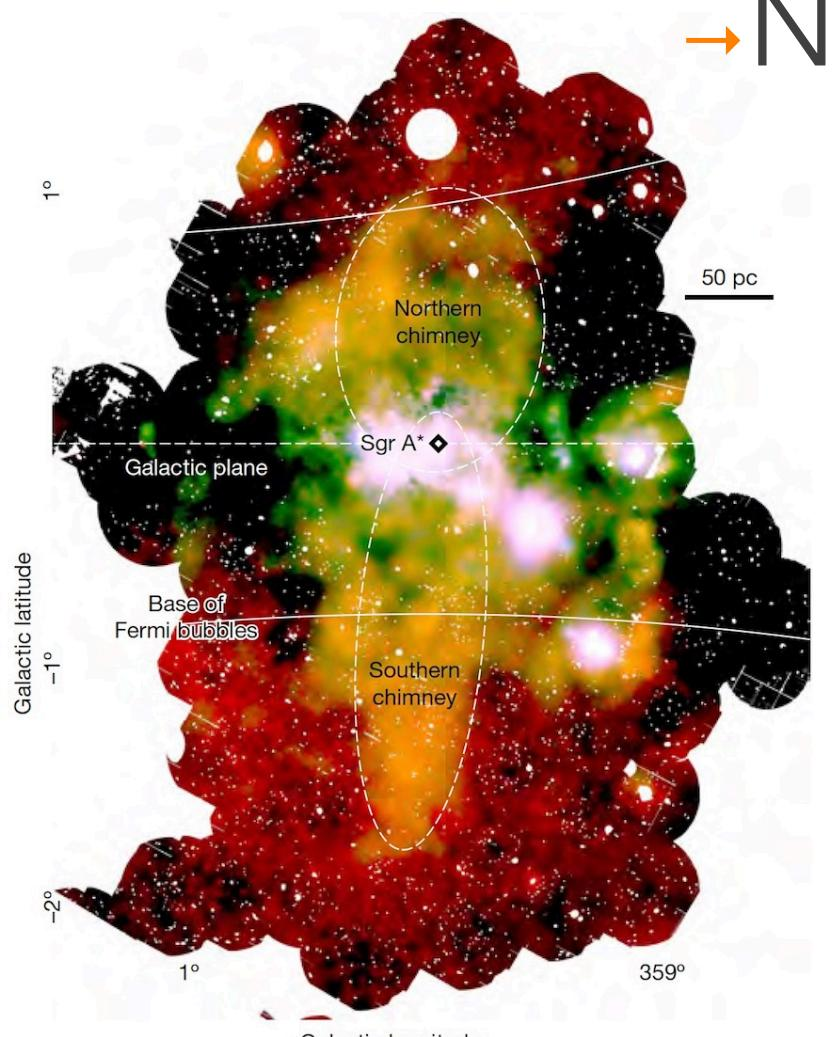
SWGO+LHAASO

Full sky map of TeV-PeV γ emission

Strongly complements new generation of neutrino instruments

Mapping out diffuse emission / separating IC from pion decay emission, Dark Matter search +++

→ Nearby transients/flares



Transients

Instantaneous / short-timescale sensitivity of ground-particle detectors is much worse than IACTs! Especially at low E!!



So why are they still interesting for transients?

100% duty cycle → higher rate of high luminosity and/or nearby events (nearby bursts are very important → GWs, EBL systematics, ¹⁰³++)

Zero observation delay - can potentially catch events with fluxes many orders of magnitude higher

No need to trigger!

Blind searches and can check offline for ‘slow’ alerts

e.g. afterglow triggers from optical and radio → look back!

e.g. cubesats ++ many new / near future alert sources which can come **hours late**

Fermi: 1 GeV
CTA/SWGO: few 100 GeV

Order of magnitude **1 minute sensitivity**: Fermi-LAT: 10^{-7} , SWGO: 10^{-9} , CTA: 10^{-11} erg/cm²/s
SWGO can bring the 10s deg² error boxes (GBM, GW) down to arcmin size

